Phosphorus Removal and Recovery from Wastewater using Sorbent Technologies

by

Holly Erin Gray

A thesis

presented to the University of Waterloo

in fulfilment of the

thesis requirement for the degree of

Doctor of Philosophy

in

Civil Engineering

Waterloo, Ontario, Canada, 2018

Examining Committee Membership

The following served on the Examining Committee for this thesis. The decision of the Examining Committee is by majority vote.

External Examiner	Yves Comeau Professor
Supervisor(s)	Wayne J. Parker Professor
	D. Scott Smith Professor
Internal Member(s)	Peter Huck Professor
	Bryan Tolson Associate Professor
Internal-external Member	Frank Gu Associate Professor

Author's Declaration

This thesis consists of material all of which I authored or co-authored: see Statement of Contributions included in the thesis. This is a true copy of the thesis, including any required final revisions, as accepted by my examiners.

I understand that my thesis may be made electronically available to the public.

Statement of Contribution

Chapter 2

This work was published by International Water Association (IWA) Publishing and can be found online at: https://www.iwapublishing.com/books/state-knowledge-use-sorption-technologies-nutrient-recovery-municipal-wastewaters-nutrients

Gray, H., Parker, W. & Smith, S. 2015. State of Knowledge of the Use of Sorption Technologies for Nutrient Recovery from Municipal Wastewaters. *Water Intelligence Online*, **14**, 9781780407319.

The paper is co-authored by myself, my supervisors Dr. Wayne J. Parker and Dr. D. Scott Smith. I did the literature search and wrote the paper.

Chapter 6

The paper is co-authored by myself, my supervisors Dr. Wayne J. Parker and Dr. D. Scott Smith, as well as Tony Powell, Chief Technical Officer at Purifics Water Inc. I carried out the lab experiments, collected and analyzed the experimental data, and wrote the paper. Mr. Powell helped with some aspects of experimental design and gave insight to interpretation of some of the results.

Chapter 7

The paper is co-authored by myself, my supervisors Dr. Wayne J. Parker and Dr. D. Scott Smith, as well as Tony Powell, Chief Technical Officer at Purifics Water Inc. I carried out the lab experiments, collected and analyzed the experimental data, and wrote the paper. Mr. Powell helped with technical support.

Abstract

Phosphorus (P) is an essential nutrient in fertilizers that are necessary for food production. Wastewater may represent a renewable source of nutrients if methods for recovering P from dilute wastewater streams can be developed. Adsorption, a low cost and efficient process, has the potential to recover P from wastewater as it can transfer contaminants from the liquid to the solid phase for easy separation.

This study evaluated fourteen commercial sorbents for potential phosphorus recovery from synthetic wastewater (SWW) using batch testing. Commercially available sorbents (*e.g.* ion exchange resins (IEX), granular ferric oxide, hybrid IEX and activated alumina) were obtained from several companies and tested for phosphate removal in a 48-hour adsorption test. Seven of the sorbents exhibited substantial phosphate removal were then tested for recovery using acidic (HCl), basic (NaOH), salt (NaCl) and basic salt (NaOH + NaCl) desorption solutions. Sorbents were evaluated with respect to P recovery from the SWW. An IEX sorbent was found to recover the largest fraction at 23 % P from the SWW; while all other sorbents recovered less than 20 % P from the synthetic wastewater.

The three top performing sorbents from batch testing were chosen for column testing to investigate their potential for P adsorption and recovery with a specific target of generating a concentrated chemical desorption effluent. Sorbents included two metal oxide sorbents (granular ferric hydroxide and activated alumina) as well as an ion exchange (IEX) resin. After the sorbents were tested for P removal in column tests, chemical desorption solutions were utilized to recover P from the spent sorbents. Recovery from metal oxide sorbents was conducted using basic (NaOH) and acidic (HCl) solutions while recovery from IEX sorbent used salt (NaCl) and basic salt (NaOH + NaCl) solutions in addition to acidic and basic treatments. Sorbents were evaluated on the basis of P adsorption as well as recovery from the sorbent and the initial synthetic wastewater (SWW) stream. The IEX sorbent demonstrated the highest removal of 64 % P from the SWW, while the metal oxide sorbents adsorbed between 23 and 43 % P. Desorption using NaOH was most effective for metal oxide sorbents, which were found to recover 39 % P (granular ferric hydroxide) and 21 % P (activated alumina) from the initial SWW. Sorbent C recovered the largest quantity of P (61%) from SWW with the use of NaCl. Due to its good performance, sorbent C was used to recover P from two wastewater samples. Using NaCl, sorbent C recovered 47 and 15 % of P from secondary and final effluent samples.

In addition to a shift in wastewater treatment to P recovery, wastewater treatment is also focusing on producing effluent that meets ultra-low effluent P discharge limits. In order to achieve this goal, non-reactive phosphorus (nRP) must be removed; nRP contains condensed phosphates and organic phosphorus (OP) species that are recalcitrant in secondary wastewater treatment and tend to remain in final effluents.

An advanced oxidation process (AOP) which couples TiO_2/UV photolysis with ultrafiltration (UF) to oxidize and remove nRP species was tested. Tests utilizing a mixture of two OP model compounds were conducted to determine the effect of TiO_2/UV photolysis on the model

compound removal and to elucidate the mechanisms of phosphorus removal; nRP was removed through adsorption and UV irradiation. The AOP was also tested for P removal from three municipal wastewaters and one automotive industry effluent. In all cases, phosphorus removal was found to occur through filtration, surface complexation onto the TiO_2 and UV oxidation. Total phosphorus removal efficiencies between 90-97 % were observed for the municipal wastewater effluents and 44 % removal was observed in the industrial effluent after treatment using AOP. Conversion of nRP to reactive P (RP) was evident during TiO_2/UV treatment of samples that had high concentrations of nRP; the total amount of phosphate liberated was not quantified due to phosphate binding to TiO_2. In summary, the AOP effectively oxidized nRP to RP, achieving a high level P removal in real wastewater effluents and retaining P on the TiO_2 solids.

Investigations into P recovery by TiO_2 nanoparticles revealed that adsorption of P onto TiO_2 was due to a combination of inner sphere complex formation and calcium bridging. Precipitation of calcium phosphate was observed at pH values above 10. Recovery of P from TiO_2 after concentrating of the TiO_2 solids and application of a chemical desorption solution was assessed. Recovery with an NaOH desorption solution was minimal due to calcium phosphate precipitation while recovery using HCl was limited, releasing only 2 % of adsorbed P. Recovery from TiO_2 nanoparticles loaded with calcium phosphate precipitates was also investigated. A recovery of 35 % P was observed from TiO_2 solids via the dissolution of the precipitates.

Acknowledgements

I would like to thank my supervisors Dr. Wayne Parker and Dr. Scott Smith for their knowledge, passion, endless patience and advice. Your guidance, encouragement and support provided me with strength, helped nurture my passion and inspired me to continue to improve at every opportunity. Thank you for enduring staying with me through all the bumps in the road caused by my crazy life. It has been a privilege to work with you.

To the members of my committee Dr. Yves Comeau, Dr. Peter Huck, Dr. Bryan Tolson and Dr. Frank Gu for reviewing my thesis, providing valuable feedback and putting up with a deluge of paperwork during the later part of my thesis.

I would like to thank the industrial partners who funded my research. To Canadian Water Network (CWN), Water Environment Research Foundation (WERF), Ostara Nutrient Recovery Technologies Inc., Suez Environnement (formally GE Water & Process Technologies), GHD Group (formally Conestoga-Rovers and Associates), Halton Region, York Region and Region of Waterloo and the companies which donated sorbents for testing. I would like to thank Tony Powell, Brian Butters, John Nelligan and Cam Honsinger from Purifics Water Inc. for letting me set up in their shop and helping me out whenever I broke something or caused a minor flood.

To my parents, family and friends for always being by my side. Finally, to my dog Boyd – you have more knowledge on nutrient recovery than anyone will ever give you credit for.

Dedication

For

Desmond Gray

Patricia Lynagh

and

Kevin James Gray

Table of Contents

List of Figures

List of Tables

List of Abbreviations

AC	Activated Carbon
AEC	Ammonia Exchange Capacity
AEP	Aminoethylphosphonate
AOP	Advanced Oxidation Process
ATP	Adenosine Triphosphate
BILS	Boston Ivy Leaf Sorbent
BM	Binary Mixture
BV	Bed Volume
CaP	Calcium Phosphate
CEC	Cation Exchange Capacity
CF	Concentration Factor
CWO	Catalytic Wet Oxidation
CRS	Calcium Rich Sepiolite
CUF®	Ceramic UltraFiltration
DOC	Dissolved Organic Carbon
DOM	Dissolved Organic Matter
EBPR	Enhanced Biological Phosphorus Removal
GAC	Granular Activated Carbon
HAP	Hydroxyapatite
HFO	Hydrated Ferric Oxide
ICP OES	Inductively Coupled Plasma Optical Emission Spectroscopy
ISE	Ion Selective Electrode
IEX	Ion Exchange
MAC	Maximum Adsorption Capacity
MAP	Magnesium Ammonium Phosphate (*i.e.* Struvite)

nRP	Non-Reactive Phosphorus
NOM	Natural Organic Matter
OCP	Octacalcium Phosphate
OP	Organic Phosphorous
P	Phosphorus
pH_{zpc}	Zero Point Charge
RP	Reactive Phosphorus
SEM	Scanning Electron Microscope
SLS	Strawberry Leaf Sorbent
SSE	Sum of Square Error
SWW	Synthetic Wastewater
TA	Total Ammonia
TN	Total Nitrogen
TOC	Total Organic Carbon
TP	Total Phosphorus
UF	Ultrafiltration
UV	Ultra-violet
WRRF	Water Resource Recovery Facility
WWTP	Wastewater Treatment Plant

List of Symbols

C_b	Breakthrough Concentration
C_e	Equilibrium Concentration
C_o	Initial Concentration
C	Concentration of P in the Aqueous Phase
G_s	Flow of Solvent
K_F	Freundlich Capacity Factor
K_{sp}	Solubility Product Constant
K_T	Mass Transfer Coefficient
R_s	Percent P Recovered from Sorbent
R_{WW}	Percent P Recovered from Wastewater
Q	Flow Rate
1/N	Freundlich Intensity Parameter
M_{PA}	Mass of Adsorbed P
M_{PD}	Mass of Desorbed P
M_{PWW}	Initial Mass of P in Wastewater
t	Time
t_b	Time at Breakthrough
X	Mass of Sorbate Adsorbed per Mass of Sorbent
V	Velocity of Adsorption Zone
V_c	Volume of Column
V_{DS}	Volume of Desorption Solution
V_{WW}	Volume of Wastewater Treated
P_{EST}	Estimated Mass Recovered P
SUR	Sorbent Usage Rate

1.0 Introduction

1.1 Problem Statement

The recognition that wastewater contains valuable resources has caused a paradigm shift from nutrient removal to recovery in wastewater treatment (LeCorre *et al*., 2009). Presently, the majority of wastewater treatment plants use chemical and biological treatment to remove phosphorus (P) from the wastewater stream, collecting it in the biosolids for disposition (Valsami-Jones, 2001). This traditional form of treatment is slowly being replaced with nutrient recovery technologies and wastewater treatment plants (WWTPs) are being renamed as water resource recovery facilities (WRRFs). As of 2015, there were six WRRFs in North America which recover P using struvite crystallization (Latimer *et al*., 2015). Struvite ($NH_4MgPO_4 \cdot 6H_2O$), is a valuable, inorganic P precipitate that can act as slow release fertilizer (Desmidt *et al*., 2015).

While the goal of P recovery is the new focus of wastewater treatment, phosphorus in wastewaters must still be removed to low concentrations to avoid the detrimental effects of eutrophication in receiving waters (Cordell *et al.*, 2009). In some cases, persistent non-reactive phosphorus (nRP) needs to be removed to achieve ultra-low effluent P concentrations. This is important in areas with sensitive receiving waters prone to eutrophication that require stricter phosphorus effluent discharge limits (Clark *et al.*,2010); nRP species can make up 26 to 81 % of the total P in treated wastewater effluents as it is more recalcitrant, and not receptive to biological and chemical nutrient removal processes (Qin *et al.*, 2015). The oxidation of nRP would benefit P recovery technologies as organic P species are not available for nutrient recovery and thus, are lost to landfill (Latimer *et al*., 2015). There is a need for technologies that

can oxidize nRP to inorganic P species which are more susceptible to removal and potentially recovery, and as such, could help reach the high levels of removal necessary in treated wastewater effluents.

Finally, a limitation of struvite-based recovery is that the concentration of P in the wastewater stream needs to be greater than 100 mg P/L for these technologies to be effective (Xie *et al*., 2016). Phosphorus concentrations in domestic wastewater influents are low (< 10 mg P/L) limiting the implementation of struvite technologies to integration with enhanced biological phosphorus removal (EBPR) where P has been concentrated to suitable levels (Ye *et al*., 2017). Wastewater treatment plants which do not utilize EBPR require technologies that can concentrate phosphorus into a stream which meets the high concentrations necessary for nutrient recovery.

In summary, with the shift to P recovery, WWTPs without EBPR require technologies for P recovery that collect P from dilute waste streams and concentrate P into a form suitable for struvite recovery. Simultaneously, a method is required to oxidize nRP in wastewater streams to allow this fraction of P to be recovered while also achieving ultra-low P concentrations in treated wastewater effluent.

1.2 Objectives and Scope

The goals of this study were:

1) To identify commercial sorbents that can adsorb and subsequently desorb large quantities of phosphorus to recover P from wastewater treatment plant effluents.

In laboratory bench testing, existing commercial sorbents were investigated for phosphorus adsorption and desorption. An ideal sorbent would have the ability to adsorb large quantities of P

and achieve high level P removal in wastewater effluents. Sorbents would also be regenerated via chemical desorption and hence, chemical desorption was also investigated. Desorption solutions were evaluated on liberation of P from the sorbent and concentration of the recovery solution. An ideal desorption solution would recover all adsorbed P and produce a recovery solution with high P concentration which would be a useful feedstock for nutrient recovery technologies (*i.e*. struvite crystallization).

The sorbent and the corresponding desorption solution that demonstrated the best performance was used to remove and recover P from real wastewater effluents.

2) To determine if a commercial advanced oxidation process could be effective at oxidizing organic P species in wastewater treatment effluent.

Two model compounds were tested in a mixture and individually, to evaluate the ability of a lab-scale commercial UV/TiO_2 advanced oxidation process (AOP) coupled with ultrafiltration to oxidizing non-reactive phosphorus to reactive phosphorus. Model compounds were used to gain insight into the mechanism of non-reactive phosphorus removal through the action of TiO_2/UV photocatalysis. The AOP unit was also used to treat real effluent samples to evaluate the ability to breakdown nRP species in a complex wastewater matrix.

3) To test TiO_2 nanoparticles as a means to concentrate P into the solid phase and then transfer to a concentrated aqueous phase suitable for struvite recovery.

Phosphorus adsorption onto TiO_2 and its potential for P recovery from wastewater was investigated using a lab scale ultrafiltration unit employed to separate the TiO_2 from the wastewater and to concentrate the TiO_2 nanoparticles. Concentration of P in the recovery stream through concentration of the P-loaded TiO_2 solids, followed by pH adjustment was examined to optimize chemical use for recovery.

4) Propose a strategy to oxidize non-reactive phosphorus and remove liberated reactive phosphorus from the liquid phase to the solid phase for subsequent recovery into a solution suitable for P recovery.

1.3 Significance

The knowledge gained in this study will give insight into methods of adsorption for phosphorus recovery. It also improves the understanding of the mechanism of nRP removal though TiO_2/UV photolysis as well as providing insight into the approaches that could be used to reduces nRP in wastewater effluents. The investigations made in this study towards nRP oxidation also provide a commercial technology that could be implemented into current practice to reduce nRP in wastewater effluents. Finally, the information obtained in this study can provide insight to use of TiO_2 nanoparticles as a seed for calcium phosphate precipitation as potential method for phosphorus recovery.

1.4 Outline of Thesis

This thesis is divided into eight chapters and including an introduction to the project in Chapter 1. The literature review portion of this thesis is divided into two chapters. Chapter 2 is a

literature review on nutrient recovery using adsorption processes which has been published as a WERF White report titled “State of Knowledge of the Use of Sorption Technologies for Nutrient Recovery from Municipal Wastewaters” (NUTRIR06x, 2014). A literature review exploring the oxidation of organic phosphorus is presented in Chapter 3. Chapter 4 contains the methodology and results from batch tests that screened commercial sorbents for phosphorus removal and recovery using chemical desorption solutions. Experimentation and results of column tests further exploring the top three performing sorbents are presented in Chapter 5. Chapter 6 describes the experimental method and results obtained from oxidation of non-reactive phosphorus using a lab-scale commercial TiO_2/UV AOP. Methodology and results from attempting to recover the liberated orthophosphate from photolysis are presented in Chapter 7. The last chapter in this thesis is Chapter 8 which summarizes the various conclusions of the experimental work and discusses recommendations for future work.

Chapters 4 through 7 are written in manuscript format and intended for submission to peer reviewed journals for publication consideration. References are provided at the end of each chapter.

2.0 Literature Review: Adsorption for Nutrient Recovery

This work was published by International Water Association (IWA) Publishing and can be found online at: https://www.iwapublishing.com/books/state-knowledge-use-sorption-technologies-nutrient-recovery-municipal-wastewaters-nutrients

Gray, H., Parker, W. & Smith, S. 2015. State of Knowledge of the Use of Sorption Technologies for Nutrient Recovery from Municipal Wastewaters. *Water Intelligence Online*, **14**, 9781780407319.

WERF

Water Environment Research Foundation

Collaboration. Innovation. Results.

State of Knowledge of the Use of Sorption Technologies for Nutrient Recovery from Municipal Wastewaters

Co-published by

IWA PUBLISHING

NUTR1R06x

STATE OF KNOWLEDGE OF THE USE OF SORPTION TECHNOLOGIES FOR NUTRIENT RECOVERY FROM MUNICIPAL WASTEWATERS

Holly Gray
Wayne Parker
University of Waterloo

Scott Smith
Wilfrid Laurier University

2015

WERF

The Water Environment Research Foundation, a not-for-profit organization, funds and manages water quality research for its subscribers through a diverse public-private partnership between municipal utilities, corporations, academia, industry, and the federal government. WERF subscribers include municipal and regional water and water resource recovery facilities, industrial corporations, environmental engineering firms, and others that share a commitment to cost-effective water quality solutions. WERF is dedicated to advancing science and technology addressing water quality issues as they impact water resources, the atmosphere, the lands, and quality of life.

For more information, contact:
Water Environment Research Foundation
635 Slaters Lane, Suite G-110
Alexandria, VA 22314-1177
Tel: (571) 384-2100
Fax: (703) 299-0742
www.werf.org
werf@werf.org

This report was co-published by the following organization.

IWA Publishing
Alliance House, 12 Caxton Street
London SW1H 0QS, United Kingdom
Tel: +44 (0) 20 7654 5500
Fax: +44 (0) 20 7654 5555
www.iwapublishing.com
publications@iwap.co.uk

Library of Congress Catalog Card Number: 2014945151
IWAP ISBN: 978-1-78040-731-9

University of Waterloo, Wilfrid Laurier University.

The research on which this report is based was developed, in part, by the United States Environmental Protection Agency (EPA) through Cooperative Agreement No. EM-83406901-0 with the Water Environment Research Foundation (WERF). However, the views expressed in this document are not necessarily those of the EPA and EPA does not endorse any products or commercial services mentioned in this publication. This report is a publication of WERF, not EPA. Funds awarded under the Cooperative Agreement cited above were not used for editorial services, reproduction, printing, or distribution.

2.1 Problem Statement

Fertilizer is an essential part of food production. It nourishes soil and prepares the ground for growing crops for human and livestock consumption. The components in fertilizers that are required for the growth of plants are phosphorus and nitrogen, nutrients which cannot be substituted (Hao *et al.*, 2013). Because nitrogen and phosphorus are absolutely necessary for food production there was cause for concern when it was reported that worldwide mining of phosphate rock is expected to peak in the year 2030; complete exhaustion of global phosphate rock stores is expected to occur in the next 50 – 100 years (Cordell *et al.*, 2009).

Due to the threat to global crops and livestock, methods to reduce use of phosphorus and nitrogen have been put into play in hopes of allowing stores to last longer (Hao *et al.*, 2013). However, the solution to the problem is not limiting the use of essential nutrients. Over time the stores of phosphorus will still be depleted. This problem has highlighted the necessity of having alternate sources of the phosphorus and nitrogen. An opportunity exists in harvesting nutrients from wastewater.

Use of wastewater as a nutrient source will be one of the biggest gains in nutrient recovery (Hao *et al*., 2013). Wastewater treatment views nutrients as nuisance contaminants that cause eutrophication in receiving waters. To lower the amount of nutrients being introduced to wastewater, manufacturers have stopped adding phosphate into their products (*e.g.* detergents). However, even with this reduced input of phosphorus, wastewater streams can deliver an average of 3 mg P/ (person-day). Hence wastewater is still a significant source of phosphorus (Daigger, 2009).

Significant effort has been put into developing treatments to achieve high levels of phosphorus and nitrogen removal. With nutrient limits getting increasingly tight, operational costs and complexity of treatments are increasing (Gu *et al*., 2007). Developing a low cost technology that recycles nutrients and produces low nutrient level effluent will not only help cut operational costs but also give wastewater treatment plants a source of income by selling the recycled nutrients back to industry (de-Bashan *et al.*, 2004). Adsorption offers a highly efficient and stable, low cost technology for phosphorus and nitrogen removal; desorption of the nutrients from the sorbent will allow phosphorus and nitrogen to be easily recycled using nutrient recycling technologies. This report summarizes the state of knowledge on the use of sorption technologies for recovering nitrogen and phosphorous from municipal wastewaters. Gaps in the literature that should be addressed to increase the viability of this application are identified.

2.2 Sustainability in Wastewater Treatment

Wastewater is rich in phosphorus (P) and nitrogen (N), nutrients that are necessary for the development of life. In the wastewater industry, these nutrients are seen as nuisance contaminants due to the negative effect their presence has on receiving waters. Eutrophication is caused by the introduction of N and P to the aquatic environment. Addition of the nutrients lead to algal blooms which cause a decrease in dissolved oxygen concentrations and ultimately death in higher aquatic organisms (van Loon and Duffy, 2000; Love *et al.*, 2010). Studies indicate that phosphorus plays the major role in eutrophication, causing eutrophic conditions to develop in oligotrophic waters with phosphorus concentrations as low was 20 µg P/L (Mayer *et al.*, 2013). Since eutrophication has such a negative impact, wastewater effluents are highly regulated and discharge limits of N and P are continually decreasing.

Conventional wastewater treatment uses technologies to remove contaminants producing clarified water that can be released back into aquatic systems without adverse effects (Metcalf and Eddy, 2003). The goal of current wastewater treatment is the outright removal of nutrient species with nitrogen being outgassed and phosphorus most often ending up in landfill bound in the sludge. Phosphorus can be removed from wastewater through chemical precipitation and enhanced biological removal (Metcalf and Eddy, 2003). In chemical precipitation, metal salts are added to wastewater to remove inorganic phosphorus (*i.e.* phosphate) through precipitation (Sedlak, 1991). Biological phosphorus removal cultures bacteria that, under the right conditions, store large amounts of phosphate in poly-phosphate deposits in their cell bodies (Grady *et al.*, 2011). In conventional treatment, N is removed from wastewater using nitrification and denitrification processes. In these processes, bacteria remove ammonia from wastewater and release it into the atmosphere as N_2 gas. This process has little to no effect on the nitrogen cycle (Mulder, 2003).

The depletion of phosphate stores worldwide has pushed phosphorus recovery into the foreground to help alleviate the strain on natural mined phosphate ore (Biswas *et al.*, 2007; Cordell *et al.*, 2009). Since there is little impact on the nitrogen cycle, nitrogen recycling has received less attention in recent years. After all, nitrogen is an abundant element with nitrogen gas making up 78% of the atmosphere (Erisman *et al*., 2008). However, implementing nitrogen recovery can reduce operating costs of wastewater treatment plants as well as reduce the cost of fertilizer production. Nitrification and denitrification require energy for aeration and pumping increasing costs which can be saved through nitrogen recycling (Malovanyy *et al*., 2013). Also, when nitrogen is released in the form of N_2 gas, it is in a form of nitrogen that cannot be reused without further processing. Nitrogen fertilizers are currently manufactured using ammonia (NH_3)

obtained through the Haber Bosch process; Figure 2-1 depicts the cycle of nitrogen through wastewater treatment and the Haber Bosch process. The Haber Bosch process converts N_2 gas to NH_3 gas through the use of high temperatures and pressures introducing high cost (Erisman *et al*., 2008). Capturing the nitrogen in wastewater can provide aqueous ammonia for various industries preventing the added step of converting N_2 gas to ammonia.

Once implemented, nutrient recovery technologies will have a significant role in the development of sustainable waste and wastewater treatments (Daigger, 2009). The evaluation of conventional P removal led to the discovery that existing technologies will prove to be difficult or impossible to use for recovery. Chemical P removal is efficient in achieving low levels of P removal however the treatment makes it difficult to recover P from the sludge because the precipitated P species are often not in a form available to plants. Phosphate is the target species for P recovery (Rittman *et al.*, 2011). On the other hand, the biosolids that remain after biological P removal can be recycled in soil. However, biosolids are land applied approximately only 1% of the time due to other contaminants in the biosolids (Rittman *et al.*, 2011).

A review of conventional treatment has led to the recognition that traditional removal methods have limitations that also drive the need for better treatment technologies in general. Existing "traditional" treatment of wastewater is unsustainable (Daigger, 2009). Chemical treatment has high associated cost and often problems arise when considering sludge handling and disposal (Rodrigues *et al*., 2010; Biswas *et al*., 2007). Biological removal has its own set of difficulties. Treatment using microorganisms is lengthy, complex and requires considerable investment in infrastructure (Long *et al*., 2011). Although there is constant push to improve conventional technologies, even the best available technologies are reaching their limits in meeting human and environmental needs (Daigger *et al.*, 2009; Mayer *et al*., 2013). These issues with conventional

treatment add to the necessity to develop a technology that can recover nutrients from wastewater.

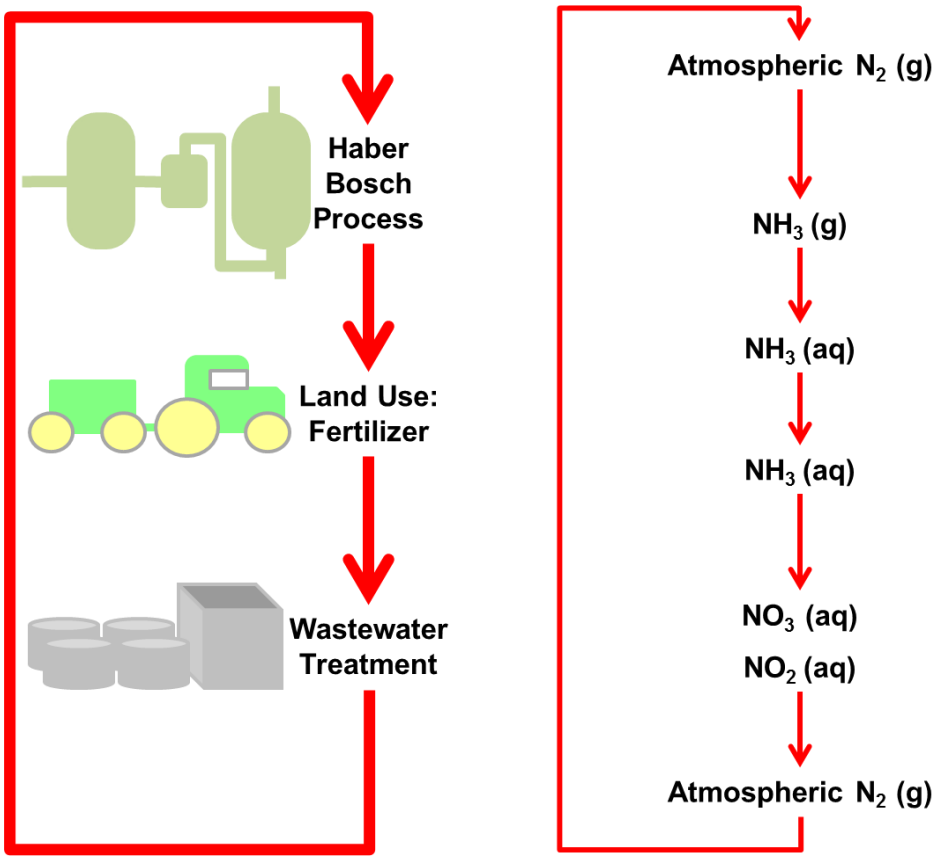

Figure 2-1: The cycle of nitrogen through wastewater treatment and the Haber Bosch process.

One of the major challenges for nutrient removal is that there are currently no economic incentives for nutrient recycling. Current financial models indicate that the cost of mined phosphate rock is lower than that of phosphate recovered from wastewater (Guest *et al.*, 2009). However, after review of the models, it was found that most models only accounted for internal cost of nutrient recovery neglecting the external environmental benefits such as reduced impact of nutrients on source waters. Once models were adjusted to include the environmental benefits

of nutrient recycling, nutrient recovery was found to be economically viable (Molinos-Senante *et al.*, 2010). Even with the support of financial modeling, more can be done to help make the process more economically viable. Use of technologies that require less energy and do not require specialized training can help reduce financial burden.

Wastewater contains a number of components other than nutrients that are valuable resources. Heat energy, carbon and water can all be recovered from wastewater adding further motivation to change treatment of wastewater to recovery (Ashley *et al*., 2011). Technologies which can capture the value added components of wastewater are slowly being implemented in wastewater treatment. One such technology includes anaerobic membrane bioreactors (AnMBR) which treat domestic wastewater without aeration, decreasing sludge production and operating costs, and producing an energy rich by-product in the form of methane biogas (Lew *et al*., 2009). The resultant AnMBR effluent is low in suspended solids and possesses a high nutrient concentration due to the limited biomass growth under anaerobic conditions. In a review of the AnMBR process, Smith *et al*. (2012) emphasized that technologies need to be employed for post-treatment to remove N and P to allow the discharge of the effluent without the risk of eutrophication.

Application of biological nutrient removal after AnMBR systems can be challenging due to insufficient quantities of chemical oxygen demand which are required by microorganisms (Smith *et al*., 2012). The gap in technology presents an opportunity for nutrient recovery processes. A nutrient recovery process exploiting microalgae to take up nutrients with the exhausted microalgae to be used in fertilizer for land application has been reported (Ruiz-Martinez *et al*., 2012). The system showed promising removal of nitrogen (67.2 %) and phosphorus (97.8 %); however, effluent nutrient concentrations fluctuated in correlation to influent concentrations that

ranged from 42.6 to 81.4 mg NH_3-N/L and 5.1 to 10.5 mg P/L. The system required pH adjustment, a source of uniform photosynthetically active radiation throughout the reactor, and the monitoring of additional variables for optimal nutrient removal that increased the operating costs for the system (Ruiz-Martinez *et al*., 2012).

A low cost, highly efficient treatment option of increasing interest for nutrient recovery is the process of adsorption. Adsorption technologies require little energy input and can be adapted to meet the needs of different wastewater treatment plants (Li *et al*., 2014; Long *et al*., 2011). Used in solid–liquid separation, adsorption is already known to be a useful technology and has been implemented in water and wastewater treatment plants worldwide (Crittenden *et al*., 2012). Currently, the limitation of adsorption lies with finding a sorbent which will be selective for phosphorus and nitrogen over other aqueous species and that under appropriate conditions will release targeted sorbates. A summary of the research that has been conducted in this area is presented in Section 2.4.

2.3 Adsorption Literature

At its essence, adsorption is the process of accumulating a material, called a sorbate, at an interface. Usually, the sorbent is a solid and the interface can lie between the solid and a liquid or gas (Crittenden *et al.*, 2012). For nutrient recovery in wastewater, the sorbent collects aqueous species from the wastewater onto its surface. The process of adsorption requires several transport steps to situate the sorbate in its final location where it will attach to the sorbent. A schematic of the adsorption process is shown in Figure 2-2. The first step of adsorption is the movement of the contaminant from the bulk solution to the outermost layer of the sorbent (Figure 2-2a); this layer is called the boundary layer. At the boundary layer, there is an envelope of stationary liquid that

the sorbate must pass through to enter the pores of the sorbent. The passage through the stationary liquid layer is driven by diffusion (Figure 2-2b). The final steps of adsorption involve the movement of the sorbate into the sorbent pores and attachment to the surface of the sorbate (Figure 2-2c) (Metcalf and Eddy, 2003).

In order for a sorbent to adsorb a sorbate, there must be a driving force for the movement of the sorbate into the pores. If a driving force is not present, the sorbate will not move into the sorbent and will not be adsorbed. Commonly the driving force in adsorption is a concentration gradient between the surface of the sorbent and the bulk solution, causing the sorbate to move into the pores of the sorbate (Thorton *et al*., 2007). Sorbent-sorbate interactions are dependent on the properties of the sorbent, sorbate, pH and presence of other species. To assist with determining the best sorbent(s) to be used for nutrient removal, the chemical species of nitrogen and phosphorus in wastewater was reviewed.

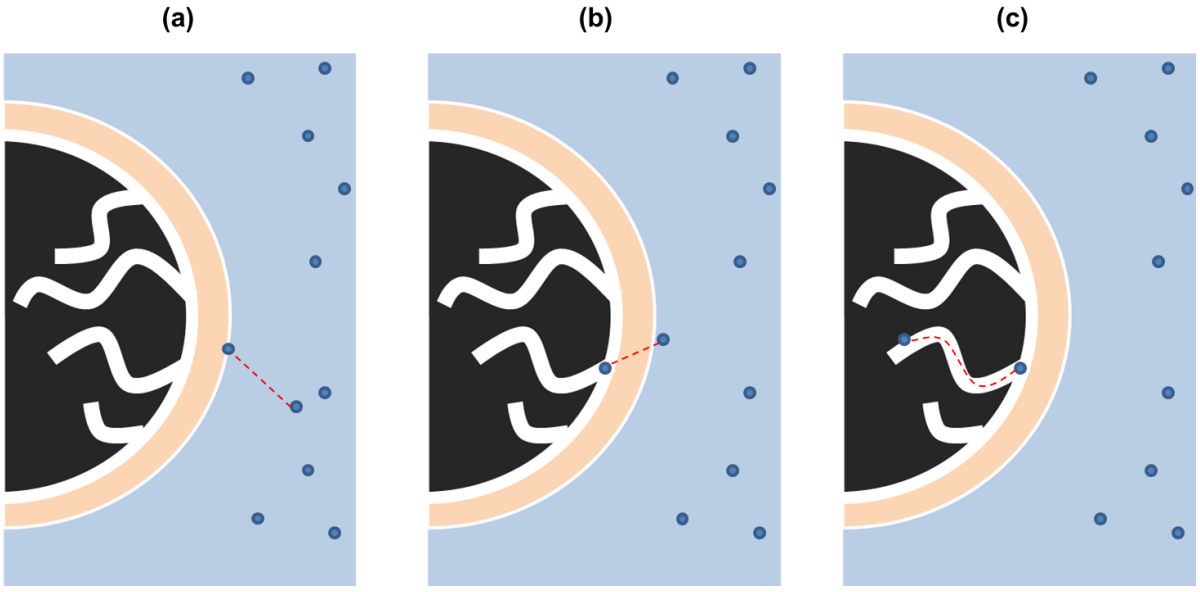

Figure 2-2: The process of adsorption of a sorbate (blue circle) onto a sorbent (black circle).

2.3.1 Nitrogen Speciation in Wastewater

Nitrogen in wastewater can come from a variety of sources including fertilizer run off, animal proteins and nitrogenous plant material. The total nitrogen (TN) in wastewater is made up of organic and inorganic fractions as shown in Figure 2-3a. The organic nitrogen fraction is made up of nitrogen in the form of amino acids, amino sugars and proteins which are long chains of amino acids. Inorganic nitrogen consists of total ammonia nitrogen (TAN), nitrate (NO_3^-) and nitrite (NO_2^-) (Metcalf and Eddy, 2003). Total ammonia nitrogen is the sum of the ammonium ion (NH_4^+) and the free ammonia (NH_3) species. The presence of either ammonium or ammonia in water is dependent on the pH of the solution. Figure 2-3b shows the distribution of the TAN species over pH which is established by the equilibrium reaction shown in Equation 2-1.

$$NH_4^+ \leftrightarrow NH_3 + H^+ \qquad pKa = 9.25 \qquad (2\text{-}1)$$

The pH of wastewater is typically 6.5 – 8.5, hence, ammonium is the dominant species (Metcalf and Eddy, 2003). Total ammonia nitrogen is one of the target sorbate species in this study; TAN recovered from wastewater will be a valuable added resource for fertilizer manufacturing.

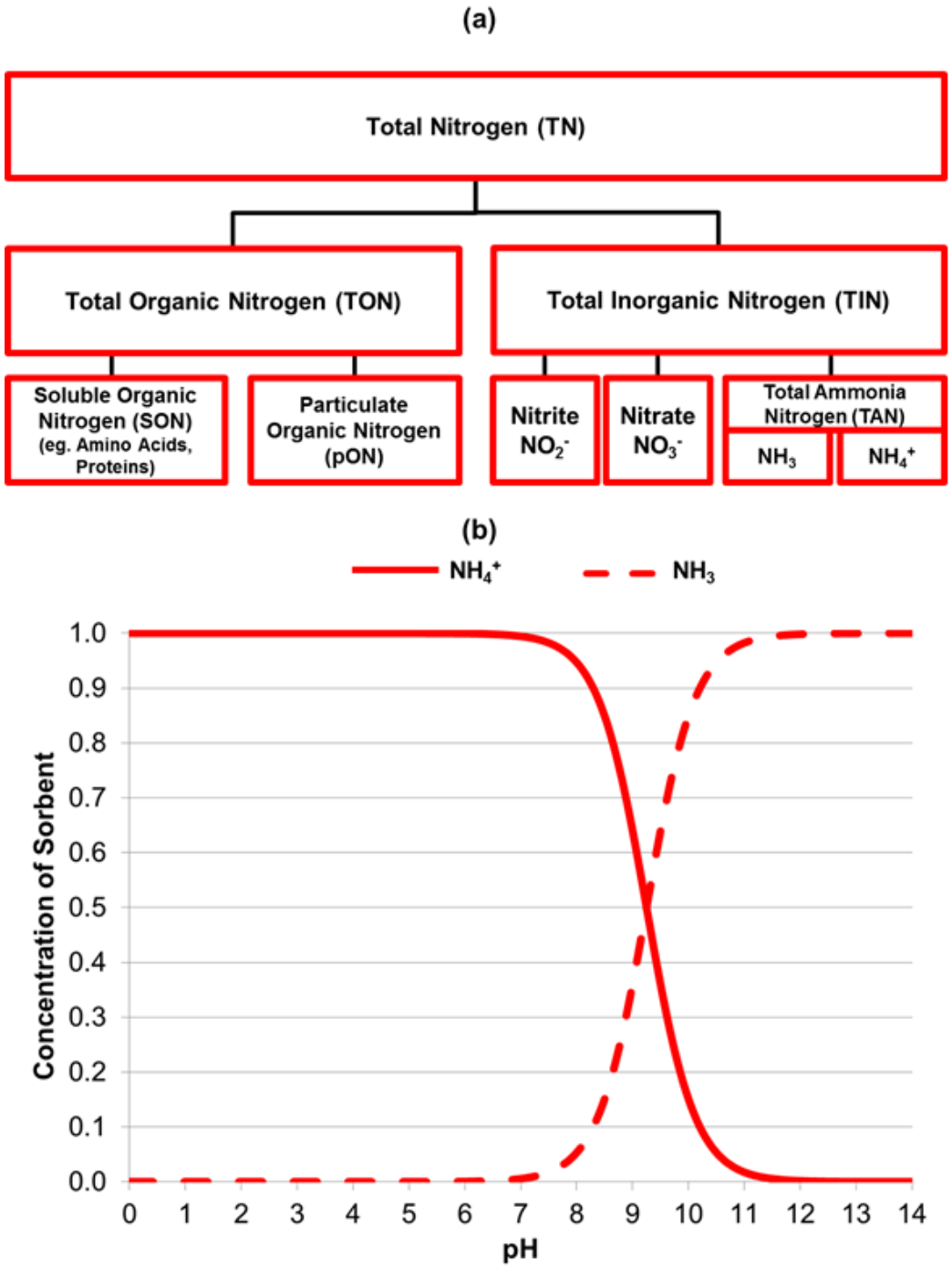

Figure 2-3: Classification of total nitrogen species (a) and the ammonium/ammonia distribution diagram (b).

2.3.2 Phosphorus Speciation in Wastewater

Total phosphorus in wastewater is also comprised of organic and inorganic species. Figure 2-4a shows the different phosphorus species that make up total phosphorus (TP). Total organic phosphorus (TOP) is made up of a variety of compounds including adenosine triphosphate (ATP), phospholipids and phosphonate (Maher and Woo, 1998). Inorganic phosphate consists of inorganic condensed phosphorus, mineral phosphorus and orthophosphate. Condensed and mineral phosphorus make up the fraction of phosphorus known as acid-hydrolyzable phosphorus (AHP) while orthophosphate is known as reactive phosphorus (RP). AHP and RP are phosphorus fractions determined by which analytical method is used for their detection. As with ammonia, orthophosphate (also referred to as phosphate) is present in water in various forms that are pH dependent. Figure 2-4b shows the relative amounts of phosphate in water with respect to pH range. The distribution diagram of phosphate was based on the following three equilibrium reactions:

$$H_3PO_4 \leftrightarrow H^+ + H_2PO_4^- \qquad pKa_1 = 2.15 \qquad (2\text{-}2)$$

$$H_2PO_4^- \leftrightarrow H^+ + HPO_4^{2-} \qquad pKa_2 = 7.20 \qquad (2\text{-}3)$$

$$HPO_4^{2-} \leftrightarrow H^+ + PO_4^{3-} \qquad pKa_3 = 12.33 \qquad (2\text{-}4)$$

In the pH range of 6.5 – 8.5, $H_2PO_4^-$ and HPO_4^{2-} are the dominant orthophosphate species. Although, phosphate is the target phosphorus sorbate species in this study, adsorption of soluble organic phosphorus (SOP) species should also be investigated due to the SOP fraction making up a large fraction of the residual TP after wastewater treatment (Gu *et al*., 2011). To achieve low levels of phosphorus, organic phosphorus (OP) must be removed and converted to orthophosphate to allow it to be readily available when recycled.

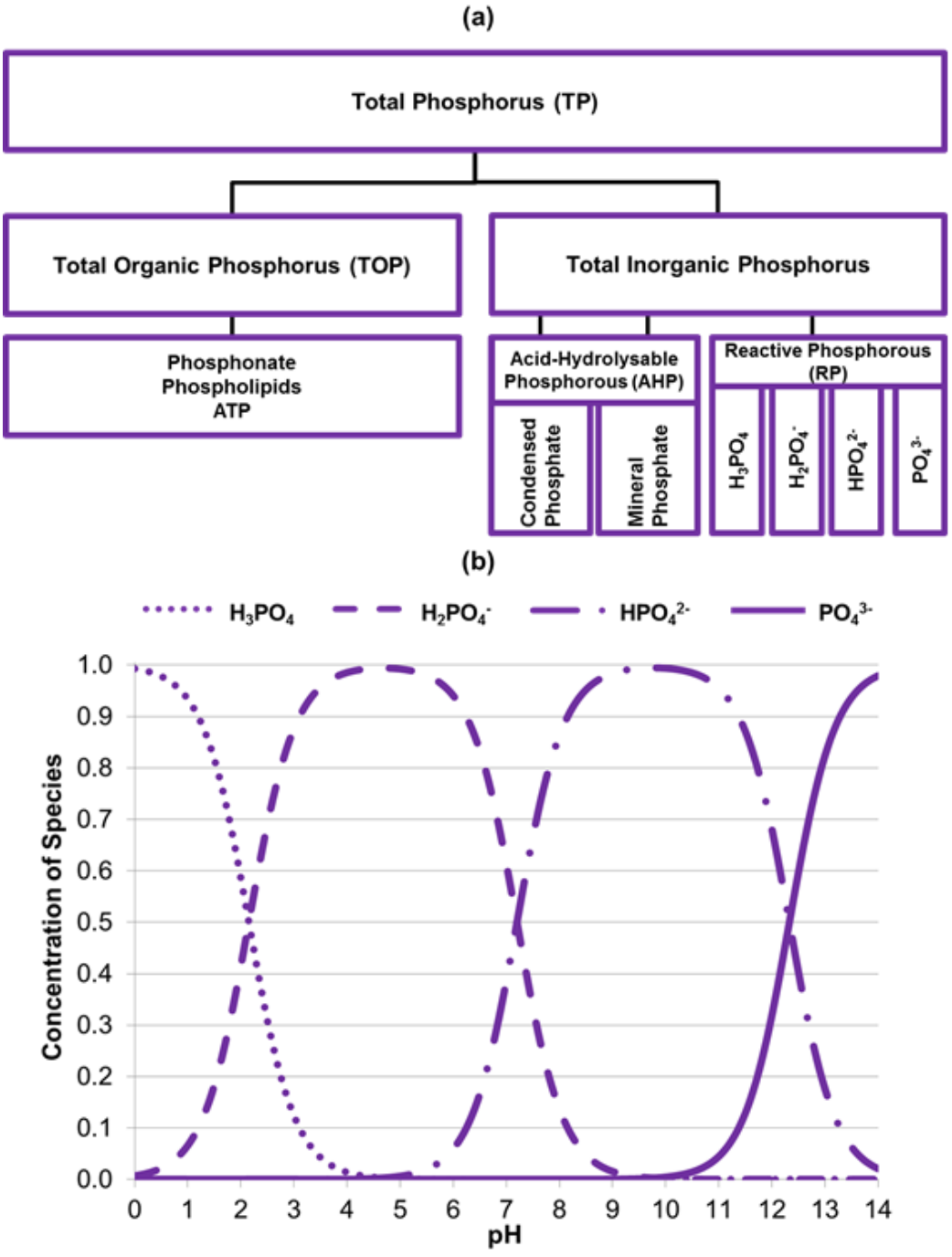

Figure 2-4: Classification of total phosphorus species (a) and the orthophosphate distribution diagram (b).

2.3.3 Characteristics of a Sorbent

When using adsorption to remove a specific target species, a good sorbent will be one that adsorbs large amounts of sorbate. The quantity of sorbate that a sorbent can adsorb is called the adsorption capacity. It is dependent on the physical and chemical attributes of the sorbent. The mass and type of sorbent in a system affects several important factors including the number of available sorption sites, adsorption capacity and selectivity of the sorption sites for the target sorbate (Crittenden *et al.*, 2012). A sorbent that is efficient in one application may not be appropriate to use in a different application. Sorbents are useful tools which can be used for a variety of different applications; however, sorbent characteristics must be reviewed and understood to determine the best sorbent to be used for nutrient recycling.

2.3.3.1. Physical Characteristics of Sorbents

The main physical characteristic that impacts the adsorption capacity of a sorbent is the surface area. Sorbents that have high surface areas have large surfaces for the sorbate to interact with, therefore giving a higher possibility of sorption (Ozacar *et al*., 2003). The surface area of a sorbent is dependent on the starting material used in its production. While small particles have a large surface area per unit mass a major contributor to surface area is the presence of porosity in the solids with large amounts of pores resulting in high surface areas (Crittenden *et al.*, 2012).

The International Union of Pure and Applied Chemistry (IUPAC) has defined three classifications of pore size; macropores have a pore diameter greater than 50 nm, mircopore diameters are less than 2 nm and the boundary diameter for mesopores fall between the mirco- and macropore sizes (IUPAC, 1982). While the presence of pores helps increase a surface area,

pore size can also limit the adsorption capacity based on the size of the target sorbate. If the sorbate of interest is larger than the pore diameter, it will be unable to diffuse into pore, thus reducing the accessible adsorption surface area (Schreier and Regalbuto, 2004). While a large surface area is required for a sorbent material, sorbent-sorbate attraction, which is dependent on the fundamental chemical composition of the sorbent, must also be considered (Mohan and Pittman, 2007).

2.3.3.2. Chemical Characteristics of Sorbents

A knowledge of the mechanism by which a sorbate is adsorbed onto the sorbent surface can help select the appropriate sorbent for use. Adsorption mechanisms can be categorized into physical or chemical sorption (Crittenden *et al.*, 2012). Physisorption is driven by physical attractions between the sorbent and the sorbate. The mechanisms behind physisorption are nonspecific and include binding in the form of van der Waal forces and electrostatic interactions (Breeuwsma and Lyklema, 1972; Crittenden *et al.*, 2012). The reaction between the sorbate and the sorbent surface is reversible and process speed is limited by mass transfer (Crittenden *et al.*, 2012). Physisorption is used widely in water treatment. It is observed in ion exchange and adsorption of contaminants onto activated carbon and some minerals (Jorgensen and Weatherley, 2003; Crittenden *et al.*, 2012). By contrast chemisorption leads to the forming of covalent bonds between the sorbate and the surface sites on the sorbent. In covalent bonding, electrons are shared or exchanged between the sorbent surface and the adsorbed species forming bonds that are considered irreversible. In chemisorption, the rate of adsorption is often dependent on the rate of the chemical reactions involved in forming the covalent bonds (Crittenden *et al.*, 2012; Su *et al.*, 2013).

The forces that drive adsorption are dependent on the reactive functional groups on the surface of the sorbent. These electrostatic forces lead to the attraction of the sorbate and can explain the selectivity of the surface. An important concept of adsorption onto sorbates is the zero point charge (pH_{ZPC}). The sorbent pH_{ZPC} is the pH value at which the surface of the sorbent has no overall charge (Shah *et al*., 1982). When the pH of the solution is below the pH_{ZPC}, the surface functional groups are protonated causing an overall positive charge of the sorbent. When solution pH is higher than pH_{ZPC}, the functional groups are deprotonated and the sorbent surface charge is negative. Surface charge of the sorbent is important characteristic due to the attraction between sorbents and sorbates when oppositely charged. If a sorbent and sorbate are similarly charged, the sorbate will be repelled by the sorbent.

2.3.3.3 Models for Adsorption Mechanism Determination

Tools are available to help determine the mechanisms that are active when a sorbate is adsorbed on the sorbate. Adsorption isotherms are models that relate the mass of sorbate accumulated onto a mass of sorbent to the liquid phase concentration at equilibrium. The nature of the adsorption model that is appropriate for a specific application is dependent on the type of sorbent surface (*i.e*. homo- or heterogeneous) in which adsorption is occurring and whether or not adsorption occurs in a mono- or multi-layer fashion (Metcalf and Eddy, 2003). In theory, the Langmuir isotherm describes a simple, ideal scenario in which monolayer adsorption of a sorbate occurs on a homogeneous surface. The Langmuir isotherm is derived from the equilibrium reaction where the sorbate (A) adsorbs to an empty site (S) on the surface of the sorbent to create an occupied surface site (SA). The equation for the Langmuir isotherm is shown in Equation 2-5. A linear form of the Langmuir isotherm is shown in Equation 2.6.

$$X = \frac{K_L Q_m C_e}{1 + K_L C_e} \quad (2\text{-}5)$$

$$\frac{C_e}{X} = \frac{1}{Q_m K_L} + \frac{C_e}{Q_m} \quad (2\text{-}6)$$

In the Langmuir equation, Ce is the concentration of the sorbate in the bulk solution at equilibrium (mg P/L), X is the amount of sorbate adsorbed per mass of sorbent (mg/g), Q_m is the equilibrium maximum adsorption capacity (MAC) expressed in mg/g and K_L is the binding constant with units of L/mg (Su *et al*., 2013).

When adsorption of the sorbate occurs on a heterogeneous surface and in multiple layers, the system is often modeled by the Freundlich isotherm. Equation 2-7 is the expression for the Freundlich equation, where K_F and N are fitting parameters called Freundlich adsorption constants. The linear form of the Freundlich is shown in Equation 2-8. A simplification of the Freundlich, when N is equal to 1, is known as the linear model (Metcalf and Eddy, 2003).

$$X = K_F C_e^{1/N} \quad (2\text{-}7)$$

$$\log X = \log K_F + \frac{1}{N} log\ C_e \quad (2\text{-}8)$$

2.3.3.4 Sorbents for Nutrient Recycling

Overall, the one characteristic that is necessary in a good sorbent is its capability to collect as much sorbate as possible. That being said, it should be recognized that the goal of nutrient recovery is to be able to collect nutrient for reuse in other applications. This objective highlights the need for sorbates to be recovered from the sorbent and possible sorbent reuse. Recovery of N

and P from the sorbent into a liquid concentrate can be important for different nutrient recycling technologies such as magnesium ammonium phosphate (MAP), also known as struvite (Rahman *et al*., 2014). Furthermore, when a sorbent can be used for multiple cycles it effectively has a much higher adsorption capacity and reduces cost because the sorbent needs to be replaced less frequently (Rodrigues *et al*., 2010).

Desorption of the sorbate from the sorbent is often dependent on how the sorbate was initially adsorbed. Since physisorption is due to electrostatic interactions and van der Waals forces, the process is considered reversible and often associated with easier desorption. Physisorption has some disadvantages, the major issue is dealing with competition for adsorption by other species (Crittenden *et al.*, 2012; Biswas *et al*., 2007). Competition will lead to a decrease in sorbent adsorption capacity that is undesirable if maximum quantities of sorbents are to be recovered. By nature physisorption is a non-selective process, adsorbing any opportunistic sorbates that happen to be attracted to the sorbent surface (Crittenden *et al.*, 2012). Wastewater is a complex matrix consisting of many aqueous species that could be potential sorbates. Therefore, having a sorbent which is highly selective is beneficial to recover target species.

Alternatively, chemisorption is more selective in the sorbent-sorbate interactions that occur; however, as previously mentioned, the bonds formed in the process are considered to be irreversible. Prior studies have been successful in determining chemisorption interactions which may be useful in water and wastewater treatment. In some cases, desorption of chemisorbed species can occur by manipulating the system conditions (*i.e.* pH adjustment). In cases where desorption cannot occur, another option is the use of the sorbent itself as a product for the fertilizer industry and can be evaluated for use in land application (Bellier *et al*., 2006).

2.4 Summary of Sorbent Research in Literature

The overall goal of this project is to find a good sorbent for nitrogen and phosphorus recycling. Understanding the advantages and disadvantages of the previously explored sorbents will help identify sorbents or reactions that are best for nutrient removal and recovery. A critical review of the literature will help pinpoint any advantages or disadvantages of choosing one sorbent composition, or mechanism, over another. The most logical starting point in investigating what will be a useful sorbent for nutrient removal is treatments which are well defined and frequently used. The review of the literature begins with conventional water and wastewater adsorption technologies.

2.4.1 Activated Carbon

One of the most widely used sorbents in conventional water treatment is activated carbon (AC). AC has been employed mainly to remove organic matter and heavy metals. It is an attractive sorbent because it is easily manufactured and can be manipulated to remove a variety of different contaminants (Mahmudov and Huang, 2011). To make AC, starting materials such as wood and coal are heated to temperatures around 700°C, creating a char which is then activated by exposure to gas (*e.g.* CO_2, steam) at temperatures between 800 - 900°C. The result of the process is a sorbent high in oxygenated functional groups and the formation of pores in the char which increases the surface area. Different activation methods can result in pore formation of different sizes (Metcalf and Eddy, 2003; Amano *et al.*, 2012). Although less common in wastewater treatment, AC has gained momentum in its use in advanced treatment (Metcalf and Eddy, 2003). Recently research groups have been investigating the use of AC to adsorb inorganic ions to establish if existing ACs are capable of removing phosphate and ammonium from wastewater.

Mahmudov and Huang (2011) investigated the adsorption of several oxyanions by commercially available granular activated carbon (GAC) Filtrasorb 400, sourced from Calgon Carbon. The results indicated that while the sorbents affinity for nitrate was fairly high (MAC of 0.29 mmol/g), very little phosphate was adsorbed (MAC of 0.10 mmol/g). Hussain *et al*. (2011) also used a commercial GAC product (Table 2-1) to test for phosphate adsorption and met with some success.

Hussain *et al*. found that the GAC was able to remove 70% of phosphate at pH 7 and an initial phosphate concentration of 20 mg P/L (Hussain *et al*., 2011). Previously Hussain *et al*. (2006) evaluated the same GAC for ammonia adsorption. The GAC was able to remove over 70% ammonia-nitrogen over the pH range of 2 – 13. Adsorption of aqueous ammonia by an unspecified commercial coconut based GAC was tested by Long *et al*. (2008) and the maximum adsorption capacity of the GAC was determined to be 17.19 mg/g. Hence, it is apparent that adsorption of different sorbates is dependent on the type of activated carbon used.

Table 2-1: Properties of GAC tested by Hussain *et al*. for phosphate and ammonia adsorption (Hussain *et al*., 2011; Hussain *et al*., 2006).

Ash Content (%)	> 5
Hardness	< 90
Moisture (%)	5
pH	9 – 10
Particle Size (mm)	0.65 – 2.36
Particle Density (kg/m^3)	1317

There has been some disagreement in the mechanism behind adsorption onto activated carbon. In most studies, the initial uptake onto the AC was fast, with the majority of adsorption occurring in

the first few minutes of treatment. This behaviour is usually indicative of physisorption (Long *et al*., 2008). Physisorption through electrostatic interactions and ion exchange is the mechanism for ammonium removal while phosphate removal studies have shown that the phosphate adsorption mechanism is actually a combination of specific chemical and electrostatic interactions (Mahmudov and Huang, 2011).

Researchers can agree, however, on the role that the surface functional groups have on adsorption. The surface of activated carbon is high in oxygenated functional groups that can be classified as either acidic or basic functional groups. Known surface functional groups of AC are shown in Figure 2-5. Studies have shown that ACs high in basic adsorption sites have higher phosphate adsorption due to the attraction of HPO_4^{2-} through hydrogen bonding. The acidic groups are negative therefore repelling the phosphate anion (Amano *et al*., 2012). Adsorption of the ammonium cation occurs on the acidic surface sites such as carbonyl or phenolic hydroxyl groups (Long *et al*., 2008).

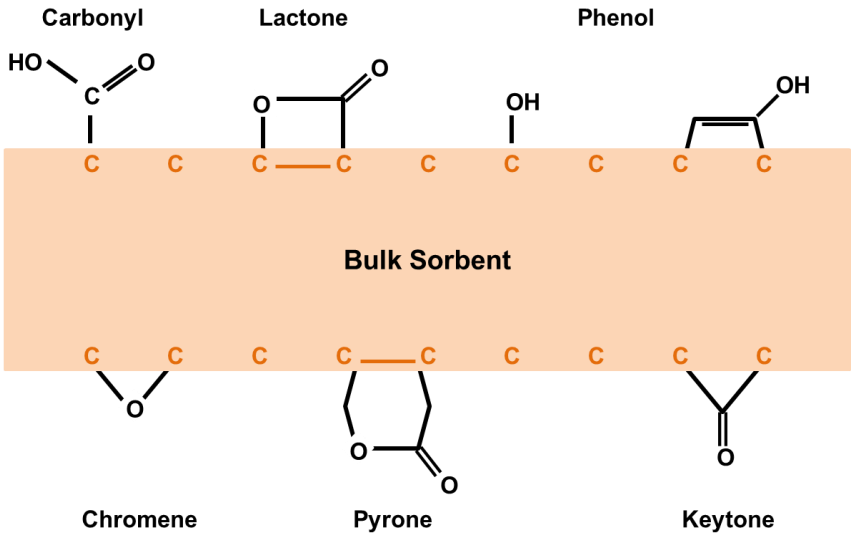

Figure 2-5: Surface functional groups of activated carbons (Long *et al*., 2008)

These functional groups also adsorb other ionic species potentially causing ammonium and phosphate adsorption to decrease in real waters due to competition effects. Prior studies have shown that competition increased in the presence of chloride, sulfate and nitrate ions, directly affecting phosphate adsorption (Mahmudov and Huang, 2011; Amano *et al*., 2012; Hussain *et al*., 2011). Another ion that decreases phosphate adsorption is hydroxyl (OH^-) ion. As pH increases the amount of phosphate adsorbed decreases due to the change in the surface charge of the AC (Amano *et al*., 2012). Hussain *et al*. (2011) saw a decrease in phosphate adsorption above pH 7 while Namasivayam and Sangeetha (2004) saw decreased phosphate adsorption at pH values higher than 11.

It is unclear which orthophosphate species adsorbs to AC. Amano *et al*. (2012) stated that it was understood that AC adsorbs both $H_2PO_4^-$ and HPO_4^{2-} equally, however upon further investigation Amano *et al*. discovered that AC adsorbs only small amounts of $H_2PO_4^-$. This could be dependent on the type of AC being used and the type of functional groups on the surface. The degree of phosphate protonation and the degree of surface charge is dependent on pH and should be monitored closely when using AC for treatment.

By comparison, ammonium adsorption had little dependence on pH. Ammonium removals of over 70% were observed over the pH range of 2 to 13 (Hussain *et al*., 2006). However, ammonium removal was dependent on temperature and initial concentrations of ammonium and activated carbon. Increased temperature enhanced ammonium removal, almost doubling the rate of uptake from 6.7 to 16.8 mg/g min by increasing temperature from 20 to 40°C (Long *et al*., 2008). Higher adsorption of ammonia also occurred with increasing initial concentrations of both GAC and sorbate. A larger initial does of sorbent leads to a decrease in capacity; however,

overall more ammonia is removed from solution due to the increase in sorbent surface area (Long *et al*., 2008).

The results of these studies have shown that while there has been some success with adsorption of phosphate and ammonia, the difficulty lies in finding the appropriate type of AC in terms of amount and type of functional groups. The ability of AC to remove different adsorbates is due to its surface properties, a characteristic easily manipulated by the organic matter and activation technique used to produce the AC. The process of activation can substantially alter the surface properties.

2.4.1.1 Surface Modification of Activated Carbon

There are different methods of activating activated carbon that can manipulate the formation of pores in the char. The pores can vary in size and number depending on the activation agents used (Crittenden *et al.*, 2012). The formation of pores increases the internal surface area of the sorbent which allows more surface for the exposed sorbate to bind. Different activation procedures can also select for the types (*i.e.* acidic or basic) of surface sites available for binding thereby affecting which species will be adsorbed to the surface (Amano *et al*., 2012). The following section summarizes research that studied the effects of activation procedures on phosphate adsorption.

From previous studies, it can be established that the qualities of activated carbon that encourage phosphate adsorption are a high surface area in which basic functional groups are predominant. The type of surface group can be altered by the choice of temperature in the final outgassing step during AC production (Amano *et al*., 2012). To demonstrate this, Amano *et al*. (2012) sourced a

wood based AC (Norit) which was de-ashed, oxidized using nitric acid and then outgassed while heated to a temperature in the range of 600 – 1000°C. Results from the study indicated that as outgassing temperature increased basic adsorption surface sites increased, thus maximizing the amount of phosphate adsorbed. There was little to no effect on AC surface area or pore size (Amano *et al*., 2012).

The number of basic functional groups on the surface of the activated carbon can also be manipulated by increasing the length of the activation process (Amano *et al*., 2012). This relationship was shown during research by Amano *et al*. on a coconut based AC (Calgon Carbon Japan). In the study, the AC was activated by heating (900°C) under the flow of CO_2 gas over time periods that varied from 0.5 to 2 hours. Overall, a 30-minute activation of the char caused the surface area to significantly increase from 14 to 756 m^2/g. Increasing the length of activation time from 30 minutes to 2 hours caused an even further increase in surface area and also improved total pore volume. The surface area changed from 756 to 1491 m^2/g while pore volume increased from 0.040 to 0.714 mL/g. Amano *et al*. discovered that phosphorus adsorption positively correlated with increasing surface area ($R^2 = 0.91$) and pore volume ($R^2 = 0.92$).

2.4.1.3 Activated Carbon for Nutrient Recovery

After a review of the literature, it can be seen that activated carbon has some challenges with its use with respect to nutrient recycling. One challenge is the low selectivity of AC for sorbates introducing competition between ions for the same surface sites. Wastewater is a complex matrix known to contain ions such as sodium, potassium and sulfate which may introduce competition

for adsorption sites thereby reducing adsorption. Another challenge that would have to be addressed to use AC is recovery of the nutrients after adsorption.

Current literature has not investigated if chemical treatment could be used to desorb nutrients from AC therefore it is unknown as to whether the adsorbed sorbate species could be recovered. Regeneration of the AC could also present a challenge. Currently AC is regenerated by reforming the char through pyrolysis – heating the AC to burn off any build up and regenerating the surface functional groups. In most cases, regeneration is rarely done because the adsorption capacity of AC has never been fully recovered (Crittenden *et al.*, 2012).

Use of exhausted AC for land application as a fertilizer is another gap in the literature. If the nutrients cannot be recovered, further study would be necessary to see if AC could work as a slow release fertilizer for land application. If the AC can be used for land application, the AC would have to be replaced regularly. Commercial activated carbons can be quite costly, therefore continuous replacement would not help reduce costs in wastewater treatment (Hussain *et al*., 2011; Hussain *et al*., 2006).

2.4.2 Natural Minerals of Sorbents

Natural materials with adsorbent qualities such as mineral and clays have been evaluated as potential sorbents. These materials typically require processing to make them ready for use as sorbents. For example, mined rock materials are crushed to increase surface area, rinsed, air dried and then sieved to separate the various sizes to increase uniformity (Bellier *et al*., 2006). Clay and mineral materials have been regarded as promising sorbents due to the surface functional groups available. The functional groups on the sorbent surface vary due to the

chemical composition of the various clay and mineral materials. Varieties include oxide minerals such as aluminum oxide, calcium carbonate and silica. (Altundoğan and Tümen, 2001). The various compositions of these materials can affect nutrient adsorption. Descriptions of the clay minerals can be found in Table 2-2. The following section reviews literature in which phosphate was the adsorbate. A summary of adsorption capacities and other experimental results of the natural clay minerals can be located in Table 2-3. Ammonium adsorption that can be achieved with a special class of sorbents (zeolites) is reviewed in Section 2.4.3.

Table 2-2: Characteristics of naturally sourced clay minerals.

Name	Formula	Description	Reference
Apatite	$Ca_{10}(PO_4)_6(X)_2$ (X = OH, F, Cl, Br)	- Structure consists of phosphate anions and calcium cations.	Cruz *et al*., 2005
Bauxite	NA	- Aluminosilicate - High in iron and aluminum oxides	Altundogan and Tumen, 2001
Bentonite	$Al_2O_3.4(SiO_2).H_2O$	- Also known as montmorillonite - Aluminosilicate - High in aluminum oxide	Sohrabnezhad *et al*., 2014
Calcite	$CaCO_3$	- Limestone has large % composition of calcite	Karageorgiou *et al*., 2007
Diatomite	NA	- Siliceous sedimentary rock - Typically 80 – 91% SiO_2 with alumina and ferric oxide	Xiong *et al*., 2008
Kaolinite	$Al_2Si_2O_5(OH)_4$	- Layered aluminosilicate mineral	Thompson and Cuff, 1985
Pyrrhotite	$Fe_{(1-x)}S$	- Iron sulfide mineral	Li *et al*., 2013
Quartz Sand	SiO_2	- Silicate mineral	Jiang *et al*., 2014
Vermiculite	NA	- Magnesium-aluminum-iron-silicate clay mineral - Expandable layers - 5 – 20% water between layers	Huang *et al*., 2014

Table 2-3: Summary of Clays and Minerals used for Phosphate Sorption from Wastewater Streams

Sorbent	Adsorption Capacity (mg P/g)	Adsorption Isotherm Model and Kinetics	Optimum pH Range	Surface Area (m^2/g)	Reference
Apatite	0.41	- Langmuir	NA	530	Bellier *et al*., 2006
Fluoroapatite	0.37	- Langmuir	NA	480	Bellier *et al*., 2006
Fluoroapatite	0.28	- Langmuir	NA	580	Bellier *et al*., 2006
Hydroxyapatite	0.31	- Langmuir	NA	720	Bellier *et al*., 2006
Hydroxyapatite	4.76	- Langmuir	- tested at pH 7	NA	Molle *et al.*, 2005
Bauxite	6.73	NA	3.2 – 5.5	NA	Altundogan and Tumen, 2001
Bauxite	0.61	- Langmuir	5.9	6.8	Drizo *et al.*, 1999
Bentonite	0.28	- Langmuir - Freundlich	8 – 10	85	Morharami and Jalali, 2013
Bentonite	0.5	NA	4 - 6	31.7	Yan *et al*., 2010
Calcium Rich Sepiolite	9.04 (pH 7)	- Langmuir - Freundlich	3 – 6	231	Yin *et al*., 2013
Calcite	1.82	NA	2 – 8	0.98	Morharami and Jalali, 2013
Calcite	19.0 (at pH 12)	NA	10.5 – 12	NA	Karageorgiou *et al*., 2007
Calcite (Limestone)	0.68	- Langmuir	7.8	7.4	Drizo *et al*., 1999
Calcite (Limestone)	1.09	- Langmuir Freundlich	NA	570	Bellier *et al*., 2006
Diatomite	10.2 (pH 4) 1.7 (pH 8.5)	- Langmuir - Freundlich	2 – 5	24.77	Xiong *et al*., 2008
Kaolinite	0.32	- Langmuir - Freundlich	2 – 4	3.66	Morharami and Jalali, 2013
Pyrrhotite	0.92	- Langmuir - Freundlich - Pseudo-Second Order	3.5 – 12.1	NA	Li *et al.*, 2013
Quartz Sand	0.17	- Langmuir - Pseudo-Second Order	NA	NA	Jiang *et al*., 2014
Vermiculite	2.65	- Langmuir - Freundlich - Pseudo-Second Order	NA	9.8	Huang *et al*., 2014

Investigations into the use of minerals and clays as sorbents have included the use of bentonite, sepiolite and quartz sand among others (Moharami and Jalali, 2013; Huang *et al*., 2014; Yin *et al.*, 2011; Jiang *et al*., 2014). Phosphate adsorption capacities reported in the literature using mineral and clays as sorbents varied greatly. Quartz sand had the lowest adsorption capacity for phosphate with an adsorption capacity of 0.17 mg P/g while calcite was the highest at 19 mg P/g (Jiang *et al*., 2014; Karageorgiou *et al*., 2007). Overall, mineral adsorbents displayed varied affinities for phosphorus adsorption, even in minerals of the same classification. An example of this variance is in the reported phosphate adsorption capacities reported for calcite (Table 2-3); Morharami and Jalali (2013) reported an MAC of 1.82 mg P/g while Karageorgiou *et al*. (2007) reported an MAC of 19 mg P/L. Similar differences in reported adsorption capacities can also be seen for bauxite, bentonite, hydroxyapatite and calcite (Table 2-3).

In addition to the adsorption affinities, mineral sorbents have been found to display various adsorption mechanisms. Jiang *et al*. (2014) stated that quartz sand displayed physical adsorption through electrostatic interaction or ion exchange. Bauxite was also determined to adsorb phosphate in this manner (Jiang *et al*., 2014; Altundoğan and Tümen, 2001). Ion exchange is the process that occurs when ions pre-existing in a material (called counterions) are replaced with different ions of the same charge entering the sorbent channels and pores. Materials that can take part in the ion exchange process usually have an overall negative or positive charge and counterions exist in the structure of the sorbent so electroneutrality is met (Crittenden *et al.*, 2012). In minerals the ion exchange occurs at the metal oxide surface sites. Aluminum oxides and zirconium oxides are examples of metal oxides known to participate in this mechanism (Tanada *et al*., 2003; Su *et al*., 2013).

Several mineral sorbents have been reported to adsorb phosphorus through adsorption driven by precipitation. Calcite, a mineral very high in calcium carbonate (98.2% $CaCO_3$), has been found to precipitate calcium phosphate (Karageorgiou *et al*., 2007). Upon addition to water, calcite forms hydrolysis products which have positive charges at pH values lower than 8.2 (8.2 is the zero point charge of calcite). At pH values lower than 8.2, physical adsorption occurs through electrostatic interactions between the negatively charged phosphate species and the positive surface sites achieving up to 75% phosphate removal and a sorbent loading of approximately 15 mg/g. However, upon closer inspection, calcite was found to perform better at pH values higher than the pH_{zpc}. At pH 12, calcite exhibited removal efficiencies reaching approximately 95% and the sorbent loading capacity reached 19 mg P/g. Enhanced adsorption with increased pH was counter intuitive. As pH increased, the overall negative charge of calcite would increase, repelling the negative phosphate ion. It was discovered that the adsorption of phosphate at high pH was due to the driving force of calcium phosphate (CaP) precipitating at the surface (Karageorgiou *et al*., 2007).

Apatite can also precipitate CaP; however, when several varieties were tested for phosphate removal, they were found to have MAPs much lower than calcite. The MAP ranged from 0.28 to 0.41 mg P/g for three igneous apatites (Bellier *et al*., 2006). The loading capacities reported for the igneous apatites were quite low when compared to other studies (2.7 – 4.8 mg P/g). This could be due to the igneous form of apatite having much lower porosity when compared to their sedimentary counter parts (Molle *et al*., 2005; Bellier *et al*., 2006). Overall, if phosphorus uptake can be optimized, precipitation of CaP is an advantage of some minerals. The mineral loaded with CaP can be marketed as a fertilizer (Bellier *et al*., 2006).

Despite the abovementioned deficiencies, minerals are widely available, inexpensive and have an affinity for phosphate adsorption making them attractive materials to use if adsorption capacities can be increased. As with activated carbon, natural minerals can be treated to change the properties of the mineral structure. Literature which employed surface modified natural minerals for phosphate removal are reviewed in the following section.

2.4.2.1 Surface Modification of Natural Mineral Sorbents

A method of enhancing nutrient adsorption in minerals is by modification of the chemical structure. Vermiculite is a layered magnesium-aluminum-iron silicate mineral that, when heated, results in water that is between the layers converting to steam to cause separation of the layers and cracks in the surface. The product of heating vermiculite is known as exfoliated or expanded vermiculite because the available surface area is increased drastically. The increase in surface area improves the ion exchange capacity of the clay mineral (Gordeeva *et al*., 2002). Expanding vermiculite can be produced at temperatures between 200 and 1000 °C. Evaporation of water occurs at temperatures at the lowest end of the temperature range while higher temperatures result in other changes stemming from the decomposition of chemical structure. While exfoliated vermiculite is normally used for metal adsorption, its adsorption properties have been evaluated for phosphate removal with limited success. The loading capacity of phosphate on the mineral was found to be 2.65 mg P/g (Huang *et al*., 2014).

Calcination is a form of modification in which heating leads to the partial decomposition of the chemical structure of the sorbent starting material; calcination involves the heating of Ca rich materials to temperatures up to 1000°C (López-Periago *et al*., 2013). The result of calcination

can be increased surface area or calcium content. Table 2-4 summarizes two studies in which calcination was used to improve phosphate adsorption. Ozacar *et al*. (2003) found that calcination of Alunite, an aluminum-potassium-sulfate mineral, led to increased surface area and increased adsorption capacity. Yin *et al*. (2013) used natural calcium rich sepiolite (CRS) to monitor the effects of calcination on phosphate uptake. The clay material was heated to a variety of temperatures within the range of 100 to 1000°C. Calcination temperatures of 500°C and below had little effect on P removal; however, temperatures exceeding 600°C increased P removal significantly with the highest loading capacity occurring with CRS calcinated at 900°C. The increase in phosphate adsorption was attributed to an increase in the CaO composition in the calcinated sorbent at higher calcination temperatures; in part, the adsorption mechanism of CRS is driven by CaP precipitation. Another effect of calcination was a change in the pH_{zpc} from 6.5 (unmodified) to 11.7 reducing the influence of pH. A high pH_{zpc} indicates that at circumneutral pH the charge of the surface of CRS is positive thereby attracting phosphate (Yin *et al*., 2013).

Table 2-4: Phosphate adsorption capacity and surface area with increasing calcination temperature and time.

Sorbent	Adsorption Capacity (mg/g)	Temperature (°C)	Time (Hrs)	Surface Area (m^2/g)	Calcium Composition (%)	
Ca-rich Sepiolite	9.04	--	2	231.1	22.3	Yin *et al*., 2013
	8	400		38.8	--	
	7.5	600		26.5	--	
	18.5	700		13.3	29.1	
	33.9	900		12.9	--	
	25	1000		7.15	33.7	
Alunite	9	--	1	29.2	--	Ozacar *et al*., 2003
	13	500		42.2	--	
	19	600		57.0	--	
	19	700		58.7	--	
	41.5	800		130	--	
	40	900		123	--	

Even though the enhancement of the mineral sorbents improved loading capacities, there are still several issues that need to be taken into consideration. The loading capacities reported for the calcinated and uncalcinated CRS were established in solutions where the initial phosphate concentration was very high (800 mg P/L) (Yin *et al*., 2013). When Yin *et al*. (2013) tested the CRS sorbents using lower initial phosphate concentrations, the loading capacity decreased drastically. In solutions containing 0.05 mg P/L, loading capacities ranged from 0.0018 to 0.0020 mg/g for uncalcinated and 900°C calcinated CRS, respectively. With typical wastewater influent concentrations being in the range of 4 to 16 mg P/L, lower loading capacity of the mineral sorbents may prove to be problematic (Metcalf and Eddy, 2003).

2.4.2.2 Natural Mineral Sorbents for Nutrient Recovery

From the literature reviewed it can be seen that while the naturally sourced mineral sorbents may be useful in areas where conventional wastewater infrastructure is limited or does not exist, issues may arise when used for nutrient recovery. One challenge with the use of natural mineral sorbents in nutrient recovery is the highly varied adsorption characteristics and the unpredictable nature of the sorbents. Natural minerals typically have impurities and imperfections that cause reduced adsorption capacity (Bellier *et al*., 2006).

There were gaps in the literature investigating natural minerals as sorbents for ammonia and phosphate. Competition effects on adsorption in the presence of other anions were not addressed by the literature. Reduced adsorption capacity due to competition could also present an obstacle in nutrient recovery as minerals and clays play acts as scavengers for cationic and anionic pollutants in nature (Moharami and Jalali, 2013). Desorption of phosphate from natural mineral

sorbents was also not investigated in literature. Reuse of sorbent would increase the overall adsorption capacity of the sorbents. The fate of the spent sorbent was also unclear in literature. In the case of CaP precipitating sorbents, it has been suggested that the spent sorbent can be land applied as fertilizer; however, few studies investigated the use of these materials as slow release fertilizers (Bellier *et al*., 2006).

2.4.3 Natural Zeolites

Substantial research has focused on a class of mineral that has excellent ion exchange capabilities. Natural zeolites are known to adsorb ammonia through cation exchange and have the benefits of other minerals such as low cost and high surface area. Natural zeolites are porous aluminosilicate materials that were first discovered in volcanogenic sedimentary rock and now can be found in zeolitic deposits around the world (Wang *et al*., 2010). There are several physiochemical characteristics that zeolites have that contribute to their utility as a sorbent material.

The aluminosilicate framework that comprises the foundation of zeolites imparts zeolites with a negative charge and the ability to exchange cations. The structure of the aluminosilicate framework can be found in Figure 2-6. Within the physical structure, the central silica atom (Si^{4+}) is substituted with an aluminum atom (Al^{3+}), leaving an overall negative charge (Wang *et al*., 2010). In natural zeolites, this substitution occurs during the formation of the material and the negative charge in the framework is balanced by the presence of mono- or divalent cations and water. The water molecules act as aqueous bridges binding atoms in the foundation to cations or bridging cations with additional cations (Wang *et al*., 2010). In addition, due to the

presence of channels in their structure, natural zeolites have large surface areas when compared to other mineral materials (Huo *et al*., 2012). The general chemical formula of zeolites is $M_{x/n}[Al_xSi_yO_{2(x+y)}]\cdot pH_2O$ where M can be Na, K, Li and/or Ca, Mg, Ba, Sr, n is the cation charge and y/x and p/x can range from 1 – 6 and 1 – 4, respectively (Wang *et al*., 2010). A collection of zeolites with corresponding chemical structures is presented in Table 2-5. Examples of chemical composition of different natural zeolites are in Table 2-6.

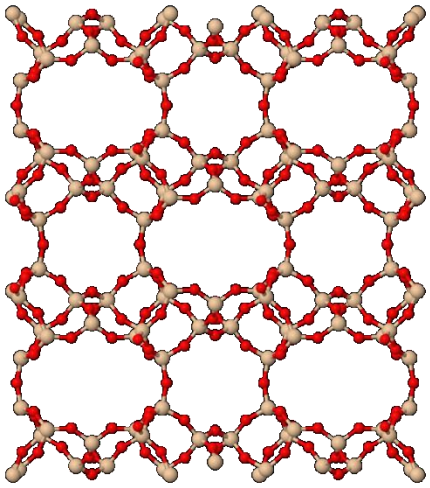

Figure 2-6: An example of the aluminosilicate framework of the zeolite clinoptilolite (Image from Mineralienatlas.de).

Table 2-5: Names of natural zeolites with corresponding chemical formula (adapted from Wang *et al*., 2010).

Name	**Chemical Formula**
Clinoptilolite	$(K_2, Na_2, Ca)_3Al_6Si_{30}O_{72}\cdot 21H_2O$
Mordenite	$(Na_2, Ca)_4Al_8Si_{40}O_{96}\cdot 28H_2O$
Chabazite	$(Ca, Na_2,K_2)2Al_4Si_8O_{24}\cdot 12H_2O$
Phillipsite	$K_2(Ca, Na_2)2Al_8Si_{10}O_{32}\cdot 12H_2O$
Scolecite	$Ca_4Al_8Si_{12}O_{40}\cdot 12H_2O$
Stilbite	$Na_2Ca_4Al_{10}Si_{26}O_{72}\cdot 30H_2O$
Analcime	$Na_{16}Al_{16}Si_{32}O_{96}\cdot 16H_2O$
Laumontite	$Ca_4Al_8S_{16}O_{48}\cdot 16H_2O$
Erionite	$(Na_2K_2MgCa_{1.5})_4Al_8Si_{28}O_{72}\cdot 28H_2O$
Ferrierite	$(Na_2, K_2, Ca, Mg)_3Al_6Si_{30}O_{72}\cdot 20H_2O$

Table 2-6: Chemical composition of reviewed zeolites.

	Natural Zeolites							
Constituent	Clinoptilolite (Turkish)	Clinoptilolite (Chinese)	Chende	Zeolite C	Clinoptilolite (Japanese)	Zeolite (Chabizite base)	Clinoptilolite (Iranian)	Zeolite (Chilean)
SiO_2	74.4	65.52	71.53	51.80	77.96	68.10	78.3	67
Al_2O_3	11.5	9.89	13.65	18.34	14.02	18.59	11.7	13
Fe_2O_3	1.1	1.04	2.82	3.40	1.30	2.84	0.51	2.0
TiO_2	0.1	0.21	0.28	--	--	--	0.018	0.2
MnO_2	< 0.001	--	--	--	--	--	--	--
MnO	--	0.61	0.05	--	--	--	--	0.04
MgO	0.5	0.61	1.61	0.96	0.46	0.75	--	0.69
CaO	2.0	3.17	1.89	4.73	1.23	0.27	0.23	3.20
BaO	--	--	--	0.35	--	--	--	--
SrO	--	--	--	0.04	--	--	0.97	2.60
Na_2O	0.6	2.31	1.86	0.60	1.15	8.32	3.2	0.45
K_2O	5.0	0.88	4.14	4.91	3.88	1.12	5.5	0.05
P_2O_5	0.02	--	--	--	--	--	--	--
H_2O	--	7.25	--	--	--	--	--	--
CuO	--	--	--	--	--	--	0.24	--
ZrO_2	--	--	--	--	--	--	0.038	--
SO_3	--	--	--	--	--	--	0.12	--
Loss on Ignition	5.85	10.02	5.60	15.14	--	--	--	--
Reference	Karadag *et al*., 2006	Wang *et al*., 2008; Du *et al*., 2005	Huang *et al*., 2010	Karapinar *et al*., 2009	Jha and Hayashi, 2009	Cyrus and Reddy, 2011	Ashrafizadeh *et al*., 2008	Englert and Rubio, 2005

Natural zeolites have been used to exchange ammonia in aquatic systems. A summary of research studies employing natural zeolites for ammonium uptake can be found in Table 2-7. Ammonium adsorption onto natural zeolites has been investigated in depth. In a review by Wang *et al*. (2010), it was reported that natural zeolites have a wide range of ammonia exchange capacities (AECs) ranging from 2.7 to 30.6 mg/g. Investigations into the effects of initial ammonium concentration on AEC and the mechanisms behind ammonium adsorption have indicated that the AEC increased with increasing initial ammonium concentration. This was attributed to the larger concentration gradient between the bulk liquid and the surface of the zeolite (Karadag *et al*., 2006).

When monitoring the effects of contact time, Karadag *et al*. (2006) discovered that 70% of total ammonia uptake was within the first ten minutes of contact. In the first few minutes, diffusion was fast onto the surface of the zeolite. After the first 10 minutes, ammonium uptake was slow and the system reached equilibrium at 40 minutes. The system was slow to reach equilibrium due to slow diffusion of ammonium into the pores of the zeolite. Fast initial uptake of ammonium followed by a slow progression to equilibrium by natural zeolites has been witnessed in other studies (Cyrus and Reddy, 2011; Karapinar *et al*., 2009; Du *et al*., 2005).

The effects of temperature, pH and sorbent dosage on ammonium uptake into the zeolite have been reported. Karadag *et al*. (2006) found that increasing operation temperature caused the rate of ammonium uptake as well as AEC to decrease. The fact that ammonium removal via zeolite worked better under lower temperatures may prove attractive for treatment processes in colder climates. Karadag *et al*. did not test their system at temperatures lower than 25°C, therefore further investigation is necessary.

Table 2-7: Summary of Natural Zeolites used for Ammonia Sorption in Wastewater Streams.

Sorbent	Adsorption Capacity (mg/g)	Adsorption Isotherm Model and Kinetics	Cation Exchange Capacity (CEC) (meq/g)	Bulk Density (kg/m^3)	Particle Size (mm)	Reference
Clinoptilolite (Turkish)	8.121 (25°C) 6.149 (40°C) 5.166 (55°C)	- Langmuir - Pseudo-Second Order - Intraparticle Diffusion	0.95 – 1.4	900 - 1100	1.0 – 1.4	Karadag *et al*., 2006
Zeolite C	23[1]	NA	235[1]	NA	< 0.06	Karapinar *et al*., 2009
Zeolite (Chabizite base)	10.84	- Langmuir	2.50	1.73	< 0.001	Cyrus and Reddy, 2011
Clinoptilolite (Chinese)	21.67[2]	- Langmuir[3] - Freundlich[4]	1.03	NA	0.45 – 0.90[4]	[3]Wang *et al*., 2008; [4]Du *et al*., 2005
Clinoptilolite (Chinese)	3.05	- Langmuir - Freundlich	NA	NA	0.45 – 0.9	Wang *et al*., 2006
Clinoptilolite	22.5	- Langmuir	NA	NA	NA	Jorgensen and Weatherly, 2003
Clinoptilolite (Japanese)	16.02	- Langmuir	2.16	NA	< 0.10	Jha and Hayashi, 2009
Zeolite (New Zealand)	20.1	NA	0.878 – 1.13	NA	$\leq$ 2.0	Bolan *et al*., 2003
Clinoptilolite 1	10.47	- Langmuir	0.93	0.982	< 2.0	Bernal and Lopez-Real, 1993
Clinoptilolite 2	13.65	- Langmuir	1.02	0.796	< 2.0	Bernal and Lopez-Real, 1993
Clinoptilolite 3	19.50	- Langmuir	1.396	0.858	< 2.0	Bernal and Lopez-Real, 1993
Clinoptilolite 4	16.52	- Langmuir	1.50	0.561	< 2.0	Bernal and Lopez-Real, 1993
Chilean Zeolite (Clinoptilolite and Mordenite)	11.4 – 14.8	- Langmuir	2.05	NA	0.013	Englert and Rubio, 2005
Clinoptilolite (Iranian)	17.8[5]	- Langmuir - Freundlich	NA	960	1 – 2	Ashrafizadeh *et al*., 2008

[1]$[NH_4^+]_o$=20 mg/L and sorbent dose = 0.5 g/L (Karapinar *et al*., 2009),[2]Optimum pH: 6 (Du *et al*., 2005).[5]$[NH_4^+]_o$ = 50 mg/L

Ion exchange capacity is also dependent on the range of pH used during treatment. The species present in solution and the charge associated with them are dependent on pH (Metcalf and Eddy, 2003). An optimum operating pH of 6 was determined by Du *et al*. for ammonium adsorption onto a Chinese clinoptilolite. At lower pH values, ammonium ions had to compete for binding sites with H+ ions, decreasing removal efficiency. Increased uptake at pH 6 could also be attributed to the removal of impurities in the natural zeolite (*i.e.* calcium carbonate), thereby increasing available surface area (Du *et al*., 2005). The effect of zeolite dosage was investigated by Karapinar *et al*. (2009) on ammonium uptake and AEC, a relationship that had not been addressed in many other studies. Karapinar observed that ammonium uptake increased and AEC decreased with higher amounts of zeolite. The optimal dose of zeolite was found to be 8 g/L for solutions containing initial ammonia concentrations of 10 to 40 mg/L. This would translate to a large mass of sorbent in a municipal wastewater treatment setting.

The impact of competition on adsorption to natural zeolites has been investigated. Malovanyy *et al*. (2013) studied the effects of K^+, Ca^{2+}, Na^+ and Mg^{2+} on the ammonium exchange capacity of a natural zeolite. In the presence of the additional ions, the AEC of the natural zeolite decreased to 6.8 mg/g from 10.8 mg/g (Malovanyy *et al*., 2013). Huang *et al*. (2010) studied the removal of ammonium from aqueous solutions through use of a Chinese natural zeolite. The research group monitored the effects cations and anions on an individual basis such that a relationship could be established between the presence of each species and NH_4^+ uptake. For each species, increased cation concentration led to a decreased AEC by the zeolite. Sodium had the largest effect, and the ranking of cations in order of competitive effect was $Na^+ > Mg^{2+} > Ca^{2+} > K^+$. The presence of anions in solution also adversely affected ammonium uptake. Having carbonate in solution caused the largest decrease in AEC, reducing removal efficiency by over 24%. The presence of

the other anionic species had much smaller influences on AEC. Removal efficiencies decreased by 6, 12 and 13.8% in the presence of chloride, sulfate and phosphate, respectively (Huang *et al*., 2010).

Ion exchange can also result in organic matter removal, and hence questions arise as to whether there would be competition effects between organic matter and ammonium uptake by natural zeolites. Jorgensen and Weatherley (2003) evaluated the impact of the presence of organic matter on ammonia adsorption onto the natural zeolite clinoptilolite. In the study, the change in maximum ion exchange was assessed when organic matter was present (*i.e*. proteins and citric acid). Jorgensen and Weatherley observed enhanced NH_4^+ adsorption at lower initial ammonium concentrations and 31 % decrease in maximum NH_4^+ capacities in the presence of organic matter.

Desorption of ammonia and zeolite regeneration has been the subject of several investigations involving natural zeolites. There are a variety of methods that can be used to regenerate expended zeolites. These methods include regeneration via acid or base solution, salt solution and heating (Li *et al*., 20111). Bolan *et al*. (2003) used 0.5 M HCl to regenerate natural zeolites from New Zealand and found that the acid released both NH_4^+ and other cations taken up by the zeolite. Bolan *et al.* were able to regenerate the natural zeolite for over twelve cycles without greatly affecting the AEC of the zeolite. Du *et al*. used a sodium chloride solution at a pH of 11 – 12 to regenerate a natural clinoptilolite. The NaCl solution concentration was 0.5 M and the pH was adjusted using NaOH. It was concluded that the ammonia removal capacity of the clinoptilolite remained constant after the second and third regeneration cycles but did not present the data collected from those runs (Du *et al*., 2005).

Overall, it has been observed that the regeneration technique can greatly affect the adsorption capacity of the zeolite. Li *et al*. (2011) evaluated three different regeneration techniques to determine which would be best to use on clinoptilolite. It was concluded that an NaCl salt solution was the best to use for regeneration, leading to practically no change in AEC. Zeolite regenerated by heat treatment (200°C, 4 hr) had the lowest ammonium capacity after regeneration, followed by acid regeneration (1.0 M HCl). Cyrus and Reddy (2011) also had mixed success when using an acid regeneration technique for the natural zeolites used to treat swine wastewater. Cyrus and Reddy found that the expended natural zeolite could be regenerated with 0.1N HCl; however, results of full regeneration of the column and testing of the regenerated zeolite were not reported. The regeneration results that were reported by Cyrus and Reddy showed that ammonia release from the zeolite was slow, only releasing up to 10 mg/L within the first 50 hours. The zeolite continued to desorb ammonium over 150 hours. Due to these results, Cyrus and Reddy suggested that the natural zeolites are promising for use as nitrogen slow release fertilizers. The HCl concentration used a close proxy to the ammonium concentration that would be present in acidic soils, leading to the slow release of ammonia.

2.4.3.1 Natural Zeolites for Nutrient Recovery

There are some challenges associated with the use of natural zeolites for nutrient adsorption. One challenge is the lower adsorption capacities of the zeolites. Ammonium exchange by natural zeolites can only occupy 6.8 - 52% of the potential maximum cation exchange capacity (Bolan *et al*., 2003). Cation exchange capacity can vary greatly between zeolites of same and different classifications (Wang *et al*., 2010). The lower adsorption capacities highlight another challenge with the use of natural zeolites – the production of a large quantity of solid waste if used in large

scale plants. It has been shown that when used in wastewater applications, the AEC of natural zeolites lie within the range of 0.2 – 0.68 meq/g, this corresponds to less than 1% nitrogen in the content of the spent zeolite (Malovanyy *et al*., 2013). One final challenge in zeolite use is that zeolites could also be cost prohibitive due to the cost of mining and transportation of the zeolite as well as cost of disposal of spent zeolite or transportation for land application (Malovanyy *et al*., 2013).

There are also some issues that have not been addressed in literature. Regeneration of zeolites have been studied; however, characterization of the desorbed solutions have not been investigated. Zeolites are known to exchange other ions (*i.e.* free metal ions) which could be introduced into the desorbed solution and potentially cause adverse effects when using nutrient recovery technologies (Wang *et al*., 2008). Another gap in the literature includes the fate of exhausted zeolites. The potential for land application use of the spent sorbent should be investigated.

2.4.4 Engineered Ion Exchange Resins

The ion exchange mechanism is a promising method for ammonium adsorption from wastewater. Ion exchange provides excellent response to shock loading of systems and if ion exchange capacities are maximized, an excellent source for ammonium recovery. Attention has also turned to engineered ion exchange resins due to their ability to have high reaction rates as well as increased reactive site availability for incoming sorbates (Thorton *et al*., 2007). Since engineered resins are manufactured, the framework of the resin can be produced in a way that has minimal impurities and inconsistencies, maximizing the capacity of the resin. Organic resins are also

being implemented in ion exchange due to their resistance to chemical change (Thorton *et al*., 2007; Jorgensen and Weatherly, 2003). Table 2-8 summarizes studies that have used ion exchange resins for ammonium and phosphate removal.

Ion exchange for ammonium removal is used often in the aquaculture industry since ammonia is toxic to aquatic species and water is recirculated throughout the system (Jorgensen and Weatherley, 2003). Jorgensen and Weatherley (2003) tested two polymeric exchangers, Dowex 50w-x8 and Purolite MN500, for their ability to exchange ammonium. The results obtained from ammonium uptake showed that the two polymeric resins had ammonium capacities higher than that of clinoptilolite. The MACs for Dowex 50w-x8, Purolite MN500 and clinoptilolite were approximately 38, 25 and 22.5 mg/ g, respectively. Jorgensen and Weatherly discovered that Purolite MN500 was also selective to ammonia over sodium ions, an ability that could prove to be useful in saline environments. In a separate study it was observed that the presence of calcium, magnesium, sodium and potassium cause the AEC of MesoLite and KU – 2 – 8 to decrease by 30 and 70 %, respectively. Optimum pH for ammonia uptake by anion exchange resins varied between 5.9 and 7 (Thorton *et al*., 2007).

Engineered ion exchange resins can also be used for anion exchange and research has investigated their use for phosphate removal. A weak base exchanger was found to work very well for phosphorus exchange. At optimum pH, the ion exchange resin had a loading capacity of 153 mg P/g (Awual and Jyo, 2011). The weak base exchanger was found to work better at low pH experiencing less adsorption as pH became more basic. While anion exchange resins may select the target sorbate over other ions in solution, overall adsorption was found to decrease up to 17 % due to competition (Awual and Jyo, 2011).

Table 2-8: Summary of Engineered Ion Exchange Resins used for Sorption in Wastewater Streams

Sorbent	Sorbate	Resin Type	Adsorption Capacity (mg sorbate/g)	Adsorption Isotherm Model	Optimum pH Range	Desorption	Reference
Dowex 50w-x8	NH_4^+	Strong Acid Cation	38	NA	NA	NA	Jorgensen and Weatherly, 2003
Purolite MN500	NH_4^+	Strong Acid Cation	25	NA	NA	NA	Jorgensen and Weatherly, 2003
MesoLite	NH_4^+	Cation	49	- Langmuir	6 – 7	NA	Thorton *et al*., 2007
Purolite C104	NH_4^+	Weak Acid Cation	21.9	- Thomas Model	-tested at 9.12	0.51 M NaCl	Malovanyy *et al*., 2013
KU – 2 – 8	NH_4^+	Strong Acid Cation	74.1	- Thomas Model	5.9	0.17 M HCl	Malovanyy *et al*., 2013
INDION 225 Na	NH_4^+	Strong Acid Cation	16.14	- Langmuir	NA	NA	Bashir *et al*., 2010
Diaion WA20	PO_4^{3-}-P	Weak Base Anion	153.45 – 43.09	NA	2 – 3	1 – 2 M HCl	Awual and Jyo, 2011
Diaion SA10A	PO_4^{3-}-P	Strong Base Anion	52.7 – 12.09	NA	3 – 7	1 – 2 M HCl	Awual and Jyo, 2011
Purolite Ferrix A33E	PO_4^{3-}-P	Strong Base Hybrid Exchange Resin	48	- Langmuir	NA	2% NaOH 2% NaCl	Nur *et al*., 2013
Amberlite IRA – 900	PO_4^{3-}-P	Strong Base Hybrid Exchange Resin	2.4[1]	NA	6 – 8	2% NaOH 2% NaCl	Blaney *et al*., 2007
LayneRT	PO_4^{3-}-P	Strong Base Hybrid Exchange Resin	9.54	- Langmuir - Freundlich	NA	NA	Sendrowski and Boyer, 2013
LayneRT	PO_4^{3-}-P	Strong Base Hybrid Exchange Resin	1.49 – 10.1	- Freundlich	NA	2% NaOH 2.5% NaCl	O'Neal and Boyer, 2013
LayneRT	PO_4^{3-}-P	Strong Base Hybrid Exchange Resin	7.68	NA	NA	4% NaOH 2% NaCl	Martin *et al*., 2009

[1]Experiments completed at $[PO_4^{3-}]_o$= 0.2 mg P/L

Other anion exchange resins have been used in conjunction with metal oxides creating what is called a hybrid anion exchange and reporting reasonable phosphate adsorption. One study reported a MAC of 48 mg P/g (Nur *et al*., 2013). Use of the hybrid anion exchange resin reduced the competition effects on phosphate adsorption due to the other ions competing for different bonding sites. The mechanism of phosphate adsorption in a hybrid anion exchange was reported to result from precipitation of phosphate with the iron oxide functional groups (Blaney *et al*., 2007). The optimum working pH for the hybrid anion exchange resins were found to be between 6 and 8 (Blaney *et al*., 2007).

Desorption has also been studied in depth using ion exchange resins and many different methods have been used to regenerate the resins. Cationic exchange resins have a high affinity for H^+ ions and can be regenerated using acidic solutions (Malovanyy *et al*., 2013). Hybrid ion exchange resins can desorb phosphate using a 2% NaOH and 2% NaCl solution. Studies reported no change in adsorption capacity after three consecutive regeneration cycles, recovering over 90% adsorbed phosphate (Blaney *et al.*, 2007; Nur *et al*., 2013). The weak base ion exchange resin was easily regenerated using 1M HCl to desorb the phosphate on the resin and the NaOH rinse returned the resin to the hydroxyl form (Awual and Jyo, 2011). The weak base ion exchange resin was able to be regenerated several times, recovering over 95% of phosphate in each cycle.

2.4.4.1 Engineered Ion Exchange Resins for Nutrient Recovery

There are challenges in the use of ion exchange resins including competition effects and optimal working pH ranges. Competition effects arise due to the ion exchange resin being non-selective for the sorbate of focus thus decreasing adsorption capacity. Decreased adsorption capacity could

also be seen at pH values which are not optimal for phosphate or ammonium exchange. While ammonium exchange can occur around neutral pH, phosphate exchange via anion exchange resins is highest at low pH, adding in a costly pH adjustment step. Investigation into overcoming these challenges in addition to the high adsorption capacities and easy regeneration of engineered ion exchange resins make them good candidates for use in nutrient removal/recovery. Additionally, the ability of ion exchange resins to adsorb quickly and handle shock loads make them attractive for use in a large-scale wastewater treatment plant.

2.4.5 Metal Oxides as Sorbents

Studies of natural mineral sorbents have demonstrated the ability of metal oxide functional groups to adsorb phosphorus. As mentioned previously, inconsistencies in the structure and impurities found in natural minerals cause decreased adsorption capacities when used as sorbents. Metal oxides can be synthesized easily in higher purity and consistency and this has allowed deeper study of their effectiveness as sorbents and better understanding of interactions between sorbate species and the metal oxides (Deliyanni *et al*., 2007). One of the benefits of engineering metal oxides is the control that can be exhibited during development. Manufacturing conditions can be manipulated in a way that during the formation, the metal oxide growth process can be halted at a stage where the metal oxide has a fully developed crystalline structure but is extremely small. These extremely small metal oxides are usually less than 100 nm one dimension classifying them as nanoparticles (Su *et al*., 2013). Nanoparticles are very attractive for use as sorbents since they can have very specific surface properties that can be highly specific, efficient and cost effective (Qu *et al*., 2013).

The mechanism of phosphorus adsorption on metal oxides is dependent on the metal oxide present. When iron and/or magnesium are present the predominant mechanism of phosphate adsorption is surface complexation (Kumar *et al*., 2014a; Tanada *et al*., 2003). In surface complexation, phosphate forms bonds on the surface of the metal oxide creating an inner sphere complex as shown in Figure 2-7. Phosphate can form bonds at the surface in a mono- or bi-dentate formation where bidentate are stronger than monodentate complexes because they involve the formation of two bonds (Li and Stanforth, 2000). In the case of aluminum or zirconium metal oxides, phosphate adsorption through ion exchange is usually due to the phosphate anion exchanging with the hydroxyl group on the surface of the iron oxide forming an outer sphere complex (Blaney *et al*., 2007; Tanada *et al*., 2003).

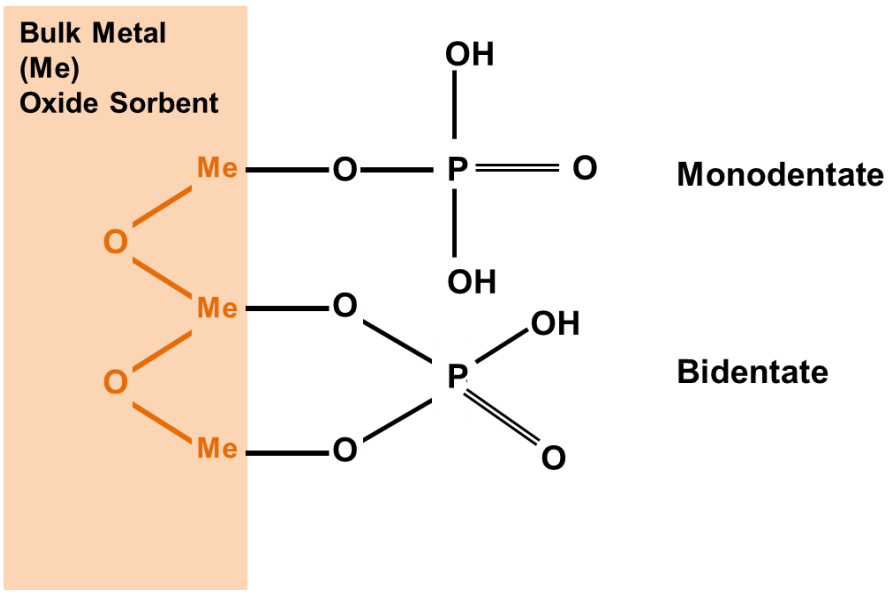

Figure 2-7: Monodentate and bidentate inner sphere complexes formed between phosphate and the metal oxide surface (adapted from Blaney *et al*., 2007).

A summary of studies that have used metal oxides for phosphate adsorption is presented in Table 2-9. Several types of iron oxide have been studied for adsorption of phosphorus from water. The surface complexation reaction between phosphorus and iron hydr(oxide) has been well studied and applied to phosphorus removal in wastewater. The adsorption and precipitation of phosphate with iron oxides is the foundation for chemical phosphorus removal (Kumar *et al*., 2014a).

A summary of the different properties of the iron minerals can be found in Table 2-10. Genz *et al*. (2004) studied an akaganeite (β-FeOOH) sorbent and found that it had a large MAC of 23 mg P/g. Akaganeite showed a higher adsorption capacity of 60 mg P/g when studied in the pure crystalline form (Deliyanni *et al*., 2007). Ferrihydrite, goethite and hematite were found to have loading capacities of approximately 18, 5 and 2.8 mg P/g Fe, respectively; note that the adsorption capacities have been normalized for iron content (Kang *et al*., 2003). In another study, an iron oxyhydroxide exhibited a much lower phosphate adsorption capacity of 1.5 mg P/g (Boujelben *et al*., 2008). In each study, the adsorption of phosphate decreased at increasing pH and as the concentration of competing anions increased. Optimum pH was found to be in the low (<5) pH range. It was also found that the presence of bicarbonate decreased phosphate uptake, while the presence of calcium and magnesium ions increased phosphate removal at high pH through precipitation (Kang *et al*., 2003).

Table 2-9: Summary of Synthesized Metal Oxides used for Phosphate Sorption in Wastewater Streams

Sorbent	Adsorption Capacity (mg/g)	Log K_L	Adsorption Isotherm Model and Kinetics	Optimum pH Range	Competing Ions	Desorption	Specific Surface Area (m^2/g)	Reference
Akaganeite (β-FeOOH)	23.3 (pH 5.5) 16.9 (pH 8.2)	1.31 0.94	- Langmuir	5.5	NA	0.6 M NaOH	280	Genz *et al.*, 2004
Akaganeite (β-FeOOH)	59.62 (25°C) 44.87 (45°C) 27.29 (65°C)	-1.69 -1.85 -1.62	- Langmuir - Freundlich - Pseudo-Second Order - Exothermic	- only tested at pH 7	NA	pH 12 (NaOH)	330	Deliyanni *et al.*, 2007
Amorphous Ferrihydrite	18	NA	- Freundlich	3	NA	0.2 M NaOH	200 – 300	Kang *et al.*, 2003
Goethite (α-FeOOH)	5	NA	- Freundlich	NA	NA	0.2 M NaOH	20	Kang *et al.*, 2003
Hematite (α-Fe_2O_3)	2.8	NA	- Freundlich	NA	NA	NA	20 – 25	Kang *et al.*, 2003
FeOOH	1.5 (pH 5)	-0.70	- Langmuir - Freundlich - Endothermic	5	NA	NA	2.609	Boujelben *et al.*, 2008
Aluminum Hydroxide (γ-alumina)	6.45	NA	- Langmuir	4	F^-, citrate, tartrate	NA	NA	Chen *et al.*, 1973
Aluminum Hydroxide (corundum)	1.24	NA	NA	NA	NA	NA	NA	Anderson and Malotky, 1979
Boehmite (AlOOH)	45 (pH 4)		- Freundlich - First Order	4	Cl^-, SO_4^{2-}, NO_3^-, CO_3^{2-}		297	Tanada *et al.*, 2003
Amorphous $ZrO(OH)_2$	15 (pH 8.8)	NA	- Freundlich	- only tested at pH 8.8	Cl^-, SO_4^{2-}	0.1 M NaOH	228	Chitrakar *et al.*, 2006
Amorphous ZrO_2	99.01 (pH 6.2)	-0.51	- Langmuir - Freundlich - Pseudo-Second Order	2 – 6	- little to no effect	0.1 M NaOH	327	Su *et al.*, 2013
La_2O_3	24.6 (pH 6)	NA	- Freundlich	4 – 6	- little to no effect	0.8 M NaOH	550 – 600	Ning *et al.*, 2008

Table 2-10: Composition of iron hydr(oxide) minerals (adapted from Kumar *et al*., 2014a).

Iron Mineral	Chemical Formula
Ferrihydrite	$Fe_5HO_8 \cdot 4H_2O/Fe_2O_3 \cdot nH_2O$
Akaganeite	β-FeOOH
Goethite	α-FeO(OH)/ ~90%Fe_2O_3
Hematite	α-Fe_2O_3
Lepidocrocite	γ-FeO(OH)/ ~90%Fe_2O_3
Magnetite	Fe_3O_4

Aluminum oxides also have a variety of forms that can be classified as aluminum oxides, aluminum hydroxides and aluminum oxyhydroxides (shown in Table 2-11). While being reviewed for their use in wastewater treatment, it was reported that aluminum oxides γ-alumina and corundum adsorbed very little phosphate and had adsorption capacities of 0.208 and 0.04 mmol/g, respectively. At pH 7, the aluminum oxyhydroxide gibbsite was determined to have an even smaller adsorption capacity of 0.015 mmol/g. Boehmite, aluminum oxyhydroxide, was determined to have the highest adsorption capacity of 1.45 mmol/g; approximately 45 mg P/g at pH 4 (Tanada *et al*., 2003; Kumar *et al*., 2014b). The presence of other anions decreased phosphate uptake onto boehmite by a small amount; however, it still showed preference for phosphate adsorption over other species. The effects of chloride, nitrate and sulfate were studied (Tanada *et al*., 2003). It was determined that pH influenced the adsorption of phosphate on aluminum oxides greatly. Adsorption of phosphate onto gibbsite decreased with increasing pH (Kumar *et al.*, 2014b). Boehmite exhibited an optimum working pH of 4. Changes in pH above or below 4 led to drastic decreases in phosphate uptake (Tanada *et al*., 2003).

Other oxides have also been investigated for phosphate adsorption. Nanoscale amorphous zirconium oxides were investigated by Su *et al*. (2013) because they have a number of traits suitable for an effective sorbent. Zirconium oxides have high strength in resisting oxidants, acids

and bases, they are non-toxic; and have a high thermal stability and very low solubility in water. Amorphous ZrO_2 was found by Su *et al*. (2013) to have one of the highest reported adsorption capacities of 99 mg/g at pH 6.2. Optimal phosphate adsorption occurred at low pH (*i.e.* ~2) and decreased only slightly from pH 2 to 6. The presence of chloride, sulfate and bicarbonate had little effect on phosphorus adsorption onto ZrO_2. Lanthanum oxide was also used for phosphate adsorption showing a good adsorption capacity of 24.6 mg/g (Ning *et al*., 2008). The optimum pH for La_2O_3 was shown to be a pH of 4 with removal decreasing for both increasing and decreasing pH. Lanthanum oxide also showed preferential uptake of phosphate over carbonate, sulfate and chloride species (Ning *et al*., 2008).

Table 2-11: Classification of aluminum oxides (adapted from Kumar *et al*., 2014b).

Classification	Name	Formula
Aluminum Hydroxide	Gibbsite	α-$Al(OH)_3$
Aluminum Oxide	γ-Alumina	γ-Al_2O_3
	Corundum	α-Al_2O_3
Aluminum Oxyhydroxide	Boehmite	γ-AlOOH

There is some uncertainty over which inner sphere complexes form in phosphate adsorption onto metal oxide surfaces. When goethite was studied, it has been shown in one study that bidentate complexes are formed between the iron atoms and phosphate at low pH while other studies have found that monodentate complexes prevail over the majority of the pH range, and bidentate formation is dependent on the phosphate speciation (Genz *et al*., 2004). Whether monodentate or bidentate complexes prevail can indicate if desorption of phosphate from the metal oxide surface will be difficult since bidentate complexation is stronger than monodentate (Li and Stanforth, 2000).

2.4.5.1 Binary Metal Oxides as Sorbents

The adsorbent capabilities of binary oxides have received considerable attention. Binary oxides combine the physical properties of two or more metal oxides and display greater adsorption abilities due to having the benefits of both parent compounds (Li *et al*., 2014). Binary oxides usually contain iron or aluminum and have shown to have large adsorption capacities ranging from 13.7 mg P/g to as high as 61.5 mg P/g (Long *et al.*, 2011, de Sousa *et al.*, 2012); a summary of mixed metal oxides can be located in Table 2-12. A review of several binary oxides, including aluminum iron hydr(oxides), iron and aluminum mesoporous spheres and an iron zirconium binary is presented below (Ayoub *et al*., 2001; de Sousa *et al*., 2012; Ren *et al*., 2012).

Ayoub *et al*. (2001) examined the use of an iron aluminum hydroxyl(oxide) to treat wastewaters which contained low levels of phosphorus. One of the challenges in wastewater treatment is to achieve low levels of phosphorus in the effluent as the concentration gradient as a driving force for adsorption is reduced. When used in a simple matrix of distilled water and 0.5 mg P/L, the filter media was able to remove over 90% of the phosphate while with a treated wastewater effluent only 48% of the phosphate was removed. The decrease in adsorption capacity was hypothesized to be due to competition among the ions present in the complex wastewater matrix.

Table 2-12: A Summary of Binary and Trimetal Oxide use for Phosphate Sorption in Wastewater Streams

Sorbent	Adsorption Capacity (mg/g)	Log K_L	Adsorption Isotherm Model and Kinetics	Optimum pH Range	Competing Ions	Desorption Conditions	Reference
Fe – La	29.5 (pH 7)	0.93	- Langmuir - Pseudo-second-order	4	F^-, SO_4^{2-}, NO_3^-	NA	Liu *et al*., 2013
Al – Mn	59.8 (pH 6)	-0.82	- Langmuir - Pseudo-second-order	5	F^-, SO_4^{2-}	NA	Wu *et al*., 2014
Fe – Cu	39.8 (pH 5) 35.2 (pH 7)	1.25 0.90	- Langmuir - Pseudo-second-order	3 – 7	F^-, SiO_3^{2-}	0.5M NaOH	Li *et al*., 2014
Fe – Mn	36 (pH 5.6)	1.13	- Freundlich - Pseudo-second-order	< 5	- little to no effect	0.1M NaOH	Zhang *et al*., 2009
Fe – Zr	33.4 (pH 5.5) 24.9 (pH 8.5)	0.67 0.84	- Langmuir - Pseudo-second-order	< 5	- little to no effect	0.5M NaOH[1]	Ren *et al*., 2012
Magnetic Fe – Zr	13.65 (pH 4) 17.87 (pH 3)	NA	- Langmuir - Pseudo-second-order	3 – 4	NO_3^-, SO_4^{2-}, citrate	0.1M NaOH[2]	Long *et al*., 2011
Fe – Al[3] (Mesoporous spheres)	20.07 (pH 3) 2.67 (pH 7)	NA 0.02	- Langmuir	3	NA	NA	de Sousa *et al*., 2012
Fe – Al – Mn	48.3 (pH 6.8)	NA	- Freundlich - Pseudo-second-order	4	SiO_3^{2-}, HCO_3^-, SO_4^{2-}	NA	Lu *et al*., 2013

[1]Ren *et al*., 2012 only observed 53% of sorbate desorb giving evidence that some adsorption is irreversible bonding.
[2]Long *et al*., 2011 reported that after five regeneration cycles, adsorption capacity only decreased to 66.7%.
[3]Ratio of Fe:Al is 1:1 (Sousa *et al*., 2012)

Competition from other aqueous species needs to be minimized in the process of adsorption. A good sorbent is selective for the sorbate of focus. A magnetic iron – zirconium (Fe-Zr) binary oxide demonstrated lower phosphate adsorption due to competition. Decreased adsorption was found to occur in the presence of nitrate, sulfate and citrate (Long *et al*, 2011). Long *et al*. observed the effects of the various competing ions separately to determine which species affected adsorption capacity the most. In the case of the magnetic Fe – Zr oxide, citrate proved to have the largest effect on phosphate sorption due to the presence of hydroxyl groups on citrate. In other studies, metal oxides have proven to be very selective for phosphate over other known competitive species in wastewater. Li *et al*. (2014) investigated the use of an iron (III) – copper (II) binary oxide for phosphate adsorption from aqueous solutions. Although initially developed for arsenic adsorption, the binary oxide proved to be selective for phosphate over arsenic. At pH 5, the adsorption capacity of Fe – Cu (1:2) was determined to be 39.8 mg P/g (Li *et al*., 2014). Other competitive species were then tested and results showed that Fe – Cu oxide adsorbed phosphate over sulfate, chloride and bicarbonate. However, the presence of high concentrations of fluorine (F^-) and silica oxide (SiO_3^{2-}) species were shown to interfere with phosphate adsorption.

The presence of potentially competing ions had little effect on the uptake of phosphate onto an iron manganese binary oxide (Zhang *et al*., 2009). Manganese oxide has proven to have scavenging abilities for ions in fresh and salt water environments. Testing the binary oxide sorbent was done to see if the combination of Mn with Fe would increase the adsorption capacity and selectivity onto the sorbent (Zhang *et al*., 2009). The Fe – Mn binary oxide was determined to have a high MAC of 33.2 mg P/g and no significant effect on phosphate adsorption due to competition effects. The Fe – Mn sorbent had an optimal working pH range of 3 to 5 with

removal decreasing with higher pH. Ionic strength had no effect on phosphate adsorption. An iron zirconium binary oxide was also found to have the same trends with respect to pH and ionic strength demonstrating a MAC of 36.28 mg P/g (Ren *et al*., 2012). Competition effects were also shown to have little to no effect on phosphorus uptake onto the Fe – Zr binary oxide.

Trimetal oxides have been recently studied for phosphate adsorption. Lu *et al*. (2013) evaluated the use of an iron aluminum manganese mixed metal oxide for phosphate adsorption. The sorbent was amorphous and had a rough, irregular surface. The ratio of Fe:Al:Mn of the mixed metal oxide was determined to be 3:3:1 (Lu *et al*., 2013). The trimetal oxide demonstrated an adsorption capacity higher than both the iron manganese and iron aluminum binary oxides. Adsorption of phosphate was negatively affected by increasing pH and higher concentrations of SiO_3^{2-}, HCO_3^- and SO_4^{2-} anions. The highest amount of phosphate removal was observed at a pH of 4 (Lu *et al*., 2013).

2.4.5.2 Desorption from Metal Oxides

Desorption of phosphate from metal oxides has been studied extensively with different methods investigated. The most widely used method of desorption is regeneration with sodium hydroxide (Genz *et al*., 2004). Sodium hydroxide desorption was successful when desorbing phosphate from nanocrystalline akaganeite with 100% desorption at pH 12 (Deliyanni *et al*., 2007). These results were in agreement with Genz *et al.* who found no significant change in adsorption capacity over three cycles using 0.6M NaOH to regenerate their granular ferric hydroxide (akaganeite). Desorption from an iron zirconium binary oxide with 0.5M NaOH was assessed; however, desorption was found to be incomplete – 53% of the adsorbed phosphate being

irreversibly bound to the sorbent (Ren *et al*., 2012). The iron copper binary oxide studied by Li *et al*. (2014) showed a 21% decrease in removal efficiency, but still had a high phosphate adsorption capacity after five regeneration cycles with 0.5 M NaOH. During the fifth cycle, the sorbent had an adsorption capacity of around 27 mg P/g. Zhang *et al*. (2009) determined that 0.1M NaOH desorbed phosphate from the iron manganese binary oxide just as well as 0.5M, showing that more dilute solutions of NaOH could be used in regeneration. By reducing the amount of sodium hydroxide, overall process cost will decrease. Other methods of desorption have been attempted but with little success. Genz *et al*. (2004) found that they lost over 20% removal efficiency with each cycle when used hydrogen peroxide to regenerate akageneite. Genz *et al*. concluded that the NaOH regeneration was more suitable for the iron oxide.

2.4.5.3 Metal Oxides for Nutrient Recovery

Challenges have emerged with use of metal oxides as sorbents which need to be taken into consideration when investigating the use of metal oxide sorbent for nutrient recovery. One challenge with the use of metal oxides is the decrease in adsorption capacity, or in some cases less phosphorus being desorbed, after each desorption cycle. While some metal oxides show preference for phosphate adsorption, in others the selectivity is lessened and competition effects are observed. Competition effects will also be a challenge in the use of metal oxides as sorbents in wastewater.

Gaps in the literature also exist and should be investigated to evaluate the use of metal oxides in nutrient recovery. One gap is the investigation of the use of exhausted sorbent after the sorbent loses adsorption capacity due to chemically irreversible bound phosphate. Use of the spent sorbent as a fertilizer should be studied as well as the breakdown of metal oxides to starting

materials for possible reuse. The second gap in the literature is implementation of metal oxide sorbents into wastewater treatment. Some treated waters have increased metal concentrations due to breakdown of the metal oxide and release into effluent waters (Kumar *et al*., 2014a). There is also a gap in the literature pertaining to the use of metal oxides for ammonium adsorption. Investigation into the above mentioned areas will help in the evaluation of metal oxides for nutrient recovery.

2.4.4 Biowastes as Low-Cost Adsorbents

The use of biowastes as potentially sustainable nutrient removal technologies has been reported. Tables 2-13 and 2-14 summarize a collection of studies that employed biowastes for phosphate and ammonium adsorption, respectively. Biowastes are typically agricultural waste products that have been dried and ground to form particles. Drying usually occurs at temperatures of 70 - 105°C over a period of several hours (Biswas *et al*., 2007; Biswas *et al*., 2008; Liu *et al*., 2010a,b,c). Sources of such biowastes include, but are not limited to, food processing plants such as juice making facilities (Nguyen *et al*., 2013; Biswas *et al*., 2007). These materials are abundant in hydroxyl functional groups that are contributed by cellulose, hemicellulose and lignin which suggests that the material would be effective as a sorbent. Biowastes have other attractive qualities such as being readily available and inexpensive, renewable sources (Nguyen *et al*., 2013). Due to their potential as sorbents and other positive attributes, research has focused on the use of biowastes in nutrient removal.

Table 2-13: Summary of Biowaste use for Phosphorus Sorption in Wastewater Streams

Sorbent	Sorbate	Adsorption Capacity (mg/g)	Adsorption Isotherm Model and Kinetics	Optimum pH Range	Competing Ions	Reference
Saw Dust	PO_4^{3-}-P	20.39	- Freundlich - Pseudo-Second Order	NA	NA	Benyoucef and Amrani, 2011
Coir Pith	PO_4^{3-}-P	4.35	NA	2 – 3.5	NA	Krishnan and Haridas, 2008
Palm Surface Fibres	PO_4^{3-}-P	4.35	NA	NA	NA	Riahi *et al*., 2008
Granular Date Stones	PO_4^{3-}-P	8.70	- Pseudo- Second Order - Intraparticle Diffusion	3 - 5	NA	Ismail, 2012
Palm Surface Fibers	PO_4^{3-}-P	8.47	- Pseudo- Second Order - Intraparticle Diffusion	3 - 5	NA	Ismail, 2012
Okara (soy bean milk by-products)	PO_4^{3-}-P	0.8	- Langmuir	3	CO_3^{2-}	Nguyen *et al*., 2013
Coir Pith impregnated with Fe (III)	PO_4^{3-}-P	68.0	NA	NA	NA	Krishnan and Haridas, 2008
Orange Waste impregnated with La, Ce and Fe	PO_4^{3-}-P	13.94	- Langmuir	5 – 7	- little to no effect	Biswas *et al*., 2007
Orange Waste impregnated with Zr	PO_4^{3-}-P	57	- Pseudo-Second Order	1 – 4	- little to no effect	Biswas *et al*., 2008
Sugar Cane bagasse fibres loaded with Fe	PO_4^{3-}-P	49.6	- Langmuir - Freundlich	NA	NA	Carvalho *et al*., 2011
Urea modified Saw Dust	PO_4^{3-}-P	29.66	- Freundlich	NA	NA	Benyoucef and Amrani, 2011

Table 2-14: Summary of Biowastes use for Ammonium Sorption in Wastewater Streams

Sorbent	Sorbate	Adsorption Capacity (mg/g)	Adsorption Isotherm Model and Kinetics	Optimum pH Range	Surface Area (m^2/g)	Competing Ions	Reference
Strawberry Leaf	NH_4^+	3.93 (15°C) 6.05 (25°C) 6.71 (30°C) 7.66 (35°C)	- Langmuir - Freundlich - Pseudo-Second Order - Intraparticle Diffusion - Endothermic	5 – 8	0.35	Zn^{2+}, Al^{3+}, HCO_3^-, CO_3^{2-} PO_4^{3-}	Liu *et al*., 2010a[1]
Boston Ivy Leaf Sorbent	NH_4^+	3.37 (15°C) 5.28 (25°C) 6.07 (30°C) 6.59 (35°C)	- Langmuir - Freundlich - Logistic Model - Endothermic	5 – 10	31.96	NA	Liu *et al*., 2010b
Strawberry Stems	NH_4^+	4.62 (30°C)	- Langmuir - Freundlich - Logistic Model	NA	0.10	NA	Liu *et al*., 2010c
Boston Ivy Stems	NH_4^+	5.01 (30°C)	- Langmuir - Freundlich - Logistic Model	NA	0.53	NA	Liu *et al*., 2010c
Southern Magnolia Leaves	NH_4^+	6.22 (30°C)	- Langmuir - Freundlich - Logistic Model	NA	1.54	NA	Liu *et al*., 2010c
Poplar Leaves	NH_4^+	6.25 (30°C)	- Langmuir - Freundlich - Logistic Model	NA	NA	NA	Liu *et al*., 2010c
Sawdust	NH_4^+	1.7 (pH 8)	- Langmuir - Freundlich - Pseudo-Second Order - Intraparticle Diffusion	6 - 10	NA	NA	Wahab *et al*., 2010

[1]Liu *et al*., (2010a) discovered that the competing ions effected adsorption due to their influence on ambient pH upon addition.

Coir pith and date-palm wastes have both been examined to determine their phosphate adsorption abilities (Krishnan and Haridas, 2008; Riahi *et al*., 2009; Ismail, 2012). Coir pith, a waste product from the production of natural fibers from coconut husks, was studied for phosphate adsorption capacity. The dried coir pith that was ground into a powder was found to have a MAC of 4.35 mg P/g and was effective over the pH range of 2 to 3.5 (Krishnan and Haridas, 2008). Date palm fibers, from the study conducted by Riahi *et al.* (2009), were found to have the same MAC (4.35 mg P/g). Ismail (2012) used granular date stones and dried palm surface fibers for phosphate adsorption. The adsorption capacities for the two biowastes used were twice as high as those found for the above mentioned studies. Granular date stones had a MAC of 8.7 mg P/g while the dried palm surface fibers which had an adsorption capacity of 8.47 mg P/g. As with the dried coir pith, the other biowastes were found to be most efficient at low pH with optimum pH ranges occurring between pH values of 2 and 5 (Riahi *et al*., 2009; Ismail, 2012).

The use of biowastes as adsorbents for ammonia removal has proven to be much more successful. Liu (2010a) reported on research projects which investigated the use of plant residues for ammonia adsorption. Liu *et al*. (2010a) dried and ground strawberry leaves into a powder to be used as the sorbent. When the strawberry leaf sorbent (SLS) was investigated using a scanning electron microscope (SEM), the surface of the powder was found to be irregular with pores ranging in size from nanometers to micrometers (Liu *et al*., 2010a). The irregular pore sizes may help explain the result obtained from modeling using known adsorption models. The results indicated that there was both monolayer adsorption on a homogenous surface (Langmuir, $R^2 > 0.97$) and multilayer adsorption onto a heterogeneous surface (Freundlich, $R^2 > 0.94$). During batch testing, 0.2 grams of SLS were added to 25 mL of test solution, a solution of

ammonia nitrogen prepared in several concentrations. The results show that ammonia adsorption increased with increased initial concentration of ammonia and increasing temperature. Liu *et al*. (2010a) conducted batch test experiments at 15, 25 and 35 °C; adsorption capabilities of the SLS, calculated using the Langmuir model, was highest at 35 °C (MAC = 7.66 mg/g), followed by 25 °C (MAC = 6.05 mg/g) and 15 °C (MAC = 3.93 mg/g).The results for the SLS were very similar to a second study by Liu *et al*. (2010b) which studied the use of Boston Ivy Leaf Sorbent (BILS) for ammonia adsorption. Unlike the strawberry leaf sorbent, BILS had a removal efficiency of 100% in a solution with an initial ammonia nitrogen concentration of 25 mg/L. SLS had a removal efficiency of 60% in the same solution (Lui *et al*., 2010c).

The main goal of using biowastes as sorbents is the reduction in the cost of wastewater treatment. However, another advantage of using biowastes is that the process takes waste products that are causing environmental burden (*i.e.* landfill space and costs) and makes these products useful. Also, the waste product themselves could be seen as a good source of nutrients, as in the case in the use of soybean milk by-products (okara). Due to popular demand for tofu and soy milk, global production of okara as waste has been estimated to be around 14 million tons per year (Nguyen *et al*., 2013). This high amount of waste has led to the investigation of okara as a sorbent for contaminant removal. Unfortunately, when tested for phosphate adsorption, okara was shown to adsorb very little with a maximum adsorption capacity of 0.8 mg/g (Nguyen *et al*., 2013). Low adsorption of phosphorus or ammonia is found frequently with biowastes sorbents, leading to the investigation of modifying these sorbents to increase nutrient adsorption.

Research has also has examined the use of biosorbents as a support for other effective sorbents for the sorbate of interest. In 2007, Biswas *et al*. modified orange waste from an orange juicing

plant with lanthanum, cerium and iron ions and increased the adsorption capacity to 14 mg P/L. Krishnas and Haridas (2008) modified the surface of coir pith by impregnation with iron (Fe(III)) and increase adsorption capacity by to 68.0 mg/g.

Use of biosorbents has several merits. They are a sustainable, low cost option that can reduce waste from other industries thereby cutting down the dependence of industry on landfills. They produce a somewhat environmentally conscious product which has exhibited phosphate and ammonium uptake. One of the challenges present in the implementation of biosorbents for nutrient recovery may be the availability of the starting materials (*i.e.* waste products). Biosorbents may be useful in localized areas where the waste products are easily available. There is also very limited information on regeneration of the biosorbent and if sorbate can be collected separate from the biosorbent post adsorption.

2.4.7 Adsorption of Phosphate and Ammonia Together

From the review of literature, it can be seen that there has been segregation between phosphorus and nitrogen recovery by sorbents. As sorbates, ammonia and phosphate require different characteristics in a sorbent. In solution ammonia is present as ammonium cations while phosphate is present in anionic forms of varying charge. Therefore, these species will be attracted to different surfaces. Hence, sorbents that can adsorb ammonia and phosphate have consisted of composite materials. A summary of the sorbents which adsorb phosphorus and ammonia together can be found in Table 2-15. Composite materials are two or more materials mixed together to create an additive effect with respect to their adsorptive capabilities. Composite materials were mentioned previously with respect to taking two materials to enhance the adsorption of a single sorbate as in the case of metal oxides. In the following section,

composite materials will be discussed with regard to combining sorbents that select for two different sorbates. In the case of ammonia and phosphate, composite materials are an attractive option due to the difference between phosphate and ammonia ion charges.

Table 2-15: Summary of Sorbents which Remove both Ammonium and Phosphate.

Sorbent	Mechanism	Adsorption Capacity (mg/g)	Adsorption Isotherm Model and Kinetics	Optimum pH Range	Reference
NaCl, $FeCl_3$ Calcinated Clinoplitolite	Ion exchange with Surface complexation	P: 1.26 mg P/g N: 2.70 mg N/g	- Langmuir	NA	Huo *et al*., 2012
Si-Rich and Ca-Rich Zeolites	Ion exchange with precipitation and adsorption	P: 1.2 mg P/g N: 9.57 mg N/g	- Langmuir - Pseudo-Second Order	P: 5 N: 9	Ji *et al*., 2013
Type-C Natural Zeolite with CaP Precipitation (Ca:P=5.01)	Ion exchange with precipitation	P: 36.8 mg P/g N: 6 mg N/g	NA	P: 9 – 10 N: 6 – 7	Karapinar, 2009
Zeolite/Fe_2O_3 Composite	Ion exchange with Surface complexation	P: 7.14 mg P/g N: 35.7 mg N/L	NA	P: 4 – 7 N: 7.5 – 9	Xie *et al*., 2014

[1]Liu *et al*., (2010a) discovered that the competing ions effected adsorption due to their influence on ambient pH upon addition.

Karapinar (2009) investigated the use of a natural zeolite to remove ammonium (Table 2-7). After the initial investigation, Karapinar investigated the use of the ammonium adsorbed zeolite as a seed material for calcium phosphate precipitation. Calcium phosphate precipitation was monitored in the pH range of 7.5 – 10. More precipitate was formed within the pH range of 9 - 10. The presence of zeolite was found not to affect the precipitation of calcium phosphate and the study confirmed that calcium phosphate was precipitating on the zeolite. However, Karapinar (2009) stated that ammonium removal and calcium phosphate precipitation need to be studied using real wastewater to prove its "real world" efficacy. While the process of ammonium

adsorption and calcium phosphate precipitation onto the natural zeolite is convenient for nutrient recycling, the success of the ammonia phosphate enriched zeolite as a fertilizer is not known and must also be studied.

Several studies have investigated the use of calcium enriched zeolites to remove ammonia and phosphate (Murayama *et al*., 2003; Wu *et al*., 2007; Zhang *et al*., 2007). These studies used silica-rich fly ash derived zeolites and treated them using $CaCl_2$ to enhance the zeolites ability to retain phosphate. While the studies showed some success, a research group led by Ji *et al*. (2013) pointed out that the method used by the researchers had some disadvantages. The calcium enrichment method increases treatment cost and produces salt solutions that then need to be handled and disposed. Although the studies had their disadvantages Ji *et al*. (2013) believed that fly ash derived zeolites were useful in nutrient removal. The research group investigated the use a mixture of silica-rich and calcium-rich fly ash derived zeolites, effectively removing the calcium enrichment step used by the other researchers. The mixed zeolites demonstrated a phosphate adsorption capacity of 3 mg P/g and an ammonium capacity of 9.6 mg NH_4^+-N/g. A challenge of using the mixed zeolites was that the working pH ranges for optimum phosphate and ammonium adsorption were different. Phosphate was adsorbed best at pH 5, while ammonium was adsorbed best at pH 9. Also, the mixed zeolites could not achieve low level removals of nitrogen and phosphorus even at high sorbent dosage. Mixed zeolite dosage of 20 g/L achieved final phosphate and ammonium concentrations of approximately 2 mg/L and 0.5 mg/L, respectively. The fact that the end product obtained by the use of the spent zeolite mixture can be used directly as a fertilizer is a major advantage for its implementation (Ji *et al*., 2013).

2.5 Summary of Literature Review

Overall, adsorption has become an attractive treatment method due to its stability, simple operating conditions and production of less waste sludge. Adsorption can be applied to treatment plants of large and small scale and is specifically beneficial for dilute waste streams (Su *et al*., 2013). Adsorption capacity and competition effects are two of the major challenges with existing sorbents. Natural zeolites and minerals have lower adsorption capacities which can be contributed by impurities in their framework and competing ions. Biosorbents had varied adsorption capacities and competition effects were tested on very few sorbents. The use of biosorbents for nutrient adsorption is attractive since the process uses waste from other industries, reducing waste and cost. However, the starting materials used to make biosorbents may only be available in localized areas. Another challenge with the use of biosorbents is the limited information on desorption of nutrients and regeneration of the sorbent.

After a review of the literature, ion exchange resins and metal oxide sorbents were deemed to have characteristics that, once optimized, have the greatest potential for use in nutrient recovery. The ability of these technologies to adsorb and desorb large amounts of ammonium and phosphate make these methods very attractive for use in wastewater treatment. Research is necessary to overcome some of the challenges posed by competition effects and desorption capabilities, but once managed the use of these sorbent materials could achieve the goals of nutrient recovery. In recent studies using sorbents to collect both ammonium and phosphate, it can be seen that there will be some compromise. Ammonium and phosphate have opposite charges, both demanding different sorbent characteristics and working pH ranges from adsorption technologies.

2.6 Gaps in the Research

Although there have been a number of studies of nutrient recovery, more needs to be done, especially focusing on recovering both phosphorus and nitrogen. The following is a summary of the gaps found in research:

- Sorbent effectiveness in real wastewater samples: Most studies have used simple test solutions as a proxy for wastewater samples. Researchers characterize real wastewater samples and transfer the determined amounts to a simple solution containing the sorbate of focus. Wastewater has a complex matrix with many species coexisting. While the majority of studies look into the effects of competition with other species, the true performance of a sorbent cannot be evaluated until subjected to real world samples.

- Organic nitrogen and phosphorus species: Organic phosphorus and nitrogen stand in the way of meeting stringent effluent regulations. They must be removed for effluent levels to reach the ultra-low concentrations needed to meet the policies of today and in the future. Also, just removing organic nitrogen and phosphorus is essentially throwing away valuable, and in the case of phosphorus, irreplaceable resources. Research must be completed to determine a method to convert organic P and N to forms that are useful in nutrient recovery.

- Sorbate desorption and sorbate reuse: Desorption of the nutrients from the sorbent also needs to be researched further. Optimizing desorption into a feedstock solution for recovery technologies (*e.g.* struvite) is required. Also, studies have focused on one or two regeneration studies, but have not established the effects of long term use.

3.0 Literature Review: Organic Phosphorus Oxidation

3.1 Problem Statement

Phosphorus removal from waste water is gaining more attention in recent years. Areas with sensitive receiving waters prone to eutrophication require stricter phosphorus effluent discharge limits (Clark *et al.*,2010). In addition, there has been a shift in wastewater treatment from phosphorus removal to recovery since P is an essential nutrient and as such, a valuable commodity in the fertilizer industry (LeCorre *et al*., 2009). The pressure towards nutrient recovery has increased recently when it was reported that worldwide mining of phosphate rock is expected to peak in the year 2030; complete exhaustion of global phosphate rock stores is expected to occur in the next 50 – 100 years (Cordell *et al*., 2009).

Phosphorus speciation in the wastewater stream affects both P recovery and the ability to achieve lower discharge limits. Organic phosphorus species can make up 26 to 81 % of the total P in treated wastewater effluents as it is more recalcitrant, and not receptive to biological and chemical nutrient removal processes (Qin *et al.,* 2015). Further, current phosphorus recovery technologies recover P in the form of an inorganic P precipitates (*i.e*. struvite) and therefore organic P species are not suitable for nutrient recovery (Latimer *et al*., 2015). Thus, a method is needed which can oxidize organic P in wastewater, making the P available for P recovery and consequently make it easier to achieve high level P removal efficiencies in wastewater treatment effluents.

3.2 Organic P in Wastewater

Total phosphorus (TP) in wastewater can exist in several forms. Particulate and dissolved P are retained or pass through a 0.45 µm membrane filter, respectively (Gu *et al.*, 2011). Organic P typically makes up 15 % of dissolved phosphates in wastewater, with the remaining fractions being 50 % orthophosphate and 35 % of condensed phosphates (Parsons and Smith, 2008; Mayer and Woo, 1998). Organic and condensed phosphates make up a fraction of TP referred to as non-reactive P (nRP), operationally defined as such since they do not react directly with the reagents used in colorimetric P detection methods (Robards *et al.*, 1994).

The nRP fraction is typically recalcitrant in wastewater treatment (Qin *et al.*, 2015). In a 2011 study by Gu *et al.*, nRP concentrations ranged from 9 – 54 µg P/L in secondary wastewater effluents, and from 3 – 42 µg P/L in tertiary wastewater effluents. Therefore, with TP regulations for sensitive receiving waters approaching 0.01 mg P/L, the presence of nRP in wastewater will have a significant impact on the ability to meet these types of limits.

Few studies have specifically investigated organic P in the wastewater stream. While information is limited, studies agree that the organic P compounds in domestic waste water mainly consist of esterized phosphorus and pyrophosphate species that contain a covalent phosphorus to oxygen to carbon bond. (Qin *et al.*, 2015). Further characterization of organic P compounds has shown that pyrophosphates and organic mono ester phosphates are hydrophilic in nature, while mono- and di- ester phosphates are more hydrophobic; Qin *et al*. (2015) found that the majority of organic P in wastewater was hydrophobic in character.

The type and quantity of nRP in a wastewater stream is dependent on the source. Depending on the area serviced by the wastewater treatment plant, industrial wastes and agricultural runoff

could be significant contributors to nRP in wastewater. The use of organic phosphorus compounds in industrial applications is increasing leading to wastewater streams high in refractory nRP; organic phosphorus compounds are used as herbicides/pesticides, chelating agents and in pharmaceuticals (Xing *et al.*, 2017a; Mangat Echavia *et al.*, 2009; Nowack, 2003; Kamel, 2015). Organic phosphorus use in industry and its existence in industrial wastewater has been well studied; many industries use phosphonates, a group of phosphorus compounds that contain a hard to break covalent carbon to phosphorus bond (Nowack, 2003). An example of a phosphonate that is in high worldwide demand is Glyphosate, a nonselective herbicide which has increased in usage due to the production of genetically modified crops that are tolerant to Glyphosate (Xing *et al.*, 2017a).

3.3 Advanced Oxidation Processes use for Organic Phosphorus Oxidation

Studies of oxidation of organic P in wastewaters have typically been limited to the removal of large quantities found in some industrial wastewaters. Wastewater streams which contain large quantities of organophosphate pesticides (*e.g.* glyphosate) have been the subjected to several advanced oxidation processes (AOPs). The section reviews prior studies of the use of AOPs in this regard.

3.3.1 Catalytic Wet Oxidation

Wet oxidation is a process that uses oxygen or air to mineralize aqueous organic compounds to CO_2 gas and water. High temperatures and pressures are often needed in the wet oxidation process to avoid partial oxidation of organics and long reaction times (Bhargava *et al.*, 2006). Catalytic wet oxidation (CWO) typically uses catalysts to improve reaction conditions, making

the process more efficient. Even with the use of catalysts, high temperature and pressure may still be required to achieve the desired results in short enough reaction times (Xing *et al*., 2017a; Xing *et al*., 2017b). Due to the elevated temperatures and pressures, the mechanism behind oxidation via CWO is complicated and involves a combination of hydrolysis, thermal decomposition and free radical oxidation (Bhargava *et al*., 2006). CWO has been identified as a suitable method to remove organic pollutants in medium to high concentration wastewaters.

Prior studies of catalytic wet oxidation in wastewater applications have mainly focused on the oxidation of glyphosate and organic P in glyphosate process wastewater. In one study, CWO was used with an activated carbon (AC) catalyst which had been modified to increase the catalytic activity of the AC surface (Xing *et al*., 2017a). Experiments were completed in a co-current upflow fixed bed reactor containing 10 mL of catalyst; a hydraulic residence time of approximately 25 minutes while the temperature and pressure were 110 – 130 ℃ and 1.0 MPa respectively. Removals of over 99 % glyphosate and 93 % organic P were observed after CWO of the glyphosate waste water where the initial glyphosate and organic P concentrations ranged from 213 – 2560 and 51 – 474 mg/L, respectively (Xing *et al*., 2017a). In another study by the same research group, CWO was coupled with a lime-catalyzed formose reaction to oxidize organic P and formaldehyde in the same glyphosate process wastewater (Xing *et al*., 2017b). In the study, the effluent collected after CWO was heated to 60 – 90 ℃ and lime was added to the reactor to initiate formaldehyde oxidation via the autocatalytic behaviour of the lime/formaldehyde mixture (Castells *et al*., 1983). More than 99% glyphosate and 90% organic P were oxidized to phosphate when optimal CWO conditions were used; the experiments employed a 3 % modified AC catalyst, a temperature of 130℃, a pressure of 1.0 MPa and a reaction time of 2 hours (Xing *et al*., 2017b). With the addition of the lime 96.2 % of total

phosphorus was removed via precipitation of phosphate. Overall, CWO was shown to effectively oxidize glyphosate and organic P in concentrated wastewater streams.

In general, the high pressures and temperatures required for wet oxidation to be an effective treatment have associated high operating cost and thus, catalysts are being explored to make the process more cost effective. However, a review by Bhargava *et al*. (2006) found that the catalysts used in CWO are costly and inefficient and there is much need for improvement. Additional research is needed to address catalyst deactivation and catalyst recovery for the CWO process to gain further industrial use (Bhargava *et al*., 2006).

3.3.2 Photocatalysis

Photocatalysis is often used in advanced oxidation processes (AOPs) to oxidize organic contaminants in water and wastewater streams. In photocatalysis, oxidation occurs through the action of hydroxyl ($^{\cdot}OH$) and superoxide ($O_2^{\cdot -}$) radicals that are formed by exposing a semiconductor to UV light; the UV light promotes an electron of the semiconductor from the valence to the conduction band leading to the formation of radicals (Benotti *et al*., 2009). Photocatalysis of organic phosphorus has been regularly reported in the literature. These studies typically coupled UV light with various forms of TiO_2 (Chen and Liu, 2007; Mangat-Echavia *et al*., 2009), hydrogen peroxide (Manassero *et al*., 2010) and ferrioxalate (Chen *et al*., 2007).

3.3.2.1 Titanium Dioxide and UV Light

The combination of titanium dioxide (TiO_2) and UV light have been used to treat wastewaters containing pesticides. The photocatalyst TiO_2 has been used in powder suspensions, or slurries

(Shifu and Yunzhang, 2007; Han *et al*., 2009; Evgenidou *et al*., 2006), as well as immobilized on silica gel (Mangat Echavia *et al*., 2009). Studies have also evaluated TiO_2/UV photocatalysis using either natural (Vela *et al.*, 2018) or artificial UV irradiation. A summary of studies investigating pesticide oxidation via TiO_2/UV photocatalysis is summarized in Table 3-1. In general, it has been reported that the use of TiO_2/UV can achieve high levels (>80%) of pesticide removal. Its performance has been found to be dependent on the duration of UV exposure, catalyst dose and initial concentration of contaminant.

Advanced oxidation processes which use TiO_2 as a photocatalyst have also been found to remove pesticides via physical adsorption (Mayer *et al.*, 2013). Chen and Liu (2007) observed glyphosate adsorption to the TiO_2 surface under dark conditions; the TiO_2 adsorption capacity for glyphosate was 1.28×10^{-6} mol/g (40 µg P/g TiO_2). Adsorption of the organic P species did not hinder oxidation, as orthophosphate was detected in solution once the UV lights were activated (Chen and Liu, 2007). In another study Han *et al*. (2009) discovered that the pesticide acephate adsorbed to TiO_2 and this was also found to not hinder oxidation. Mangat Echavia *et al.* (2009) reported complete removal of 0.1 mM glyphosate after adsorption to TiO_2 and 60 minutes of UV exposure. RP was not released after oxidation of the glyphosate suggesting that the liberated orthophosphate and other intermediate compounds were removed via adsorption.

Several studies have addressed the liberation of inorganic ions during the oxidation of pesticides. Degradation via photolysis can take numerous pathways as the radical species that form are non-selective (Legrini *et al*., 1993; Westeroff *et al*., 2009). As such, most studies have monitored orthophosphate (inorganic P species) to gauge if complete mineralization of the parent compounds had occurred. In one study, liberation of orthophosphate was observed with photooxidation, however the quantity of PO_4^{3-} released was low when compared to the

stoichiometry of the amount of glyphosate degraded (Mangat Echavia *et al*., 2009). Han *et al*. (2009) observed only 2 % of P was mineralized into orthophosphate. The release of lower than expected orthophosphate could be due to adsorption onto the TiO_2 catalyst or due to incomplete mineralization of the compound studied. Several by-products have been identified in experiments by Evgenidou *et al*. (2006) studying the pesticides dimethoate and dichlorvos; nine organic compounds were identified as by-products of dimethoate oxidation while three organic compounds were observed for dichlorvos oxidation. Longer UV irradiation times have the potential to completely mineralize parent compound and any additional organic by-products.

The use of TiO_2/UV to oxidize organic contaminants has both advantages and limitations. The advantages include the efficacy of the treatment over a wide range of pH, little chemical requirements other than the addition of the catalyst (*i.e.* TiO_2) and no need for additional treatment post-oxidation (Shon *et al*., 2006). Photocatalysis is however limited by the transmission of the UV light. The wastewater stream being treated must allow good transmission of the UV light as water with high turbidity will interfere with oxidation of contaminants (Gogate and Pandit, 2003). In addition, due to the energy requirements of the system, the overall cost of TiO_2/UV photolysis could be higher than other methods of treatment (Shon *et al*., 2006).

Table 3-1: Summary of studies investigating UV/TiO_2 oxidation on organophosphate containing pesticides. Removal efficiencies based on detection of parent compounds in solution.

Method	Contaminant of Focus	Removal Efficiency (%)	Irradiation Time (min)	Comments	Reference
UV/TiO_2	Dimethoate ($C_5H_{12}NO_3PS_2$)	100 %	60	- TiO_2 was immobilized onto silica gel. - Removal of glyphosate was due to photocatalysis and adsorption. - Initial pesticide concentrations were 0.1 mM (3.1 mg P/L).	Mangat Echavia *et al., 2009*
	Glyphosate ($C_3H_8NO_5P$)	100 %	60		
	Acephate ($C_4H_{10}NO_3PS$)	100 %	105		
UV/TiO_2	Malathion ($C_{10}H_{19}O_6PS_2$)	100 %	240	- Optimal TiO_2 dose: 200 mg/L - Natural sunlight used as UV light source. - Pesticides were treated as a mixture dosed in wastewater treatment plant effluent - Initial concentrations of 0.3 mg/L (0.04 – 0.06 mg P/L) per pesticide was used.	Vela *et al*., 2018
	Fenotrothion ($C_9H_{12}NO_5PS$)	80 ± 8 %			
	Quinalphos ($C_{12}H_{15}N_2O_3PS$)				
	Dimethoate				
UV/TiO_2	Glyphosate	> 90 %	210	- Initial glyphosate concentration: 2.5 x 10^{-4} M (7.7 mg P/L) - Optimal TiO_2 dose: 6 g/L	Shifu and Yunzhang, 2007
UV/TiO_2	Acephate	> 90 %	60	- Optimal TiO_2 dose: 4 g/L - Initial acephate concentration: 0.40 mM (12.4 mg P/L)	Han *et al*., 2009
UV/TiO_2	Dimethoate	100 %	120	- Initial pesticide concentrations: 20 mg/L (2.7 – 2.8 mg P/L) - TiO_2 dose: 100 mg/L	Evgenidou *et al*., 2006
	Dichlorvos ($C_4H_7O_4PCl_2$)	100 %	30		
UV/TiO_2	Dimethoate	100 %	30	- Initial concentration: 10 mg/L (1.35 mg P/L) - TiO_2 dose: 100 mg/L	Evgenidou *et al*., 2005

3.3.2.2 Hydrogen Peroxide and UV Light

The exposure of hydrogen peroxide (H_2O_2) to UV light produces hydroxyl radicals which oxidize organic compounds to CO_2, H_2O and inorganic ions (Malato *et al*., 2000). This method has been employed to treat solutions containing glyphosate (Manassero *et al*., 2010). The study investigated the effects of initial glyphosate concentration (27 – 91.3 mg/L), H_2O_2 concentration and pH on the performance of the process. Optimal glyphosate conversion was observed to occur at H_2O_2/glyphosate molar ratios in the range of 7 – 19 and above pH 7. Overall, oxidation of over 70 % glyphosate to orthophosphate was observed after 5 hours at pH 7 and with a H_2O_2 dose between 75 – 200 mg/L (Manassero *et al*., 2010).

Relatively few studies have investigated the use of H_2O_2/UV light for organic P oxidation and this may be due to limitations of the method. One disadvantage is that hydroxyl radical formation from H_2O_2 at 254 nm is slow, leading to long reaction times. In addition, hydroxyl radical formation can be inhibited in the presence of dissolved and suspended solids (Ikehata and El-Din, 2006). Municipal wastewaters are known to have large dissolved and suspended solids concentrations (Shon *et al*., 2006). High dissolved and suspended solids concentrations in combination with the large volumes of wastewater that need to be treated will likely limit the use of H_2O_2/UV treatment for organic P oxidation in wastewater.

3.3.2.3 Ferrioxalate

The ferrioxalate system combines Fe(III) with oxalate and UV light to produce hydroxyl radicals which then oxidize organic contaminants. Chen *et al*. (200) reported photodegradation of glyphosate in a ferrioxalate system with 60.6 % conversion to RP at pH values between 3.5 and

5; initial glyphosate concentrations were 5.0 mg/L. When the pH was raised to a value of 6, the conversion lowered to 42.1 %. It was found that use of the acidic pH range was necessary for effective oxidation due to the prevalence of $Fe(C_2O_4)_2^-$ and $Fe(C_2O_4)_3^{3-}$ which are more efficiently photolyzed over other ferrioxalate species (Chen *et al*., 2007). The pH adjustment needed for optimal oxidation is a limitation of the use of the ferrioxalate method. Adjusting the pH of large volumes of municipal wastewater would be costly. Therefore, the ferrioxalate method would be best used in industrial wastewater streams which are already acidic.

3.4 Literature Review Summary

In summary, oxidation methods are potentially attractive for oxidizing organic phosphorus in wastewater. The literature suggests that TiO_2/UV photocatalysis has the greatest potential for nRP oxidation in wastewater treatment effluents due the limited chemical addition and efficacy at circumneutral pH. Research is however necessary to determine if TiO_2/UV could be an effective method for nRP oxidation in wastewater effluents which contain a mixture of OP species in addition to phosphonates. Additionally, wastewaters typically contain natural dissolved organic matter which could impact the efficacy of TiO_2/UV photocatalysis; additional research questions include catalyst dosage and length of UV irradiation necessary for different wastewater effluents. With additional research, the use of TiO_2/UV photocatalysis could achieve the goal of nRP oxidation in wastewater streams.

3.5 Gaps in Literature

Overall, the literature indicates that AOPs are effective at oxidizing organic phosphorus compounds to inorganic RP however there are a number of areas that require further research. The following is a summary of gaps in the literature:

- Use of oxidation methods on real wastewater samples: The majority of studies reported in the literature have focused on pesticides in simple test solutions. Waste water is a complex matrix with other constituents that may affect the efficiency of oxidation on organic P in wastewater effluents.
- Organic phosphorus species: Prior studies have focused on organophosphate containing pesticides (phosphonates). Wastewater effluents are known to contain a variety of different organic P compounds (*i.e.* esterized phosphorus, pyrophosphates). The efficacy of oxidation methods for solutions containing the mixture of nRP species found in municipal wastewater effluents should be investigated.
- Organic phosphorus concentrations: In the literature, experiments have targeted treatment of concentrated pesticide waste streams. Organic P concentrations in typical municipal wastewaters are low in comparison and therefore, different treatment issues may arise.
- Competition between natural organic matter and organic phosphorus: In municipal wastewater, organic P species are less concentrated in comparison to organic matter. hydroxyl radicals non-selectively attack organic contaminants in solution, therefore photolysis may not be as effective on organic P compounds in wastewaters with high organic matter such as municipal wastewater.

4.0 Screening of Commercially Available Sorbents for Phosphorus Recovery from Synthetic Wastewater Test Solution

4.1 Summary

An opportunity exists to harvest nutrients from wastewater, a source rich in phosphorus. Using adsorption and desorption tests, this study evaluates 14 commercial sorbents for potential phosphorus recovery from synthetic wastewater. Commercially available sorbents (*e.g.* ion exchange resins (IEX), granular ferric oxide, hybrid IEX and activated alumina) were obtained from several companies and tested for phosphate removal from the wastewater in a 48-hour adsorption test. Sorbents which exhibited substantial phosphate removal were then tested for recovery using acidic (HCl), basic (NaOH), salt (NaCl) and basic salt (NaOH + NaCl) desorption solutions. Sorbents were evaluated with respect to P recovery from both the spent sorbent (adsorbed fraction) and from the synthetic wastewater stream. In terms of recovery of phosphate from the initial synthetic wastewater stream, the IEX sorbent C was found to recover the largest fraction at 23 % P; while all other sorbents recovered less than 20 % P from the synthetic wastewater. Additional desorption solutions (carbonate and magnesium sulfate) were tested on sorbents A (granular ferric hydroxide) and D (IEX) and it was found that these solutions can increase phosphorus recovery from wastewater.

KEYWORDS: Nutrient Recovery, Wastewater, Adsorption, Desorption

4.2 Introduction

Phosphorus is an essential nutrient in fertilizers that are necessary for food production. Conventional practices used to produce P based fertilizers are costly and unsustainable;

phosphate rock is mined worldwide with total depletion of phosphate stores projected to occur within the next 50 to 100 years (Erisman *et al.*, 2008; Cordell *et al.*, 2009; Hao *et al.*, 2013). Wastewater may represent a renewable source of nutrients if methods for harvesting P are developed. The quality of effluents and cost of wastewater treatment may also be enhanced by replacing nutrient removal with nutrient capture and recycling since phosphorus and nitrogen often must be removed to reduce toxicity, or to mitigate the effects of eutrophication.

The literature shows that methods for nutrient recovery from waste water range from conceptual, proof-of-concept studies to monitoring of full-scale implementation into water resource recovery facilities (WRRFs). A number of studies have focused on phosphorus recovery from wastewater, leading to several literature reviews on the subject (de Bashan and Bashan, 2004; Xie *et al*., 2016; Mehta *et al*., 2015); some examples of methods investigated include reverse osmosis, adsorption and electrochemical methods. To date, only technologies which produce struvite ($NH_4MgPO_4 \cdot 6H_2O$) have been implemented in full scale wastewater treatment plants (Latimer *et al*., 2015). Although these technologies are in use, there is an interest in the development of economical and efficient recovery methods for nutrients (de Bashan and Bashan, 2004).

Adsorption is a low cost and efficient process that can transfer contaminants from the liquid to the solid phase for separation (Metcalf and Eddy, 2003). Since adsorption requires little energy input there has already been some deployment in wastewater treatment (Li *et al.*, 2014; Long *et al.*, 2011). Challenges can however arise when selecting a sorbent suitable for nutrient removal. Identifying sorbents that adsorb large quantities of nutrients may lead to the use of two sorbents of different compositions to adsorb N and P due to the differing properties of nitrogen and

phosphorus bearing compounds. The adsorption of nutrients must also be reversible if nutrients are to be recovered, a functionality which is dependent upon adsorbent properties (Rittman *et al.*, 2011). If nutrients cannot be desorbed, sorbents will not be an effective recovery technology.

This study used commercially available sorbents of different compositions to obtain insight into the effect of adsorption mechanisms on phosphorus recovery. The mechanisms of focus in this study include ion exchange and surface complexation. Ion exchange resins (IEX) incorporate an exchange mechanism where one ion replaces another at the resin surface while metal oxide sorbents can bind phosphate via surface complexation or ion exchange depending on the metal present. In practice several commercially available IEX resins include metal oxides in their structure to increase sorption capacity (Blaney *et al.*, 2007; Kumar *et al.*, 2014a; Tanada *et al.*, 2003).

Ion exchange resins (IEX) and metal oxides have been employed to remove various contaminants from aqueous solutions. Ion exchange resins are known to have quick response to shock loading and large reactive site availability for certain sorbates (Thorton *et al.*, 2007). Ion exchange resins have been previously employed to capture phosphate ions from the liquid phase. Nur *et al.* (2013) used a strong base hybrid exchange resin that achieved an adsorption capacity of 48 mg P/g sorbent. O'Neal and Boyer (2013) also used a strong base hybrid exchange resin to remove phosphorus from grey water and reported adsorption capacities ranging from 1.5 to 10.1 mg P/g sorbent.

Known for forming surface complexes with phosphate (Smith *et al.*, 2008), metal oxide based sorbents have also been tested for removal of phosphate from aqueous environments (Kumar, 2014a). A granular ferric hydroxide, that was used to remove phosphate from water, had a reported adsorption capacity of 24 mg P/g sorbent at pH 6 (Sperlich, 2010). Aluminum hydroxide has been shown to adsorb 45 mg P/g sorbent at a pH of 4 (Tanada *et al.*, 2003).

Regeneration of metal oxides and hybrid ion exchange resins with either basic and/or salt solutions has been reported (Blaney *et al.*, 2007; Malyovanny *et al.*, 2013). While desorption has been reported, in most cases the studies were conducted to regenerate the sorbent and not to collect adsorbed species (Blaney *et al.*, 2007; Nur *et al.*, 2013). Prior studies have suggested that sorbents have the potential for multiple regeneration cycles with little effect on adsorption capacity (Rodrigues *et al.*, 2010). It is therefore anticipated that desorption of nutrients into a feedstock suitable for fertilizer production would require minor adjustments from current regeneration methods.

The purpose of this study was therefore to test whether commercially available sorbents could be employed to recover phosphorus from wastewater. In this study emphasis was placed on desorption of P from the sorbent by assessing different desorption solutions to investigate which combinations of solution and sorbent were most suitable for nutrient recovery. The sorbents were evaluated based on P adsorption capacity from a synthetic wastewater (SWW) and the recovery of P from the SWW; desorption solutions were assessed through nutrient recovery from the spent solids. The results of this research will provide guidance to the wastewater treatment industry

when making decisions when selecting appropriate adsorbent technologies for nutrient removal and recovery.

4.3 Methodology

4.3.1 Synthetic Wastewater

An inorganic synthetic wastewater (SWW) that emulated the complexity of secondary-treated wastewater in terms of ionic composition was modified from that described by Jung *et al.* (2005). The common components of the synthetic wastewater solution (Table 4-1) included magnesium sulfate ($MgSO_4 \cdot 7H_2O$, Sigma-Aldrich, St. Louis, MO), calcium chloride ($CaCl_2 \cdot 2H_2O$, Fisher Scientific, Fair Lawn, NJ), sodium bicarbonate ($NaHCO_3$, EMD Chemicals Inc., Gibbstown, NJ), sodium acetate (CH_3COONa, BDH Chemicals, Toronto, ON). Potassium phosphate monobasic (KH_2PO_4) (BDH, VWR International LLC., West Chester, PA) was also included and concentration was dependent on the experiment and are subsequently described in further detail. The synthetic wastewater was prepared using ultra pure water (18.2MΩ, MilliQ) and adjusted to a pH of 7.0 ± 0.05 using hydrochloric acid (HCl, EMD Chemicals Inc., Gibbstown, NJ) or sodium hydroxide (NaOH, Sigma-Aldrich, St. Louis, MO). All chemical reagents used in this study were reagent grade or higher.

Table 4-1: Synthetic wastewater recipe adapted from Jung *et al.* (2005). Potassium phosphate monobasic (*a*) concentration was dependent on target phosphorus concentration.

Compound	Concentration (mg/L)
Magnesium Sulfate ($MgSO_4 \cdot 7H_2O$)	24.0
Calcium Chloride ($CaCl_2 \cdot 2H_2O$)	2.4
Sodium Bicarbonate ($NaHCO_3$)	300.0
Sodium Acetate (CH_3COONa)	820.3
Potassium Phosphate Monobasic (KH_2PO_4)	***a***

4.3.2 Commercial Adsorbents

Fourteen commercially available sorbents were obtained from vendors based on supplier recommendations on the sorbent's potential to adsorb P from solution via chemical adsorption or ion exchange. The sorbents utilized in this study represent a small fraction of commercial adsorbents available and varied in chemical composition, summarized in Table 4-2. Sorbents included ion exchange resins (IEX), titanium dioxide, granular activated alumina, silica hydrogels and ferric hydroxide based materials; sorbents are referred to by an alphabetic code to maintain anonymity of the supplier. In addition, Table 4-2 gives conventional uses of these commercial sorbents to demonstrate their potential as nutrient sorbing agents. The uses include phosphate removal but also, given the strong chemical similarity included arsenate removing resins.

4.3.3 Adsorption Isotherm Experiments

Adsorption isotherms were developed using data gathered from batch tests. In the batch tests the solutions were prepared by adding known amounts of KH_2PO_4 standard solution to 50 mL of the synthetic wastewater to yield final nominal concentrations of 0, 5, 10, 20, 40 and 80 mg P/L; adsorption isotherm experiments of select sorbents included test solutions with a nominal concentration of 100 mg P/L. For these batch tests 50 mL polypropylene tubes (Corning Inc., Tewksbury, MA) were used. After a known amount of sorbent addition, the tubes were continuously mixed on a rocker for 48 hours after which equilibrium was assumed. The contents of the tube were then filtered using 0.45 µm polyethersulfone membrane filters (VWR International LLC., West Chester, PA). Filtrates were subsequently analyzed for total phosphorus concentration using the methods described below.

4.3.4 Nutrient Recovery Experiments

In the chemical desorption experiments, a known amount of sorbent was added to the synthetic wastewater test solution with a nominal phosphate concentration of 40 mg P/L (1.29 mmol P/L) and the pH of the test solution was adjusted to 7.0 $\pm$ 0.05. After 48 hours, the sorbent was filtered from the solution using a 0.45 µm cellulose nitrate membrane filter (Whatman, Germany) and rinsed with 25 mL ultrapure water (18.2MΩ, MilliQ). The spent sorbent was then soaked in 50 mL of desorption solution for 48 hours. The desorption solutions that were tested included 0.1 M NaOH, 0.1 M HCl, 0.1 M NaCl and 0.1 M NaOH + 0.1 M NaCl. After 48 hours, the desorption solution was filtered through 0.45 µm membrane filter and the filtrate was brought to a neutral pH by adjusting with 0.1 M HCl or NaOH. Desorption filtrates were analyzed for total phosphorus concentrations using the methods described below.

Table 4-2: Commercial sorbents tested.

Sorbent	Description	Conventional Use
A	Granular ferric hydroxide based sorbent	- Phosphate adsorption
B	Ion exchange resin (IEX)	- General deionization and chemical processing applications - $R\text{-}N\text{-}(CH_3)^+Cl^-$ functional group
C	IEX	- General deionization and chemical processing applications - Dimethylamine functional group
D	IEX	- General deionization and chemical processing applications - Trimethylamine functional group
E	IEX with hydrated ferric oxide (HFO) nanoparticles	- Arsenate adsorption
F	Granular activated alumina	- Strong affinity for polar compounds - Nonspecific contaminants
G	Hybrid IEX	- Arsenate adsorption - Trimethylamine functional group
H	Aluminum and Titanium Oxide based sorbent	- General contaminant removal - Metal removal
I	Aluminum and Titanium Oxide based sorbent	- General contaminant removal - Metal removal
J	Synthetic amorphous silica hydrated	- Strong affinity for polar compounds and proteins
K	Synthetic amorphous silica hydrated/citric acid	- Strong affinity for polar compounds and proteins
L	Synthetic amorphous silica hydrated	- Strong affinity for polar compounds and proteins
M	Synthetic amorphous silica hydrated	- Strong affinity for polar compounds and proteins
N	TiO_2	- Photochemical reactions

4.3.5 Evaluation of Alternative Desorption Solution

Additional chemical desorption tests were conducted on selected sorbents; these experiments followed the same protocol as the previously described nutrient recovery experiments, apart from

the desorption solutions used. The alternate desorption solutions included 0.5 M $MgSO_4$, 1.0 M NaOH, 0.1, 0.5 and 1.0 M $NaHCO_3$. A mixture of 0.5 M NaOH + 0.5 M $NaHCO_3$ was also tested for phosphorus recovery.

4.3.6 Phosphorus Measurements

Phosphorus was measured using Inductively Coupled Plasma Optical Emission Spectrometry (ICP-OES); intensities were measured at a wavelength of 213.617 nm. Calibration solutions used for ICP-OES measurements were prepared each day of analysis using KH_2PO_4 in ultrapure water (18.2MΩ, MilliQ). Phosphorus standards prepared from certified reference material (H_3PO_4, Lot BCBM9148V, 1002 ± 4 mg P/L) purchased from Sigma Aldrich were included in all runs for quality assurance.

4.3.7 Data Analysis

Results from the batch adsorption isotherm testing were fit to the Freundlich isotherm (Equation 4-1) that is commonly used to describe adsorption of species to sorbents with heterogeneous surfaces; Equation 4-1 was fit to the results of the batch isotherm testing using non-linear regression; isotherm fit was optimized to minimize least squares error using the nlinfit function of MATLAB™.

$$X = K_F C_e^{1/N} \tag{4-1}$$

In Equation 4-1, C_e is the concentration of the sorbate in the bulk solution at equilibrium (mg P/L), X is the amount of sorbate adsorbed per mass of sorbent (mg P/g sorbent). The fitting parameters of the Freundlich isotherm K_F ((mg/g)(L/mg)$^{1/N}$) and 1/N (unitless) are known as the

Freundlich capacity factor and Freundlich intensity parameter, respectively (Liu *et al.*, 2010a). The sum of squared error (SSE) reported for the fit of each sorbent to the Freundlich isotherm was calculated using Equation 4-2.

$$\text{SSE} = \sum_{i=0}^{n} \left(X_{e,experimental} - X_{e,model} \right)_i^2 \quad (4\text{-}2)$$

The recoveries of phosphorus from the sorbent (Equation 4-3) and the initial synthetic wastewater (Equation 4-4) were estimated:

$$R_s = \frac{M_{PD}}{M_{PA}} x\ 100\ \% \quad (4\text{-}3)$$

$$R_{WW} = \frac{M_{PD}}{M_{PWW}} x\ 100\ \% \quad (4\text{-}4)$$

where M_{PD} is the mass of desorbed P, M_{PA} is the mass of adsorbed P and M_{PWW} is the initial mass of P in the synthetic wastewater; all expressed in milligrams. To extend the results to evaluate column testing, Equations 4-5 and 4-6 from Crittenden *el al.* (2012) were employed to determine sorbent usage rate (SUR, g/L) and the volume of wastewater treated (V_{WW}, L/g) per kilogram of sorbent, respectively. The calculations were performed with the assumption that the P loading on the sorbent was in equilibrium with the influent P concentration and the mass transfer zone is small compared to the length of the column (Crittenden *et* al., 2012).

$$\text{SUR} = C_e/K_F C_e^{1/N} \quad (4\text{-}5)$$

$$V_{WW} = \text{SUR}^{-1} \quad (4\text{-}6)$$

Statistical analysis of the sorbents was conducted using ANOVA and T-tests. Results of ANOVA and T-tests are indicated by reporting the result of the F or t value, respectively, as well as the corresponding *p* value; degrees of freedom of the statistical test are reported in brackets.

4.4 Results and Discussion

Nutrient recovery with adsorption involves initial adsorption of the target sorbate (*i.e.* phosphorus) and subsequent release of sorbate from the spent sorbent. The results of adsorption and desorption tests are presented separately below.

4.4.1 Adsorption Screening Tests

Adsorption screening experiments were completed to determine which commercial sorbents substantially adsorbed phosphorus and to determine the adsorption capacity of each sorbent. It was expected that sorbents with larger adsorption capacities would have the potential to recover, larger quantities of nutrients, an important criterion that can impact the overall efficiency of any potential recovery process.

The initial screening of the fourteen sorbents established that eleven of them could adsorb phosphorus; sorbents L, M and N did not demonstrate P adsorption and were not included in further testing. The screening involved testing of sorbate adsorption at nutrient concentrations relevant to medium strength domestic wastewater with average orthophosphate concentration of 5 mg P/L (Metcalf and Eddy, 2003). Sorbents were evaluated based on sorbate removal with a cut-off threshold of 30%; any sorbents which demonstrated less than 30 % P removal were not included in further testing. The removal results of the sorbent screening are shown in Figure 4-1

with the cut-off threshold indicated. In terms of P removal, the performance of iron oxides (sorbent A), anion exchange resins (sorbents B through E and G) and activated alumina (sorbent F) based sorbents varied but on average, performed above the 30 % threshold; these sorbents were studied further in adsorption isotherm tests. Sorbents H through K displayed limited adsorption of phosphorus removing between 1 – 6 % P; sorbents in this group consisted of synthetic amorphous silica based sorbents, aluminum/titanium based metal oxides and TiO_2 powder. Due to their ineffective performance, sorbents H through K were discarded from further investigation.

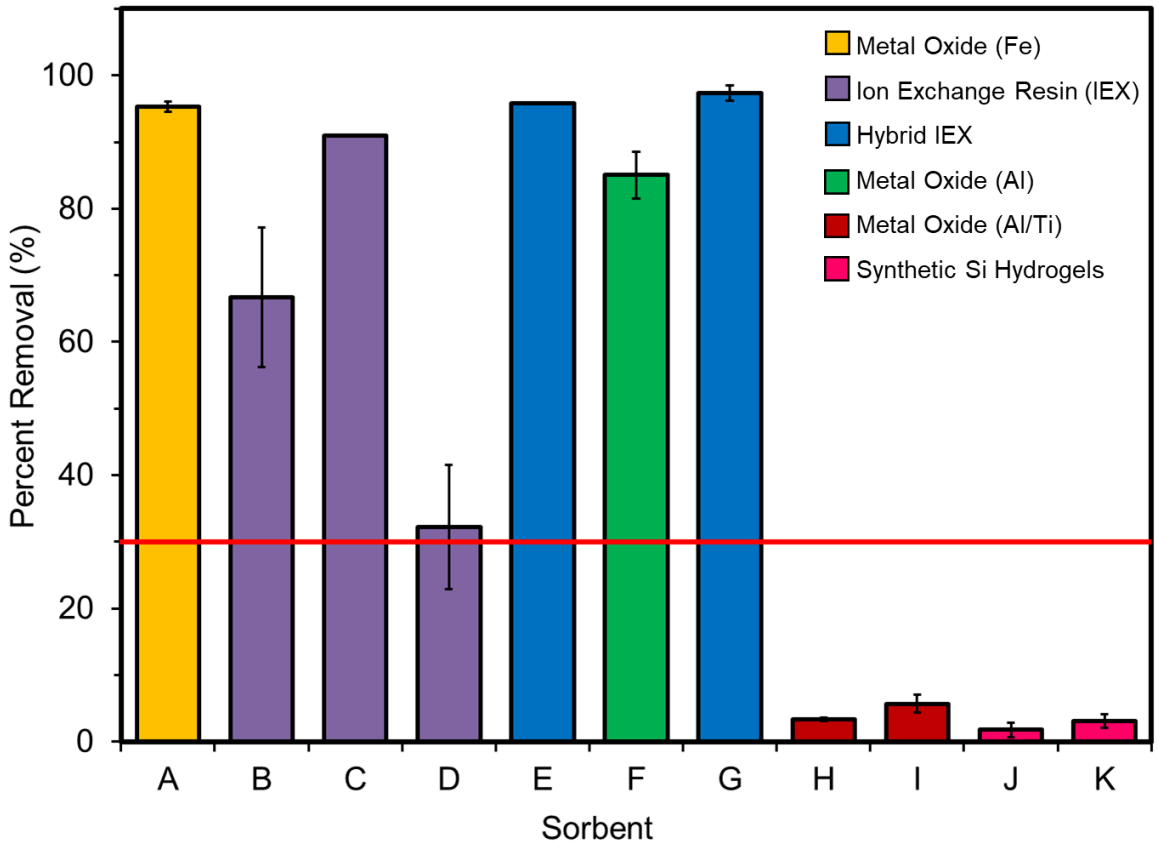

Figure 4-1: Phosphorus Removals for sorbents which exhibited nutrient adsorption. Colours depict different sorbent compositions. Sorbents with a percent removal below the cut-off threshold of 30 % (red line) were excluded from additional testing. Initial phosphate concentration was and 5 mg P/L.

4.4.2 Adsorption Isotherms

Seven sorbents met the adsorption performance threshold and were further characterized by adsorption isotherm experiments, the results of which were fit with isotherms (Figures 4-2 and 4-3). Adsorption capacity did not become saturated for any of the seven sorbents over the range of phosphorus concentrations tested, therefore the Freundlich isotherm was found to best describe the sorption responses. The best fit Freundlich parameters 1/N and K_F are summarized in Table 4-3. It should be noted that due to the mathematical structure of the Freundlich equation (Equation 4-1), the Freundlich parameters are closely related and estimates of one parameter will impact the second parameter (Vlad, 2015). Results of the sorbents which successfully adsorbed P are discussed in detail below.

The quality of fit of the Freundlich isotherm to the data obtained from adsorption isotherm tests were examined for further insight into the adsorption behaviours of the sorbents. A trend was observed with respect to sorbent composition in the values obtained for R^2 and sum of squared error. The fits for metal oxide sorbents A and F corresponded to R^2 values of 0.96 and 0.98, while hybrid IEX sorbents E and G had R^2 values of 0.87 and 0.86, respectively. Sorbents that were solely IEX based had smaller R^2 values; sorbents B and C both had R^2 values of 0.72 whereas sorbent D had the smallest R^2 of 0.54. The error associated with the fit of the Freundlich isotherm to the data of the various sorbents was also higher with IEX sorbents. The sum of squared error (SSE) values (Equation 4-2) obtained in fitting the adsorption isotherms were 0.75 $(mg\ P/g)^2$ or higher; metal oxide sorbents had SSE values of 0.43 $(mg\ P/g)^2$ or less. The better fit obtained for the metal oxide sorbents could be due to the adsorption process onto metal oxide sorbents being more heterogeneous, and therefore well described by the Freundlich isotherm,

while adsorption via IEX can occur more stoichiometrically (Crittenden *et al*., 2012). Additionally, results from adsorption isotherm testing with IEX sorbents was also highly variable and therefore could have also affected the fit of the Freundlich isotherm; results in experiments with IEX sorbents could be more variable due to the sorbents being non-selective for P, adsorbing any opportunistic ion (Thorton *et al*., 2007; Sengupta and Pandit, 2011). Altogether, it is evident that the Freundlich isotherm better describes sorbents containing metal oxides over the ion exchange resins.

The adsorption isotherm experiments were performed to identify which sorbents exhibited larger adsorption capacities, and therefore have the potential to recover larger quantities of P. The Freundlich capacity factor K_F describes the mass of P adsorbed by the sorbent under the test conditions performed (Liu *et al*., 2010a). Evident from the range of K_F values listed in Table 4-3, the sorbents exhibited different P adsorption capacities with no observable trends, however, the resulting K_F could be grouped into three categories; high and medium capacity sorbents had K_F values in the ranges of 2.72 – 2.38 and 1.69 - 1.25 $(mg/g)(L/mg)^{1/N}$ respectively while one sorbent (D, IEX) had a low capacity with a K_F of 0.54 $(mg/g)(L/mg)^{1/N}$. The high capacity sorbents included IEX sorbents B and D as well as the granular ferric hydroxide sorbent A and sorbent E, a hybrid IEX that incorporates metal oxide nanoparticles. The two sorbents with mid-range K_F factors were sorbent F (activated alumina) and sorbent G (IEX). The Freundlich isotherm was also used to describe P adsorption from source-separated urine and wastewater streams onto a hybrid IEX (O'Neal and Boyer, 2013). The K_F values obtained in this study were lower than the range of K_F values observed using a hybrid IEX in the different water matrices;

the K_F values ranged from 3.37 to 13.0 $(mg/g)(L/mg)^{1/N}$ (O'Neal and Boyer, 2013). Overall, sorbent B exhibited the largest K_F value of the sorbents tested.

Values for 1/N determined through fitting adsorption data to the Freundlich isotherm were also examined. The 1/N term is indicative of the degree of heterogeneity of the surface adsorption with heterogeneity decreasing as 1/N approaches 1 (Foo and Hameed, 2010); heterogeneity of surface adsorption is due to adsorption sites having a distribution of energies, indicating that a number of different interactions (*e.g*. electrostatic, acid-base) are occurring (O'Neal and Boyer, 2013). Freundlich intensity parameters (1/N) for the seven sorbents ranged between 0.32 (sorbent E) and 0.82 (sorbent D); the values for 1/N obtained for the rest of the sorbents studied were in the midrange, between 0.68 and 0.52. Overall, there was no observable trend between the 1/N value and sorbent composition however insight can be gained when examining the sorbents with the largest (IEX sorbent D) and smallest (hybrid IEX sorbent E) values of 1/N. For IEX sorbent B, the 1/N value approached 1 indicating adsorption is more homogeneous. In other words, the adsorption sites on the surface are of similar type which could decrease the selectivity of phosphorus at the surface; a sorbent which preferentially adsorbs P over other ions would demonstrate higher selectivity of phosphorus. Alternatively, 1/N for sorbent E approached 0 which has been interpreted as indicating many different sites available for P adsorption and could have increased selectivity. The 1/N value obtained for sorbent E (0.32) fell within the range of values obtained in another study which investigated P adsorption onto another hybrid IEX for use in source separated urine (O'Neal and Boyer, 2013); 1/N ranged from 0.15 and 0.4 in diluted urine and urine streams mixed with wastewater. In the study, the lower 1/N values were attributed to the combination of electrostatic and Lewis acid-base interactions that were

occurring at the surface (O'Neal and Boyer, 2013). Therefore, adsorption is potentially less favourable in sorbents with high values of 1/N (*i.e.* sorbent B) due to the possibility of increased competition in complex waste water streams where ions may compete for the same surface sites unless the surface sites are highly selective for the target sorbate.

Table 4-3: Freundlich isotherm parameters determined for sorbents which adsorb phosphorus; K_F and 1/N, known as the Freundlich capacity factor and Freundlich intensity parameter, respectively.

Sorbent	Freundlich Isotherm Fitting Parameters			
	K_F	1/N	R^2	SSE
A	2.38	0.52	0.96	0.11
B	2.66	0.53	0.72	0.75
C	2.47	0.61	0.72	1.17
D	0.54	0.83	0.54	1.19
E	2.72	0.32	0.87	0.03
F	1.25	0.65	0.98	0.07
G	1.69	0.68	0.86	0.42

In summary, the commercial sorbents which exhibited phosphorus adsorption varied with respect to their Freundlich capacity factors and 1/N values. The types of sorbents investigated in this study could potentially all have qualities that could be beneficial for P recovery. An example of this can be highlighted with the comparison of sorbents E and B. Hybrid IEX sorbent E and IEX sorbent B were found to have high K_F values but differed with respect to 1/N values. From the literature, the results suggest that Sorbent E, which incorporates metal oxides, could be capable of selectively adsorbing P from the synthetic wastewater while IEX sorbent B may be more susceptible to competition from other ions in solution. Whether the sorbent is selective for P or prone to competition could both hinder or benefit P recovery in wastewater. While competition

during the adsorption phase may decrease the P adsorbed, any P that is adsorbed may be desorbed easily with the right competitive ion. On the other hand, sorbents which select for P may have stronger bonds with P at the surface and could prevent P from being desorbed easily. Therefore, the results from adsorption isotherms needed to be evaluated with respect to P recovery to obtain further insight into the effectiveness of the sorbents for P recovery.

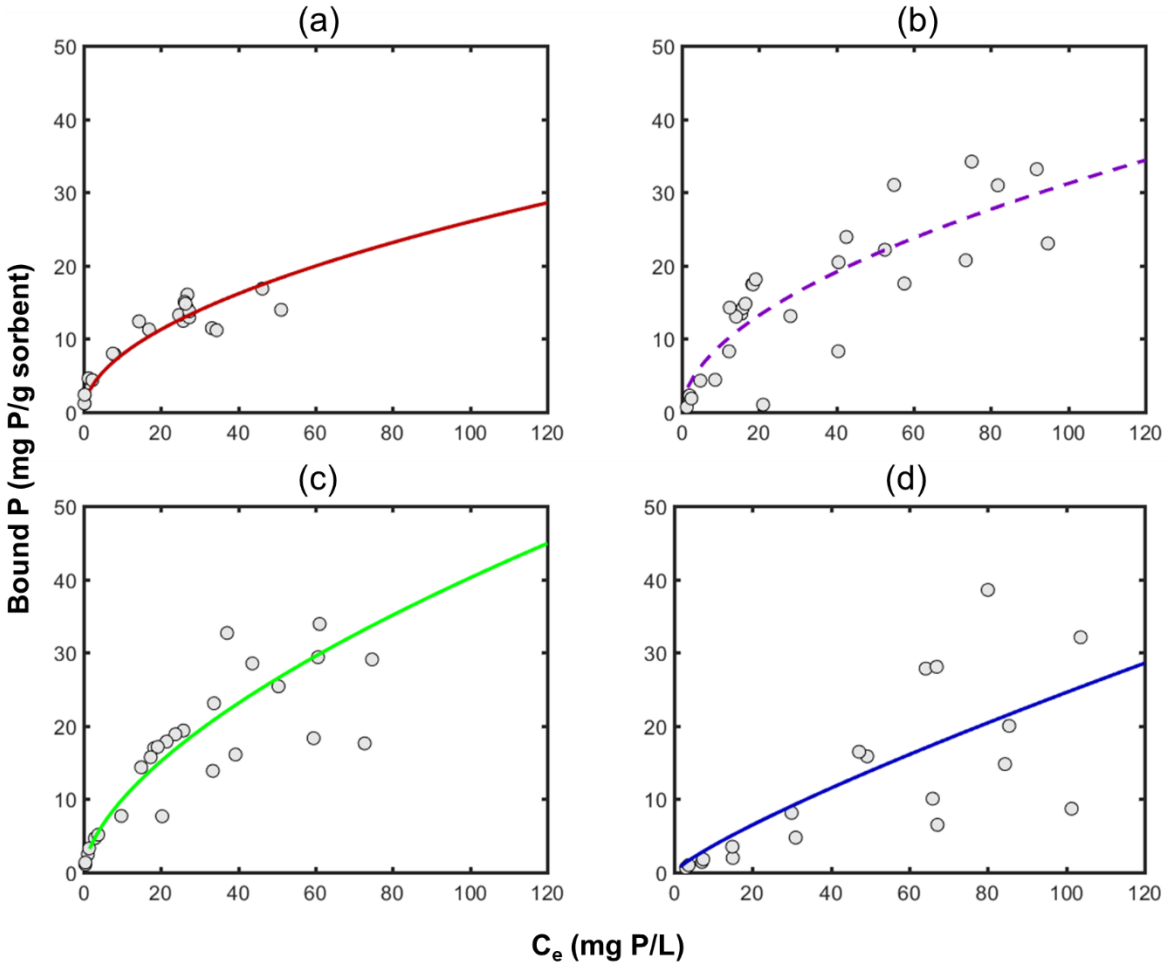

Figure 4-2: Freundlich adsorption isotherms for (a) granular ferric hydroxide sorbent A (red, solid) and ion exchange resin sorbents (b) sorbent B (purple, dashed), (c) sorbent C (green, dashed) and (d) sorbent D (blue, solid).

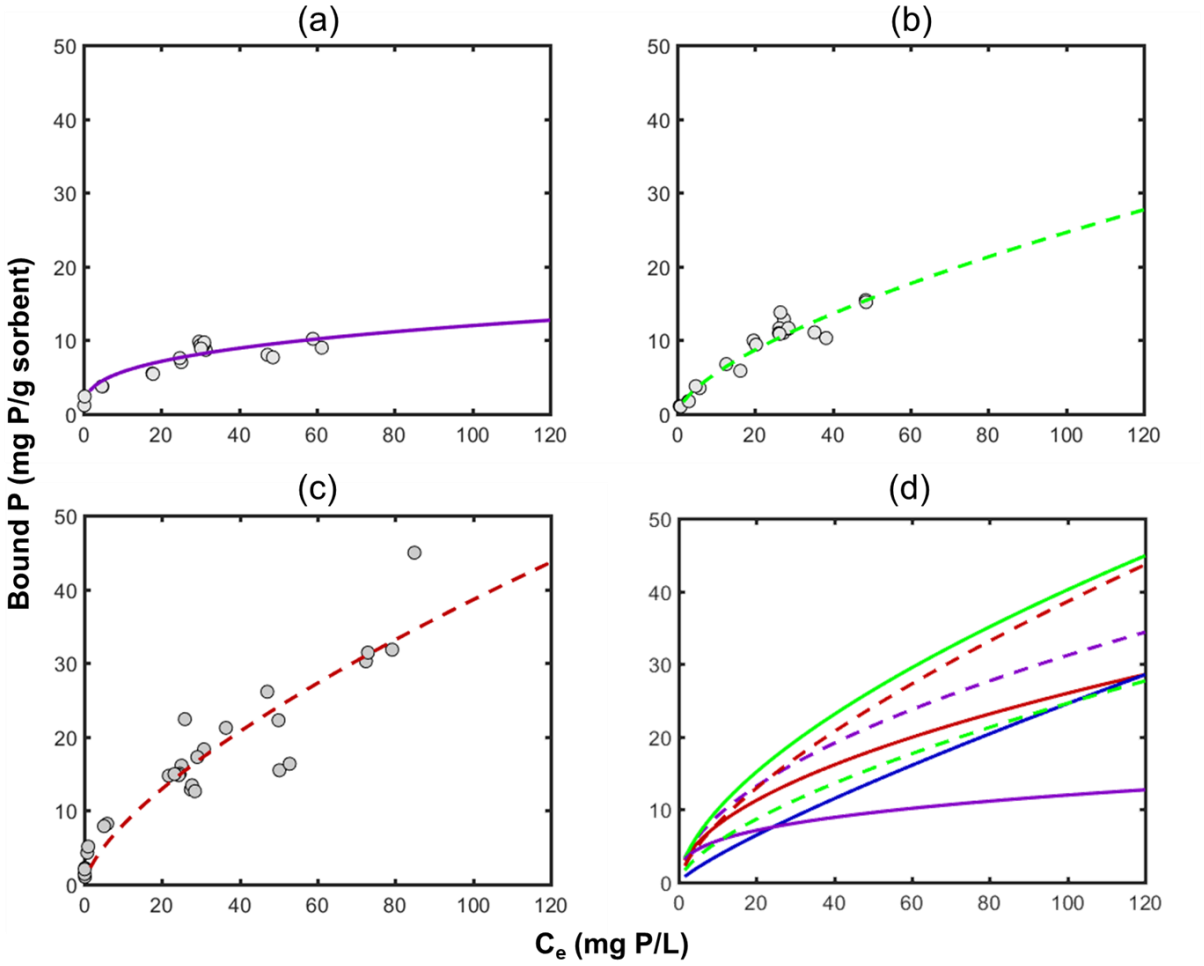

Figure 4-3: Freundlich adsorption isotherms for (a) IEX with metal oxide nanoparticles sorbent E (purple, solid), (b) activated alumina sorbent F (green, dashed) and (c) IEX sorbent G (red, dashed). Figure 4b plots all seven Freundlich isotherms for sorbents; colours and line styles are consistent with individual plots.

4.4.3 Nutrient Recovery

An important criterion for selection of a sorbent for nutrient recovery is that the sorbate (*i.e.* phosphorus) must be able to be desorbed. Ideally, the desorption process would result in 100 % recovery of P from the sorbent resulting in sorbent regeneration and no loss of surface binding sites. Any irreversibly bound phosphorus would occupy binding sites for addition P sorption,

thereby lessening the adsorption capacity of the sorbent and potential for nutrient recovery. Recovery of the sorbate from a sorbent is often dependent on the type of sorbent and the desorption method used. Chemical desorption is used in current adsorption processes for sorbent regeneration, regaining binding sites for another round of treatment; acidic, basic and salt desorption solutions have all be used to regenerate various sorbents for reuse over many cycles (Blaney *et al.*, 2007; Nur *et al.*, 2013).

The current study evaluated solutions typically used for sorbent regeneration but focused on sorbate collection in the used desorption solution rather than reuse of the sorbent. Due to the variety of sorbents utilized in this study, basic (0.1 M NaOH), acidic (0.1 M HCl), salt (0.1 M NaOH) and basic salt (0.1M NaOH + 0.1 M NaCl) solutions were used to determine which sorbents had promise for nutrient recovery. Figure 4-4a shows the P recovered from the spent sorbents using the four desorption solutions as calculated using Equation 4-3. The recovery results are discussed in terms of phosphorus recovery from the sorbent and total recovery from the wastewater solution below.

Recovery of P from granular ferric hydroxide sorbent A using NaOH, HCl, NaCl and NaOH + NaCl desorption solutions yielded average desorbed masses of 5.32, 3.71, 2.56 and 5.13 mg P/g sorbent respectively. The amount of P recovered was found to be dependent on the desorption solution used ($F(7) = 75.438$, $p = 0.001$). Recovery of P via the salt desorption solution was the least effective for sorbent A, recovering 18.2 % of P adsorbed to the surface. The HCl desorption solution improved recovery in comparison to NaCl, increasing recovery to 26.4 % ($t(2) = 9.85$, $p = 0.01$). Use of NaOH further increased P recovery from sorbent A, with 37.8 % P being

desorbed (NaCl: t(2) = 9.51, p = 0.01; HCl: t(2) = 5.86, p = 0.03). The mixture of NaOH + NaCl did not improve P recovery from sorbent A over the use of NaOH alone; 36.5 % P was recovered from sorbent A using the basic salt mixture which was not significantly different from the quantity recovered through the use of NaOH (t(2) = 0.692, p =0.561). Overall, the desorption solutions NaOH and NaOH + NaCl recovered the largest quantities of P from sorbent A.

Treatment of IEX sorbent B with NaOH, HCl, NaCl and NaOH + NaCl recovered 3.31, 5.54, 5.28, and 5.88 mg P/g sorbent B, respectively. The amount of P recovered was determined to be dependent on the desorption solution used (F(7) =15.861, p = 0.011). Application of the NaOH desorption solution recovered 21.6 % P, the lowest recovery observed of the four desorption solutions (HCl: t(2) = -69.5, p < 0.001; NaCl: t(2) = -4.50, p = 0.05; NaOH + NaCl: t(2) = -6.74, p = 0.02). The remaining three desorption solutions recovered similar quantities of P which were not statistically different; desorption using HCl, NaCl, and NaOH + NaCl corresponded in P recoveries of 36.1, 34.4, and 38.4 % from sorbent B. Therefore, desorption solutions containing chloride recovered the largest quantities of P from Sorbent B.

Recovery from the IEX sorbent C with NaOH, HCl, NaCl and NaOH + NaCl desorption solutions resulted in recoveries of 6.63, 6.13, 7.76 and 9.20 mg P/g respectively. The amount of P recovered was found to be dependent on the desorption solution used (F(7) =19.233, p = 0.008). The 38.4 and 35.5 % P recoveries with NaOH and HCl desorption solutions, respectively, were not statistically different (t(2) = 1.11, p = 0.382). The combination of NaOH + NaCl recovered 53.3 % P from sorbent C, an increase from the recoveries obtained through the use of NaOH (t(2) = -6.30, p = 0.02) and HCl (t(2) = -6.45, p = 0.02). Desorption using NaCl recovered

45.0 % P from sorbent C and was not statistically different from the quantities of P recovered through application of the other three desorption solutions (NaOH: $t(2) = -2.84$, $p = 0.105$; HCl: $t(2) = -3.50$, $p = 0.07$; NaOH + NaCl: $t(2) = -3.37$, $p = 0.08$). This suggests that the presence of the chloride ion was enough to compete for the adsorption sites of sorbent C occupied by P thereby causing P to be liberated, however there may be a slight enhancement in having the exchange between Cl^- and P occurring at basic pH. Overall, NaCl and NaOH + NaCl recovered the largest quantities of P from sorbent C.

The recovery of P from IEX sorbent D with NaOH, HCl, NaCl and NaOH + NaCl desorption solutions resulted in average recoveries of 2.29, 2.88, 3.38 and 3.47 mg P/g sorbent, respectively. The amount of P recovered was found to be dependent on the desorption solution used ($F(7) = 24.57$, $p = 0.005$). NaOH recovered the least amount of P from sorbent D, desorbing 9.5 % P (HCl: $t(2) = -7.99$, $p = 0.02$; NaCl: $t(2) = 5.24$, $p = 0.03$; NaOH + NaCl: $t(2) = -21.91$, $p = 0.002$). The chloride-containing desorption solutions HCl, NaCl and NaOH + NaCl recovered 12.1, 13.1 and 13.5 % P. The recoveries obtained using chemical desorption in the presence of Cl^- were statistically similar apart from HCl and the combination of NaOH + NaCl where the acidic conditions recovered less P ($t(2) = -8.795$, $p = 0.01$). Therefore, at neutral and basic pH, desorption solutions containing the chloride ion recovered more P from sorbent D.

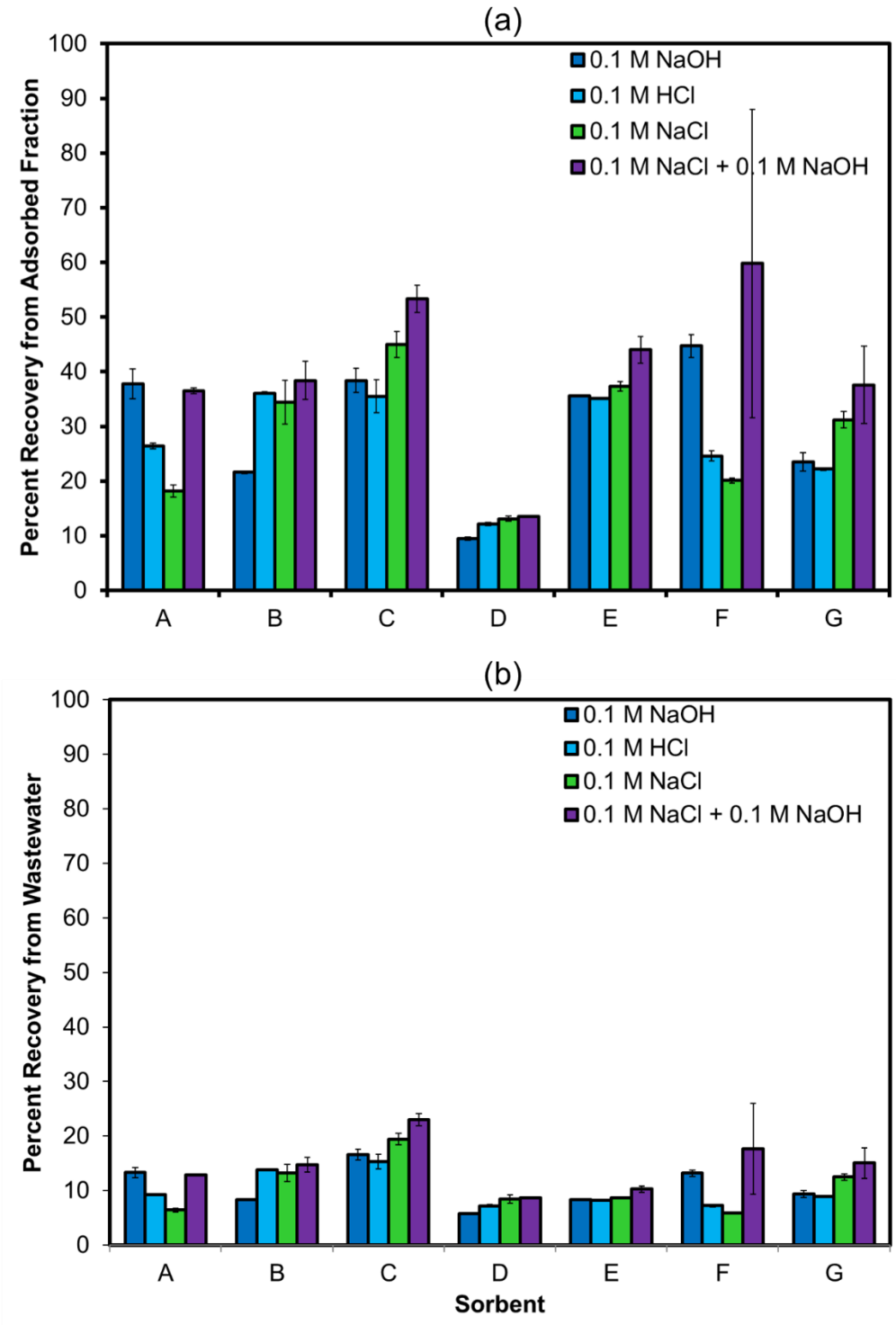

Figure 4-4: Percent recovery of P from the (a) adsorbed fraction on sorbent and (b) original synthetic wastewater solution. P was recovered using basic (blue), acidic (light blue), salt (green) and basic salt (purple) solutions.

Phosphorus recovery from Hybrid IEX sorbent E yielded average recoveries of 3.31, 3.27, 3.47 and 4.10 mg P/g sorbent using NaOH, HCl, NaCl and NaOH + NaCl, respectively; the quantity of P recovered was found to be dependent on the desorption solution used ($F(7) = 20.699$, $p = 0.007$). Application of NaOH recovered 35.6 % P which was not statistically different from the 35.1 and 37.3 % P recovered using HCl and NaCl desorption solutions, respectively (HCl: $t(2) = 4.025$, $p = 0.06$; NaCl: $t(2) = -2.952$, $p = 0.10$). Use of the combination of NaOH + NaCl recovered 44.0 % P from sorbent E, higher than the quantity of P recovered by NaOH ($t(2) = -4.928$, $p = 0.04$) and HCl ($t(2) = -5.216$, $p = 0.035$) and NaCl recoveries ($t(2) = -4.928$, $p = 0.039$). Therefore, the basic salt desorption solutions demonstrated the best recovery from sorbent E.

Recovery from activated alumina sorbent F with NaOH, HCl, NaCl and NaOH + NaCl desorption solutions corresponded to recoveries of 5.27, 2.90, 2.37 and 7.05 mg P/g sorbent F which were not statistically different ($F(7) = 3.379$, $p = 0.135$). Desorption recovered between 20.1 and 59.8 % P through use of the four desorption solutions.

Phosphorus desorption from the Hybrid IEX sorbent G with NaOH, HCl, NaCl and NaOH + NaCl desorption solutions corresponded to recoveries of 3.75, 3.55, 4.99 and 6.02 mg P/g sorbent. The amount of P recovered was found to be dependent on the desorption solution used ($F(7) = 7.539$, $p = 0.04$). Desorption using NaOH and HCl recovered similar quantities of P; NaOH recovered 23.5 % P while HCl recovered 22.2 % P ($t(2) = 1.04$, $p = 0.408$). The use of NaCl recovered 31.2 % P from sorbent G, a recovery that was significantly higher than those obtained using NaOH ($t(2) = -4.864$, $p = 0.04$) and HCl ($t(2) = -8.342$, $p = 0.014$). Phosphorus

recovery using the combination of NaOH + NaCl was variable but on average 37.6% P was recovered from sorbent G; P recovered using the basic salt solution was not significantly different from the quantities liberated by NaOH ($t(2) = -2.761$, $p = 0.110$), HCl ($t(2) = -3.085$, $p = 0.091$) and NaCl ($t(2) = -1.259$, $p = 0.335$). Therefore, recovery using NaCl was the best desorption solution used for recovery from sorbent G; NaOH + NaCl could also prove useful however the results were not as reproducible when compared to NaCl.

Further examination of P recovery from the sorbents provided insight into which chemical desorption solution was best for the different types of sorbents studied. The sorbents that included metal oxides released larger quantities of P with basic and basic salt desorption solutions. Ion exchange sorbents exhibited greater P recovery with desorption solutions containing chloride. In sorbents that incorporate metal oxides, recovery using acidic and basic desorption solutions have proven to be the most effective due to the changes in sorbate and surface charge caused by the change in pH (Chitrakar *et al*., 2006). The pH_{zpc} (zero-point charge) of metal oxides can be in the circumneutral pH range; at pH values above the pH_{zpc}, the surface of the sorbent will become negative (Luster *et al*., 2017) Therefore, the high recoveries obtained with NaOH with the metal oxide sorbents were consistent with the literature as the charge of phosphate becomes more negative at high pH, which would be repelled by the negatively charged sorbent surface. With respect to IEX sorbents, liberation of sorbate (*i.e.* phosphate) occurs when a counter ion exchanges with P at the surface. Chloride is known to be an effective counter-ion for IEX sorbents and has been previously used in regeneration studies (Thorton *et al.*, 2007). Thus, the elevated P recovery using desorption solutions with Cl^- with IEX resins was consistent with theory. The optimal conditions for the exchange between P and Cl- were at

circumneutral pH. Hybrid IEX sorbents consist of a combination of IEX and metal oxides, therefore both mechanisms of recovery could be employed during desorption. The composition of hybrid IEX sorbents could explain why there was an enhancement in recovery observed when the combination of NaOH + NaCl was used for hybrid IEX sorbent E. Therefore, the desorption solutions used to obtain the maximum recoveries from the sorbents were dependent on sorbent composition and mechanism of adsorption.

An examination of the percent P recovered from the sorbent was employed to indicate which sorbent was able to recover the most adsorbed P. Sorbents with higher percent recoveries could have more sorption sites available for subsequent cycles of P adsorption and recovery. There was an observed difference in % P recovered by the sorbents under optimal desorption conditions ($F(25) = 17.429$, $p < 0.001$). The difference in percent recoveries separated the sorbents into two groups. The first group consisted of sorbents B, D and G, which recovered statistically similar amounts of P using the best desorption solution suited for each of the sorbents. The second group included sorbents A, B, C, E, F and G which had optimal recoveries that were statistically similar. The lowest % recovery of adsorbed P was recorded for IEX sorbent D which liberated a maximum of 13.5 % P (NaOH + NaCl) from the sorbent; this indicates that sorbent D had the largest fraction of irreversibly bound phosphorus on the sorbent. With the exception of sorbent D, the remaining sorbents exhibited similar optimal recoveries ranging from of 31 to 60 % adsorbed P.

While recovery from the solid phase of the sorbent was deemed to be important, it does not quantify the total mass of sorbate recovered from the wastewater stream being treated. Retrieving the largest quantity of nutrient from the initial wastewater stream is the goal of nutrient recovery. Hence, the P recoveries from the initial wastewater were calculated (Equation 4-4) for the sorbents and are shown in Figure 4-4b. Sorbents were evaluated in terms of largest recovery of P from the synthetic wastewater stream using NaOH, HCl, NaCl and NaOH + NaCl desorption solutions; the desorption solution used to achieve optimal P recovery from each sorbent is identified in brackets. Sorbents D (NaCl) and E (NaCl + NaOH) had the poorest performance of the sorbents recovering 8.7 and 10.3 % from the synthetic wastewater, respectively. Sorbents A (NaOH), B (HCl, NaCl, NaOH + NaCl), F (NaOH, HCl, NaCl, NaOH + NaCl) and G (NaCl) had midrange recoveries corresponding to 13.3, 14.7, 17.6 and 15.1 %. Ion exchange resin, sorbent C (NaCl, NaOH + NaCl) reclaimed 23.0% P from the wastewater stream. A difference in total P recovered from the initial SWW was observed based on the sorbent used ($F(25) = 8.974$, $p < 0.001$). Through statistical analysis, the sorbents were grouped into categories that recovered similar quantities of P from the SWW; some sorbents were found to overlap in the three categories. The first group, which recovered the least amount of P from the SWW, included IEX sorbents D and B, hybrid IEX sorbents E and G and metal oxide sorbent A. The mid-range group of sorbents included IEX sorbent B, hybrid IEX sorbent E and G, and metal oxide sorbents A and F. The group of sorbents with the highest recoveries included IEX sorbent C and metal oxide sorbent F. When ranked in terms of total P recovery, the sorbent order was C (IEX) ≥ F (activated alumina) ≥ G (IEX), B (IEX), A (granular ferric hydroxide), E (IEX with metal oxide nanoparticles) ≥ D (IEX). In summary, ion exchange resin sorbent C and activated alumina sorbent F were able to recover the largest quantity of P from the wastewater stream.

4.4.4 Recovery Experiments with Alternative Desorption Solutions

Alternative desorption solutions containing competitive ions were evaluated for their potential to increase the driving force of P off specific sorbents. Sorbent A, a granular ferric hydroxide, and sorbent D, an IEX, were tested with the alternative desorption solutions. Past research has shown that iron oxide based sorbents preferentially adsorb carbonate over phosphate (Wilfert *et al.*, 2015). To take advantage of competition effects with the goal of greater P recovery, sorbent A was tested with a 0.1M, 0.5M and 1.0M $NaHCO_3$ solutions, a mixture of 0.5 M $NaHCO_3$ + 0.5 M NaOH (pH 11.7) and a solution of 0.5 M $MgSO_4$. The recoveries using alternative desorption solutions on sorbents A and D were evaluated on the basis of P recovery from the solid phase and total P recovered from the SWW test solution.

The experiments testing the recovery of P using alternative desorption solutions were performed at a later date than initial desorption tests and therefore the potential for changes in P adsorption by sorbent A and D was investigated. In the additional recovery tests, sorbent A adsorbed 11.42 ± 1.27 mg P/g sorbent while sorbent D adsorbed 9.22 ± 0.72 mg P/g sorbent. Hence, the adsorption capacities for sorbent A and D were approximately 19 and 51 % lower, respectively, than that observed in initial desorption testing; mass of P adsorbed by sorbent A and D were significantly different from initial adsorption experiments (A: $t(12) = 3.968$, $p = 0.002$; D: $t(12) = 3.083$, $p = 0.009$). The decrease in adsorption was attributed to changes of the surface of the sorbents from exposure to air as the sorbents used in initial desorption tests were taken from sealed packaging. Due to the change in adsorption, recovery calculations performed for

alternative desorption solutions were expected to be lower because of the reduced quantities of P adsorbed by the sorbents.

The results obtained through treatment of sorbent A with the additional desorption solutions were examined to see if P recovery improved relative to the previously described sorbents. The percent P recovered from the solid phase and from the initial SWW are presented in Figure 4-5a and 4-5b, respectively. Exposure of sorbent A to 0.1, 0.5 M, 1.0 M $NaHCO_3$ resulted in 0.97, 2.01 and 6.91 mg P/g sorbent being desorbed while exposure to the combination of 0.5 M $NaHCO_3$ + NaOH resulted in the liberation of 3.63 mg P/g sorbent. Recovery using 0.5 M $MgSO_4$ was also investigated and resulted in the desorption of 0.68 mg P/g sorbent. Finally, 0.74 mg P/g sorbent A was liberated through use of ultra pure water; ultrapure water was included as a control. Limited P desorption was observed with the use of 0.5 M $MgSO_4$ and 0.1 M $NaHCO_3$ as desorption solutions. The quantities of P that were desorbed by these solutions were not statistically different from that observed when using ultra pure water ($MgSO_4$: $t(2) = 0.417$, $p = 0.717$; 0.1 M $NaHCO_3$: $t(2) = 1.014$, $p = 0.417$) and therefore, the solutions were considered unsuitable as P desorbing agents. Alternatively, increased P recovery was observed with increasing $NaHCO_3$ concentrations ($r = 0.936$, $p = 0.006$). An average of 62 % P was liberated from sorbent A using 1.0 M $NaHCO_3$, which was approximately 46 % more than that which was recovered with 0.5 M $NaHCO_3$ ($t(2) = 5.349$, $p = 0.033$). Therefore, solutions containing 0.5 M and 1.0 M $NaHCO_3$ were found to substantially desorb P from sorbent A.

Recoveries obtained through the application of alternative desorption solutions were further investigated to determine their performance when compared to the original four desorption

solutions. The average percent P recovered from the sorbent and total percent P recovered from sorbent A obtained through the use of the NaOH, HCl, NaCl and NaOH + NaCl desorption solutions are indicated by dashed lines on Figure 4-5a and 4-5b, respectively; 0.1 M NaOH was determined to be the best desorption solution for sorbent A of the four solutions tested. The quantity of P desorbed by $NaHCO_3$ + NaOH was higher than the P liberated using the same concentration of $NaHCO_3$ alone ($t(2) = -5.032$, $p = 0.0037$). When compared to the initial 0.1 M NaOH desorption solution, the quantity of P liberated using the $NaHCO_3$ + NaOH mixture was not statistically different ($t(2) = -4.076$, $p = 0.055$). However, the percent P recovered from the sorbent ($t(2) = -7.454$, $p = 0.018$) and from the initial SWW ($t(2) = -6.206$, $p = 0.025$) were lower when using the combination of $NaHCO_3$ + NaOH due to lower quantity of P initially adsorbed. Recovery from sorbent A using $NaHCO_3$ + NaOH was also compared to the recovery obtained using 1.0 M $NaHCO_3$ and the two quantities were not statistically different ($t(2) = 3.396$, $p = 0.077$). The quantity of P recovered by 1.0 M $NaHCO_3$ was not statistically different from the amount recovered using 0.1 M NaOH ($t(2) = 1.672$, $p = 0.236$. Overall, the percent of P liberated from sorbent A and the percent recovered from the initial SWW both increased by approximately 5 % using 1.0 M $NaHCO_3$ however due to variability and lower initial adsorption, effect on P recovery was not statistically significant.

Sorbent D was chosen for further testing to evaluate the possibility of increased recovery as it was observed to have the highest adsorption capacity yet recovered the smallest fractions of P from both the adsorbed fraction and synthetic wastewater while using the original four desorption solutions. The percent P recovered from sorbent D and from the initial SWW are presented in Figure 4-5a and 4-5b, respectively. Desorption using 0.5 M $NaHCO_3$, 0.5 M

$NaHCO_3$ + 0.5 M NaOH (pH 11.7) and 1.0 M NaOH resulted in the recovery of 7.25, 5.86, and 5.79 mg P/g, respectively. Desorption with ultra pure water was also conducted and resulted in the liberation of 0.02 mg P/g sorbent. While the average mass of P recovered from sorbent D using 1.0 M NaOH was greater than the average mass of P adsorbed, the two amounts were not significantly different and therefore effectively all of the P was desorbed from sorbent D ($t(4) = -0.2195$, $p = 0.837$). The masses of P recovered using $NaHCO_3$, NaOH and the $NaHCO_3$ + NaOH mixture were not statistically different ($F(5) = 4.840$, $p = 0.115$). Overall, use of $NaHCO_3$, NaOH and the $NaHCO_3$ + NaOH mixture recovered around 60 to 100 % of P adsorbed to sorbent D, a significant increase (~70 %) from the recoveries observed with NaCl and NaOH + NaCl ($F(9) = 22.867$, $p = 0.001$); 0.1 M NaCl and the mixture 0.1 M NaOH + 0.1 M NaCl demonstrated the top performance of the four original desorption solutions tested. Therefore, alternative desorption solutions increased the P recovered from sorbent D and thus, increased the P recovered from the initial SWW test solution.

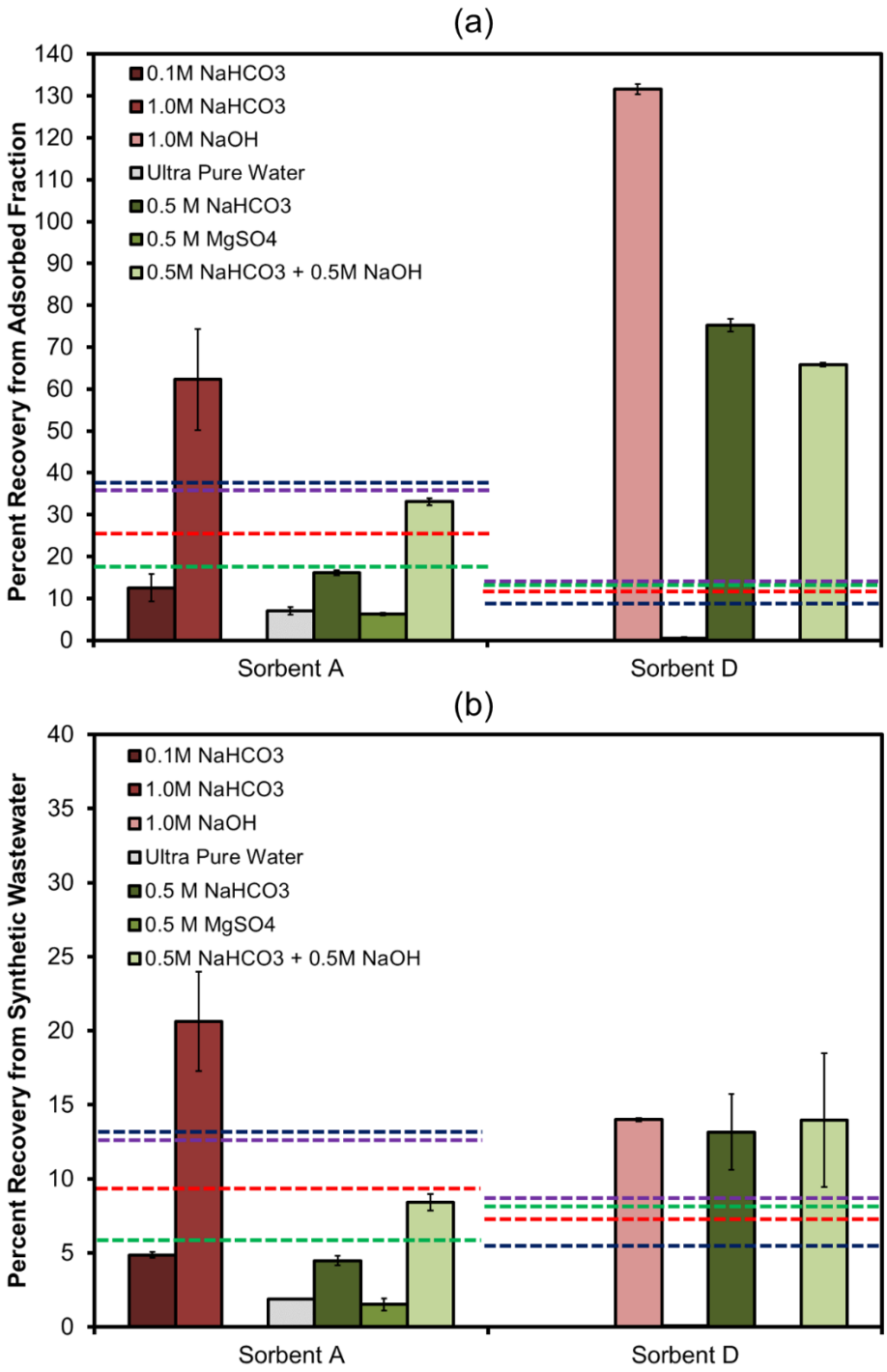

Figure 4-5: Percent recovery of P from the (a) adsorbed fraction on sorbent and (b) synthetic wastewater. To increase driving force, P was recovered using carbonate and magnesium sulfate solutions. Dashed lines indicate percent recovery obtained from desorption using acidic (red), basic (navy), salt (green) and basic salt (purple) solutions.

4.4.5 Implications for Recovery in Practical Use

Additional analysis was conducted to extend the results from batch testing to give insight as to how the sorbents would perform in column applications. In practice, sorbents are typically employed in a series of adsorption columns and hence calculations were performed to predict the sorbent usage rate (SUR, Equation 4-5) and volume of wastewater treated per kilogram of sorbent (V_{WW}, Equation 4-6). Additionally, the estimated mass of P recovered (P_{EST}) from the adsorption column was calculated using the percent recovery obtained from the best desorption solution for the sorbent of focus. Finally, the volume of desorption solution (V_{DS}) required to meet a target desorption effluent concentration for nutrient recovery technologies was calculated. Calculations of P_{EST} and V_{DS} are described in detail below. The column calculations were performed for the three sorbents which demonstrated a characteristic that could contribute to increased phosphorus recovery. Sorbents C (IEX), and F (activated alumina) were chosen on the basis of its potential to recover the largest quantity of P from the SWW, while sorbent A (granular ferric hydroxide) had increased recovery through the application of the alternative desorption solutions. Results from the above calculations for the select sorbents are summarized in Table 4-4 and discussed below.

Ideally, a sorbent would be able to treat a large volume of waste water before the adsorption column is exhausted and hence, the sorbent usage rate (SUR) and volume of wastewater treated (V_{WW}) was calculated for the three sorbents. Using Equation 4 and the fitting parameters obtained from the Freundlich isotherm (Table 4-3), the SUR was calculated for the three sorbents treating a typical domestic wastewater with an influent P concentrations of 5 mg P/L (Metcalf and Eddy, 2003); the V_{WW} treated is the inverse of the SUR. Sorbents A, C and F had SURs of

910, 758 and 1 250 mg sorbent/L wastewater treated, respectively, corresponding to V_{WW} of 1.10, 1.32 and 0.71 L/mg sorbent. The results indicate sorbent C would treat the largest quantity of wastewater before exhaustion of the column. The calculations for SUR and V_{WW} do not consider if the column can be regenerated and used again and as such, the estimates can only be applied to the first cycle of adsorption. Looking to the literature, the SUR values calculated for sorbents A, C and F did not fall within the range of carbon usage rates for a granular activated carbon (GAC) that has been used in pilot tests to remove pharmaceuticals in municipal wastewater; the study reported carbon usage rates ranging between 30 to 100 mg GAC/L wastewater treated (Kårelid *et al*., 2017). This suggests that the sorbent usage rates of the three sorbents may not be reasonable for use in P recovery. As described above, the fitting parameters of the Freundlich isotherm are related and different values for K_F and 1/N can produce the same X values in Equation 4-1 (Vlad, 2015), therefore, the values obtained in Table 4-4 could be improved with further investigation of the sorbents. In addition, the SUR could be lowered, increasing $V_{WW,}$ with regeneration and reuse of the sorbents.

Table 4-4: Sorbent usage rate (SUR) and volume wastewater treated (V_{WW}), estimated P recovered (P_{EST}) and minimum volume desorption solution (V_{DS}) calculations performed for sorbents A (granular ferric hydroxide), C (IEX) and F (activated alumina).

Sorbent	SUR (g sorbent /L)	V_{WW} (L/g sorbent)	P_{EST} (g/kg sorbent)	V_{DS} (L/kg sorbent)
A	0.91	1.10	2.1	21
C	0.76	1.32	2.1	21
F	1.25	0.71	3.5	35

The recovery phase of the adsorption column is also an important indicator of the practicality of a sorbent's use, particularly the amount of desorbing agent needed as chemical requirements

would increase the cost of the process. Hence, the estimated mass of P recovered (P_{EST}) from a hypothetical exhausted column containing 1 kg of sorbent was calculated by multiplying the total mass of P adsorbed by the optimal desorption efficiency obtained by the best desorbing solution. The resulting concentration of the recovery effluent was also considered to be important as it is desirable for the desorption stream to have a target final concentration of 100 mg P/L, the minimum concentration suited for struvite formation (Xie *et al*., 2016). Therefore, a target concentration of 100 mg P/L was set when calculating the maximum volume of desorption solution (V_{DS}); if recovery requires volumes of desorption solutions larger than the V_{DS}, the final recovery effluent concentration would not meet the concentration required for nutrient recovery technologies. Results from these calculations are summarized in Table 4-4 and discussed further below.

Sorbents that require smaller desorption volumes are preferential when evaluating if the sorbents use for nutrient recovery is practical. As predicted by the results of batch testing, sorbents A and C recovered similar quantities of P (2.1 g Pkg sorbent) from the exhausted adsorption column while sorbent C is predicted to recover the largest quantity of P (3.5 g P/kg sorbent).. Due to the quantities of P_{EST} calculated, the V_{DS} calculated for sorbents A, C and F were 21, 21 and 35 L/kg sorbent per recovery cycle. Therefore, the estimated P that can be recovered from the sorbents would have to desorb within the corresponding V_{DS} for the blended recovery stream to have a concentration that meets the 100 mg P/L threshold for nutrient recovery technologies.

In summary, the results of this study provided insight into the impact of sorbent composition on P recovery. When fitting the adsorption data with the Freundlich isotherm, it was evident that

two adsorption mechanisms could have benefits for P removal from wastewater. Metal oxide sorbents were selective for P over IEX sorbents, which could help with P uptake by the sorbent in complex wastewater streams. Ion exchange sorbents were less selective for P but exhibited large adsorption capacities which was shown in adsorption column calculations to be beneficial for the recovery process. Although both sorbents are susceptible to competition, IEX sorbents are more prone to adsorption of any accessible ion. This trait of IEX sorbents can help in P recovery as IEX sorbents demonstrated desorption of P in most solutions containing an appropriate counter-ion. Therefore, both IEX and metal oxide sorbents have potential for use in phosphorus recovery.

4.5 Conclusions

The purpose of this study was to screen commercial sorbents for P adsorption and evaluate recovery of P from the sorbents through chemical desorption. Of 14 commercial sorbents, seven sorbents were able to adsorb practical quantities of phosphate. With respect to sorbent composition, there were no trends were observed in the Freundlich isotherm parameters K_F and 1/N however sorbents which incorporated metal oxides had improved quality of fit to the isotherm over IEX sorbents. Overall, the commercial sorbents with the largest Freundlich capacity factors (K_F) were IEX sorbents B (2.66) and C (2.41) as well as hybrid IEX resin E (2.72).

Phosphorus recovery testing was completed on sorbents A through G using basic, acidic, salt and basic salt solutions. The most effective desorption solution was dependent on sorbent composition; IEX sorbents recovered the most P with NaCl desorption solutions, P was

recovered from metal oxide sorbents using NaOH while hybrid IEX sorbents required a mixture of both desorbing agents to get optimal P recovery. Sorbent F (activated alumina) released the largest fraction of adsorbed phosphorus from the solid phase (54.7 %), followed by sorbent E (43.8 %) and IEX sorbent G (43.0%, IEX). In terms of recovery of phosphate from the initial synthetic wastewater stream, sorbent C and F was found to recover the largest quantity of phosphate from the synthetic wastewater stream, recovering 23 and 17.6 % P, respectively. Overall, both IEX and metal oxide sorbents were proven to have potential for use in phosphorus recovery.

ACKNOWLEDGEMENTS

The authors would like to thank our partners: Water Environment Research Foundation (WERF), Ostara Nutrient Recovery Technologies Inc., Suez Environnement (formally GE Water & Process Technologies), GHD Group (formally Conestoga-Rovers and Associates), Halton Region, York Region and Region of Waterloo. The authors would also like to acknowledge the companies which donated the sorbents for testing.

5.0 Column Testing of Commercial Sorbents for Phosphorus Recovery

5.1 Summary

With wastewater treatment shifting to resource recovery, a method of phosphorus recovery is needed to concentrate P from dilute wastewater streams in treatment plants without enhanced biological nutrient removal. This study evaluates three commercially available sorbents for P adsorption and recovery to generate a concentrated chemical desorption effluent. Sorbents included granular ferric hydroxide (sorbent A) and activated alumina (sorbent B) based sorbents as well as an ion exchange (IEX) resin (sorbent C). After the sorbents were tested for P removal in column tests, chemical desorption solutions were utilized to recover P from the spent sorbents. Recovery from the metal oxide sorbents A and B was conducted using basic (NaOH) and acidic (HCl) solutions while recovery from sorbent C used salt (NaCl) and basic salt (NaOH + NaCl) solutions in addition to acidic and basic solutions. Sorbents were evaluated on the basis of P adsorption as well as recovery from the sorbent and the initial synthetic wastewater (SWW) stream. Sorbent C demonstrated the highest removal of 55 % P from the SWW, while sorbents A and B adsorbed approximately 20 % P. Desorption using NaOH was most effective for sorbents A and B, which were found to recover 21 and 17 % P from the initial SWW. Sorbent C recovered the largest quantity of P (52 %) from SWW with the use of NaCl. Due to its good performance, sorbent C was used to recover P from two wastewater samples. Using NaCl, sorbent C recovered 37 and 16 % of P from secondary and final effluent samples.

KEYWORDS: Nutrient Recovery, Wastewater, Adsorption, Desorption

5.2 Introduction

Typically, phosphorus is removed from waste water to mitigate the effects of eutrophication in receiving waters. Phosphorus removal in traditional wastewater treatment occurs through chemical P removal and enhanced biological nutrient removal where P is taken up into the biosolids (Valsami-Jones, 2001). Traditional nutrient removal in wastewater treatment plants (WWTPs) is slowly being replaced with nutrient recovery technologies such that WWTPs are being renamed as water resource facilities (WRRFs); as of 2015, six WWRFs aim to recover P using struvite crystallization (Latimer *et al*., 2015). Due to P concentrations in domestic wastewater being < 10 mg P/L, nutrient recovery technologies can only be implemented after EBNR where P has been concentrated to suitable levels for struvite crystallization (Ye *et al*., 2017). A method to concentrate phosphorus in a recovery stream is needed for non-EBNR wastewater treatment plants.

Adsorption is a low cost and efficient process for wastewater treatment that can transfer contaminants from the liquid to the solid phase for easy separation (Metcalf and Eddy, 2003; Li *et al.*, 2014; Long *et al.*, 2011). Adsorbents with large adsorption capacities would be beneficial for P recovery since any P adsorbed onto the sorbent is potentially available for recovery. Additionally, adsorbents that have a high selectivity for P may remove significant amounts of P, producing an effluent that could meet strict discharge limits. The sorbents employed in this study, ion exchange resins (IEX) and metal oxides, have been known to demonstrate the features mentioned above and thus have been used in the past to remove contaminants from aqueous solutions. Iron and aluminum (hydr)oxides are known for forming surface complexes with phosphate while IEX resins have large reactive site availability for ions; in wastewater at

circumneutral pH, phosphate exists as $H_2PO_4^-$ and HPO_4^{2-} (Kumar *et al.*, 2014a; Thorton *et al.*, 2007). Metal oxide and IEX resins have the potential for P recovery from waste water.

Liberation of the adsorbed P from the sorbent is necessary to ensure P is recovered into a concentrated recovery stream for struvite crystallization technologies. The type of sorbent will determine whether adsorption is reversible (Rittman *et al*., 2011). Metal oxide sorbents and IEX resins are known to be regenerated easily using simple desorption solutions. Desorption of the adsorbed P has the potential to produce a concentrated P recovery stream suitable for nutrient recovery technologies if the amount of desorption solution used is small. Desorption has been studied for both ion exchange resins and metal oxides with desorption solutions including basic and/or salt solutions, used for metal oxides and hybrid ion exchange resins (Blaney *et al*., 2007; Malyovanny *et al*., 2013); more information on desorption from sorbents can be found in Chapter 4. While desorption has mostly been studied with respect to sorbent regeneration, P recovery in the desorption stream is now being examined. Zhang *et al*. (2013) found that a proprietary hydrated ferric oxide nanocomposite could recover 97 % of P from a dilute wastewater effluent (~ 2 mg P/L); P was desorbed from the sorbent using a NaCl/NaOH binary solution. It was noted that P in the recovery stream was 100x more concentrated than the wastewater effluent tested. Therefore, recovering adsorbed P into a concentrated recovery stream is possible and could be the outcome of desorption from the sorbents used in P recovery.

In this study, column tests were used to investigate the phosphorus adsorption capacity and evaluate the P recovery potential of three commercial sorbents. The sorbents and their corresponding desorption solutions were chosen based on results from batch testing (Chapter 4).

Phosphorus recovery by chemical desorption was evaluated in terms of the percent P recovered from the exhausted adsorption columns, the percent P recovered from the initial synthetic wastewater (SWW) solution as well as the concentration of P in the spent recovery solution. The sorbent that demonstrated the highest potential for P adsorption and recovery in tests with the SWW was used to treat two wastewater samples. The results of this study will provide direction to the wastewater treatment industry when making decisions when selecting appropriate adsorbent and sorbent regeneration technologies for phosphorus removal and recovery.

5.3 Methodology

5.3.1 Commercial Adsorbents

Three commercially available sorbents were used in column testing; the three sorbents demonstrated potential for use in P recovery in a previous study where a variety of sorbents were screened using batch testing (Chapter 4) for P recovery via chemical desorption. The sorbents used in this study were of different compositions and are referred to by an alphabetic code to maintain anonymity of the supplier. Sorbent A is a granular ferric hydroxide sorbent that is marketed for phosphate adsorption. Sorbents B and C are both marketed as sorbents that target non-specific contaminants; sorbent B is an activated alumina sorbent while sorbent C is an ion exchange resin (IEX) with a surface that had been functionalized with dimethylamine.

5.3.2 Synthetic Wastewater

To simulate the complexity of wastewater in terms of ionic composition, a synthetic wastewater (SWW) modified from Jung *et al.* (2005) was employed in column tests. The components of the synthetic wastewater solution included magnesium sulfate ($MgSO_4 \cdot 7H_2O$, Sigma-Aldrich, St.

Louis, MO), calcium chloride ($CaCl_2 \cdot 2H_2O$, Fisher Scientific, Fair Lawn, NJ), sodium bicarbonate ($NaHCO_3$, EMD Chemicals Inc., Gibbstown, NJ), sodium acetate (CH_3COONa, BDH Chemicals, Toronto, ON) and potassium phosphate monobasic (KH_2PO_4) (BDH, VWR International LLC., West Chester, PA); quantities of the individual components are listed in Table 5-1. The synthetic wastewater was prepared using ultra pure water (18.2MΩ, MilliQ) and adjusted to a pH of 7.0 $\pm$ 0.05 using either hydrochloric acid (HCl, EMD Chemicals Inc., Gibbstown, NJ) or sodium hydroxide (NaOH, Sigma-Aldrich, St. Louis, MO). All chemical reagents used in this study were reagent grade or higher.

Table 5-1: Synthetic wastewater recipe adapted from Jung *et al.* (2005).

Compound	**Concentration (mg/L)**
Magnesium Sulfate ($MgSO_4 \cdot 7H_2O$)	24.0
Calcium Chloride ($CaCl_2 \cdot 2H_2O$)	2.4
Sodium Bicarbonate ($NaHCO_3$)	300.0
Sodium Acetate (CH_3COONa)	820.3
Potassium Phosphate Monobasic (KH_2PO_4) (mg P/L)	20.6 ± 1.0

5.3.3 Wastewater Samples

Wastewater effluent samples were collected from two conventional activated sludge municipal wastewater treatment plants in Ontario, Canada. Samples included a secondary effluent sample and a final effluent; the secondary effluent was collected after aeration and before alum addition. The collected samples were stored a 4 ℃ until testing.

5.3.4 Column Experiments

Adsorption column runs were carried out in HDPE columns that were 2 cm in length with a 1.27 cm inner diameter. The influent was pumped into the column in an up-flow direction using peristaltic pumps, MasterFlex L/S Multichannel Pump, Model 7535 - 04 (Cole-Parmer, Montreal, QC). Influent flow rates and sorbent weights are summarized in Table 5-2. Effluent samples from the columns were collected and analyzed for total P concentrations.

Phosphorus recovery was performed similarly by passing the desorption solution in an up-flow direction. The desorption solutions that were tested consisted of 0.5 M NaOH, 0.5 M HCl, 0.5 M NaCl and 0.5 M NaOH + 0.5 M NaCl. The desorption solution used in the experiments depended on the sorbent being tested. Metal oxide sorbents adsorb P through surface complexation which is pH dependent (Chitrakar *et al*., 2006) therefore, desorption solutions consisting of 0.5M HCl and 0.5M NaOH were utilized in P recovery from sorbent A and B. Recovery from IEX sorbent C require an ion that competes for the P adsorption site, therefore, desorption solutions of 0.5M NaCl and 0.5M NaCl + NaOH were tested in addition to the acidic and basic solutions. Composite samples were collected approximately every 5 minutes throughout the recovery phase except for recovery from sorbent C with NaOH and NaOH + NaCl desorption solutions in which composite samples were taken approximately every 20 minutes. Samples collected during desorption were analyzed for total phosphorus concentration.

A similar adsorption and recovery protocol was used in experiments with wastewater samples. Wastewater experiments were completed after the identification of the sorbent and corresponding desorption solution that demonstrated the greatest potential for P recovery.

Table 5-2: Average influent flow rate, sorbent weight and bed volume for the three commercial sorbents used in adsorption column tests. Freundlich capacity and intensity factors from previous work (Chapter 4) are also listed.

	Sorbent A	Sorbent B	Sorbent C
Sorbent Type	Granular ferric hydroxide	Activated alumina	Ion exchange resin
Sorbent Mass (g)	2.87 ± 0.04	3.66 ± 0.10	2.14 ± 0.05
Flow Rate (mL/min)	2.06 ± 0.24	2.06 ± 0.27	2.09 ± 0.09
Freundlich Capacity Factor (K_F)	2.38	1.25	2.47
Freundlich (1/N)	0.52	0.65	0.61
Desorption Solutions Tested	NaOH, HCl	NaOH, HCl	NaOH, HCl, NaCl NaOH + NaCl

5.3.5 Phosphorus Analysis

Total P (TP) was measured using Inductively Coupled Plasma Optical Emission Spectroscopy (ICP-OES). Intensities were measured in axial mode at a wavelength of 213.617 nm with the viewing height set to 15 mm above the induction coil; the flow rate of the sample pump was set to 2 mL/min, argon was used as the plasma and auxiliary gas, set to 15 and 0.5 L/min, respectively. In wastewater samples, reactive P (RP) concentrations were measured using ascorbic acid colorimetric determination at 660 nm as per method G-103-93 Rev. 10 (Seal Analytical, WI) in accordance to Method 4500 P.E in Standard Methods (Standard Methods, 2005). Reactive and total P were measured wastewater samples and non-reactive P (nRP) concentrations were calculated by difference between TP and RP.

Calibration solutions were prepared each day of analysis using KH_2PO_4 in ultrapure water (18.2MΩ, MilliQ). A certified reference material (H_3PO_4, Lot BCBM9148V, 1002 ± 4 mg P/L) purchased from Sigma Aldrich was used to prepare P standards included in all runs for quality

assurance. The method detection limits of the colorimetric and ICP-OES methods were 2 and 25 µg P/L, respectively (Ateeq, 2015).

5.3.6 Data Analysis

Breakthrough curves that presented the effluent concentration divided by the initial influent concentration (C/C_o) over the number of bed volumes of wastewater treated were prepared. The number of bed volumes (BV) was calculated using Equation 5-1

$$BV = V_C (Q\ t)^{-1} \quad (5\text{-}1)$$

where t is the time of sample (min), V_C is the volume of the column occupied by the sorbent (mL) and Q is the flow rate of the influent (mL/min). The total mass of phosphorus adsorbed was calculated using the area under the breakthrough curve.

Composite samples were taken over the duration of the recovery phase of each column and therefore the recovered P was calculated as the cumulative sum of the product of the P concentration of the desorption solution and the volume of the desorption sample. The recoveries of phosphorus from the sorbent (Equation 5-2) and the initial synthetic wastewater (Equation 5-3) were calculated:

$$R_S = (M_{PD}/M_{PA}) \times 100\ \% \quad (5\text{-}2)$$

$$R_{WW} = (M_{PD}/M_{PWW}) \times 100\ \% \quad (5\text{-}3)$$

where M_{PD} is the mass of desorbed P, M_{PA} is the mass of adsorbed P and M_{PWW} is the initial mass of P in the synthetic wastewater; all expressed in milligrams.

Statistical analysis of the sorbents was conducted using ANOVA and T-tests. Results of ANOVA and T-tests are indicated by reporting the result of the F or t value, respectively, as well as the corresponding *p* value; degrees of freedom of the statistical test are reported in brackets.

5.3.7 Breakthrough Modelling

The Clark Model (Clark, 1987) is a simple model based on mass-transfer and the Freundlich isotherm. The generalized equation used to fit to the breakthrough profiles is shown in Equation 5-4

$$C = \left(\frac{C_i^{n-1}}{1 + Ae^{-rt}}\right)^{1/n - 1} \quad (5\text{-}4)$$

where C is the concentration of P in the aqueous phase (mg P/L), C_i is the initial P concentration (mg P/L), n is the Freundlich intensity parameter (unitless), t is time (minutes). The term A is dependent on breakthrough time (t_b) and breakthrough concentration of P (C_b) and is calculated using Equation 5-5.

$$A = \left(\frac{C_i^{n-1}}{C_b^{n-1}} - 1\right) e^{rt_b} \quad (5\text{-}5)$$

The term r was calculated (Equation 5-6) as a function of the mass-transfer coefficient (K_T), the flow of the solvent (G_s) and velocity of the adsorption zone (V) to the Freundlich intensity parameter.

$$r = V\left(\frac{K_T}{G_S}\right)(1 - n)^{-1} \quad (5\text{-}6)$$

The full derivation of the model is reported in Clark (1987).

In this study, the Clark model was heuristically fit to the breakthrough profiles by modifying the values for term A and r to minimize the sum of squared errors (SSE, Equation 5-7) between the model and the data.

$$\text{SSE} = \sum_{i=1}^{n} (C_{e,experimental} - C_{e,model})_i^2 \quad (5\text{-}7)$$

5.4 Results and Discussion

5.4.1 Column Adsorption Testing

The column tests were designed to assess the adsorption and subsequent desorption of P from the sorbents. An ideal sorbent for P recovery would adsorb large quantities of P which would then be chemically desorbed into a highly concentrated recovery stream suitable for nutrient recovery technologies. The sorbents investigated in this study were screened during batch testing (Chapter 4) and each was shown to remove and recover P in a synthetic wastewater (SWW) solution. In addition, the sorbents included in this study were chosen for characteristics, described below, that could be beneficial for P recovery in wastewater.

To further investigate the feasibility of using the sorbents for P recovery, column testing with SWW was conducted to establish loading capacities and removal capabilities of three commercial sorbents. To quickly load the sorbent columns with large quantities of P, the initial P concentration (C_o) of the SWW was 20 mg P/L, which is higher than typical concentrations found in wastewater effluents. Breakthrough curves obtained by column tests with the commercial sorbents are shown in Figure 5-1. The breakthrough curves were heuristically fit with the Clark model to help compare the concentration profiles (Clark, 1987). Sorbents were evaluated on P removal efficiency and bed volumes of SWW treated at breakthrough ($0.1C_o$), nearing exhaustion of the sorbent ($0.5C_o$) and exhaustion ($1.0C_o$). Table 5-3 summarizes mass and percent P removals as well as loading capacities of the sorbents tested; mass and percent removals were calculated for the duration of the column test (until sorbent was exhausted). The

results of the experiments and the evaluation of each sorbent's P removal performance are subsequently discussed.

Granular ferric oxide sorbent A was included in column tests because of its high affinity for phosphate. The breakthrough profile of Sorbent A is presented in Figure 5-1a. Effluent P concentrations averaged $0.1C_o$ after approximately 37 BVs, removing an average of 95.4 ± 1.6 % P. Effluent P concentrations sharply increased to $0.5C_o$ by approximately 165 BVs; 68.2 ± 4.4 % P was removed by 153 BVs. Increased initial effluent P concentrations is potentially be due to short-circuiting in the column. The column was determined to be exhausted by 1035 BVs. The breakthrough curve obtained from Sorbent A was described well by the Clark model (SSE = 786.71, $R^2 = 0.831$). At exhaustion, adsorption onto sorbent A removed 15.7 mg P and had an average P loading of 5.45 mg P/g sorbent. In a study by Chitrakar *et al.* (2006), synthetic iron oxides goethite and akageneite demonstrated higher P loading of 10 mg P/g and at lower equilibrium P concentrations (0.3 mg P/L). In another study, three iron oxide based sorbents were found to have maximum P loadings of ranging from 61 to 98 mg P/g (Kunaschk *et al.*, 2015). The loading capacity obtained in this study was less than those observed in other studies and may be due to short circuiting of the column and to the presence of competing ions (*e.g.* carbonate) in the SWW. During column testing, Sorbent A removed 43.4 ± 4.7 % P that passed through the adsorption column.

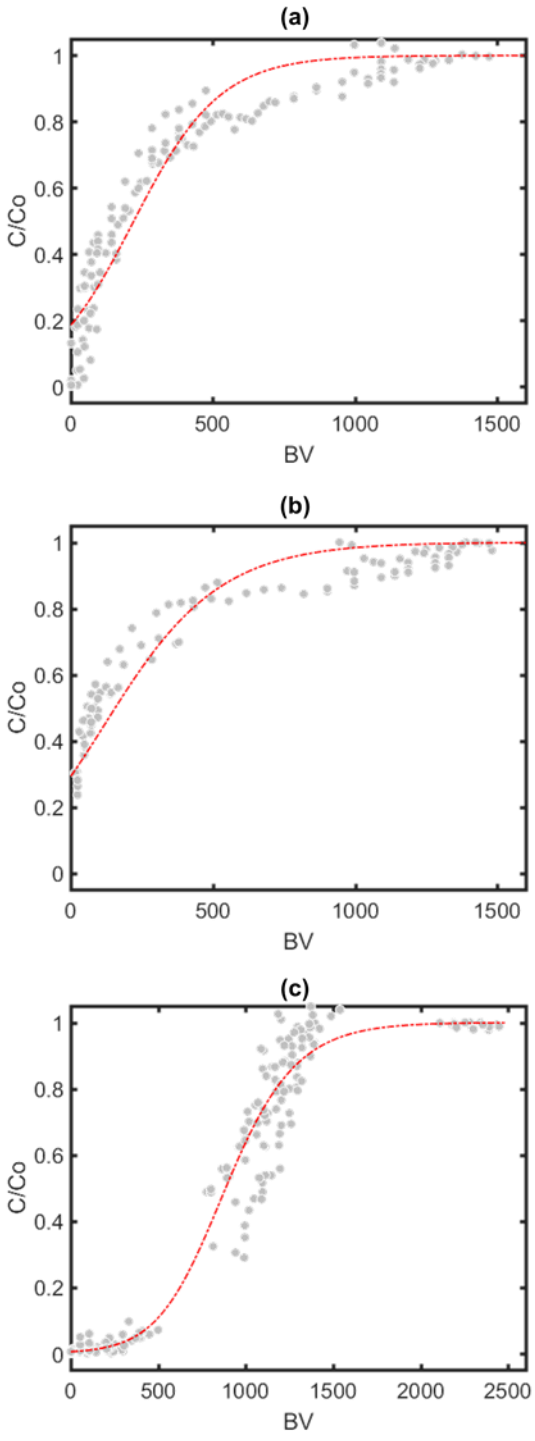

Figure 5-1: Breakthrough curves fit with Clark Model (red dashed line) for (a) granular iron oxide Sorbent A (SSE = 786.71, R^2 = 0.831), (b) activated alumina Sorbent B (SSE = 1849, R^2 = 0.252) and (c) IEX Sorbent C (SSE = 859.34, R^2 = 0.952).

Table 5-3: Percent phosphorus removed when column effluent P concentration is 10%, 50% and 100% of the influent concentration (C_o = 20.6 mg P/L). Average mass of phosphorus removed, sorbent loading after exhaustion ($1.0C_o$) and Clark fitting parameters are also reported. The $0.1C_o$ effluent threshold was not met by sorbent B therefore, percent removal is not reported.

Sorbent		A	B	C
Number of Trials		7	6	21
% Removed ($0.1C_o$)		95.4 ± 1.6	--	96.8 ± 0.9
% Removed ($0.5C_o$)		68.2 ± 4.4	69.4 ± 1.4	81.4 ± 3.9
% Removed ($1.0C_o$)		43.4 ± 4.7	23.4 ± 3.2	64.0 ± 5.1
Mass Removed (mg)		15.7 ± 4.5	15.3 ± 3.4	42.2 ± 5.3
Loading (mg/g)		5.45 ± 1.57	4.19 ± 0.95	19.7 ± 2.4
Clark Model Fitting Parameters	**A**	3.77	0.94	29.98
	r	4.5×10^{-3}	3.8×10^{-3}	3.7×10^{-3}

Sorbent B, an activated alumina based sorbent, demonstrated high P adsorption in batch test studies (Chapter 4) and therefore were also included column testing. The breakthrough profile for sorbent B is shown in Figure 5-1b. Effluent P concentrations increased immediately after the pump was activated; effluent P concentration after 15 BVs was $0.24C_o$. Phosphorus concentrations increased to $0.5C_o$ by 82 BVs, removing 69.4 ± 1.4 % P from the SWW. The column was exhausted at 1150 BVs, respectively. Fitting the breakthrough profile for sorbent B to the Clark model produced poor results (SSE = 1849, R^2 = 0.252). The poor fit to the Clark model could be due to the steep increase in P measured in the adsorption column effluent, followed by a slow increase after 500 BVs until exhaustion of the column which indicates two types of adsorption are potentially occurring; studies have proposed that metal oxide sorbents

that contain Al can remove P via surface complexation, ion exchange and precipitation (Li *et al.*, 2016). At exhaustion, sorbent B removed 15.3 mg P from the test solution which resulted in a P loading capacity of 4.19 mg P/g sorbent. The loading capacity in this study was similar to a study using activated alumina to adsorb P from a membrane bioreactor which observed a loading capacity of 5 mg P/g sorbent (Genz *et al*., 2004). The loading capacity observed for sorbent B was found to lie between the loading capacities observed for two aluminium hydroxide based sorbents which had loading capacities of 6.45 and 1.24 mg P/g sorbent (Chen *et al.*, 1973; Anderson and Malotky 1979). At exhaustion, adsorption onto the column of sorbent B removed 23.4 ± 3.2 % P.

Sorbent C (IEX) demonstrated the highest removal and recovery of P during batch testing and hence was included in the column test experiments. As shown in Figure 5-1c, P effluent concentrations were low throughout the first 350 BVs, removing 96.8 ± 0.9 % P. Effluent P concentrations slowly increased to $0.5C_o$ by approximately 910 BVs at which 81.4 ± 3.9 % P was removed by sorbent C. Column exhaustion occurred around 1320 BVs. The breakthrough curve for sorbent C fit well to the Clark model (SSE = 859.34, R^2 = 0.952). At exhaustion, sorbent C removed 42.2 mg P corresponding to a P loading of 19.7 mg P/g sorbent. The P capacity of sorbent C after exhaustion was higher than the range in capacities observed by Liu *et al*. (2016) who studied P removal using an IEX from an anaerobic membrane bioreactor effluent; in the study loading capacities ranged from 6 to 11 mg P/g sorbent. Loading capacities observed by Liu *et al*. may have been lower due to the presence of higher concentrations of competing ions in the anaerobic membrane bioreactor effluent when compared to the SWW test solution. In total, sorbent C removed 64.0 ± 5.1 % P that passed through the adsorption column.

Percent P removal and BVs of SWW treated at breakthrough (0.1Co) during treatment with the three sorbents were analyzed. The trend observed in increasing BVs of SWW treated of the three sorbents at breakthrough was sorbent B << sorbent A < sorbent C. As described above, effluent from the sorbent B column was not observed to go below $0.24C_o$ over the duration of the test and therefore percent removal and number of BVs SWW treated was not quantified. The number of BVs SWW treated was higher for sorbent C (350 BVs) than sorbent A (40 BVs) ($t(7) = -17.10$, $p < 0.001$). Sorbents A and C removed 95.4 and 96.8 % P when effluent P concentrations were $0.1C_o$ ($t(7) = -1.373$, $p = 0.212$). Sorbent C treated the largest volume of SWW before breakthrough was observed.

Percent P removal and BVs of SWW treated when effluent P concentration were $0.5C_o$ during treatment with the three sorbents were analyzed. The volume of SWW treated was dependent on the sorbent used ($F(18) = 135.25$, $p < 0.001$). Sorbents A and B treated 165 and 82 BVs of SWW, respectively, when effluent P concentrations were $0.5C_o$ ($p < 0.001$). An average of 911 BVs of SWW was treated by sorbent C when effluent P concentration were $0.5C_o$ ($p < 0.001$). Therefore, when effluent P concentrations were $0.5C_o$, the trend observed in increasing BVs of SWW treated was sorbent B < sorbent A < sorbent C. The percent P removed was also dependent on the sorbent used ($F(18) = 135.254$, $p < 0.001$). Percent P removed by sorbent A and B were similar, averaging 70 % P removed ($p = 0.841$) while sorbent C removed approximately 80 % P ($p < 0.001$). Therefore, sorbent C treated the largest volume of SWW when effluent concentrations met the $0.5C_o$ threshold.

At exhaustion ($1.0C_o$), the trend in increasing BVs of wastewater treated was sorbent A ≈ sorbent B < sorbent C ($F(24) = 11.898$, $p < 0.001$). Sorbents A and B treated approximately 1030 and 1150 BVs of SWW prior to exhaustion; due to variability in the tests, the average BVs treated were statistically similar ($p = 0.246$). Sorbent C treated an average of 1320 before exhaustion of the column ($p < 0.001$). Overall, sorbent C treated a larger volume of SWW compared to sorbents A and B.

Sorbent P loadings were compared to determine which of the three sorbents removed the largest quantity of P after saturation of the sorbent. The calculated P loading onto metal oxide based sorbents A and B were similar ($t(11) = 1.769$, $p = 0.107$). Similarities in P loading could be due to both the sorbents being metal oxide based with specific surface areas in the range of 230 to 300 m^2/g; adsorption by metal oxide sorbents occur via surface complexation. The ion exchange Sorbent C demonstrated significantly higher removals and P loadings when compared to sorbents A and B. Sorbent C adsorbed over 2.5 times more P than sorbents A and B (A: $t(12) = -12.82$, $p < 0.001$; B: $t(13) = -14.90$, $p < 0.001$). The P loading of sorbent C was almost 4 times higher than the other two sorbents (A: $t(16) = -18.07$, $p < 0.001$; B: $t(21) = -23.95$, $p < 0.001$). Overall, sorbent C displayed the best removal performance when compared to sorbents A and B.

The Clark model was fit to the breakthrough profiles to further compare the three sorbents. The Clark model is a simplified model developed to predict the performance of granular activated carbon adsorption columns for the removal of organic compounds however it has been shown to perform well for a variety of systems and under different conditions (Clark, 1987; Xu *et al*., 2013). Of the three sorbents, sorbent C was best described by the Clark model. The good fit was

attributed to the high adsorption capacity of the sorbent capturing the P onto the column resulting in low effluent P concentrations in the first section of the breakthrough curve and giving the concentration profile the “S” shape typically observed. Sorbents A and B both adsorbed less P, with effluent P concentrations detected within minutes of tests being initiated. The duration of low P concentration prior to breakthrough was short for sorbent A and not observed in the breakthrough profile of sorbent B and hence, the shapes of the concentration profiles deviated from what is normally observed in adsorption tests. In a review of mathematical models used to describe fixed-bed adsorption columns, it was noted that there is no model that can accurately describe a system when the breakthrough curve deviates from the expected shape (Xu *et al*., 2013). To improve the fit of sorbent A and B data to a model, the column length would need to be increased or the influent P concentration decreased to possibly capture the typical breakthrough profile curve. Therefore, the goodness of fit to the Clark model is dependent on adsorption capacity of the sorbent as well as column test design.

For more insight into the different removal performances demonstrated by the sorbents, the Clark model fitting parameters were examined. The term A (Equation 5-5) is related to the time and concentration of breakthrough while r (Equation 5-6) relates to the velocity of the adsorption zone and the mass transfer coefficient. The A and r values fit to the breakthrough column for the three sorbents are report in Table 5-3. The trend observed for increasing r value was sorbent C < sorbent B < sorbent A. The low A and r values can explain the poor fit of the Clark model to the breakthrough profile of sorbent B. The r value indicates that mass transfer coefficient is low, which is consistent with the initial rapid increase in P concentration at the start of the test and slow increase in P concentration before exhaustion of sorbent B. The trend in increasing A value

observed was sorbent B < sorbent A < sorbent C and agreed with the trend observed for the increasing number of BVs of SWW treated until breakthrough.

5.4.2 Phosphorus Recovery

In terms of P recovery, a high adsorption capacity of a sorbent is only beneficial if the adsorption can be reversed. Therefore, recovery of the P adsorbed by the three sorbents was investigated using chemical desorption. During the recovery phase, composite samples were collected over the duration of desorption. The total P recovered from the sorbent was calculated by summing the products of the P concentration and volume of each sample taken. The P concentrations of the collected samples from the different sorbents and desorption solutions are presented in Figure 5-5. The mass and percentage of P recovered with the three sorbents are summarized in Table 5-3. The recovery of P from the three sorbents using the different desorption solutions was evaluated on the basis of the quantity of P recovered from the adsorption column. The results obtained in recovery experiments are presented and discussed below.

The recovery from sorbent A using acidic and basic desorption solutions was examined to determine the quantity of P recovered from the spent adsorption column and to evaluate the performance of the two recovery solutions. Figure 5-2a presents the P concentrations in the recovery effluent versus BV for two trials of 0.5M NaOH (red) and 0.5M HCl (blue) desorption. In trials using 0.5 M NaOH, the effluent P concentrations reached a maximum within the first 5 BVs of desorption (average [P] = 450 mg P/L) and quickly decreased to less than 10 mg P/L after 38 BVs. In trials using 0.5 M HCl, the effluent P concentration increased above 100 mg P/L around 6 BVs, further increased to approximately 130 mg P/L by 9 BVs and then remained around 100 mg P/L for an additional 60 BVs. After 75 BVs, the P concentrations slowly

decreased but remained above 10 mg P/L for the duration of the desorption phase. In total, 14.1 and 20.5 mg P were desorbed from sorbent A using NaOH and HCl, respectively, corresponding to recoveries of 90 and 95 % which were not statistically different ($t(2) = -4.71$, $p = 0.13$). Therefore, over 90 % of P adsorbed by sorbent A could be recovered through use of acidic or basic desorption solutions.

Desorption of P from activated alumina sorbent B was investigated using acidic (0.5 M HCl) and basic (0.5 M NaOH) desorption solutions. The effluent P concentrations of desorption solution used are shown versus BV in Figure 5-2b. Using 0.5 M NaOH, effluent P concentrations increased to an average of 530 mg P/L after 6 BVs of desorption solution and then decreases to approximately 90 mg P/L by 23 BVs. Phosphorus concentrations in the NaOH desorption effluent continued to slowly decrease for the remaining time of the recovery test. The P concentrations in the effluent remained above 10 mg P/L until around 60 BVs of desorption solution had passed. Phosphorus concentrations in the HCl desorption effluent were also observed to peak however the highest effluent P concentration was 336 mg P/L which was observed after ~ 6 BVs. In total, NaOH and HCl desorption solutions liberated 18.4 and 14.0 mg P from Sorbent B, respectively, with NaOH recovering more P than HCl ($t(2)=60.9$, $p < 0.001$). The phosphorus recoveries were estimated as 120 and 91 % for NaOH and HCl. Desorption using NaOH recovered larger quantities of P than adsorbed by Sorbent B, however the mass desorbed was not statistically different from the mass adsorbed by sorbent B ($t(5) = 2.235$, $p = 0.07$). Overall, almost all the adsorbed P was recovered from sorbent B with the NaOH desorption demonstrating better recovery.

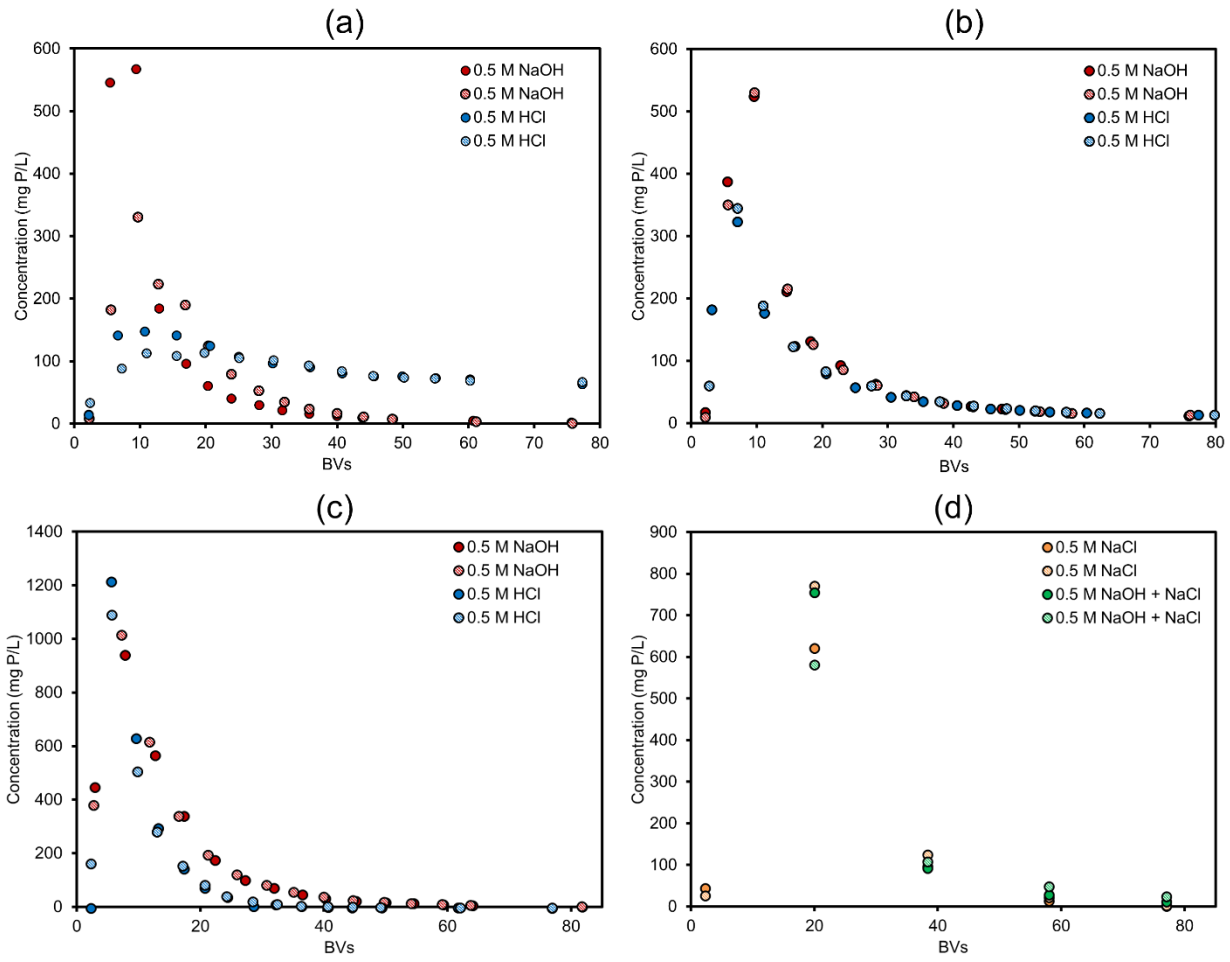

Figure 5-2: Phosphorus concentration of desorption solution over desorption BVs obtained using 0.5 M NaOH (red), 0.5 M HCl (blue) for (a) granular iron oxide sorbent A, (b) activated alumina sorbent B and (c) IEX sorbent C. Desorption solutions 0.5 M NaCl (green) and 0.5 M NaOH + NaCl (orange) were also used with (d) sorbent C. The results from both desorption trials are shown.

Table 5-4: Mass and percent P recovered from sorbents A, B and C using chemical desorption solutions. Bed volumes of the desorption solution required to liberate 90 % recoverable P from the sorbents and calculated final concentration of the blended recovery solution (mg P/L) are also reported.

Sorbent	A		B		C			
Desorption Solution	0.5M NaOH	0.5M HCl	0.5M NaOH	0.5M HCl	0.5M NaOH	0.5M HCl	0.5M NaCl	0.5M NaOH + NaCl
Number of Trials	2	2	2	2	2	2	8	4
Mass Recovered (mg)	14.1 ± 1.9	20.5 ± 0.5	18.4 ± 0.1	14.0 ± 0.1	32.8 ± 0.24	21.8 ± 0.6	40.3 ± 5.3	44.5 ± 8.1
% Recovered	90 ± 12	95 ± 1	120 ± 1	91.3 ± 0.4	78 ± 1	52 ± 1	96 ± 13	106 ± 20
Blended Recovery Concentration (mg P/L)	180 ± 29	80 ± 3	124 ± 3	65 ± 1	411 ± 39	468 ± 20	382 ± 59	362 ± 52
Average BVs	27	95	53	78	29	17	29	38

Desorption with acidic (0.5 M HCl), basic (0.5 M NaOH), salt (0.5M NaCl) and basic salt (0.5 M NaOH + NaCl) solutions was investigated to determine which solution would best recover phosphorus from Sorbent C. In trials with NaOH and HCl (Figure 5-2c), effluent P concentrations peaked between 3 and 5 BVs with concentrations of 982 and 1160, respectively. The effluent P concentrations in trials using NaCl and NaOH + NaCl peaked at 700 and 671 mg P/L, respectively, around 13 BVs. Overall desorption using basic, acidic, salt and basic salt solutions liberated 32.8 (77.9%), 21.8 (51.8%), 40.3 (95.5%) and 44.5 (105 %) mg P from Sorbent C, respectively.

Recovery results obtained from desorption of P from Sorbent C using the four desorption solutions were further investigated to determine which solution was best suited for P recovery. There was a statistical difference in % P recovered by sorbent C with the different desorption conditions ($F(15) = 7.997$, $p = 0.003$). Despite higher P concentrations in the recovery stream, HCl recovered 26 % less P than NaOH ($t(2) = 25.204$, $p = 0.002$). Comparing NaOH and NaOH + NaCl desorption solutions, NaOH recovered around 22 % less P than the combination of NaOH+ NaCl ($t(3)= -2.88$, $p = 0.03$). There was no statistical difference between the quantities of P recovered through desorption using NaCl and NaOH + NaCl solutions ($t(4) = -0.95$, $p = 0.39$). Results from the basic, salt and basic salt desorption tests show that that introducing Cl^- to exchange with phosphate on the surface of the sorbent may be the more effective way to recovery P and regenerate the sorbent. Using NaCl was deemed to be preferential to NaOH + NaCl since there would be additional costs associated with subsequent pH readjustment after the addition of NaOH. Therefore, 0.5 M NaCl solution proved to be the favoured desorption solution due to its high P recovery and lower chemical cost.

Recovery efficacy with respect to producing a concentrated feedstock for nutrient recovery technologies was also investigated for the three sorbents. The phosphorus concentration in the desorption solutions all exceeded the 100 mg P/L threshold required for some nutrient recovery technologies during the recovery phase however, the highest concentrations were normally at the beginning of the desorption where less than 50 % of the total recoverable P had been released from the sorbent. Liberation of over 90 % recoverable P from the sorbent is desirable to minimize loss of P and maximize the regeneration of the sorbent for reuse. Therefore, to evaluate the final concentration of the blended desorption effluent, a target of 90 % of total recoverable P was set. The concentration of the blended desorption effluent was calculated by dividing the cumulative mass P recovered by the cumulative desorption volume required to liberate 90 % recoverable P. The final desorption effluent concentration calculated for the three sorbents are reported in Table 5-3 and discussed below.

The final concentration of the blended recovery solution using NaOH and HCl desorption solutions were examined for granular ferric hydroxide sorbent A (Table 5-3). Using 0.5 M NaOH and 0.5 M HCl, 90 % of recoverable P was liberated in approximately 27 and 95 BVs, respectively. The resulting concentrations of the blended recovery solutions were 180 mg P/L (NaOH) and 80 mg P/L (HCl). The concentration of the HCl recovery solution effluent was below the 100 mg P/L concentration cut off needed for nutrient recovery technologies. Therefore, use of NaOH desorption solution on sorbent A produced a recovery effluent with a concentration suitable for nutrient recovery.

The concentrations resulting from NaOH and HCl desorption solutions were also examined for activated alumina sorbent B. During recovery of sorbent B (Table 5-3), 90 % of the recoverable P was desorbed in approximately 53 and 78 BVs using 0.5 M NaOH and 0.5 M HCl, respectively. The final P concentration of the blended NaOH and HCl recovery solutions corresponded to 124 and 65 mg P/L. The concentration of the HCl desorption solution after P recovery did not meet the concentration threshold for nutrient recovery technologies. Therefore, NaOH proved to produce the better desorption effluent for P recovery technologies from sorbent B.

Concentration of the blended recovery effluents obtained using NaOH, HCl, NaCl and NaOH + NaCl desorption solutions on sorbent C were analyzed (Table 5-3). The four desorption solutions recovered 90% of the P adsorbed to sorbent C with final P concentrations of the blended effluent ranged from 362 to 469 mg P/L. Desorption of 90 % recoverable P from sorbent C was collected in 29 and 17 BVs of NaOH and HCl desorption solutions, respectively. Desorption of 90 % recoverable P was achieved in 29 and 38 BVs for NaCl and NaOH + NaCl desorption solutions. All four desorption solutions produced an effluent that is a concentration suitable for nutrient recovery.

The number of desorption BVs needed to recover 90 % P from the sorbents were examined in the desorption solutions that produced effluent concentrations that met the threshold for nutrient recovery technologies. The final concentration of the blended recovery solution is a result of the cumulative mass of P liberated and total volume of desorption solution used. A low volume requirement, low BVs, is beneficial as it will lower the chemical demand needed and thus, lower

the cost of the recovery process. Of the sorbents, sorbent B required the largest volume of desorption solution (53 BVs NaOH) to recover 90 % adsorbed P. Sorbent A (NaOH) and sorbent C (NaOH, NaCl, NaOH + NaCl) required desorption volumes between 27 and 38 BVs. Recovery from sorbent C using HCl required the smallest volume of desorption solution, desorbing 90 % of recoverable P in 17 BVs.

Using the adsorption and recovery results for the three sorbents it is possible to identify which sorbent has the greatest potential for P recovery. From the initial SWW, IEX Sorbent C removed larger quantities of P (64.0 %) over metal oxide Sorbents A (43.44 %) and B (23.4 %). While P recoveries from the surface of sorbents A and B were > 90 % during recovery tests, initial P adsorption demonstrated by sorbent A and B were low, therefore overall P recoveries from the initial SWW test solution were approximately 39 % and 21 %, respectively. Sorbent C proved to be stable under all four desorption solutions tested. Phosphorus recoveries from sorbent C were > 95 % in desorption solutions containing NaCl. Desorption of P from sorbent C using NaCl also required a low volume of desorption solution to recover ~90 % of the total desorbed P and produced a desorption effluent of a concentration suitable for P recovery. With its high adsorption capacity and the ability to recover > 95 % of P adsorbed, sorbent C recovered approximately 61 % from the initial SWW test solution. Of the three sorbents tested, sorbent C proved best suited for P recovery under the conditions tested.

5.4.3 Real Wastewaters

Phosphorus adsorption from two wastewater samples was investigated to evaluate the performance of sorbent C with a more complex water matrix. The performance of a sorbent

when treating real wastewater could change due to competition by higher concentrations of other species that could also adsorb onto the sorbent. Ion exchange resins, such as sorbent C, are non-selective and will adsorb any anions available in the wastewater stream. The two municipal wastewater samples used for testing with sorbent C, consisted of a secondary effluent sample that was collected after the aeration basin and before chemical P removal, and a final effluent sample; the samples were collected from different wastewater treatment plants. The secondary effluent had an initial TP concentration of 0.81 ± 0.09 mg P/L with 0.54 ± 0.10 mg P/L in the reactive P (*i.e.* orthophosphate) form. The final effluent had an initial TP concentration of 0.21 ± 0.02 mg P/L, which consisted entirely of reactive P as the measured TP and RP (0.18 ± 0.02 mg P/L) concentrations of the final effluent were not statistically different ($t(8) = -1.299$, $p = 0.23$). The results of P adsorption by sorbent C from the wastewater samples are presented and discussed in the subsequent text.

Adsorption results from treating secondary effluent with sorbent C are presented in the breakthrough curve in Figure 5-3a. Phosphorus was detected in the effluent of the adsorption column immediately after the start of the adsorption phase; secondary effluent P concentrations did not go below $0.3C_o$ (0.24 mg P/L). The column effluent P concentration slowly increased, reaching $0.5C_o$ by 300 BVs and column exhaustion around 1200 BVs. Sorbent C removed 61.9 ± 1.5% P when effluent concentrations were $0.5C_o$. The breakthrough profile of P adsorption from the secondary effluent fit well to the Clark model despite the high initial effluent concentrations (SSE = 0.0546, $R^2 = 0.940$). When fitting the breakthrough curve of the secondary effluent, the Clark fitting parameters A and r were determined to be 1.30 and 2.1×10^{-3}, respectively. Clark fitting parameter obtained in fitting the secondary effluent decreased when compared to the

fitting parameters obtained from treatment of SWW with sorbent C. The lower values of A and r are consistent with the low BVs of wastewater treated and a slower rate of mass transfer. The high initial P concentration in the adsorption column effluent suggests that approximately 30 % of P in the secondary effluent was not susceptible to adsorption. The secondary effluent had 0.27 mg P/L which was non-reactive P, making up approximately 33 % of TP in the secondary effluent. Non-reactive P is made up of organic and condensed P species that might not have the properties (*e.g.* size, surface charge) which would favour adsorption on sorbent C. At saturation, sorbent C removed 39.6 ± 3.7 % of P from the secondary effluent.

Figure 5-4b presents the adsorption results from treating the final effluent with Sorbent C. As shown in the breakthrough profile, the effluent P concentrations with the final effluent sample were low until the $0.1C_o$ breakthrough concentration was met after approximately 260 BVs, removing 95.5 ± 1.2 % P. After breakthrough, the P concentrations continued to increase to $0.5C_o$ by approximately 440 BVs with 85.3 ± 0.1 % P removed. Column exhaustion occurred at 1140 BVs. Results from treatment of the final effluent with sorbent C fit well to the Clark model (SSE = 0.0014, R^2 = 0.989). When fitting the breakthrough curve of the final effluent, the Clark fitting parameters A and r were determined to be 26.57 and 7.7 x 10^{-3}, respectively. The value of A was similar to the value obtained from fitting the breakthrough curve from treatment of SWW with sorbent C, while the value of r increased indicating a faster rate of mass transfer. Sorbent C adsorbed 46.5% P from the final effluent sample at saturation.

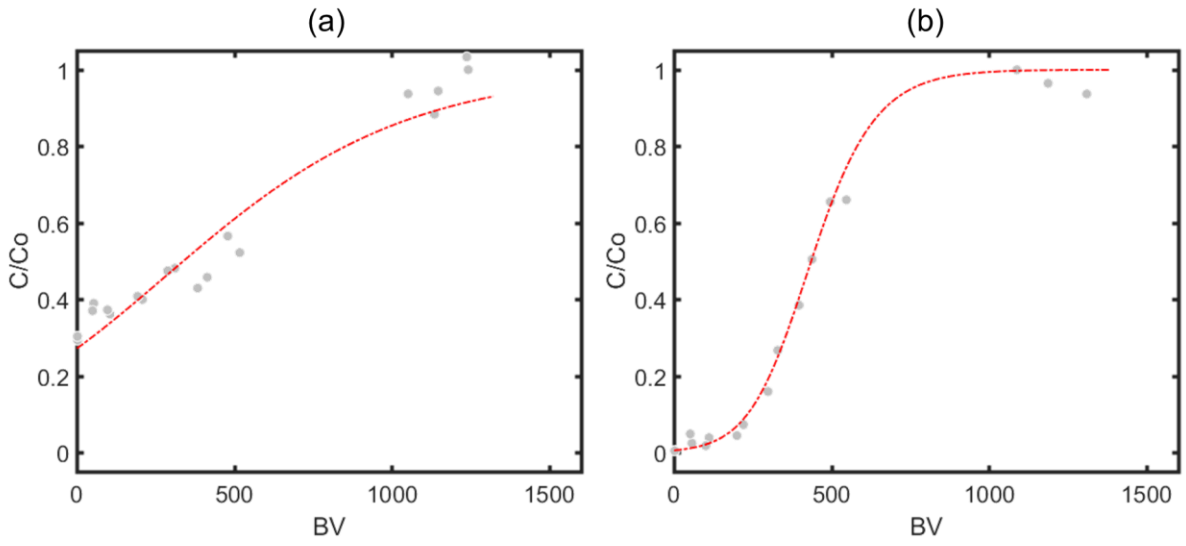

Figure 5-3: Breakthrough profiles fit with Clark Model (red dashed line) obtained through treatment of (a) secondary effluent (SSE = 0.055, R^2 = 0.94) and (b) final effluent (SSE = 0.0014, R^2 = 0.99) with Sorbent C.

Comparison of the adsorption performance of sorbent C in the two waste waters provides insight into potential application of adsorption in the wastewater treatment train. Sorbent C treated 440 BVs of final effluent before the breakthrough concentration was met ($0.1C_o$); P concentrations in the secondary effluent after adsorption by sorbent C did not go below $0.3C_o$ during treatment. Adsorption by sorbent C removed P from the final effluent to lower levels than in the secondary effluent. During adsorption of P from final effluent, P concentrations were below the breakthrough ($0.1C_o$) for 440 BVs. Sorbent C demonstrated higher removal in the final effluent (85 %) compared to the secondary effluent (61.9 %) when P concentrations after adsorption were $0.5C_o$ ($t(2) = 21.697$, $p = 0.002$). Sorbent C also treated a larger volume of final effluent (440 BVs) compared to secondary effluent (300 BVs) ($t(2) = 11.703$, $p = 0.007$). The lower removal observed in secondary effluent is most likely due to the large fraction of nRP (~33 % TP) that was not prone to adsorption by sorbent C. Therefore, sorbent C demonstrated higher levels of P removal and treated larger volumes of wastewater during adsorption of P from final effluent.

For more insight into the P adsorption by sorbent C, the resulting P loadings from treatment of secondary and final effluents were compared. Phosphorus removed in secondary and final effluents resulted in P loadings of 0.46 ± 0.07 and 0.13 ± 0.01 mg P/g sorbent. The P loading on sorbent C after treatment with secondary effluent was higher than the P loading after treatment of final effluent ($t(2) = -7.078$, $p = 0.01$) and was most likely due to the difference in initial P concentration of the two wastewater effluents. Even though 30 % of the P in the secondary effluent was not susceptible to adsorption by Sorbent C, the concentrations of the remaining aqueous P were almost twice those of the final effluent. The increased P concentration leads to a larger concentration gradient between the solid and aqueous phase, increasing the driving force of mass loading onto the sorbent. The difference in initial P concentration has much to do with the degree of treatment in the two samples. Secondary effluent was collected upstream from chemical P removal and therefore will have a higher initial P concentration when compared to final effluent which has fully treated. Therefore, Sorbent C has demonstrated P adsorption in real wastewater samples however performance was dependent on initial P concentration and speciation of the wastewater stream.

Desorption of P from the Sorbent C adsorption columns that were exhausted through treatment of secondary and final effluent was investigated using 0.5 M NaCl. For each trial, the desorption effluent was collected as one sample over the duration of the recovery phase due to the low initial P concentrations and the volume of waste water treated via adsorption. The final P concentrations of the desorption solutions used to recover P from the columns treating secondary and final effluent were 3.20 ± 0.07 and 0.30 ± 0.02 mg P/L, respectively. Hence desorption

recovered 0.99 ± 0.04 mg P from the secondary effluent and 0.10 ± 0.00 mg P from the final effluent. Therefore, the 0.5 M NaCl solution recovered 102 ± 4 and 38 ± 1 % P adsorbed by Sorbent C from the secondary and final effluent, respectively. The quantity of P recovered from the secondary effluent was almost 10 times greater than the P recovered from final effluent ($t(6) = -47.73$, $p < 0.001$). In desorption tests recovering P from SWW samples, desorption from Sorbent C was quick, occurring within the first 30 BVs. The composite sample collected during recovery from the wastewater samples was collected over 130 BVs which should have captured all recoverable P. Any P remaining on the sorbent after desorption phase is potentially irreversibly adsorbed to Sorbent C. Overall, Sorbent C recovered around 39.6 and 17.7 % P from secondary and final effluents, respectively.

The desorption effluent concentrations obtained through NaCl desorption of the sorbent C adsorption columns were also examined. As mentioned above, the concentration of the desorption effluent from the secondary effluent after 130 BVs was 3.20 mg P/L, almost 4 times more concentrated than the initial wastewater. The concentration of the desorption effluent for the final effluent was 0.30 mg P/L, approximately 1.4 times more concentrated than the initial concentration. The concentrations of the blended desorption solution are much lower than the 100 mg P/L threshold needed for struvite recovery technologies.

The trends observed during desorption of the SWW were used to interpret the exhausted desorption columns. Trends observed for desorption from sorbent C when testing SWW predicted that 90 % of P recovered from the sorbent could be collected in approximately 30 BVs. Therefore, the maximum concentration of the desorption effluent was calculated by dividing the mass of P recovered from the sorbent at this point by the volume associated with 30 BVs. The resulting concentrations for the desorption effluents were estimated as 11.7 and 1.23 mg P/L for

secondary and final effluents, respectively. Hence, while the phosphorus concentrations were predicted to be higher than that of the initial wastewater streams, the estimated maximum concentrations of the desorption stream were still below the concentration required for nutrient recovery technologies.

The results from treating the real wastewater effluents provide insight into the use of sorbents for P removal and recovery in wastewater treatment. Adsorption of P from the wastewater stream can be affected by several possible factors. Examples include initial phosphorus concentration, initial phosphorus speciation, presence of competing ions and possibly the presence of dissolved organic matter. Initial phosphorus concentration can help or hinder adsorption onto IEX sorbents depending on whether the concentration is high or low, respectively. A higher concentration in the aqueous phase provides a larger concentration gradient between the surface and solution, encouraging P adsorption onto the surface. Phosphorus speciation also may play a role as some forms of P are recalcitrant and may not be susceptible to adsorption, as was observed in this study, and thus, cannot be recovered. While not investigated in this study, the presence of dissolved organic matter could also reduce P adsorption through possible fouling of the sorbent surface (Bazri and Mohseni, 2016). The results of this study give evidence that P recovery in a concentrated P effluent through adsorption/desorption can be achieved however, further study into the factors mentioned above may provide useful information with regards to the wastewater stream to be treated.

5.5 Conclusions

The purpose of this study was to determine the phosphorus removal and recovery potential of three commercial sorbents through column testing. Once saturated, the granular ferric hydroxide

(sorbent A) removed 43.4 % P while activated alumina (sorbent B) removed 23.4 % P from the SWW test solution. The mass removed by sorbents A and B were similar and corresponded to a P loading of approximately 5 mg P/g sorbent. The ion exchange (sorbent C) removed the largest quantity of P from the SWW, removing 64.0 % P corresponding to a P loading of 19.7 mg P/g sorbent.

All of the desorption solutions tested were found to desorb P from the exhausted adsorption columns. Acidic (0.5 M HCl) and basic (0.5 M NaOH) desorption solutions both recovered over 90 % of the adsorbed P from sorbent A. NaOH recovered more P (> 99 %) from sorbent B than HCl (~ 90 %). Of the four desorption solutions used on sorbent C, 0.5 M NaCl and 0.5M NaOH + 0.5M NaCl both demonstrated the largest recoveries, desorbing over 95 % adsorbed P. Desorption from sorbent A and B with NaOH produced a desorption effluent with a P concentration that met the threshold concentration for nutrient recovery technologies (100 mg P/L) while use of all four desorption solutions on sorbent C produced a desorption effluent with a P concentration greater than 100 mg P/L. With the use of the optimal desorption solution of each sorbent, the percent recoveries of P from the initial SWW were 39, 21 and 61 % P for sorbents A, B and C, respectively.

Sorbent C proved to be the sorbent best suited for P recovery under the conditions tested and therefore was used for P removal and recovery from secondary and final wastewater treatment effluent. At exhaustion, sorbent C removed approximately 39.6 and 46.5 % P from secondary and final effluent, corresponding to P loadings of 0.46 and 0.13 mg P/g sorbent. Using 0.5 M NaCl, sorbent C recovered around 40 and 18 % P from secondary and final effluents, respectively.

6.0 Organic Phosphorus Removal using an Integrated Advanced Oxidation-Ultrafiltration Process

Holly E. Gray[1], Tony Powell[2], D. Scott Smith[3], Wayne J. Parker[1]

[1]Department of Civil and Environmental Engineering, University of Waterloo, 200 University Ave. W., Waterloo, ON N2L 3G1.
[2]Purifics Water Inc., London, ON
[3]Department of Chemistry and Biochemistry, Wilfrid Laurier University, 75 University Ave. W., Waterloo, ON N2L 3C5.

6.1 Summary

Non-reactive phosphorus (nRP) contains condensed phosphates and organic phosphorus (OP) species that are recalcitrant in secondary wastewater treatment and tend to remain in final effluents. To meet ultra-low effluent P discharge limits, persistent nRP must usually be removed. The objective of this study was to test an advanced oxidation process (AOP) which couples TiO_2/UV photolysis with ultrafiltration (UF) to oxidize and remove nRP species. Initial tests utilized a simple mixture of two OP model compounds to determine the effect of TiO_2/UV photolysis on them and to elucidate the mechanisms of phosphorus removal. The AOP was also tested for P removal from three municipal wastewaters and one automotive industry effluent. In all cases, phosphorus removal was found to occur through filtration, surface complexation onto the TiO_2 and UV oxidation. Total phosphorus removal efficiencies between 90-97 % were observed for the municipal wastewater effluents and 44 % removal was observed in the industrial effluent after treatment using AOP. Conversion of nRP to reactive P (RP) was evident during TiO_2/UV treatment of samples that had high concentrations of nRP. In summary, the AOP effectively oxidized nRP to RP, achieving high levels of P removal in real wastewater effluents and retaining P on the TiO_2 solids.

Keywords: Organic phosphorus, non-reactive phosphorus, phosphorus removal, advanced oxidation process, adsorption, UV/TiO_2, ultrafiltration.

6.2 Introduction

Total phosphorus (TP) in wastewater exists as two operationally defined fractions based on colourimetric P detection methods, termed reactive (RP) and non-reactive phosphorus (nRP) (Robards *et al*., 1994); soluble or particulate forms of TP are defined by whether they pass through or are retained by a 0.45 µm filter, respectively (Gu *et al*., 2011). Over 75 % of TP in wastewater is RP, an inorganic fraction made up of orthophosphate, that reacts directly to the reagents in colorimetry (Water Environment Federation, 2010). Alternatively, nRP contains condensed phosphates and organic phosphorus (OP) species which require digestion (*e.g.* persulfate oxidation) prior to being measured using colorimetric methods (Standard Methods, 2005). Conventional wastewater treatment can usually achieve TP discharge limits of 1 mg P/L, with some plants able to meet limits of 0.3 mg P/L (US EPA, 2007). However, traditional biological and chemical treatments target the RP fraction more effectively than nRP and it has been reported that 26 – 81 % of TP in treated effluents is in the form of dissolved nRP (Qin *et al*., 2015).

Areas with receiving waters more prone to hypertrophication are requiring stricter effluent standards to mitigate eutrophication (Clark *et al*., 2010). To meet the more demanding effluent quality standards, removal of only RP may not be sufficient and nRP must also be removed. Hence, industries with waste streams that have high concentrations of nRP will benefit from an effective and efficient nRP treatment technologies. It is expected that the need for these technologies will increase with time as the demand for organic phosphorus compounds in industrial uses is on the rise (*i.e.* herbicides/pesticides, chelating agents and in pharmaceuticals (Xing *et al*., 2017a; Mangat Echavia *et al*., 2009; Nowack, 2003; Kamel, 2015)). Further, while the goal of current wastewater treatment technologies is P removal, P is a valuable resource and

hence the implementation of nutrient recovery technologies is an emerging priority for treatment facilities. As of 2015, six water resource recovery facilities (WRRFs) in North America recover or will be recovering nutrients by implementing struvite ($NH_4MgPO_4 \cdot 6H_2O$) crystallization (Latimer *et al*., 2015). Therefore, the potential benefits of developing a technology that transforms nRP to RP is two-fold; oxidation of nRP to RP will eliminate the refractory P in effluents and will increase the fraction of P available for recovery technologies.

The types of non-reactive phosphorus in wastewater will depend on the wastewater source. Historically, nRP forms in domestic wastewater have included condensed phosphates (*e.g.* pyrophates) and phosphorus covalently bound to organic matter (*e.g.* adenosine 5'- triphosphate (ATP), phospholipids) (Maher and Woo, 1998). The characterization of nRP remaining in treated domestic waste waters has been limited, however the few studies that exist indicate that the organic P compounds mainly consist of esterized phosphorus and pyrophosphate species (Qin *et al*., 2015) that contain a covalent phosphorus to oxygen to carbon bond. The presence of organic phosphorus in industrial wastewaters has been well studied. It has been found that many industries use phosphonates, a group of phosphorus compounds that contain a resilient covalent carbon to phosphorus bond (Nowack, 2003). An example of a phosphonate that is in high worldwide demand is glyphosate, a nonselective herbicide which has increased in usage due to the production of genetically modified crops that are tolerant to glyphosate (Xing *et al*., 2017a). Regardless of composition, the need to reduce the quantity of nRP in the effluents is expected to increase.

In advanced oxidation processes (AOPs), organic compounds are non-selectively oxidized by highly reactive hydroxyl radicals that can be produced by photolysis (Legrini *et al*., 1993; Westeroff *et al*., 2009). Industrial wastewater streams that contain large quantities of

organophosphate pesticides (*e.g.* glyphosate) have been treated with AOP processes that couple UV and TiO_2 to enhance photocatalysis (Chen and Liu, 2007; Mangat Echavia *et al*., 2009). Chen and Liu (2007) studied photocatalysis of glyphosate using a TiO_2 powder and discovered 15 and 92 % of glyphosate was degraded after 30 minutes and 3.5 hours, respectively. In another study the oxidation of the organophosphate pesticides acephate and dimethoate using TiO_2 immobilized onto silica gel was assessed (Mangat Echavia *et al*., 2009). In a clean water matrix, 0.1 mM solutions of the pesticides acephate and dimethoate were both found to be degraded by photocatalysis after 60 and 105 min, respectively. Overall, the results indicate that AOPs are potentially effective at oxidizing OP compounds to form inorganic RP.

Advanced oxidation processes which use TiO_2 as a photocatalyst have the added benefit of the presence of a surface available for physical adsorption (Mayer *et al.*, 2010); metal oxides are known to complex with P compounds in solution (Li *et al.*, 2016). In both above-mentioned studies, glyphosate removal was determined to be due to adsorption onto TiO_2 as well as photolysis. Chen and Liu (2007) observed glyphosate adsorption to the TiO_2 surface under dark conditions; TiO_2 adsorption capacity for glyphosate was 1.28×10^{-6} mol/g (216 µg glyphosate/g TiO_2). Once exposed to UV light, RP was liberated from the TiO_2 (Chen and Liu, 2007). Mangat Echavia *et al.* (2009) reported complete removal of 0.1 mM glyphosate after adsorption and 60 minutes of UV exposure. RP release after oxidation of glyphosate was not observed suggesting that the liberated orthophosphate and other intermediate compounds were removed via adsorption.

Most studies investigating the use of AOPs for organic phosphorus removal have focused on industrial chemicals while the treatment of nRP in municipal wastewater has not been reported. Hence, the current study sought to extend the use of AOPs to treat dilute mixtures of different

organic P compounds typical of those found in municipal wastewater effluents. In this study, two model compounds were tested in a mixture and individually, to evaluate the ability of a commercial UV/TiO_2 AOP coupled with ultrafiltration to oxidize nRP species. The model compounds were chosen on the basis of the similarity of their structures with those reported in municipal waste waters. ATP contains two phosphoanhydride bonds (condensed phosphorus) and a phosphoester bond that are common in the nRP present in wastewater effluent streams while 2-aminoethylphosphonate (AEP) has a similar structure to the phosphonates reported in industrial wastewaters. The AOP unit was also used to treat real effluent samples to evaluate the ability to breakdown nRP species in a complex wastewater matrix. Based on the results obtained in this study, P removal mechanisms are proposed and the implications for phosphorus removal and recovery are discussed.

6.3 Methodology

6.3.1 Integrated Advanced Oxidation Process/Ultrafiltration System

The experiments were completed using a lab-scale Photo-Cat® system from Purifics Water Inc. (London, Ontario, Canada). The Photo-Cat® system couples a UV/TiO_2 photocatalysis unit with a ceramic ultrafiltration membrane. The Photo-Cat® system was run in batch mode with a maximum capacity of 16 L. Reagent grade titanium dioxide (Degussa P25, Dusseldorf, Germany) was used in a slurry that was continuously circulated within the system. Degussa P25 consists of a mixture of anatase and rutile TiO_2 nanoparticles in the ratio of 3:1; average particle size is 21-25 nm, however nanoparticles aggregate to form particles on the scale of hundreds of nanometers (Ohno *et al*., 2001; Gerrity *et al*., 2008). Additional information on the Photo-Cat® system has been reported by Westeroff *et al*. (2009).

6.3.2 Model Compounds and Test Solution Preparation

Two model compounds were used in this study to evaluate nRP behaviour in the AOP; ATP was used in the form of adenosine 5'-triphosphate disodium salt hydrate while AEP was in form 2-aminoethyl phosphonic acid. Both model compounds had 99 % purity and were purchased from Sigma Aldrich (St. Louis, MO). The model compounds were tested together in a binary mixture (BM) as well as individually. The molar concentrations of ATP and AEP employed in the BM were maintained in individual tests apart from the control test where less AEP was added. Test solutions were prepared as 1 L concentrates to add to the sample tank of the AOP which contained 16 L of tap water.

6.3.3 Wastewater Samples

Treated effluent samples were collected from three conventional activated sludge municipal wastewater treatment plants (WWTP) in Ontario, Canada prior to disinfection. The municipal wastewater treatment plants are referred to by an alphabetic code (A, B, C) to maintain anonymity. In addition, an untreated wastewater sample that was known to contain substantial nRP was collected directly from the outlet of the collection well of an automotive industrial facility and contained a mixture of industrial and domestic wastewaters. Apart from the samples obtained from WWTP A, the collected samples were stored at 4 ℃ until testing; samples from WWTP A were tested the same day as sampling.

6.3.4 Experimental Method

In tests with model compounds, the reaction tank of the AOP was filled with 16 L of tap water then dosed with 1 L of model compound concentrate and subsequently the system pump was

activated. When UV irradiation was being used, a known mass of TiO_2 was added to the system and allowed to mix thoroughly for 10 minutes before UV activation occurred. This approach was followed to allow the mercury lamps time to warm prior to testing. Samples were taken at each step and in 5 minute intervals up to 35 minutes once the UV lamps were on. In control tests, after TiO_2 addition, the system was mixed continuously for 30 minutes without UV irradiation and samples were taken after 5, 15, 25 and 35 minutes of mixing. Between tests, the AOP system was cleaned out using the automatic purge settings in the control system. A similar protocol was used in experiments with wastewater samples. All experiments were completed in triplicate.

6.3.5 Analysis

Total P was measured using Inductively Coupled Plasma Optical Emission Spectroscopy (ICP-OES). Intensities were measured in axial mode at a wavelength of 213.617 nm with the viewing height set to 15 mm above the induction coil; the flow rate of the sample pump was set to 2 mL/min, argon was used as the plasma and auxiliary gas, set to 15 and 0.5 L/min, respectively. Reactive P concentrations were measured using ascorbic acid colorimetric determination at 660 nm as per method G-103-93 Rev. 10 (Seal Analytical, WI) in accordance with Method 4500 P.E in Standard Methods (Standard Methods, 2005). Reactive and total P were measured in all samples and nRP concentrations were calculated by difference between TP and RP.

Calibration solutions were prepared each day of analysis using KH_2PO_4 in ultrapure water (18.2MΩ, MilliQ). A certified reference material (H_3PO_4, Lot BCBM9148V, 1002 ± 4 mg P/L) purchased from Sigma Aldrich was used to prepare P standards included in all runs for quality assurance. The method detection limits of the colorimetric and ICP-OES methods were 2 and 25 µg P/L, respectively (Ateeq, 2015).

Organic carbon was measured in wastewater samples using a SHIMADZU TOC-LCPH Carbon and Nitrogen Analyzer. Total organic carbon (TOC) was measured on unfiltered samples, while dissolved organic carbon (DOC) was measured on filtered samples.

6.3.6 Data Analysis

Statistical analysis of the sorbents was conducted using ANOVA and T-tests. Results of ANOVA and T-tests are indicated by reporting the result of the F or t value, respectively, as well as the corresponding *p* value; degrees of freedom of the statistical test are reported in brackets.

6.4 Results and Discussion

6.4.1 Model Compounds

The non-reactive phosphorus present in wastewaters typically represents a mixture of several compounds therefore ATP and AEP were used in a binary solution to simulate a simple mixture and test the AOP technology for organic P oxidation. Figure 6-1a shows the phosphorus concentrations in the BM tests throughout the treatment stages. Treatment stages included addition of TiO_2 nanoparticles followed by subsequent UV exposure. A BM control test was also conducted, in which the test solution was mixed in the reactor for the length of UV exposure but without UV light. With TiO_2 addition, 54.3 % P was removed from the solution via adsorption. Both RP and nRP were adsorbed onto TiO_2 however 86 % of the adsorbed P was nRP. With UV exposure, a slow decrease in nRP was observed over 35 minutes, reducing nRP and RP concentrations by an additional 22 and 48 %, respectively. After treatment with the AOP, over 83 % of TP was removed. Previous studies observed an increase in RP concentration as a result of the oxidation of organic P in pesticides (Chen and Liu, 2007). Although this was not observed

in the current study, the removal of TP during UV exposure suggests that nRP was being oxidized since removal was not observed in the control test without UV light. Therefore, while TP was reduced in the organic P mixture through adsorption onto TiO_2 and photocatalysis in the AOP treatment, there was no direct evidence of nRP oxidation.

It was unclear from the BM experiments if both forms of organic P were reacting to TiO_2/UV treatment in the same way, hence solutions of ATP and AEP were treated with the AOP separately to obtain additional insight into the behaviour of the two compounds throughout treatment. Results from individual treatment of ATP and AEP are shown in Figure 6-1b and 6-1c, respectively. Total P in the ATP tests was reduced by 93 % with the addition of TiO_2 and this was followed by a further reduction of 5 % with 15 minutes of UV irradiation. No further removal was observed with continued UV exposure and the TP concentration of ATP remained around the detection limit of < 25 µg P/L. During treatment of AEP, adsorption removed 38 % of TP and an additional 48 % TP was removed with 35 minutes of UV exposure. In total, AOP treatment of the individual model compounds yielded TP removals of 98 and 86 % in the ATP and AEP test solutions, respectively. TiO_2 adsorption had a large impact on nRP removal in the ATP trials while P adsorption in the AEP trials was low in comparison. The decreased adsorption may have been due to the AEP solutions having higher initial RP concentrations than ATP; initial RP concentrations in AEP and ATP trials were 540 and 84 µg P/L, respectively. RP and nRP were removed in similar proportions in the AEP sorption tests. Preferential adsorption of small phosphate anions over larger organic P species (*i.e.* glyphosate) onto metal oxide in soils has been observed in previous studies (Gimsing and Borggaard, 2007; Gimsing and Borggard, 2002). This behaviour may account for the reduced adsorption of nRP in treatment of AEP. Overall, AOP treatment of the two model compounds

yielded different results; while adsorption of nRP onto TiO_2 was the main mechanism of removal for ATP both adsorption and oxidation contributed to the removal nRP when present as AEP.

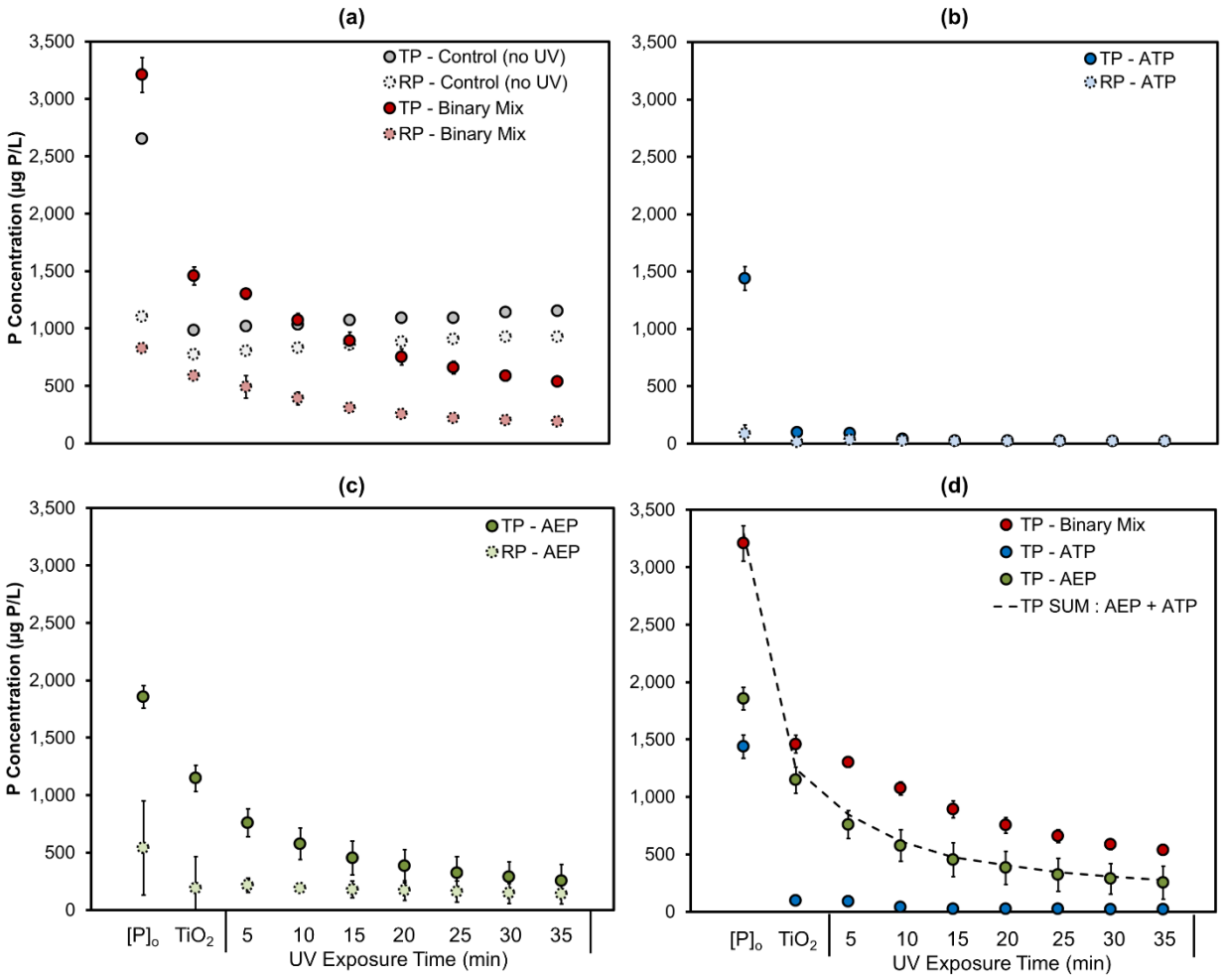

Figure 6-1: Phosphorus concentrations throughout AOP of (a) binary mixture (red), treatment of individual model compounds (b) AEP (green) and (c) ATP (blue). Total phosphorus (TP) concentrations indicated by closed circles, reactive phosphorus (RP) indicated by hatched circles. (d) Total phosphorus concentration measured for binary mix and individual model compounds as well as the sum of TP of the two individual model compounds is also shown (dashed line). Binary mixture comprised of adenosine triphosphate (ATP), aminoethylphosphonate (AEP).

The results obtained from treatment of the individual model compounds were compared with those from treatment of the BM to elucidate the mechanism of removal by the AOP. The predicted removal of a mixture of the two compounds, based on the individual compound tests (dashed line in Figure 6-1d) was found to be higher than the removals observed for the binary mixture suggesting that in the mixture ATP competitively binds to the TiO_2 surface, effectively blocking surface binding sites from AEP. With UV irradiation, the ATP on the surface is oxidized to RP thereby clearing surface sites which became available for adsorption and oxidation of AEP. The two-step removal, adsorption and oxidation of ATP and AEP, was consistent with a mechanism proposed by Mangat Echavia *et al*. (2009) when studying photocatalytic degradation of phosphonate glyphosate using TiO_2 immobilized on silica gel. In the current study RP was not observed to be released during oxidation of ATP or AEP, treated individually or in a mixture; thus, reactive P liberated from nRP was also adsorbed to the TiO_2 consequently removing P from the aqueous phase. Overall, the AOP technology proved to be an effective method to oxidize nRP associated with the model compounds.

6.4.2 Wastewater Effluents

Following the successful oxidation of the model compounds in the AOP, it's performance in treating P in real wastewater effluents was explored. Final effluent samples were collected prior to disinfection from three conventional activated sludge wastewater treatment plants (WWTPs) and one industrial effluent. The industrial waste water was from an automotive industry and included in this study due the large quantities of nRP that were present in the process wastewater. Some notable differences in the WWTPs include the rated average daily capacity, WWTP A has the largest capacity of approximately 27 000 m^3/day while WWTP B and C had

capacities of around 9 300 and 5 400 m^3/day; it should be noted that WWTP B does not have primary clarification and WWTP C includes tertiary cloth disk filtration.

The AOP removed both nRP and RP fractions in treatment of model compounds, therefore total and reactive P were measured in the tests with wastewater effluents. The initial P speciation results for the effluents are summarized in Table 6-1. The samples ranged in TP concentrations from 1 900 to 198 µg P/L; the industrial sample and WWTP B had the highest and lowest TP concentrations; respectively. The total P of the industrial sample was approximately 98 % nRP. Of the three WWTP samples, the effluent from WWTP C had the highest nRP concentration of 977 µg P/L, over 80 % of the TP. WWTPs A and B had lower nRP concentrations compared to WWTP C; total phosphorus in the two plants consisted of 6 and 30 % nRP, respectively.

Table 6-1: Characterization of wastewater samples prior to treatment with AOP. Total organic carbon was not measured for the Industry sample.

			WWTP A	WWTP B	WWTP C	Industry
Sample Date			07-06-2017	20-07-2017	28-07-2017	17-07-2017
Concentration	**µg P/L**	**$[TP]_o$**	346 ± 4	198 ± 49	1 190 ± 20	1 900 ± 100
		$[RP]_o$	310 ± 1	141 ± 15	216 ± 3	35 ± 6
		$[nRP]_o$	36 ± 3	58 ± 34	977 ± 17	1 860 ± 90
	[TOC] (mg C/L)		9.54 ± 2.05	10.74 ± 0.39	16.42 ± 0.37	--

Wastewater effluents contain organic matter, a component not included in the model compound trials therefore the effect of AOP treatment on organic matter was also evaluated in this study. The dissolved organic matter in wastewater effluents is known to be rich in P (Maizel and

Remucal, 2017), therefore it was anticipated that removal of DOC would coincide with nRP removal. The initial total organic carbon (TOC) of the of the wastewater samples are reported in Table 6-1; TOC was not measured on the industrial effluent due to the viscosity of the sample. The effluent from WWTP C had the highest average TOC concentration of 16.4 mg C/L while WWTPs A and B had concentrations of 9.5 and 10.7 mg C/L, respectively.

In this portion of the study, phosphorus removal was evaluated after a series of steps that sequentially added ultrafiltration, TiO_2 addition and UV irradiation since each step was hypothesized to remove P. Filtration was expected to have little effect on the RP concentration since orthophosphate could pass through the ceramic membrane while any nRP associated with particulate phosphorus species or organic matter would be removed from the effluent. It was expected that a small fraction of nRP might be adsorbed as observed in model compound trials however, it was expected that a majority of P removal through the addition of TiO_2 would be due to RP adsorption. Finally, photocatalysis was anticipated to target and remove nRP. Results obtained in AOP treatment will be discussed with respect to these hypotheses. Graphs of TP and RP concentrations throughout AOP treatment of the wastewater effluents are shown in Figure 6-2. Figure 6-3 summarizes the percent removal of DOC observed in the wastewater effluents after filtration, adsorption and UV oxidation. Results are presented and discussed below.

In treated wastewaters, phosphorus exists in particulate and colloidal fractions which can be removed via filtration and hence, the removal of P species through filtration was evaluated in this study. Graphs of TP and RP concentrations throughout AOP treatment of the wastewater effluents are shown in Figure 6-2. Phosphorus concentrations obtained after ultrafiltration of wastewater effluent from are labelled UF. After filtration TP concentrations of 248, 34, 707 and

1630 µg P/L were measured in the effluents from WWTP A (Figure 6-2a), B (Figure 6-2b), C (Figure 6-2c) and Industry (Figure 6-2d), respectively. Hence, it is apparent that the TP concentrations were reduced with ultrafiltration of all the wastewater effluents. The largest quantity of TP removed was in WWTP C where approximately 480 µg P/L was removed. Filtration of the industrial sample reduced TP by roughly 270 µg P/L. WWTP A and B had the smallest quantities of TP removed; approximately 97 and 155 µg P/L was removed via filtration of WWTP A and B effluent, respectively. Therefore, TP was removed via ultrafiltration in all effluents and further investigation into which P fractions were removed is discussed subsequently.

Filtration was expected to remove nRP thus changes in nRP concentrations through ultrafiltration were examined. The average concentrations of nRP in the filtered samples were 33, 25, 640 and 1600 µg P/L in WWTPs A, B, C and the industrial sample, respectively. After UF, nRP concentrations decreased by 32, 337 and 260 µg P/L for WWTP B, WWTP C and the industrial sample, respectively. nRP removal was not observed in ultrafiltration of wastewater effluent from WWTPA. As expected, the decrease in nRP concentration in the industrial effluent accounted for the total removal observed however, nRP removal only partly explained the TP removals observed in WWTP B and C effluents. Additionally, TP in WWTP A was decreased via UF while no removal of nRP was observed. Thus, removal of nRP was observed in effluents from WWTP B, C and industry but did not account for total removals observed from filtration of the wastewater effluents.

Examination of the TP and nRP removals obtained through UF inferred that RP fractions were also removed and hence, RP concentrations after filtration were evaluated. The reactive P

concentrations measured in WWTP A, B and C effluents after filtration were 216, 19 and 67 µg P/L, respectively; RP in the industrial effluent was not affected by UF. With filtration, the effluent from WWTP C exhibited an average reduction of 150 µg P/L while the effluent from WWTP A yielded a removal of 97 and 122 µg P/L was removed via filtration of WWTP B effluent. Therefore, RP was also removed through filtration of effluents from WWTP A, B and C.

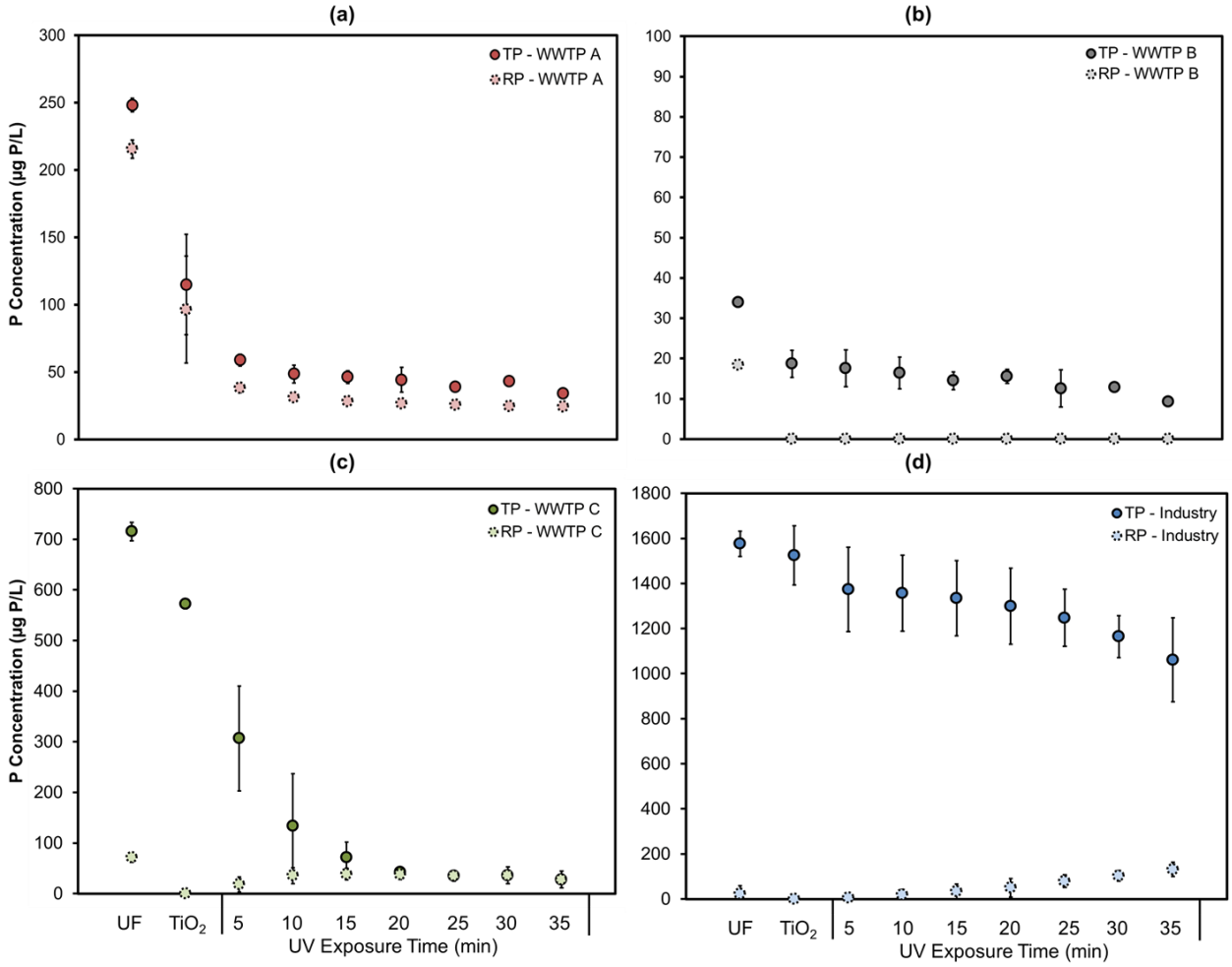

Figure 6-2: Phosphorus speciation after ultrafiltration (UF), with TiO_2 addition and over UV exposure time of wastewater effluents from (a) WWTP A, (b) WWTP B, from (a) WWTP C and (b) Industry.

Conceptually, RP was predicted to pass through the ceramic membrane however RP removal was observed through UF of WWTP A, B and C. The quantities of RP removed from effluents from WWTP A, B and C were not statistically different ($F(8) = 1.982$, $p = 0.218$) despite the wastewater effluents having different P speciation. Also, effluents from WWTP C had higher concentrations of TOC than WWTP B ($t(2) = 4.30$, $p < 0.01$) which could suggest that waste water composition had little impact on RP removal. The observed reduction of RP may have occurred because of the composition of the membrane, which remained consistent in all tests. Ceramic membranes are known to be negatively charged at pH greater than the pH zero-point charge (pH_{zpc}), the pH where the average surface charge is neutral; ceramic membranes have reported pH_{zpc} in the range of 4.5 to 8 (Sarma and Mahiuddin, 2014; Elzo *et al.*, 1998). When the membrane is negative, the surface will reject phosphate which is also negatively charged at circumneutral pH (Brandhuber and Amy, 2001). The pH of the wastewater effluents during treatment ranged from 7.4 to 8.2. With the pH of effluents measured in the high end of the reported pH_{zpc}, it is likely that RP removal was due to rejection by the negatively charged ceramic membrane.

Ultrafiltration has been reported to remove phosphorus associated with organic matter larger than 10 µm (Benotti *et al.*, 2009), therefore DOC concentrations after UF of WWTP effluents were examined in this study. The effects of UF on DOC in effluent from WWTP A will not be discussed as the sample was lost. Filtration yielded DOC concentrations of 5.8 and 9.7 mg C/L, in the effluents from WWTP B and C, respectively. Hence, filtration decreased the DOC concentrations by 4.9 and 6.7 mg C/L in WWTP B and C, respectively, corresponding to removals of 46 and 41%. Larger quantities of organic carbon were removed via ultrafiltration of WWTP C when compared to WWTP B ($t(4) = -6.84$, $p = 0.02$). Removal of organic carbon in

the effluents coincided with nRP removals in the two samples, where nRP removals in WWTP C were also higher than removals observed in WWTP B ($t(4)=-12.96$, $p = 0.01$). Therefore, organic matter was removed in WWTP B and C via ultrafiltration and this appeared to contribute to nRP removal.

The impact of adsorption was assessed by examining the TP in response to the addition of TiO_2 in the four wastewater effluents. After dosing with TiO_2, TP concentrations of 115, <25, 571 and 1520 µg P/L were measured in effluents from the A, B, C and Industry effluents, respectively. The true extent of removal in WWTP B was not known as concentrations were consistently below the method detection limit (25 µg/L). Addition of TiO_2 to WWTP A and C generated TP reductions of 133 and 136 µg P/L, respectively. While a decrease in the average TP concentrations were observed with adsorption in the industrial sample and WWTP B effluent, the TP concentrations were not significantly different from the concentrations obtained post filtration (WWTP B: $t(4) = 1.41$, $p = 0.229$; Industry: $t(4)=1.10$, $p = 0.33$); therefore phosphorus removal by adsorption from these effluents will not be discussed. Overall, adsorption removed TP in WWTP A and C while there was no significant effect on WWTP B and the industrial sample.

Adsorption was expected to remove RP on the basis of the results obtained with the model compounds hence, RP concentrations after TiO_2 addition to the WWTP A and C effluents were studied. TiO_2 addition yielded RP concentrations of 96 µg P/L in WWTP A while RP concentrations were below detection (2 µg P/L) in the WWTP C effluent. Thus, RP was removed via adsorption, reducing RP concentrations by 119 and > 67 µg P/L for the WWTP A and C effluents, respectively.

Removal of nRP species in the wastewater effluents via adsorption was also investigated in WWTP A and C. With TiO_2 addition, nRP concentrations of 19 and 571 µg P/L were detected in WWTP A and C, respectively. Higher removal was observed in WWTP C where 70 µg P/L was adsorbed onto TiO_2 whilst adsorption yielded a removal of 15 µg P/L in WWTP A. Thus, nRP was adsorbed in both wastewater effluents.

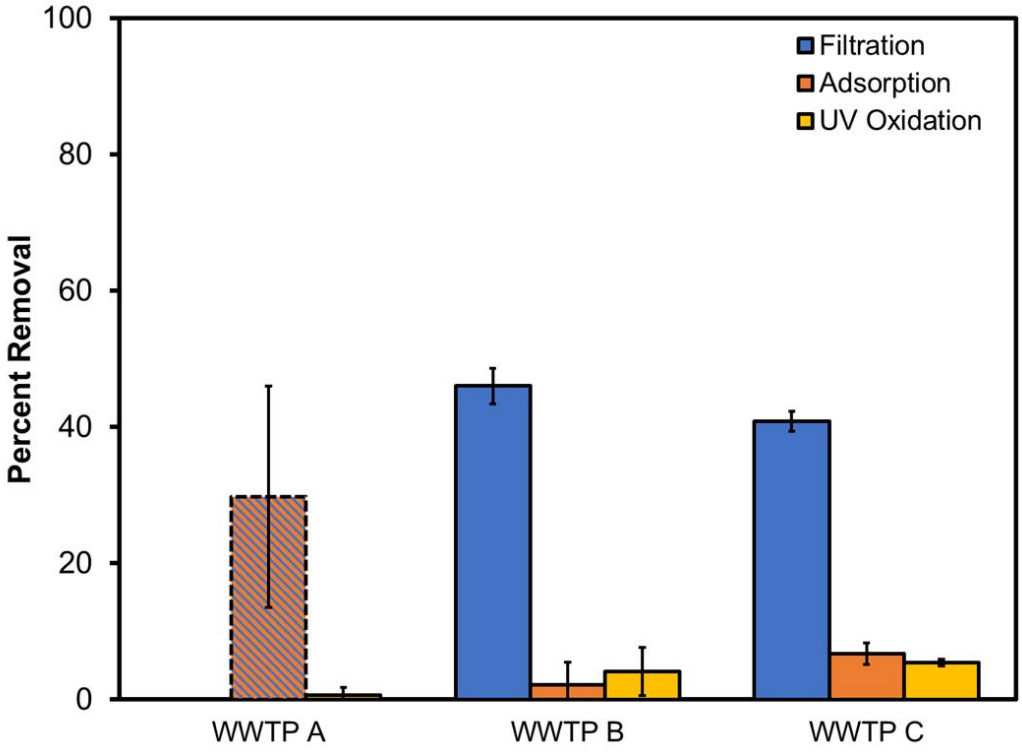

Figure 6-3: Percent removal of DOC obtained from AOP treatment of the four wastewater samples. Percent removal in WWTP A (hatched column) due to the combination of filtration and TiO_2 adsorption (sample from filtration lost).

Since, non-reactive P removal was associated with removal of organic matter during filtration, the DOC concentrations were also examined after adsorption to assess whether similar responses

were obtained. After TiO_2 addition, the DOC concentration in WWTP C effluent was 8.6 mg C/L. Adsorption reduced DOC in WWTP C by 1.1 mg C/L ($t(4) = 7.19$, $p = 0.002$). As observed during filtration, removal of DOC in WWTP C coincided with removal of nRP via adsorption. The concurrent removal of DOC and nRP in WWTP C provided further evidence that the nRP removed may be associated with the fraction of DOC also removed in treatment. Therefore, DOC was removed through adsorption in WWTP C and could potentially account for simultaneous nRP removal.

The P speciation after adsorption was examined for possible trends with respect to phosphorus removal. In summary, WWTP A and C both had reductions in TP, nRP and RP concentrations with TiO_2 addition. While the amounts of TP removed from the two wastewater effluents were similar, WWTP C yielded higher nRP removal via adsorption ($t(4) = -5.529$, $p = 0.005$). The higher nRP removals in WWTP C were most likely due to the P speciation of the effluent prior to adsorption. Before TiO_2 addition, nRP accounted for 90 % of the total P in WWTP C. When comparing the effluents, the nRP fraction in WWTP C was almost 20 times higher than that of WWTP A, while the initial RP concentration was more than 3x times lower. Adsorption of RP yielded concentrations in WWTP C below the method detection limit of 2 µg P/L, possibly exhausting the RP available for adsorption. The adsorption of RP to low levels when a large fraction of nRP was still available suggests that RP was adsorbed preferentially, and that remaining adsorption sites on the TiO_2 nanoparticles were available for adsorption of nRP species.

The total P concentrations after UV oxidation were evaluated to assess whether photolysis caused any change in concentrations. From Figure 6-2, it can be seen that the TP concentrations

in the WWTP A, C and industrial effluent samples slowly decreased after TiO_2/UV photolysis was initiated. After 35 minutes of exposure, the TP concentrations in the WWTP A (Figure 6-2a), WWTP C (Figure 6-2c) and industrial samples (Figure 6-2d) were 34, 29 and 1060 µg P/L, respectively. The total and reactive P concentrations in the WWTP B effluent were below detection prior to UV treatment and as such, will not be discussed. The removals during photolysis were found to be statistically significant, reducing TP concentrations by 81 µg P/L in WWTP A ($t(4)=3.75$, $p = 0.02$), 542 µg P/L in WWTP C ($t(4) = 56.9$, $p < 0.001$) and 460 µg P/L in the industrial sample ($t(4) = 3.50$, $p = 0.02$). The largest removals were observed in the WWTP C effluent and the industrial sample which had higher nRP concentrations than WWTP A. Overall, UV oxidation removed TP in effluents from the WWTP A, C effluents and the industry sample. The changes in nRP, RP and DOC that were associated with these tests are subsequently discussed.

It was anticipated that UV oxidation would impact on the levels of organic P in the wastewater, therefore nRP concentrations were monitored. The oxidation of effluents from WWTP A, C and the industrial sample yielded nRP concentrations of 10, 8 and 930 µg P/L, respectively, corresponding to reductions of nRP of 8, 563 and 593 µg P/L. The decrease in nRP was statistically significant in all cases (WWTP A: $t(4) = 4.11$, $p = 0.01$; WWTP C: $t(4) = 55.48$, $p <0.001$; Industry: $t(4) = 4.33$, $p = 0.01$). Thus, nRP was removed in effluents from WWTP A, C and industry with TiO_2/UV photolysis.

Due to the concurring removals of nRP and organic removal observed during UF and adsorption phases of treatment, DOC concentrations were also examined in WWTP A, B and C after UV oxidation. The dissolved organic matter in the wastewater was expected to decrease during

TiO_2/UV photolysis since oxidation of organic matter by hydroxyl radical formation is non-selective and larger or more abundant fractions of organic matter may be targeted over mineralization of nRP (Gerrity *et al.*, 2009). Concentrations of 6.8 and 7.7 mg C/L were measured in the WWTP A and C effluents, respectively, after 35 minutes of UV irradiation. Hence, oxidation reduced the DOC by 0.9 mg C/L in the WWTP C effluent ($t(4) = 25.31$, $p = 0.002$), while there was no effect on DOC in WWTP A ($t(4) = -0.87$, $p = 0.44$). In WWTP C, a statistically significant decrease in DOC coincided with a large nRP removal (563 µg P/L) while there was no observed effect on DOC through oxidation of WWTP A, coinciding with low nRP removal (10 µg P/L); nRP removal in WWTP C was over 50 x larger then removal observed in WWTP A. These results suggest that large quantities of nRP removed via oxidation may be the result of DOC oxidation. Therefore, DOC was removed via photolysis in WWTP C while there was no observed effect on DOC in WWTP A.

Reactive P concentrations were examined in this study as evidence of oxidation of P-bearing organics by TiO_2/UV photocatalysis as reported elsewhere (Chen and Liu, 2007). After 35 minutes of UV oxidation, both WWTP A and C had RP concentrations of 24 µg P/L while the industrial sample had an RP concentration of 131 µg P/L. As a result of oxidation, the RP concentration in the WWTP A effluent underwent a statistically significant decrease of 73 µg P/L ($t(4) = 3.56$, $p = 0.03$). RP concentrations in the WWTP C effluent and the industry sample yielded RP concentrations above the detection limit with UV oxidation; RP concentrations in both samples were below detection prior to UV light activation. The increase of approximately 22 µg P/L observed in WWTP C was not statistically significant ($t(4) = -1.97$; $p = 0.12$) due to RP levels in one trial remaining below detection. The greater than 129 µg P/L increase in the industrial sample was significant ($t(4) = -7.24$, $p = 0.002$) and the RP concentration obtained

after 35 minutes of UV exposure was higher than the initial RP concentration of the industrial sample prior to any AOP treatment. The increased RP concentration provides evidence that RP was liberated by photolysis of nRP in the industrial sample. Overall, UV oxidation generated different responses in the treated effluents, with RP decreasing in WWTP A and increasing in the industrial sample; there was no significant change in RP concentrations during oxidation of WWTP C.

In summary, phosphorus was found to be removed from the effluents via ultrafiltration, adsorption and oxidation. The responses to AOP differed between WWTPs and hence the fractions of total P removed by filtration, TiO_2 addition and UV exposure were summarized in Figure 6-4 to facilitate overall comparisons. The total removal in WWTB is indicated by a dashed line since the TP and RP concentrations were below the method detection limit. Viewed collectively, the AOP reduced both nRP and RP in the municipal WWTP effluents to low levels, retaining P in the TiO_2 solids. Treatment of the effluent from WWTP B resulted in an overall removal of > 87 %; P concentrations after ultrafiltration were below the method detection limits and the effects of UV oxidation on the sample could not be studied. Treatment of WWTP A and C effluents resulted in overall phosphorus removals of 90 and 97 %, respectively The AOP also removed 44 % TP from the more recalcitrant automotive industry sample. Overall, the AOP effectively removed nRP in the wastewater samples treated, achieving high level removal of TP in real wastewater effluents.

Overall, the results of this study indicate that the nature of the organic matter in the wastewater influenced the efficacy of the AOP treatment. Controlling for process step (*i.e.* filtration, adsorption, oxidation), nRP removal correlated to DOC removal throughout the AOP treatment

(df (14), r = 0.692, p = 0.003). This was expected since nRP is known to consist of organic P species which are covalently bound to organic matter such as humic substances (Mayer and Woo, 1998; Maizel and Remucal, 2017; Moran and Zepp, 1997). Organic matter larger than10 µm will be removed, along with any associated P, via ultrafiltration (Benotti *et al.*, 2009). There is also evidence in the literature that adsorption of large natural organic matter molecules, such as humic substances onto TiO_2 nanoparticles occurs within minutes of addition (Gora and Andrews, 2016). Finally, the radicals formed in TiO_2/UV photolysis are non-selective and will target large organic matter molecules over smaller, less abundant fractions (Gerrity *et al.*, 2009). This may explain why higher nRP removal was not observed in WWTP A, which initially had low nRP concentrations (34 µg P/L), while TOC was relatively abundant (9.54 mg C/L). Therefore, nRP removal in waste waters with initially low nRP concentrations may be hindered due to organic matter out-competing the limited quantities of nRP for adsorption sites.

The composition of nRP may also influence the efficacy of TiO_2/UV photolysis, therefore nRP removals obtained from oxidation of WWTP C and industry effluents were compared since both contained high initial nRP concentrations. Initially, the WWTP C and industrial effluents had nRP concentrations of 977 and 1860 µg P/L, respectively. In both effluents, nRP was reduced after the filtration and adsorption steps to concentrations of 571 and 1600 µg P/L for WWTP C and industry, respectively. A comparison of P speciation in the WWTP C effluent (Figure 6-2c) and the industrial sample (Figure 6-2d) throughout UV exposure reveals that P removal from the WWTP C effluent was more rapid than that observed in the industrial sample. The WWTP C effluent demonstrated a significant decrease of 250 µg P/L in nRP concentration after 5 minutes of UV exposure (t(4) = 3.67, p = 0.02) while 5 minutes of UV exposure did not have a significant effect on the nRP concentration of the industrial sample (t(4) = 2.11, p = 0.10). The

industrial sample required 15 minutes of UV exposure for the nRP concentrations to decrease by 316 µg P/L ($t(4) = 2.68$, $p = 0.02$). With 15 minutes of UV exposure in WWTP C, a total of approximately 520 µg P/L of nRP had been removed ($t(4) = 22.98$, $p < 0.001$). The delayed reduction of nRP in the industrial sample suggests that the nRP in WWTP C was more susceptible to UV oxidation while the nRP in the industrial sample was more recalcitrant.

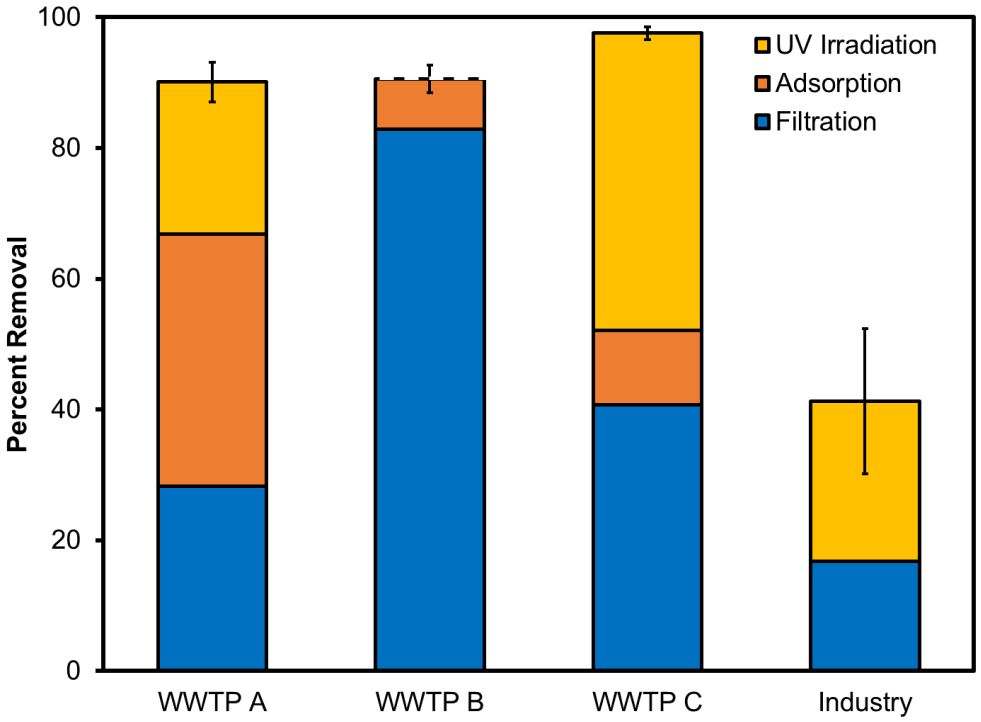

Figure 6-4: Total phosphorus percent removal obtained from AOP treatment of the four wastewater samples. Total phosphorus removal in WWTP B indicated by dashed line since TP and RP concentrations were below detection limits of the measurement methods used.

These results highlight the importance of pilot testing to determine the appropriate treatment method to achieve effluent water quality. The AOP effectively removed P in WWTP A through filtration, adsorption and oxidation, reducing TP to 34 µg P/L. However, in a 2007 report

focusing on low effluent P, the U.S. EPA found that WWTPs that implement chemical P removal with tertiary filtration were able to achieve effluent P concentrations as low as 10 µg P/L. Almost 90 % of the TP in WWTP A was RP which is known to be readily removed through chemical P removal. Treatment of waste water like that of WWTP A with the AOP could lead to wasting resources (*e.g.* TiO_2 and energy). Application of AOP is best suited for waste water with large quantities and/or difficult to remove nRP fractions as seen in WWTP C and the industrial wastewater samples.

Coupling TiO_2 and UV light with ultrafiltration may prove to be beneficial for nutrient recovery technologies. Nutrient recovery technologies (*e.g.* struvite production) aim to make a product devoid of significant organic matter (Latimer *et al*., 2015). Treatment with the AOP led to oxidation of both nRP and DOC, increasing the quantity of RP available for recovery and producing an effluent low in residual phosphorus since the liberated RP was adsorbed onto the TiO_2 solids. Ultrafiltration retains the phosphorus loaded solids which can be used for P recovery; P can be desorbed back into solution if phosphorus species are not irreversibly bound. Further information is needed to determine whether P can be recovered off the TiO_2 solids. With an appropriate desorption method, ultrafiltration coupled with TiO_2/UV photolysis has the potential to be a pre-treatment for nutrient recovery technologies.

6.5 Conclusions

Coupling ultrafiltration with TiO_2/UV proved to be effective at removing both model compounds via adsorption onto the TiO_2 as well as oxidation via UV irradiation. Tests with individual model compounds gave insight into the adsorption and oxidation behaviour of different model

compounds during treatment. The main mechanism of ATP removal was adsorption of nRP onto TiO_2 while both adsorption and oxidation contributed to the removal of nRP in AEP.

Phosphorus removal from the WWTP effluents and industrial samples was found to occur through ultrafiltration, adsorption and UV irradiation. After 35 minutes of UV irradiation, 90 %, > 87 % and 97 % total phosphorus removals were observed for effluents from WWTPs A, B and C, respectively. Treatment of the industrial sample yielded a total phosphorus removal of 44 % after UV irradiation. It was evident in oxidation of the industrial sample that RP was being liberated through nRP oxidation as UV time elapsed. Throughout AOP treatment nRP reduction correlated with removal of dissolved organic matter. In summary, the commercial AOP effectively oxidized nRP to RP, achieving high level removal of TP in real wastewater effluents and since the generated reactive P was retained on the TiO_2 solids.

7.0 Recovery of Phosphorus from TiO_2 Nanoparticles: Effect of Solution Calcium Concentration

Holly E. Gray[1], Tony Powell[2], D. Scott Smith[3], Wayne J. Parker[1]

[1]Department of Civil and Environmental Engineering, University of Waterloo, 200 University Ave. W., Waterloo, ON N2L 3G1.
[2]Purifics Water Inc., London, ON
[3]Department of Chemistry and Biochemistry, Wilfrid Laurier University, 75 University Ave. W., Waterloo, ON N2L 3C5.

7.1 Introduction

The focus in wastewater treatment is shifting to resource recovery, especially with respect to nutrients in wastewater (*i.e.* phosphorus and nitrogen). Presently, the majority of wastewater treatment plants use chemical and biological treatment to remove P from the wastewater stream, collecting it in the biosolids for disposition (Valsami-Jones, 2001). This traditional form of treatment is slowly being replaced with nutrient recovery technologies and wastewater treatment plants (WWTPs) are being renamed as water resource recovery facilities (WRRFs). As of 2015, there were six functional WRRFs in North America which recover P using struvite crystallization (Latimer *et al*., 2015). Struvite ($NH_4MgPO_4 \cdot 6H_2O$), is a valuable, inorganic P mineral that acts as slow release fertilizer (Desmidt *et al*., 2015). One limitation of struvite-based recovery is that the concentration of P in the wastewater stream needs to be 100 mg P/L or higher for the technology to be effective (Xie *et al*., 2016). Phosphorus concentrations in domestic wastewater influents are low (< 10 mg P/L), limiting the implementation of struvite technologies to after enhanced biological phosphorus removal where P has been concentrated to suitable levels (Ye *et al*., 2017). Wastewater treatment plants which do not utilize EBPR will require a method to concentrate phosphorus into a stream which meets the high concentration requirements of nutrient recovery processes.

Adsorption processes have potential to concentrate P in wastewater. Recovery of the adsorbed P through use of chemical desorption solutions can concentrate P depending on total volume of recovery stream. In this regard, nanoparticles have the potential to be used in wastewater treatment. Adsorbents which combine metal oxide nanoparticles have been of interest due to their high adsorption capacities and potential selectivity towards P adsorption (Hua *et al.*, 2013). Hybrid anion exchange resins, which incorporate iron oxide nanoparticles, have been shown to recover over 90 % of P in source-separated urine using a NaCl/NaOH desorption solution, although concentration of the recovery stream was not discussed (O'Neal and Boyer, 2013). Zhang *et al*. (2013) used a proprietary hydrated ferric oxide nanocomposite to recover 97 % P from a dilute wastewater effluent (~ 2 mg P/L), also using a NaCl/NaOH binary solution; P in the recovery stream was 100x more concentrated than wastewater effluent tested. Nano-sized titanium dioxide has also been highlighted as a promising P adsorbent due to its high surface area. In solutions containing 50 mg P/L, TiO_2 nanoparticles out performed Al_2O_3 and Fe_3O_4 nanoparticles by having the highest maximum adsorption capacity of 28.3 mg P/g (Moharami and Jalali, 2014). However, little information is available about P recovery from TiO_2 nanoparticles, which is the focus of this study.

TiO_2 nanoparticles are currently used in advanced oxidation processes (AOPs) for wastewater treatment. AOPs utilize TiO_2 nanoparticles in combination with UV light (photolysis) to oxidize organic contaminants through the action of non-selective hydroxyl radicals (Westeroff *et al*., 2009). Studies have indicated that photocatalysis with TiO_2-based AOPs can liberate a fraction of phosphorus from organic contaminants that would not originally be available for P recovery. The oxidation of organic phosphorus containing pesticides (*e.g.* glyphosate, acephate) via TiO_2/UV photooxidation has been found to result in the liberation of phosphate, which can bind

to the TiO_2 surface (Mangat-Echavia *et al.*, 2009). Since liberated phosphate is retained on the TiO_2 solids, total P in treated wastewater effluent decreases (Clark *et al.*,2010). Hence, not only can the AOP process increase P available for recovery, it also has the added benefit of oxidizing organic matter in wastewater which has an inhibitory effect on mineral precipitation, competing for active crystal growth sites or slowing reaction kinetics (Sindelar *et al*., 2015; Capdevielle *et al*., 2016). For these reasons coupling photolysis and adsorption in wastewater treatment is an attractive method with respect to P recovery.

Currently WRRFs typically use struvite precipitation for P recovery (Latimer *et al*., 2015) however there are other methods of P recovery that are considered preferential and should be investigated (Hao *et al*., 2013). Calcium phosphate (CaP) minerals are preferred P recovery products to struvite because it is the raw product (*i.e.* phosphate rock) used by industry (Valsami-Jones, 2001). Studies have highlighted that TiO_2 nanoparticles has been observed to enhance CaP precipitation. Although there is debate as to whether this effect is due to surface morphology versus chemistry, the presence of TiO_2 particles with increased surface area was shown to accelerate CaP precipitation and this further improved when suspensions of anatase or rutile were added to solutions (Damen *et* al., 1991; Chusuei *et al*., 1999; Murphy *et al*., 2016). Calcium phosphate precipitation could also become the preferential P recovery method for wastewater streams which are known to have high concentrations of Ca; the presence of Ca is known to have a negative impact on struvite precipitation effecting crystal morphology and purity (LeCorre *et al*., 2015).

Phosphorus adsorption by TiO_2 nanoparticles was demonstrated during their use as a photocatalyst in the AOP studied in Chapter 6. This study further investigated P adsorption onto TiO_2 and its potential for P recovery from wastewater. The concentration of P in the recovery

stream through concentration of the P-loaded TiO_2 solids, followed by pH adjustment was examined to optimize chemical use for recovery. A commercial ultrafiltration unit was employed to separate the TiO_2 from the wastewater and to concentrate the TiO_2 nanoparticles. Adsorption and recovery experiments were completed at different calcium concentrations to observe the effects of Ca on P removal and recovery. The results are discussed with respect to implications for phosphorus removal and recovery.

7.2 Methodology

7.2.1 Ultrafiltration System

Experiments were completed using a lab-scale Ceramic UltraFiltration (CUF®) system from Purifics Water Inc. (London, Ontario, Canada) that was operated in a batch mode. The CUF® system contains a proprietary silica carbide membrane with a pore size of < 1 µm. The CUF® system was run in batch mode and has a maximum reservoir capacity of approximately 60 L.

7.2.2 Reagents

Experimental stock solutions were prepared using calcium chloride ($CaCl_2 \cdot 2H_2O$, Fisher Scientific, Fair Lawn, NJ) or potassium phosphate monobasic (KH_2PO_4) (BDH, VWR International LLC., West Chester, PA) in ultra pure water (18.2MΩ, MilliQ). Adjustments to pH were made using hydrochloric acid (HCl, EMD Chemicals Inc., Gibbstown, NJ) or sodium hydroxide (NaOH, Sigma-Aldrich, St. Louis, MO). All chemical reagents used in this study were reagent grade or higher.

In experiments with TiO_2, reagent grade titanium dioxide (Degussa P25, Dusseldorf, Germany) was used in a slurry that was continuously circulated within the CUF® system. Degussa P25 consists of a mixture of anatase and rutile TiO_2 nanoparticles in a 3:1 ratio. The average particle size is 21-25 nm, however nanoparticles aggregate to form particles on the scale of hundreds of nanometers (Ohno *et al*., 2001; Gerrity *et al*., 2008).

7.2.3 Calcium Concentrations

Three initial calcium concentrations were used in the experiments. In trials using a low calcium concentration, a matrix of ultra-pure water was used, and the ionic strength of the ultra pure water test solution was adjusted to 0.01M with KNO_3. Due to the configuration of the lab scale CUF® system, residual calcium remained in solution after rinsing and flushing the system with tap water and as such, the calcium concentrations of the ultra pure water trials were measured and are reported as low Ca conditions. In trials with medium calcium concentrations, a tap water matrix was used. In the high concentration trials, the initial calcium concentrations were achieved by starting with a tap water matrix and adding $CaCl_2$.

7.2.4 Experimental Method

7.2.4.1 Phosphorus Adsorption versus pH

Low Ca concentrations were used in experiments investigating pH effects on P adsorption onto TiO_2. In the experiments, the reaction tank of the CUF® was filled with 41 L of water and dosed with 205 mL of P stock solution and the system pump was initiated. Once the pH of the P solution stabilized, a known mass of TiO_2 was added to the system and was allowed to mix

thoroughly for 10 minutes before the pH was adjusted incrementally using HCl or NaOH solutions. After the pH had stabilized, permeate samples were taken from the sample port; all experiments were completed in duplicate. Samples were analyzed for total phosphorus and calcium concentrations. Experiments were completed in duplicate.

7.2.4.2 Adsorption of P onto TiO_2 at Circumneutral pH

The adsorption of P onto TiO_2 at circumneutral pH was tested under low, medium and high calcium concentrations. During the adsorption experiments, the CUF® reaction tank was filled with 41 L of water and dosed with 205 mL of P stock solution. Mixing was induced through activation of the system pump. Once the pH of the P solution stabilized, a known mass of TiO_2 was added to the system followed by four sequential additions of 100 mL P stock solution; after each addition the solution was mixed thoroughly, and the pH was allowed to stabilize. Permeate samples were taken after each experimental step and analyzed for P and Ca concentrations. Experiments were completed in triplicate for each Ca concentration tested.

7.2.4.3 Recovery of P from TiO_2

The recovery of P adsorbed onto TiO_2 was conducted at low and medium calcium concentrations. Under both conditions, P was adsorbed onto the TiO_2 as described previously (Section 7.2.4.2). P recovery through incremental addition of NaOH and HCl, respectively was evaluated. In the recovery experiments conducted with the medium Ca concentration, the TiO_2 solids were concentrated by discharging effluent until final volumes of approximately 10 and 4 L remained in the system. The final volumes of 10 and 4 L corresponded to concentrating the TiO_2

solids by 4 and 11 times, respectively. The volume remaining in the reactor was determined from the read out of the CUF® system software. The system pump was kept on throughout the duration of P recovery experiments and hence the reactor was well mixed at all time. Permeate samples were taken after each experimental step and analyzed for P and Ca concentrations. Replicate experiments were conducted for both Ca concentrations.

7.2.4.4 Calcium Phosphate Precipitation without TiO_2

The precipitation of CaP without TiO_2 was examined in solutions with low, medium and high calcium concentrations. During the precipitation experiments, the CUF® reaction tank was filled with 41 L of water and dosed with 205 mL of P stock solution. Mixing was induced through activation of the system pump. The pH of the test solution was adjusted incrementally using HCl or NaOH and the pH was allowed to stabilize at each target value. Permeate samples were taken after each experimental step and analyzed for P and Ca concentrations. Experiments were completed in duplicate for each Ca concentration.

7.2.4.5 Calcium Phosphate Precipitation with TiO_2

The precipitation of CaP was examined in solutions with low, medium and high calcium concentrations; CaP was used as a descriptor for any calcium phosphate precipitates that could potentially form. Precipitation was induced by increasing the pH of the test solution to above 10 with NaOH following adsorption of P at circumneutral pH as described in Section 7.2.4.2. Permeate samples were taken after the precipitation step and analyzed for P and Ca concentrations. Experiments were completed in triplicate for each Ca concentration tested.

7.2.4.6 Recovery from CaP-Loaded TiO_2

Phosphorus recovery from CaP loaded TiO_2 was completed under medium and high Ca concentrations. Prior to recovery, the experimental method followed the CaP experiments described in Section 7.2.4.4. After the CaP precipitation step, the TiO_2 solids were concentrated by discharging effluent until the TiO_2 solids were concentrated by either 4 and 11 times. After concentrating the solids, the pH was adjusted incrementally using HCl. The system pump was kept on throughout the duration of P recovery experiments to keep the reactor contents mixed. Permeate samples were taken after each experimental step and analyzed for P and Ca concentrations. Experiments were completed in duplicate for both Ca and solids concentrations.

7.2.5 Analysis

All samples were measured simultaneously for total P and Ca using Inductively Coupled Plasma Optical Emission Spectroscopy (ICP-OES). Phosphorus and calcium intensities were measured in axial mode at wavelengths 213.617 and 317.993 nm, respectively, with the viewing height set to 15 mm above the induction coil; the flow rate of the sample pump was set to 2 mL/min, argon was used as the plasma and auxiliary gas, set to 15 and 0.5 L/min, respectively.

Calibration solutions were prepared each day of analysis using KH_2PO_4 in ultrapure water (18.2MΩ, MilliQ). A one-point calibration using a certified multielement standard was used for Ca analysis (PlasmaCAL Quality Control Standard No. 4, Lot S150326010, 100.2 ± 0.7 mg Ca/L) and certified A certified reference material (H_3PO_4, Lot BCBM9148V, 1002 ± 4 mg P/L) purchased from Sigma Aldrich was used to prepare P standards included in all runs for quality

assurance. The method detection limits of ICP-OES method for P and Ca were 25 and 240 µg P or Ca/L, respectively.

7.2.6 Equilibrium Modelling

Equilibrium modelling of the chemical speciation in the various tests was completed using MATLAB^{TM}. An equilibrium model was used in which speciation was calculated based on fixed P and Ca concentrations as well as pH. The speciation at equilibrium was determined by simultaneously solving for mass action (K and K_{sp} values) and mass balance expressions using the in-house MATLAB® script to solve the Newton Raphson optimization to minimize the residuals of the mass balance and saturation index (if solids were present). The method followed the general equations of Carrayrou *et al.* (2002). More information on the equilibrium model is provided by Smith (2013). Equilibrium constants for hydroxyapatite (HAP, $K_{sp} = 10^{-8.42}$) and octacalcium phosphate (OCP, $K_{sp} = 10^{-46.9}$) were taken from Stumm and Morgan (1995), an experimental equilibrium constant for OCP ($K_{sp} = 10^{-48.7}$) was taken from Lu and Leng (2005) and finally an amorphous CaP precipitate ($Ca_3(PO_4)$, $K_{sp} = 10^{-28.92}$) was taken from the National Institute of Standards database (NIST, 2001). Equilibrium constants for calcite were also included (Ksp = $10^{-8.42}$, Stumm and Morgan, 1995).

7.2.7 Data Analysis

Statistical analysis of the sorbents was conducted using linear regression, ANOVA and T-tests. Results of linear regression are reported as Pearson's r values. Results of ANOVA and T-tests

are indicated by reporting the result of the F or t value, respectively, as well as the corresponding *p* value; degrees of freedom of the statistical test are reported in brackets.

7.3 Results and Discussion

7.3.1 Phosphorus Adsorption onto TiO_2 and Recovery under Low Calcium Conditions

Changes in phosphate adsorption onto TiO_2 nanoparticles due to changing pH was investigated. Phosphate desorption from metal oxide sorbents is usually completed through the application of acidic or basic desorption solutions and thus, the change in P adsorption onto TiO_2 nanoparticles due to varying pH will help determine if an acidic or basic desorption solution would increase P recovery. To study this effect, P was adsorbed onto TiO_2 at circumneutral pH and then the pH was adjusted incrementally to pH values in the range 3 to 11. The result of P adsorption over pH are presented in Figure 7-1. To minimize the effects of potential interfering or competitive ions, the experiments were completed in the commercial ultrafiltration (UF) system with an ultra-pure water matrix; initial P ($[P]_o$) and Ca ($[Ca]_o$) concentrations were 4.53 mg P/L and 8.76 mg Ca/L, respectively. As pH increased, the adsorption of P onto TiO_2 was observed to decrease ($r = 0.579$, $R^2 = 0.355$, $p = 0.012$). Phosphorus loading on the TiO_2 nanoparticles ranged from 2.32 to 0.92 mg P/g TiO_2 over the pH range of 3.15 to 10.5. These results indicate that at high pH, the attraction between phosphate and the TiO_2 surface decreased, causing P to be released into solution. Therefore, desorption from TiO_2 may be accomplished using a basic desorption solution.

The literature was reviewed for insight into why P adsorption onto TiO_2 decreased with increasing pH and how this could affect the recovery process. This behaviour has been observed in other studies and is attributed to the surface charge of the TiO_2. With a zero point charge (pH_{zpc}) of 6.3, the surface of the TiO_2 nanoparticles is neutral around circumneutral pH (Luster *et al*., 2017). When the pH is below pH_{zpc}, the TiO_2 surface becomes positive and hence can attract negatively charged phosphate species leading to increased adsorption. When the pH increases above the pH_{zpc}, the TiO_2 surface becomes more negatively charged and phosphate anions are repelled (Moharami and Jalali, 2014; Kang *et al*., 2011). This behaviour suggests that to optimize recovery, P adsorption should be performed at low pH, TiO_2 solids could then be concentrated and a basic desorption solution could be employed to recover the adsorbed P. The pH adjustment to basic values would lead to larger quantities of P recovered from the surface. The adjustments of pH for both adsorption and recovery processes may be impractical in many wastewater treatment applications as large volumes of wastewater would need to be pH adjusted, requiring large quantities of acid. Maintaining circumneutral pH for the P adsorption phase and then concentrating the P loaded TiO_2 solids will lower the chemical demand of the recovery process. Therefore, for TiO_2 to be useful in P recovery, suitable quantities of P would have to be adsorbed at circumneutral pH and recovered after concentration of the TiO_2 solids.

The adsorption of P by TiO_2 was investigated under circumneutral pH. Experiments were completed in ultra pure water to reduce the effects of competing ions. The results from adsorption experiments are summarized in Table 7-1; initial P and Ca concentrations as well as TiO_2 dose are also reported in Table 7-1. Adsorption onto TiO_2 removed 26 % of P, resulting in a P loading of 4.79 mg P/g TiO_2. The P loading obtained under low calcium concentrations and at circumneutral pH was higher than the P loading observed by Kang *et al.* (2011) where P loading

of approximately 2.5 mg P/g TiO_2 at pH 7 and an ionic strength of 0.01 M were reported. The P concentration used by Kang *et al*. (2011) was approximately 20 mg P/L. In another study investigating the effect of TiO_2 nanoparticles on P removal (Moharami and Jalali, 2014), a P loading of 6.7 mg P/g TiO_2 was reported and this was slightly higher than observed in this study. Viewed collective it can be concluded that TiO_2 nanoparticles can achieve P adsorption at circumneutral pH in the absence of competing ions.

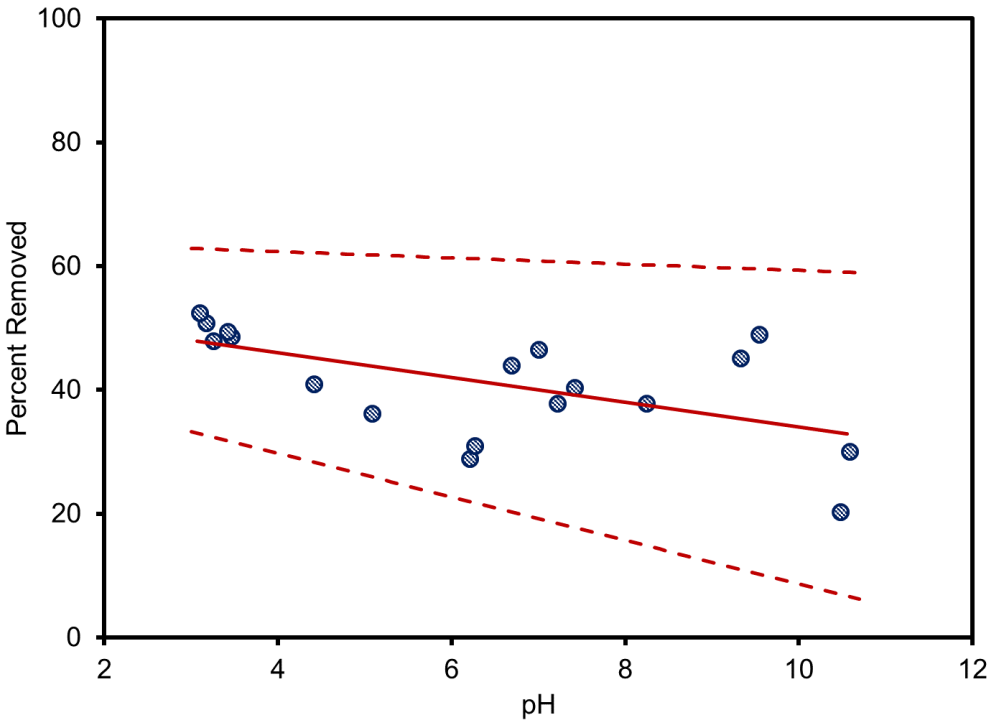

Figure 7-1: Percent P removed via adsorption onto TiO_2 with changing pH performed at low calcium concentrations (ultra-pure water). Solid line indicates the line of best fit, while dashed lines indicate the 95 % confidence intervals (r = 0.579, R^2 = 0.355, *p* = 0.012).

Table 7-1: Percent P adsorbed onto TiO_2 and P loading initial phosphorus ($[P]_o$) and calcium ($[Ca]_o$) concentrations as well as TiO_2 dose and P loading onto TiO_2 nanoparticles measured for experiments which examine P adsorption under different experimental conditions.

	Low [Ca] (ultra-pure water)	Medium [Ca] (tap water)	High [Ca] (tap water + Ca)
N	4	4	4
$[P]_o$ (mg P/L)	19.1 ± 0.2	20.8 ± 1.7	19.1 ± 1.4
$[Ca]_o$ (mg Ca/L)	4.50 ± 2.67	34.0 ± 2.6	69.9 ± 5.8
TiO_2 dose (g/L)	1.03 ± 0.02	1.03 ± 0.01	1.03 ± 0.02
pH	6.45 ± 0.49	7.52 ± 0.40	7.61 ± 0.04
% Removed	26 ± 5	41 ± 6	50 ± 5
P Loading (mg P/g TiO_2)	4.79 ± 0.84	8.38 ± 1.26	9.28 ± 4.87

The recovery of P from the TiO_2 nanoparticles was investigated by adjusting the solution pH. The TiO_2 solids were not concentrated during recovery of P under low Ca conditions as a "proof-of-concept" approach to avoid any complicating factors caused by concentrating the TiO_2 solids. Prior to pH adjustment, the free P that was not adsorbed onto TiO_2 had a concentration of 14.0 ± 0.9 mg P/L. To recover P adsorbed onto the TiO_2 nanoparticles, the pH was raised to 10.6 ± 0.4 to liberate P adsorbed on the surface. The resulting P concentration in the aqueous phase was 16.6 ± 1.6 mg P/L. On average, the aqueous P concentration was observed to increase, liberating 13.4 % P from the TiO_2 ($t(3) = -2.416$, $p = 0.047$). Hence, P was liberated by increasing pH to above 10.

The limited P recovery could potentially have been due to the type of adsorption occurring between P and the TiO_2 nanoparticles. A previous investigation into phosphate adsorption onto TiO_2 revealed that the reversibility of P adsorption was dependent on the pH at which the P was initially adsorbed (Kang *et al*., 2011). Kang *et al.* noted that P uptake onto TiO_2 at pH of 4.5 was

mostly irreversible due to inner sphere surface complexation. However, the results obtained with adsorption of P onto TiO_2 at pH values of 7 and 9 showed the possibility for P desorption with increasing pH due to the increased heterogeneity of surface complexes forming. In the present study, adsorption under low calcium concentrations was conducted around a pH of 6.5, a pH that is on the lower end of circumneutral and may have resulted in the limited recovery from the TiO_2. Kang *et al*. (2011) also found that adsorption of P onto TiO_2 increased with increasing ionic strength; ionic strength was adjusted in the study using NaCl. The results of Kang *et al*. suggested that P uptake onto the TiO_2 nanoparticles may be increased in a more complex water matrix and as such, may potentially increase the P recovery from the TiO_2 nanoparticles. Hence, higher calcium concentrations and a tap water matrix were investigated in the current work.

7.3.2 Phosphorus Adsorption onto TiO_2 and Recovery under Medium Calcium Conditions

Phosphorus adsorption onto TiO_2 in a tap water matrix was investigated to test the hypothesis that P adsorption will increase due to higher ion strength of the solution. The results from the adsorption experiments conducted in tap water are summarized in Table 7-1; initial P and Ca concentrations as well as TiO_2 dose are also reported in Table 7-1. Initial P concentrations were kept consistent with the tests that were conducted in ultra-pure water ($t(6) = 1.942$; $p = 0.10$). It was found that in tap water, adsorption onto TiO_2 removed 41 % of the P, resulting in a P loading of 8.38 mg P/g TiO_2. Hence adsorption in the tap water matrix increased P removal by 15 % ($t(6) = 4.22$; $p = 0.006$) and P loading by 3.59 mg P/g TiO_2 ($t(6) = 4.714$, $p = 0.003$). It was concluded that in a more complex matrix (*i.e.* tap water) P adsorption onto TiO_2 is increased.

The increased P adsorption onto TiO_2 may have been due to the presence of increased calcium concentrations in the tap water. Changing the water matrix from ultra pure water to tap water

increased the Ca concentration from 4.50 to 34 mg Ca/L ($t(6) = 15.88$, $p < 0.001$). As discussed previously, at pH values near the pH_{zpc} and above, the surface of TiO_2 is neutral or negative and would not be attracting negatively charged $H_2PO_4^-$ and HPO_4^{2-} species present in solution (Li *et al.*, 2002). However, in the presence of calcium, phosphate will complex with Ca^{2+} to the TiO_2 surface through calcium ion bridging (Chusuei *et al.*, 1999). Therefore, observing an increase in P adsorption in the presence of higher Ca concentrations was attributed to calcium bridging at the TiO_2 surface.

Changes in calcium concentrations with P adsorption were investigated to establish if there was evidence of Ca removal which could be attributed to the formation of Ca bridging. Figure 7-2 plots the moles of Ca removed versus the moles of P removed via adsorption onto TiO_2 in tap water. As shown in Figure 7-2, calcium was also removed as P was adsorbed onto TiO_2 ($r = 0.693$, $R^2 = 0.481$, $p < 0.001$). This relationship supports the previously stated hypothesis that calcium bridging was occurring in tap water at circumneutral pH.

With improved P adsorption under the medium Ca conditions, P was still detected in the aqueous phase after adsorption and hence, effluent P concentrations were analyzed during concentration of the TiO_2 solids to determine if there was any change in mass adsorbed onto the TiO_2. Two trials of P adsorption followed by concentration of solids were completed under medium Ca concentrations (tap water); the total P concentration of the two trials was 14.5 ± 0.1 mg P/L and TiO_2 dose was 1.10 ± 0.02 g/L. Figure 7-3a presents the percent of total P that was adsorbed onto the TiO_2 and remaining in the aqueous phase during the adsorption and concentration steps; pH at both experimental steps is also reported. Adsorption onto TiO_2 removed approximately 66 ± 3 % of the P that was added to the UF system, resulting in a P loading of 8.69 ± 0.22 mg P/g; the P loading on TiO_2 was not statistically different from P loading obtained in previous tap water

experiments reported in Table 7-1 (t(3) = 0.488, p = 0.66). After adsorption, the P remaining in the aqueous phase had an average concentration of 4.46 ± 0.09 mg P/L. After the TiO_2 nanoparticles were loaded with P, the solids were concentrated by discharging effluent from the UF system until a final volume of 4 L remained in the system, concentrating the TiO_2 solids by approximately 11 times. The removal of permeate resulted in approximately 29 ± 1 % of total P being removed from the system in the permeate. There was no observed change in the mass of adsorbed P during concentration of the TiO_2 solids.

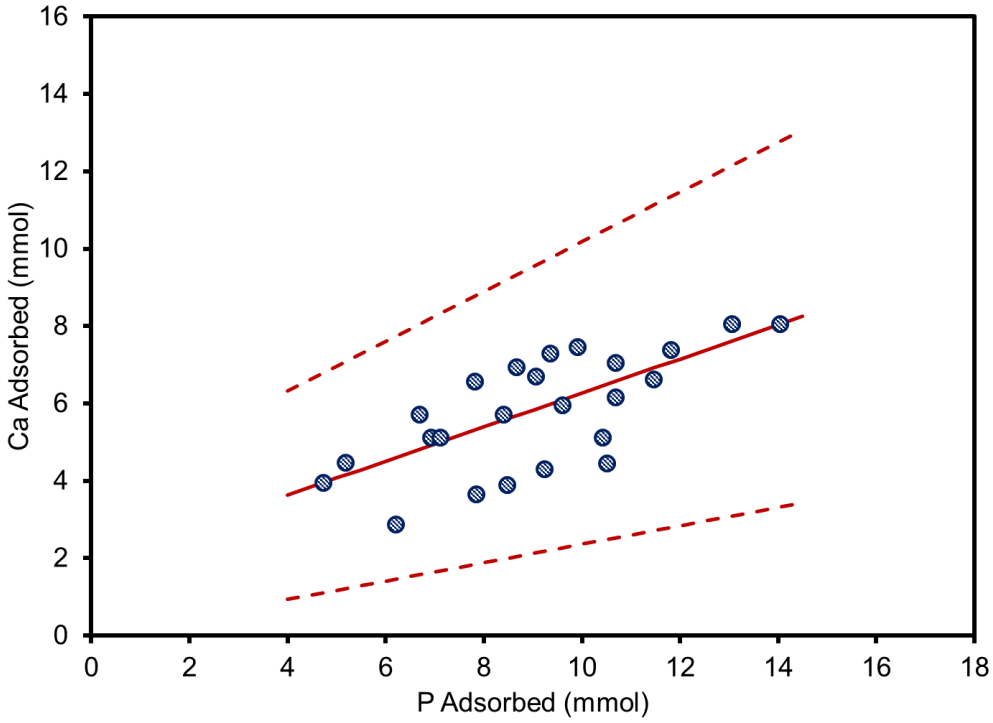

Figure 7-2: Coinciding calcium (mmol) and phosphorus (mmol) removals via adsorption. Line of best fit indicated by solid red line (r = 0.693, R^2 = 0.481, p ¸0.001); dashed lines indicate 95 % confidence intervals.

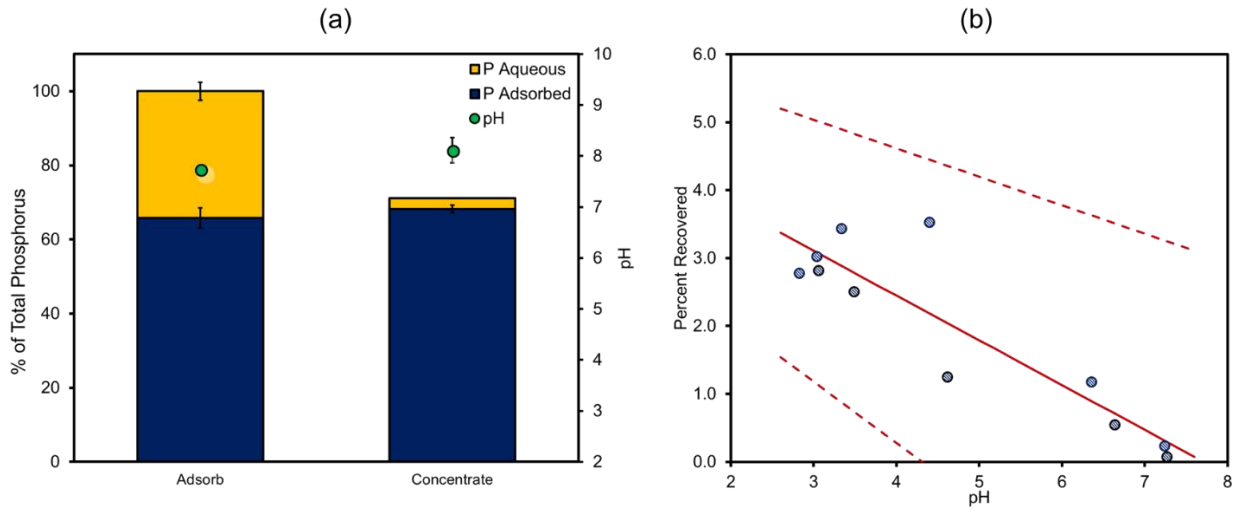

Figure 7-3: (a) Percent of total P adsorbed onto TiO_2 and in the aqueous phase after adsorption and concentration of P-loaded TiO_2 solids; pH at experimental steps are also reported. (b) Percent P recovery from the TiO_2 solids over pH ($r = 0.90$, $R^2 = 0.81$, $p < 0.001$); solid line indicates line of best fit while dashed lines represent 95 % confidence intervals.

The recovery of P from the concentrated TiO_2 solids was investigated by altering the pH of the remaining volume of test solution in the UF system. The concentrations of P and Ca in the aqueous phase prior to recovery were 4.46 ± 0.09 mg P/L and 26.9 ± 5.6 mg Ca/L, respectively. The percent recoveries obtained from incremental changes in pH are presented in Figure 7-3b. Due to the presence of Ca, P recovery through HCl addition was tested as it has been known to be an effective method to recover P from metal oxide based sorbents (Chapter 5). By contrast the use of a basic (NaOH) desorption method could improve conditions for calcium phosphate (CaP) precipitation which forms at high pH (Kunaschk *et al.*, 2015), removing P from the aqueous phase instead of recovering it. Conceptually, as pH decreases with HCl addition, the calcium bridges which formed during adsorption would be disrupted as the surface charge of the TiO_2 changes from negative to neutral, leading to the possible release of P. Incremental changes in pH were made to identify the peak P desorption prior to the TiO_2 surface becoming positive and thus adsorb the liberated P. Phosphorus recovery was observed with decreasing pH ($r = 0.90$,

$R^2 = 0.81$, $p < 0.001$). Adjustment of pH to below pH 4 resulted in higher percent P recovered from the TiO_2 solids; recoveries obtained below pH 4 were not statistically different ($F(4) = 0.08$, $p = 0.796$). Overall, the recovery from the TiO_2 was low with only 3 % of P liberated from the TiO_2 surface.

7.3.3 High Calcium Conditions

Phosphorus adsorption onto TiO_2 was also investigated in a tap water matrix with additional $CaCl_2$ added. The experiments investigating P adsorption at high Ca concentrations were conducted to assess Ca concentrations often found in wastewater; some wastewater effluents can have Ca concentrations upwards of 80 mg Ca/L (MetCalf and Eddy, 2003). The results obtained from P adsorption onto TiO_2 with an average calcium concentration of approximately 70 mg Ca/L are reported in Table 7-1. Initial P concentrations were kept consistent with previous adsorption tests ($t(10) = -0.939$; $p = 0.36$). With the additional Ca, adsorption onto TiO_2 removed 50 % of the P, resulting in a P loading of 9.28 mg P/g TiO_2. Increasing Ca concentrations from medium to high levels did not have a significant effect on P adsorption ($t(6) = 0.884$, $p = 0.411$) or P loading onto TiO_2 ($t(6) = 0.184$, $p = 0.369$). The results suggest that the adsorption capacity of the TiO_2 may have become saturated. Therefore, there was no significant difference in P adsorption or P loading on the TiO_2 solids in the presence of high concentrations of calcium.

7.3.4 Calcium Phosphate Precipitation

It was hypothesized that the presence of the TiO_2 nanoparticles may have enhanced CaP precipitation and hence, additional experiments investigating CaP precipitation with TiO_2 were conducted. There is precedent for addition of hydrated lime ($Ca(OH)_2$) in wastewater and water

treatment. Lime has been used in water treatment to remove iron and manganese ions in water, as well as non-carbonated hardness (Crittenden *et al*., 2012). In wastewater treatment, lime was used as an early method to remove biochemical oxygen demand before biological treatment was implemented however modern use of lime in wastewater treatment is used to remove P by promoting CaP precipitation (Yeoman *et al*., 1988; Metcalf & Eddy, 2003). Although pH adjustment of wastewater tends to be avoided in current wastewater treatment practice, the method may be more attractive if a valuable product is obtained post treatment.

The effect of CaP precipitation on phosphorus removal in the UF system was investigated. Experiments combining adsorption with CaP precipitation were conducted to establish if the P associated with the TiO_2 solids could be increased and thereby lessen P loss during the concentration step. Precipitation was initiated after P adsorption by TiO_2 (Table 7-1) by adjusting the pH to 10.8 ± 0.4 after phosphorus adsorption onto TiO_2. The percent of total P removed via adsorption and precipitation for the three calcium concentrations is presented in Figure 7-4. As mentioned previously, increasing pH above 10 in experiments with low Ca concentration ([Ca] < 10 mg/L) did not have a significant effect on P in solution and therefore there was no precipitation observed ($t(df=3) = -2.416$, $p = 0.09$). In experiments with medium and high Ca concentrations, 45 and 49 % P was removed by increasing the pH to 10.8, the quantity of P precipitated at medium and high Ca concentrations were not significantly different ($t(6) = 0.167$, $p = 0.87$); the additional P removal at pH 10.8 was attributed to precipitation. The combination of adsorption and precipitation removed between 87 and 98 % P in experiments where calcium concentrations exceeded 30 mg Ca/L.

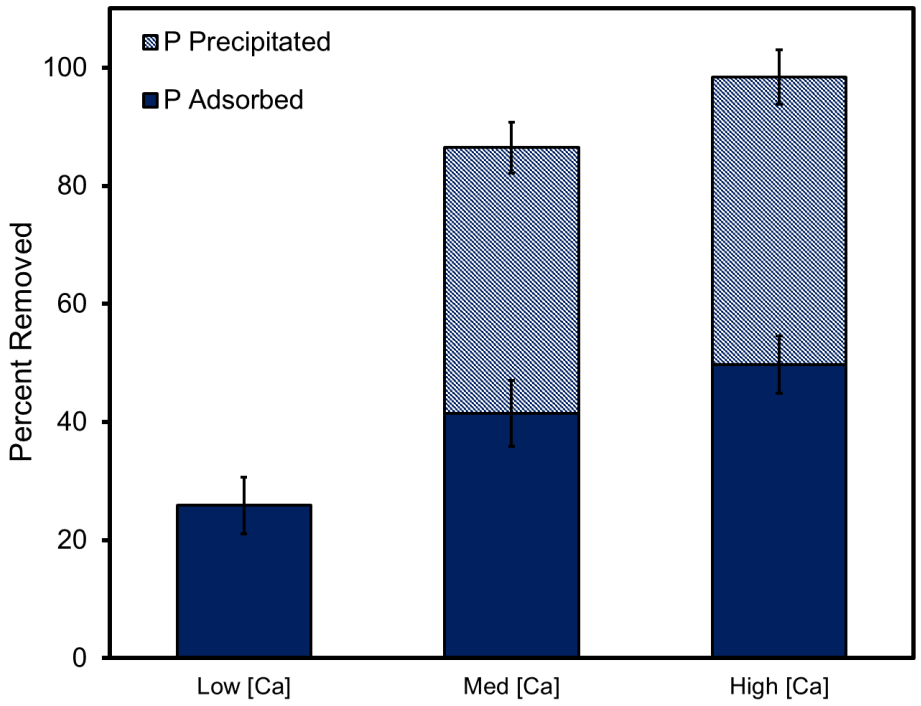

Figure 7-4: Percent P removed via adsorption (dark blue) and precipitation (light blue) at three calcium concentrations.

The calcium phosphorus (Ca/P) molar ratios obtained at pH 7.5 and 10.8 under medium Ca concentrations ([Ca] ~ 30 mg/L) were compared to obtain insight into whether CaP precipitation was occurring. This approach has been used in prior studies to identify the mineral phase precipitating (Habraken *et al.*, 2013; Luster *et al*., 2017; Seckler *et al*., 1996). The Ca/P ratio was calculated by dividing the moles of Ca removed by the moles of P removed during the treatment. At circumneutral pH when P removal was potentially due to calcium bridging, the Ca/P ratio obtained was 0.66 ± 0.14 while at high pH when precipitation was known to occur, the Ca/P ratio was calculated to be 1.23 ± 0.08. The Ca/P molar ratio at pH 10.8 was higher than the molar ratio of Ca/P removed at pH 7.5 ($t(7) = -11.65$, $p < 0.001$). The larger Ca/P molar ratio indicates that with increased pH, more P and Ca was removed to levels that were more than what could be due

to calcium bridging. Therefore, the Ca/P ratio determined for calcium and phosphorus removal at high pH suggested that the additional removals were most likely due to CaP precipitation.

The changes in the Ca/P molar ratio during removal by TiO_2 that were observed at high pH at medium and high Ca concentrations were also investigated. The average Ca/P ratio calculated for removal under high Ca conditions ([Ca] ~ 70 mg/L) was 1.74 ± 0.16. The Ca/P ratio calculated for the high Ca scenario was higher than the ratio obtained under medium Ca concentrations ($t(6) = -5.842$, $p = 0.001$). Hence, more Ca was removed under high Ca concentrations with similar quantities of P removed under both conditions; ($t(6) = -3.925$, $p = 0.008$). Therefore, in solutions with higher Ca concentrations ([Ca] ~ 70 mg/L), precipitation was occurring, and the mineral phase contained around 50 % more Ca than the precipitates form under medium Ca ([Ca] ~ 30 mg/L) conditions.

A comparison of the Ca/P ratios calculated for removals under medium and high calcium conditions was examined to assess which CaP mineral may have been precipitating. The Ca/P molar ratios of known CaP minerals include hydroxyapatite (HAP, Ca/P = 1.67), octacalcium phosphate (OCP, $Ca_4H(PO_4)_3$, Ca/P = 1.33) and brushite ($CaPO_4^-$, Ca/P = 1) (Stumm and Morgan, 1995). The Ca/P ratios determined under the medium and high calcium conditions were 1.23 and 1.74, respectively. Hence, the Ca/P ratios were in the range of the CaP minerals reported in literature. Under the medium calcium conditions, the Ca/P ratio was most similar to that of OCP, while under high calcium conditions the Ca/P ratio was closer to HAP. Therefore, the results suggest that OCP and HAP may have been precipitating onto TiO_2 under the medium (~30 mg/L) and high (~70 mg/L) Ca concentrations, respectively.

7.3.5 Experiments without TiO_2 nanoparticles

To further assess whether precipitation was occurring experiments were conducted in the UF system without the presence of TiO_2. Initial phosphorus and calcium concentrations used in experiments are reported in Table 7-2. Figure 7-5a presents the fraction of total P in the aqueous phase as the pH was varied in the system. When calcium concentrations were low ([Ca] < 10 mg/L), little to no P removal was observed until the pH increased to above 10.5, when approximately 30 % of P was removed. Under the medium Ca conditions ([Ca] ~ 38 mg/L), P in the aqueous phase began to decrease slowly from pH 6 until the pH was above 8 where there was a rapid decrease in soluble P to very low levels (at pH 10.5, [P] = 5% $[P]_o$). This was also observed at high calcium concentrations however the transitional pH values were lower, shifting to pH values of 5 and 7 (pH 9.7, [P] = 5% $[P]_o$). Overall, P removal increased with increasing pH under the various calcium concentrations.

Table 7-2: Initial phosphorus (mg P/L) and calcium (mg Ca/L) concentrations in calcium phosphate precipitation experiments.

	Low [Ca]	**Medium [Ca]**	**High [Ca]**
N	4	4	3
$[P]_o$ (mg P/L)	4.8 ± 0.32	6.0 ± 1.20	5.2 ± 0.74
$[Ca]_o$ (mg Ca/L)	7.3 ± 1.98	38.4 ± 4.80	73.3 ± 2.04

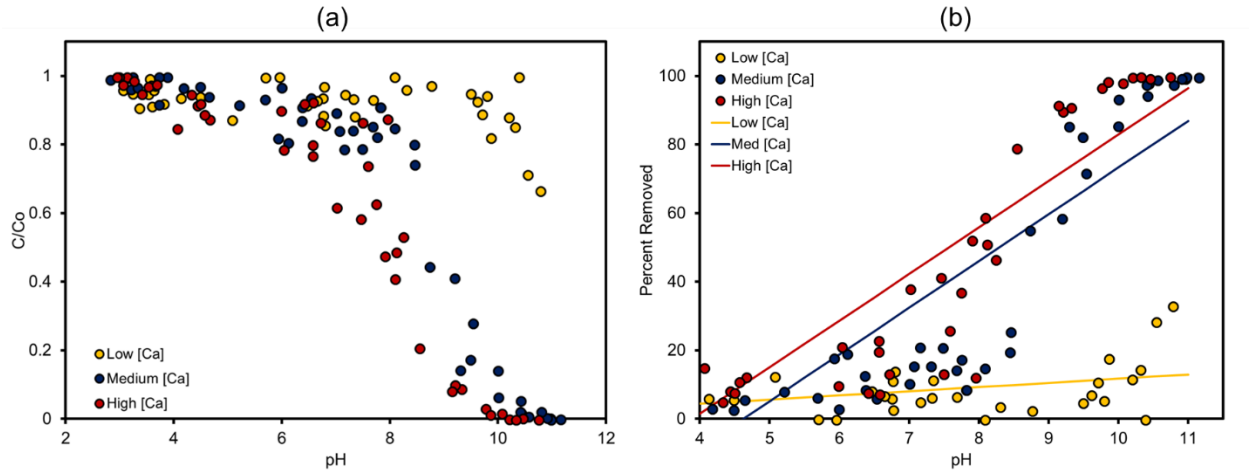

Figure 7-5: (a) Fraction of P in the aqueous phase and (b) percent P removed over pH measured in experiments with low (yellow), medium (blue) and high (red) calcium concentrations. Linear regression indicated by solid lines in corresponding colours (low [Ca]: r = 0.44, R^2 = 0.194, *p* = 0.006; medium [Ca]: r = 0.884, R^2 = 0.782, *p* < 0.001; high [Ca]: r = 0.904, R^2 = 0.818, *p* < 0.001).

The P removals were examined further to gain insight into the effect of the initial solution calcium concentration on P removal as pH was adjusted. Figure 7-5b plots the percent P removed over the range of pH values tested for the different initial Ca concentrations. Using linear regression, the relationship between P removal and pH was found to be significant for all Ca conditions. The relationship between pH and P removal was lowest under low Ca ([Ca] < 10 mg/L) which was attributed to the limited Ca availability in solution (r = 0.44, R^2 = 0.194, *p* = 0.006). Medium ([Ca] ~ 38 mg/L) and high Ca ([Ca] ~ 70 mg/L) conditions resulted in strong relationships between pH and P removal (medium [Ca]: r = 0.884, R^2 = 0.782, *p* < 0.001; high [Ca]: r = 0.904, R^2 = 0.818, *p* < 0.001). A statistical analysis of the linear regression coefficients of medium and high Ca results shows that the two relationships were not different (t = -1.149, *p* = 0.254). Hence, the relationship between P removal pH was similar when aqueous calcium concentrations were greater than 30 mg/L.

To develop more information on the possible mineral phases precipitating at medium and high Ca concentrations, the Ca/P molar removal ratios were determined. Figure 7-6 plots the millimoles of P removed versus millimoles Ca removed (blue data points) through precipitation under the different calcium conditions tested. Using linear regression, the relationship between Ca and P removal was examined and the Ca/P molar ratio of removed was obtained from the slope of the regression lines. In experiments with low Ca (Figure 7.6a), the relationship between removals was not statistically significant ($r= 0.442$, $p = 0.27$) as CaP precipitation was minimal. In experiments where there was evidence of CaP precipitation, the correlations between Ca and P removals were greater. The Ca/P molar ratios for precipitates formed under medium (Figure 7-6b) and high (Figure 7-6c) calcium conditions were determined to be 1.84 ($r = 0.985$, $R^2 = 0.969$, $p < 0.001$) and 2.24 ($r = 0.976$, $R^2 = 0.951$, $p < 0.001$), respectively.

The Ca/P molar ratios obtained in experiments performed under medium and high calcium conditions were compared to assess whether Ca availability affected mineral formation. A statistical analysis of the regression coefficients indicated that the relationships were significantly different ($t=6.09$, $p < 0.001$). Similar quantities of P were removed under both calcium conditions therefore, the higher Ca/P ratio obtained in trials conducted under high Ca concentrations (~ 70 mg/L) suggests that more calcium was being precipitated from solution than that observed under medium Ca concentrations (~ 38 mg/L). Both Ca/P molar ratios obtained in experiments were higher than Ca/P ratios of known CaP mineral phases (Figure 7-6). The higher Ca/P ratios in the precipitates could be due to the formation of an amorphous CaP precipitates in solution.

To obtain more insight into the possible mineral phases forming under the experimental conditions, the results of the experiments without TiO_2 were compared to soluble and solid

speciation predicted by equilibrium modelling. Equilibrium modelling is a useful tool that can predict precipitation of minerals based on equilibrium association and solubility constants. The equilibrium model was employed to predict the CaP mineral phases on the basis of the initial P and Ca concentrations for the medium Ca scenario (Table 7-2). The modeling solved for one CaP mineral phase at a time and the results were compared against the experimental data.

The equilibrium model was initially solved for HAP precipitation under low, medium and high initial Ca concentrations. Figure 7-7 presents the predicted fraction of P in the aqueous phase as predicted by the equilibrium model along with the experimental results obtained under the same conditions. The model predicted HAP precipitation would start to precipitate at pH values of 6.7, 6.1 and 5.9 for the low, medium and high Ca concentrations, respectively. In the experiments, the shift in P removal to a lower pH when Ca increased from medium to high concentrations was not statistically different. However, the model predicted that HAP would precipitate at lower pH under high Ca conditions. Therefore, the model predicted that at a fixed P concentration, increasing the initial Ca concentration increased the likelihood of CaP precipitation and potentially shifted the induction of precipitation to a lower pH which was generally consistent with the experimental results.

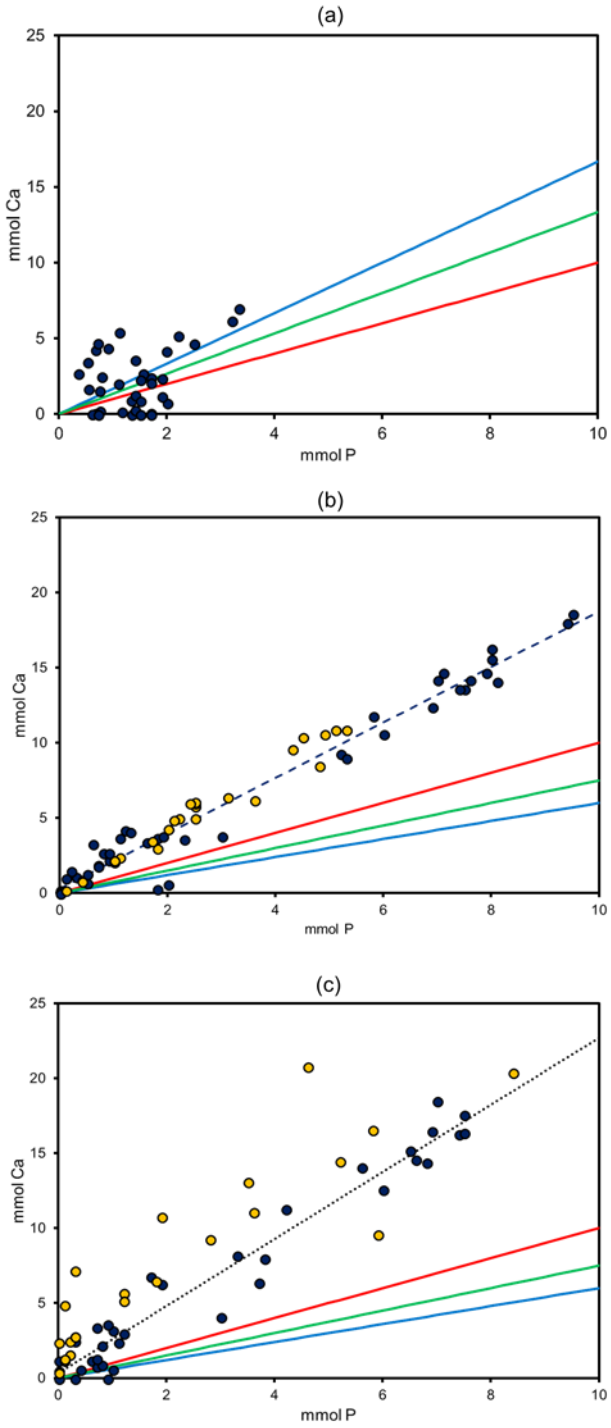

Figure 7-6: Corresponding phosphorus and calcium removals (blue) and recoveries (yellow) observed in solution with (a) low ([Ca] < 10 mg/L), (b) medium ([Ca] ~ 35 mg/L) and (c) high ([Ca] ~ 70 mg/L) calcium conditions. Dashed and dotted linear regression lines are shown for medium and high Ca, respectively. Solid coloured lines represent molar ratio lines for hydroxyapatite (blue), octacalcium phosphate (green) and brushite (red).

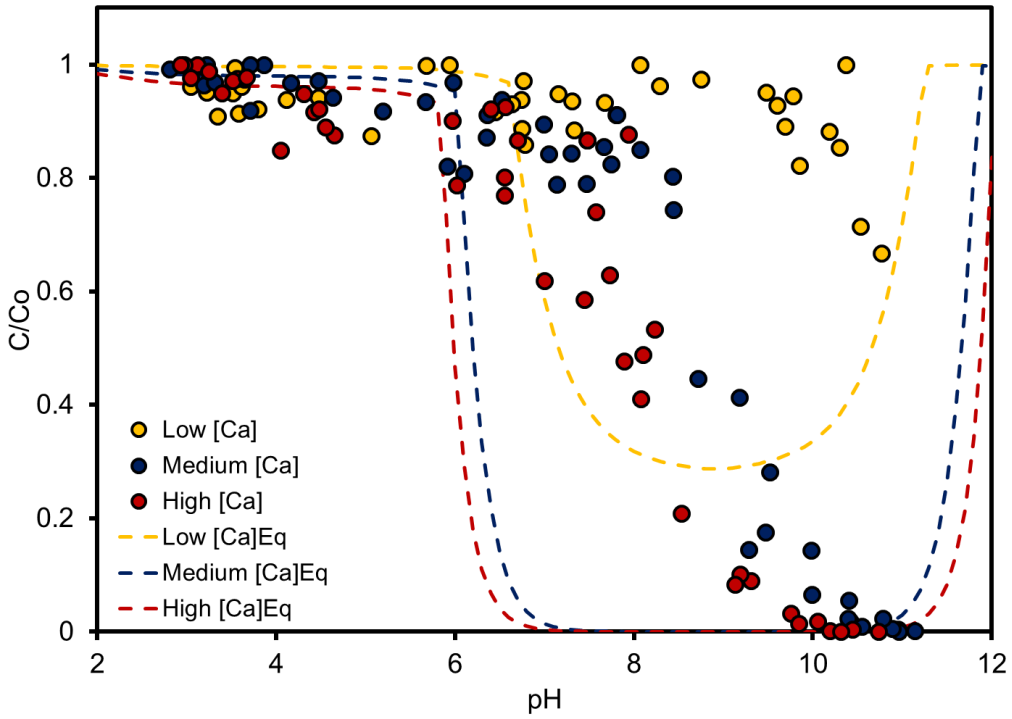

Figure 7-7: Fraction of total P in the aqueous phase over pH measured in experiments (data points) and predicted by equilibrium modelling (dashed lines) under low (yellow), medium (blue) and high (red) calcium concentrations. Equilibrium modelling was solving for hydroxyapatite (HAP) precipitation.

The phosphorus concentrations obtained in the CaP experiments were compared to the model predictions to obtain insight into which CaP mineral phase was precipitating. For simplicity, only results from experiments examining CaP precipitation under medium Ca (~ 38 mg/L) are reported as the removals under medium and high Ca conditions were similar and CaP precipitation was limited under low Ca conditions (<10 mg/L). Figure 7-8a presents the fraction of total P in the aqueous phase observed versus pH in the experiments and predicted by the model. From Figure 7-8 it can be seen that the model predicted that four possible CaP

precipitates could form and would start to precipitate between pH 6 and 7 under medium Ca concentrations. On the basis of HAP precipitation, the model predicted that aqueous P concentrations decrease rapidly after HAP precipitation is initiated with over 95 % P removed at pH 6.8. On the basis of OCP precipitation (using 2 different literature K_{sp} values), the reduction of aqueous P was low between pH 7 and 8, but by pH 8.2 over 95 % of P is predicted to be removed. A small quantity of the amorphous CaP was predicted to precipitate under medium calcium conditions; a small reduction in aqueous P concentration was predicted around pH 7 but then declines to over 95 % removed by pH 8.2.

In Figure 7-8, the decrease in P concentrations observed between pH 6 and 10 during experiments fell within the range of pH values where CaP was predicted to precipitate by the model. It was not possible to infer which mineral phase was forming as the observed P responses overlapped the predictions from all four mineral phases between pH 6 and 7 which did not match the predicted aqueous P concentrations when pH was above 7. The lack of agreement was most likely due to the experimental system not being at equilibrium and hence the CaP precipitates did not have sufficient time to form completely. In summary, it was concluded that the equilibrium model predicted that CaP precipitation was expected under the experimental conditions, but the predictions did not quantitatively agree with the experimental results due to the experimental system not being at equilibrium.

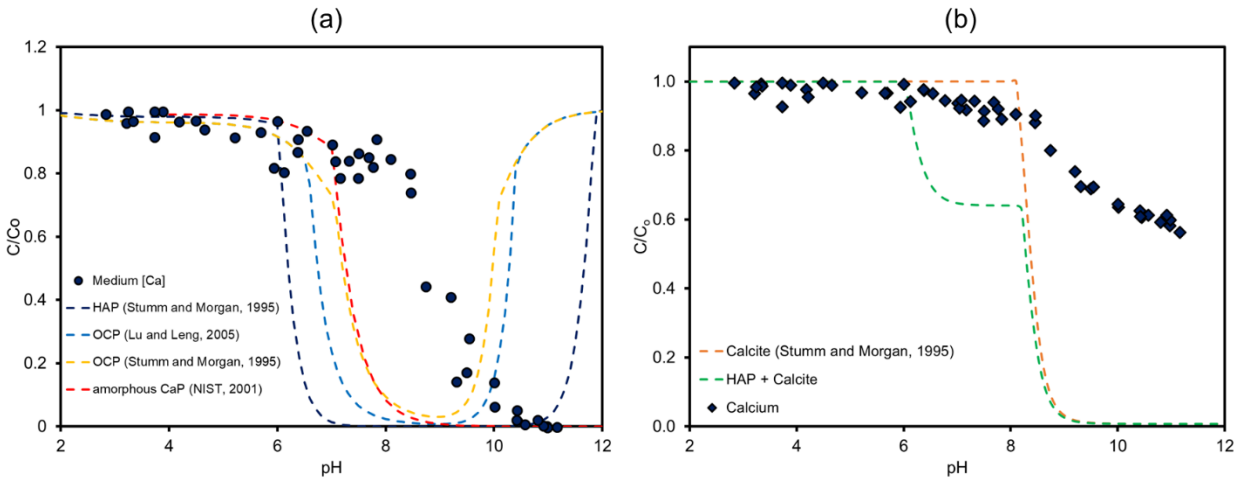

Figure 7-8: (a) Fraction of total P and (b) fraction of total Ca in the aqueous phase over pH in experiments conducted under medium Ca conditions ([Ca] ~ 35 mg/L). Data points represent measured P (circle) and Ca (diamond) while dashed lines are predicted values for CaP and $CaCO_3$ mineral phases that could potentially precipitate.

The calcium responses were also predicted by the model under the medium Ca ([Ca] ~ 38 mg/L) conditions. Figure 7-8b presents the fraction of total Ca in the aqueous phase over pH measured in experiments (data points) and predicted by the model (dashed lines). The model was used to solve for calcite ($CaCO_3$) precipitation at the P and Ca concentrations measured under medium Ca concentrations as shown in Table 7-2. When the model simulated calcite precipitation alone, Ca was not removed until pH was above 8 however when both CaP and calcite were included, Ca concentrations started to decrease around pH 6 where approximately 40 % of the Ca was precipitated as HAP. In this scenario the predicted aqueous Ca concentrations decrease above pH 8 due to calcite formation. The experimental calcium concentrations were not described quantitatively by the model however, Ca was observed to decrease by 10 % above pH 6 and this was followed by a steeper decrease after pH 8. The trends observed in the experiments were generally consistent with Ca uptake with CaP formation, followed by Ca removal in calcite precipitation. Again, the difference between experimental and modeling results were attributed to

the system not being at equilibrium and CaP and calcite precipitates may not be fully formed; amorphous calcite has been found precipitate prior to the systems reaching equilibrium (Gebauer *et al.*, 2008). Overall, the equilibrium model predicted that CaP and calcite precipitation could be expected under the experimental conditions. This could account for the high Ca/P ratios observed under the medium and high Calcium conditions.

The results obtained in experiments without TiO_2 present were assessed to gain insight into the types of precipitates that were occurring on the TiO_2 nanoparticles. The higher Ca/P ratios observed in the experiments without TiO_2 indicated that amorphous CaP and amorphous calcite was precipitating in the experiments. Additionally, solutions with higher Ca concentrations showed evidence of increased amorphous calcite formation. The experiments with TiO_2 had a similar duration as the experiments without TiO_2, and hence it was expected that the system with TiO_2 was also not at equilibrium. Overall, there was evidence supporting CaP precipitation in the UF system with and without TiO_2.

7.3.6 Recovery of P from Calcium Phosphate Precipitates from TiO_2

Experiments were conducted to determine whether the P that had precipitated onto TiO_2 could be recovered from the solids. It was previously demonstrated that approximately 50 % of the P removed in experiments with TiO_2 was precipitated onto the surface. It was anticipated that the P precipitated onto the surface could be recovered via dissolution of the CaP with acid. Further, concentrating the solids in a small volume could potentially make recovery for feasible as chemical use could be reduced and the recovered P may be more concentrated in the small volume; P recovery in a concentrated form is typically desirable for nutrient recovery technologies (Ye *et al*., 2017). Therefore, recovery experiments were conducted where the P

loaded TiO_2 solids were concentrated in the UF system and reduced volumes of acid were added to the concentrated solids to recover the precipitated P.

Dissolution of CaP precipitates liberates both Ca and P, increasing their concentration in solution which can potentially limit the amount of P that can be recovered due to reduced solubility. Due to this possible limitation, P recovery was investigated from TiO_2 solids in which CaP had precipitated under medium and high Ca concentrations. In addition, the TiO_2 solids were concentrated to two levels (4x and 11x concentrated) to observe the effects of increasing the TiO_2 solids.

Recovery of P from TiO_2 that had precipitated at medium and high Ca concentrations were investigated (Figure 7-9) over a range of pH values. The recovery of P under both Ca conditions was found to increase as pH decreased (medium [Ca]: r = -0.687, p <0.001; high [Ca]: r = -0.876, p < 0.001). The recovery under the medium Ca ([Ca]~30 mg/L) scenario was 36 % P at a pH of approximately 2.5 while a recovery of 35 % P was observed at around pH 2 in the high Ca ([Ca] ~ 70 mg/L) scenario. Overall, the recoveries observed under medium and high Ca conditions were not statistically different (r = 0.217, p = 0.162). Hence, approximately 35 % P was liberated from the TiO_2 for Ca conditions that are typical of wastewaters.

To obtain further insight into the dissolution response, the ratio of moles of P and Ca recovered from CaP precipitates formed on the TiO_2 was investigated (Figures 7-6b and 7-6c). The data points in Figure 7-6b fall along the same Ca/P line as the precipitates that were formed under medium Ca concentrations suggesting that dissolution of the CaP precipitates released similar proportions of P and Ca that were originally precipitated. Alternatively, the data points in Figure 7-6c were slightly above the Ca/P line determined for precipitates that formed under high Ca

concentrations. This indicates that more calcium was released from precipitates as compared to P and provides more evidence of a calcite precipitate being present under high Ca conditions. In summary, while the same amount of P was recovered from the precipitates, higher quantities of Ca were released from precipitates that formed under high Ca concentrations ([Ca] ~70 mg/L).

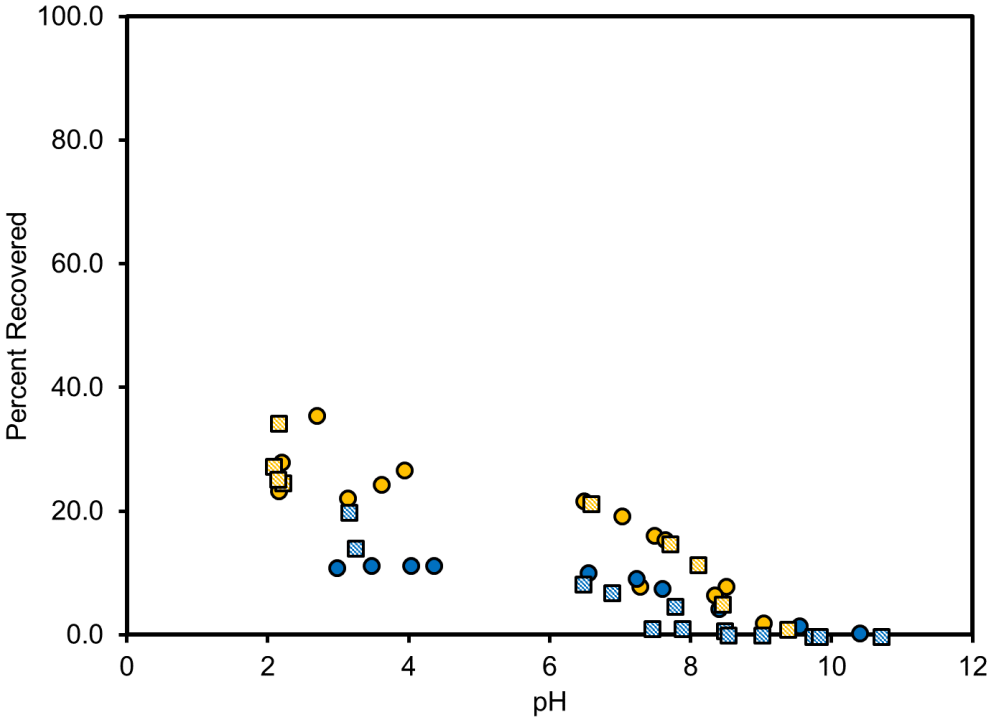

Figure 7-9: Percent P recovered over pH from precipitates that formed on TiO_2 under medium (circle) and high (square) calcium concentrations. Blue and yellow data points indicate TiO_2 solids that had been concentrated in the ultrafiltration system by 4x and 11x, respectively.

During the recovery experiments, the P-loaded TiO_2 nanoparticles were concentrated to two concentration factors to observe the effect of increasing the solids on recovery (Figure 7-9). TiO_2 that had been concentrated by 4x (TiO_2 concentration 4.67 ± 0.72 g/L) liberated between 23 to

35 % P while recoveries ranging from 14 to 20 % were observed from TiO_2 that had been concentrated by 11x (TiO_2 concentration 12.30 ± 1.36 g/L). Overall, higher recoveries were obtained from TiO_2 with lower solids concentrations ($r = -0.658$, $p < 0.001$). The limited recovery observed with higher TiO_2 solids concentrations was possibly due to solubility limits and increased interactions between soluble CaP species and TiO_2 nanoparticles. The latter mechanism has been employed when seed particles have been used to enhance precipitation (Valsami-Jones, 2001). Therefore, higher P recovery will occur when the TiO_2 solids concentration is lower.

The final concentration of P after recovery of P from CaP precipitates was investigated to establish if P could be recovered in a concentrated solution. The phosphorus concentrations in the final recovery effluents ranged from 22.2 to 34.0 mg P/L across both Ca conditions and solids concentrations. Higher recovery effluent concentrations were obtained at the higher CF even though less P was recovered; this was due to final volume of the recovery effluent being half of that of the higher CF. Final P concentrations did not meet the threshold concentrations desired for nutrient recovery.

The results of this study highlight the advantages and disadvantages of using TiO_2 nanoparticles for phosphorus recovery. While P adsorption on TiO_2 was limited, TiO_2 nanoparticles allowed calcium phosphate precipitation to occur displaying a potential for the use of TiO_2 as a seed material to select for CaP precipitation. The system did not however reach equilibrium in this study suggesting that need for enhancement of the process to achieve equilibrium which could produce more valuable forms of CaP. Hao *et al.* (2013) suggested that forms of P recovery other than struvite should be investigated. The use of TiO_2 for P recovery may be able to produce CaP

which is preferred over struvite as it is in a form that can be used directly in industry (Valsami-Jones, 2001).

7.4 Conclusions

The potential to use TiO_2 nanoparticles with ultrafiltration for P recovery was evaluated through a combination experimentation and equilibrium modelling. Phosphorus adsorption onto TiO_2 nanoparticles was found to be dependent on solution pH and initial calcium concentrations. Adsorption onto TiO_2 was observed to increase with decreasing pH in experiments where calcium concentrations were less than 10 mg/L suggesting that chemical desorption may occur at basic pH. The P loading onto TiO_2 adsorbed at circumneutral pH with low Ca concentrations was approximately 4.8 mg P/g TiO_2, consistent with values found in literature. Approximately 13 % P was recovered in chemical desorption tests at low pH with NaOH. Adsorption of P at circumneutral pH increased with increasing calcium concentrations due to the presence of calcium bridging resulting in a P loading of approximately 9 mg P/g TiO_2. Recovery from concentrated TiO_2 solids with HCl was low with only 3 % of P liberated from the TiO_2 surface.

Calcium phosphate was observed to precipitate onto TiO_2 at pH values above 10. The CaP mineral appeared to be amorphous CaP when calcium concentrations were over 30 mg Ca/L; and increasing Ca concentrations lead to the precipitation of calcite. Phosphorus was recovered from the CaP loaded TiO_2 nanoparticles via acid dissolution of the CaP precipitates. Concentration of the TiO_2 solids was found to reduce P recovery. Approximately 35 % of P was recovered from CaP loaded TiO_2.

8.0 Conclusions

8.1 Conclusions

This research provided insight into the use of adsorbents as a method for P removal and recovery from synthetic wastewater solutions and real wastewater effluents. This research also provided understanding on the potential to couple ultrafiltration with a TiO_2/UV advanced oxidation process (AOP) to remove model organic P compounds and non-reactive P (nRP) from real wastewater effluents. From this research, the following conclusions were made:

1. **Surface complexation and ion exchange adsorption mechanisms are both beneficial for P removal and recovery from wastewater.**

   A metal oxide sorbent and ion exchange resin (IEX) were identified as the top performing sorbents after screening of commercial sorbents for P adsorption and recovery from synthetic wastewater, recovering 17.6 and 23 %, respectively (Chapter 4). Overall, both IEX and metal oxide sorbents were proven to have potential for use in phosphorus recovery. Metal oxide sorbents were selective for P over IEX sorbents, which could help with P uptake by the sorbent in complex wastewater streams. Ion exchange sorbents were less selective for P but exhibited large adsorption capacities which was shown to be beneficial for the recovery process in adsorption columns. Although both sorbents are susceptible to competition, IEX sorbents were more prone to competition by opportunistic ions. This trait of IEX sorbents enhanced P recovery as IEX sorbents demonstrated desorption P in most solutions containing an appropriate counter-ion such as chloride.

2. **The adsorbent characteristics determine the optimal desorption solution used for P recovery.**

   Phosphorus recovery testing from sorbents using basic, acidic, salt and basic salt solutions was assessed during the screening of commercial sorbents for P recovery (Chapter 4). The most effective chemical desorption solution was dependent on the specific P adsorption mechanism. Metal oxides adsorb P through surface complexation and required a chemical desorption solution that alters the conditions of the surface thereby lessening the attraction between P and the surface site. Depending on pH, protons or hydroxide can compete with phosphate for surface sites on metal oxides. Thus, acidic or basic desorption solutions proved most effective at removing P from metal oxides. Ion exchange resins remove P by surface complexation or ion exchange and will desorb P from the surface when an appropriate counter ion is present and therefore chemical desorption solutions that contained chloride were more effective. Hybrid ion exchange resins are a combination of IEX and metal oxides and the optimal recovery was obtained with a chemical desorption solution that contained both components (pH change and counter-ion).

3. **The concentration of the chemical desorption recovery stream has the potential to meet target concentrations for nutrient recovery technologies.**

   For recovery of P from wastewater, current technologies require elevated P concentrations to be economically feasible. The application of desorption solutions to P saturated metal oxide and IEX sorbents produced desorption effluent concentrations in excess of the 100 mg P/L target of some nutrient recovery technologies. In column testing (Chapter 5), phosphorus liberation from both metal oxide and IEX sorbents

peaked during the first 10 bed volumes of desorption solution. The final concentration of the blended recovery solution was dependent on the desorption solution used, as some chemical desorption solutions liberated adsorbed P more slowly and thus increased the total volume required for recovery. The final P concentration of the blended recovery solution decreased with increasing volume after the initial peak of P had been recovered.

4. **Mechanism of nRP removal depends on the composition of the nRP present in the wastewater being tested.**

   The mechanism of nRP removal was found to depend on whether it was particulate or dissolved in addition to the molecular size and surface charge. In experiments using the AOP to treat solutions with model compounds (Chapter 6), nRP was removed through adsorption onto the TiO_2 and through the action of UV irradiation. Removal via adsorption was due to the attraction of nRP to the surface of the TiO_2 which was enhanced by the surface charge of both the sorbate and surface. In experiments using the AOP to treat wastewater treatment effluents, nRP removal was observed to occur with ultrafiltration in addition to adsorption and UV irradiation. Removal via ultrafiltration was due to size exclusion of the nRP.

5. **Non-reactive P removal correlated with removal of dissolved organic matter throughout AOP treatment.**

   As reported in Chapter 6, treatment with the AOP demonstrated removal of both nRP and DOC at each step during treatment. This was consistent with nRP being present as organic P species which are covalently bound to organic matter such as humic substances. Organic matter that was larger than the size cut off of the ultrafiltration membrane was retained by the filter, also retaining any associated nRP. Adsorption and

oxidation of organic matter was also observed in this study. Oxidation by hydroxyl radicals was non-selective and targeted larger organic matter which contained nRP.

6. **Production of a concentrated P stream suitable for nutrient recovery through concentrating P-loaded TiO_2 nanoparticles was limited by calcium phosphate precipitation.**

   Phosphorus adsorption onto TiO_2 nanoparticles was found to be dependent on solution pH, with P adsorption increasing with decreasing pH (Chapter 7). The recovery of adsorbed P was low in solutions with low calcium concentrations (< 10 mg Ca/L) due to irreversible binding. In solutions containing levels of calcium usually present in wastewater, P adsorption onto TiO_2 increased due to calcium bridging at circumneutral pH. Recovery from concentrated TiO_2 solids with HCl was low with only 3 % of P liberated from the TiO_2 surface. HCl was used to recover P to disrupt calcium bridging and avoid calcium phosphate precipitation observed to precipitate onto TiO_2 at pH values above 10. Phosphorus was recovered from the CaP loaded TiO_2 nanoparticles via acid dissolution of the CaP precipitates. Concentration of the TiO_2 solids was found to reduce P recovery. Approximately 35 % of P was recovered from CaP loaded TiO_2 due to low solubility of the precipitates.

8.2 Implications for Non-Reactive Phosphorus Removal and Recovery

A strategy to treat high nRP wastewater is proposed using the information gained from this research. The combination of UV/TiO_2 photolysis followed by an adsorption column could decrease residual nRP and recover phosphate in a concentrated form. Photolysis will mineralize nRP to phosphate which will pass, along with unaltered phosphate from the original sample, into

the adsorption column and adsorb onto the solid phase. Once the adsorption column is saturated, P can be recovered through chemical desorption into a recovery solution where P is concentrated enough for nutrient recovery technologies (*i.e.* 100 mg P/L). Use of an ion exchange resin in the adsorption column would be beneficial as a salt solution could be used to recover P and no pH adjustment is necessary. In this proposed arrangement, positioning UV/TiO_2 photolysis prior to the adsorption column is beneficial as photolysis will mineralize dissolved organic matter, reducing the potential of competition for adsorption sites on the column. As seen in Chapter 5, natural wastewater matrices do not perform as well as "cleaner" solutions. Thus, using oxidation prior to the column will enhance removal and ability to recover P.

8.3 Recommendations for Future Work

From this study, the following recommendations are suggested for future studies in P recovery.

1. **There is a need for a sorbent that has the high adsorption capacity and easy regeneration of an IEX resin and the selectivity of an iron oxide.**

   Development of sorbents that include both materials (*i.e.* hybrid ion exchange resins) have started to improve P adsorption in more complex water matrices such as wastewater, however sorbent performance is still greatly variable in different situations. An example of this can be seen in a study that used a strong base hybrid exchange resin to remove phosphorus from grey water and reported adsorption capacities ranging from 1.5 to 10.1 mg P/g sorbent (O'Neal and Boyer, 2013).

2. **There is a need for investigations into using different catalysts and the possibility of using different light sources in advanced oxidation processes.**

Use of light-emitting diodes (LED) instead of mercury lamps will help decrease the energy requirements and operational costs of the advanced oxidation process. In addition, use of another catalyst that does not adsorb P will reduce any potential loss of recoverable P during the oxidation of nRP. One example includes zinc oxide which has been highlighted in literature as a promising photocatalyst for water and wastewater treatment (Lee *et al.*, 2016). Incorporation of the photocatalyst into an ion exchange resin could also help increase adsorption and recovery of phosphate liberated by photocatalysis.

3. **There is a need for investigations into using TiO_2 nanoparticles as a seed for calcium phosphate precipitation.**

Further investigation into the calcium phosphate (CaP) mineral(s) that precipitate onto TiO_2 nanoparticles will help determine if TiO_2 can be used as a seed to recover P from wastewater. TiO_2 nanoparticles are low in toxicity (Vela *et al.*, 2018) and as such, could have potential for direct land application of calcium phosphate loaded TiO_2 as a fertilizer if desirable CaP minerals can be encouraged to precipitate.

Copyright Permissions

Permission was granted from Carrie Capuco (ccapuco@werf.org), Director of Communications at the Water Research Foundation to include report NUTR1R06x: State of Knowledge of the Use of Sorption Technologies for Nutrient Recovery from Municipal Wastewaters (Chapter 2) in this thesis. Permission was granted with the knowledge that this thesis will be open access.

References

Abdulgader, H. A., Kochkodan, V. and Hilal, N. (2013) Hybrid ion exchange – Pressure driven membrane processes in water treatment: A review. *Separation and Purification Technology*, **116**; 253 – 264.

Altundogan, H. S. and Tumen, F. (2001) Removal of phosphates from aqueous solutions by using bauxite I: Effect of pH on the adsorption of various phosphates. *J. Chem. Technol. Biotechnol.*, **77**; 77 – 85.

Amano, Y., Misugi, Y. and Machida, M. (2012) Adsorptive behaviour of Phosphate onto Activated Carbons Varying Surface Physicochemical Properties. *Separation Science and Technology*, **47**: 2348 – 2357.

Anderson, M. A. and Malotky, D. T. (1979) The adsorption of protolyzable anions on hydrous oxides at the isoelectric pH. *Journal of Colloid and Interface Science*, **72** (3); 413 – 427.

Ashley, K., Cordell, D. and Mavinic, D. (2011) A brief history of phosphorus: From the philosopher's stone to recovery and reuse. *Chemosphere*, **86** (6); 737 – 746.

Ashrafizadeh, S. N., Khorasani, Z. and Gorjiara, M. (2008) Ammonia removal from aqueous solutions by Iranian natural zeolite. *Separation Science and Technology*, **43**; 960–978.

Ateeq, F. (2016) "Chemical removal of total phosphorus from wastewater to low levels and its analysis". *Theses and Dissertations (Comprehensive)*. 1889. http://scholars.wlu.ca/etd/1889.

Awual, M. R. and Jyo, A. (2011) Assessing of phosphorus removal by polymeric anion exchangers. *Desalination*, **281**; 111 – 117.

Ayoub, G. M., Koopman, B. and Pandya, N. (2001) Iron and Aluminum Hydroxy(Oxide) Coated Filter Media for Low-Concentration Phosphorus Removal. *Wat. Environ. Res.*, **73** (4); 478 – 485.

Bashar, R., Gungor, K., Karthikeyan, K. G. And Barak, P. (2018) Cost effectiveness of phosphorus removal processes in municipal wastewater treatment. *Chemosphere*, **107**; 280 – 290.

Bashir, M. J. K., Aziz, H. A., Yusoff, M. S. and Adlan, M. N. (2010) Application of respose surface methodology (RSM) for optimization of ammoniacal nitrogen removal from semi-aerobic landfill leachate using ion exchange resin. *Desalination*, **254**; 154 – 161.

Bazri, M. M. and Mohseni, M. (2016) Impact of natural organic matter properties on the kinetics of suspended ion exchange process. *Wat. Res.* **91**; 147 – 155.

Bellier, N., Chazarenc, F. and Comeau, Y. (2006) Phosphorus removal from wastewater by mineral apatite. *Wat. Res.*, **40**; 2965 – 2971.

Benotti, M. J., Stanford, B. D., Wert, E. C. and Snyder, S. A. (2009) Evaluation of a photocatalytic reactor membrane pilot system for the removal of pharmaceuticals and endocrine disrupting compounds from water. *Wat. Res.*, **43**; 1513 – 1522.

Benyoucef, S. and Amrani, M. (2011) Removal of phosphorus from aqueous solutions using chemically modified sawdust of Aleppo pine (*Pinus halepensis Miller*): kinetics and isotherm studies. *Environmentalist*, **31**; 200 – 207.

Bernal, M. P. and Lopez-Real, J. M. (1993) Natural zeolites and sepiolite as ammonium and ammonia adsorbent materials. *Bioresource Technology*, **43**; 27 – 33.

Bhargava, S. K., Tardio, J., Prasad, J., Foger, K., Akolekar, D. B. and Grocott, S. C. (2006) Wet oxidation and catalytic wet oxidation. *Ind. Eng. Chem. Res.*, **45**; 1221 – 1258.

Biswas, B. K., Inoue, K., Ghimire, K. N., Ohta, S., Harada, H., Ohto, K. and Kawakita, H. (2007). The adsorption of phosphate from an aquatic environment using metal-loaded orange waste. *Journal of Colloid and Interface Science* **312**; 214 – 223.

Biswas, B. K., Inoue, K., Ghimire, K. N., Harada, H., Ohto, K. and Kawakita, H. (2008) Removal and recovery of phosphorus from water by means of adsorption onto orange waste gel loaded with zirconium. *Bioresource Technology*, **99**; 8685 – 8690.

Blaney, L. M., Cinar, S., SenGupta, A. K. (2007) Hybrid anion exchanger for trace phosphate removal from water and wastewater. *Wat. Res.*, **41**; 1603 – 1613.

Bolan, N. S., Mowatt, C., Adriano, D. C. and Blennerhassett, J. D. (2003) Removal of ammonium ions from Fellmongery Effluent by Zeolite. *Communications in Soil Science and Plant Analysis*, **34** (13 & 14); 1861 – 1872.

Bond, T., Huang, J., Templeton, M. R. and Graham, N. (2011) Occurrence and control of nitrogenous disinfection by-products in drinking water – A review. Water Research, **45**; 4341 – 4354.

Boujelben, N., Bouzid, J., Elouear, Z., Feki, M., Jamoussi, F. and Montiel, A. (2008) Phsophorus removal from aqueous solution using iron coated natural and engineered sorbents. *Journal of Hazardous Materials*, **151**; 103 – 110.

Brandhuber, P. and Amy, G. Arsenic removal by a charged ultrafiltration membrane – influences of membrane operating conditions and water quality on arsenic rejection. *Desalination*, **140**; 1 – 14.

Breeuwsma, A. and Lyklema, J. (1972) Physical and Chemical Adsorption of Ions in the Electrical Double Layer on Hematite (α-Fe_2O_3). *Journal of Colloid and Interface Science*, **43** (2); 437 – 449.

Capdevielle, A., Sýkorová, E., Béline, F. And Daumer, M.-L. (2016) Effects of organic matter crystallization on struvite in biologically treated wastewater. *Environmental Technology*, **37** (7); 880 – 892.

Carrayrou, J., Mosé, R. and Behra, P., (2002) New efficient algorithm for solving thermodynamic chemistry. *AIChE Journal* **48**; 894–904.

Carvalho, W. S., Martins, D. F., Gomes, F. R., Leite, I. R., da Silva, L. G., Ruggiero, R. and Richter, E. M. (2011) Phosphate adsorption on chemically modified sugarcane bagasse fibres. *Biomass and Bioenergy*, **35**; 3913 – 3919.

Castells, J., Lopezcalahorra, F. and Geijo, F. (1983) The Formoin reaction. *Carbohydrate Research*, **116** (2); 197 – 207.

Chen, S. and Liu, Y. (2007) Study on the photocatalytic degradation of glyphosate by TiO_2 photocatalyst. *Chemosphere*, **67**; 1010 – 1017.

Chen, Y.-S. R., Butler, J. N. and Stumm, W. (1973) Adsorption of phosphate on alumina and kaolinite from dilute aqueous solutions. *Journal of Colloid and Interface Science*, **43**; 421 – 436.

Chen, Y., Wu, F., Lin, Y., Deng, N., Bazhin, N. and Glebov, E. (2007) Photodegradation of glyphosate in the ferrioxalate system. *Journal of Hazardous Materials*, **148**; 360 - 365.

Chitrakar, R., Tezuka, S., Sonoda, A., Sakanem K., Ooi, K. and Hirotsu, T. (2006) Selective adsorption of phosphate from seawater and wastewater by amorphous zirconium hydroxide. *Journal of Colloid and Interface Science*, **297**; 426 – 433.

Chusuei, C. C., Goodman, D. W., Van Stipdonk, M. J., Justes, D. R., Loh, K. H. and Schweikert, E. A. (1999) Solid-liquid adsorption of calcium phosphate on TiO_2. *Langmuir*, **15**; 7355 – 7360.

Clark, D.L., Hunt, G., Kasch, M.S., Lemonds, P.J., Moen, G.M., Neethling, J., (2010) Nutrient management: regulatory approaches to protect water quality. Review of existing practices vol. 1. (NUTR1R06i) Water Environment Research Foundation.

Clark, R. M. (1987) Evaluating the cost and performance of field-scale granular activated carbon systems. *Environ. Sci. Technol.*, **21**; 573 – 580.

Cordell, D., Drangert, J. and White, S. (2009). The story of phosphorus: Global food security and food for thought. *Global Environmental Change*, **19**; 292 – 305.

Crittenden, J. C., Trusssell, R. R., Hand, D. W., Howe, K. J. and Tchobanoglous, G. (2012) Water Treatment: Principles and Design. 3rd ed. Montgomery Watson Harza (MWH), John Wiley & Sons, Inc. New Jersey.

Cruz, F. J. A. L., Canongia Lopes, J. N. and Calado, J. C. G. (2005) A molecular dynamics study of the thermodynamic properties of calcium apatites. 1. Hexagonal phases. *J.Phys. Chem. B*, **109**; 24473 – 24479.

Cyrus, J. S. and Reddy, G. B. (2011) Sorption and desorption of ammonium by zeolite: Batch and column studies. *Journal of Enviromental Science and Health, Part A: Toxic/Hazardous Substances and Environmental Engineering*, **46** (4); 408 – 414.

Daigger, G. T. (2009) Evolving Urban Water and Residuals Management Paradigms: Water Reclamation and Reuse, Decentralization and Resource Recovery. *Water Environment Research*, **81** (8); 809 – 823.

Damen, J. J. M., Ten Cate, J. M. and Ellingsen, J. E. (1991) Induction of calcium phosphate precipitation by titanium dioxide. *J. Dent. Res.*, **70**(10); 1346 – 1349.

de-Bashan, L.E. and Bashan, Y. (2004). Recent advances in removing phosphorus from wastewater and its future use as fertilizer (1997 – 2003). *Water Research*, **38** (19), 4222 - 4246.

Deliyanni, E. A., Peleka, E. N. and Lazardis, N. K. (2007) Comparative study of phosphates removal from aqueous solutions by nanocrytalline akaganeite and hybrid surfactant-akaganeite. *Separation and Purification Technology*, **52**; 478 – 486.

Desmidt, E., Ghyselbrecht, K., Zhang, Y., Pinoy, L., Van der Bruggen, B., Verstraete, W., Rabaey, K. and Meesschaert, B. (2015). Global phosphorus scarcity and full-scale P-recovery techniques – a review. *Critical Reviews in Environmental Science and Technology*, **45**; 336 – 384.

de Sousa, A. F., Braga, T. P., Gomes, E. C. C., Valentini, A. and Longhinottie, E. (2012) Adsorption of phosphate using mesoporous spheres containing iron and aluminum oxide. *Chemical Engineering Journal*, **210**; 143 – 149.

Dionisiou, N. S., Matdi, T. and Misopolinos, N. D. (2013) Phosphorus Adsorption-Desorption on a Surfactant-Modified Natural Zeolite: A Laboratory Study. *Water Air Soil Pollut*, **224**: 1362 – 1372.

Drizo, A., Frost, C.A., Grace, J. and Smith, J.K. (1999) Physico-chemical screening of phosphate-removing substrates for use in constructed wetland systems. *Water Res.*, **33**; 3595–3602.

Du, Q., Liu, S., Cao, Z. and Wang, Y. (2005) Ammonia removal from aqueous solution using natural Chinese clinoptilolite, *Separation and Purification Technology*, **44**; 229–234.

Elzo, D., Huisman, I., Middelink, E., Gekas, V. (1998) Charge effects on inorganic membrane performance in a cross-flow microfiltration process. *Colloids and Surfaces*, **138**; 145 – 159.

Englert, A. H. and Rubio, J. (2005) Characterization and environmental application of a Chilean natural zeolite. *International Journal of Mineral Processing*, **75**; 21–29.

Erisman, J. W., Sutton, M. A., Galloway, J., Kilmont, Z. and Winiwarter, W. (2008) How a century of ammonia synthesis changed the world. *Nature Geoscience*, **1**; 636 – 639.

Evgenidou, E., Fytianos, K., and Poulios, I. (2005) Photocatalytic oxidation of dimethoate in aqueous solutions. *Journal of Photochemistry and Photobiology A: Chemistry*, **175**; 29 - 38.

Evgenidou, E., Konstantinou, I., Fytianos, K., and Albanis, T. (2006) Study of the removal of dichlorvos and dimethoate in a titanium dioxide mediated photocatalytic process through the examination of intermediates and the reaction mechanism. *J. of Hazardous Materials*, **B137**; 1056 – 1064.

Gebauer, D., Gunawidjaja, P. N., Ko, J. Y. P., Bacsik, Z., Aziz, B., Liu, L., Hu, Y., Bergström, L, Tai, C., Sham, T., Edén, M. and Hedin, N. (2010) Proto-calcite and proto-vaterite in amorphous calcium carbonates. *Angew. Chem.* **122**; 9073 – 9075.

Gebauer, D., Völkel, A. and Cölfen, H. (2008) Stable prenucleation calcium carbonate clusters. *Science*, **322**; 1819 – 1822.

Geng, B., Jin, Z., Li, T. and Qi, X. (2009) Preparation of chitosan-stabilized Fe(0) nanoparticles for removal of hexavalent chromium in water. *Sci. Total Environ*, **407**; 4994 – 5000.

Genz, A., Kornmüller, A. and Jekel, M. (2004) Advanced phosphorus removal from membrane filtrates by adsorption on activated aluminum oxide and granulated ferric hydroxide. *Water Res.*, **38**; 3523–3530.

Gerrity, D., Ryu, H., Crittenden, J. and Abbaszadegan, M. (2008) Photocatalytic inactivation of viruses using titanium dioxide nanoparticles and low-pressure UV light. *J. of Environmental Science and Health Part A*, **43**; 1261 – 1270.

Gimsing, A. L. and Boggaard, O. K. (2001) Effect of phosphate on the adsorption of glyphosate on soild, clay minerals and oxides. *Intern. J. Environ. Anal. Chem.*, **82** (8-9); 545 – 552.

Gimsing, A. L. and Boggaard, O. K. (2007) Phosphate and glyphosate adsorption by hematite and ferrihydrite and comparison with other variable-charge minerals. *Clays and Clay Minerals*, **55** (1); 108 – 114.

Gogate, P. R., and Pandit, A. B. (2003) A review of imperative technologies for wastewater treatment I: Oxidation technologies at ambient conditions. *Adv. Environ. Res*. **8**(3–4); 501–551.

Gora, S. L. and Andrews, S. A. (2017) Adsorption of natural organic matter and disinfection byproduct precursors from surface water onto TiO_2 nanoparticles: pH effects, isotherm modelling and implications for using TiO_2 for drinking water treatment. *Chemosphere*, **174**; 363 – 370.

Gordeeva, L.G., Moroz, E.N., Rudina, N.A. and Aristov, Y.I. (2002) Formation of porous vermiculite structure in the course of swelling, Russ. J. Appl. Chem. **75**; 357–361.

Grady, C. P. L., Daigger, G. T., Love, N. G. and Filipe, C. D. M. (2011) Biological Wastewater Treatment, 3rd ed. Boca Raton, FL: CRC Press.

Gu, A. Z., Liu, L., Neethling, J. B., Stensel, H. D. and Murthy, S. (2011) Treatability and fate of various phosphorus fractions in different wastewater treatment processes. *Water Science & Technology*, **63**(4); 804 – 810.

Guest, J. S., Skerlos, S. J., Barnard, J. L, Beck, M. B., Daigger, G. T., Hilger, H., Jackson, S. J., Karvazy, K., Kelly, L., Macpherson, L., Mihelcic, J. R., Pramanik, A., Raskin, L., van Loosdrecht, M. C. M., Yeh, D. and Love, N. G. (2009) A new planning and design paradigm to achieve sustainable resource recovery from wastewater. *Envrion. Sci. & Tech.*, **43**; 6126 – 6130.

Habraken, W. J. E. M., Tao, H., Brylka, L. J., Friedrich, H., Bertinetti, L., Schenk, A. S., Verch, A., Dmitrovic, V., Bomans, P. H. H., Frederik, P. M., Laven, J., van der Schoot, P., Aichmayer, B., de With, G., DeYoreo, J. J. and Sommerdijk, N. A. J. M. (2013) Ion-association complexes unite classical and non-classical theories for the biomimetic nucleation of calcium phosphate. Nature Communications, **4** (1507); doi: 10.1038/ncomms2490.

Han, S., Li, J., Xi, D., Zuo, Y. and Zhang, J. (2009) Photocatalytic decomposition of acephate in irradiated TiO_2 suspensions. *J. of Hazardous Materials*, **163**; 1165 -1172.

Hao, X., Wang, C., van Loosdrecht, M. C. M. and Hu, Y. (2013) Looking beyond struvite for P-recovery. *Envion. Sci. Technol*., **47**; 4965 – 4960.

Harris, D.C. (2003) Quantitative Chemical Analysis. 6th ed. W. H. Freeman and Company, New York, USA.

Hua, M., Zhang, S. J., Pan, B. C., Zhang, W. M., Lv, L., and Zhang Q. X. (2012) Heavy metal removal from water/wastewater by nanosized metal oxides: a review. *J. Hazard. Mater.* **211**; 317 – 331.

Huang, H., Xiao, X., Yan, B. and Yang (2010) Ammonium removal from aqueous solutions by using natural Chinese (Chende) zeolite as adsorbent. *Journal of Hazardous Materials*, **175**; 247 – 252.

Huang, H., Xiao, X., Yang, L. and Yan, B. (2010) Recovery of nitrogen from saponification wastewater by struvite precipitation. *Water Science & Technology*, **61** (11); 2741 – 2749.

Huang, W., Li, D., Liu, Z., Tao, Q., Zhu, Y. Yang, J. and Zhang, Y. (2014) Kinetics, isotherm, thermodynamic and adsorption mechanism studies of $La(OH)_3$-modified exfoliated vermiculites as highly efficient phosphate adsorbents. Chemical Engineering Journal, **236**; 191 – 201.

Huo, H., Lin, H., Dong, Y., Cheng, H., Wang, H. and Cao, L. (2012) Ammonia-nitrogen and phosphates sorption from simulated reclaimed waters by modified clinoptilolite. *Journal of Hazardous Materials*, **229 – 230**; 292 – 297.

Hussain, S., Aziz, H. A., Isa, M. H. Adlan, M. N. and Assaari, F. A. H. (2006) Physico-chemical method for ammonia removal from synthetic wastewater using limestone and GAC in batch and column studies. *Bioresource Technology*, **98**: 874 – 880.

Hussain, S., Aziz, H. A., Isa, M. H. Ahmad, A., van Leeuwen, J., Zou, L., Beecham, S. and Umar, M. (2011) Orthophosphate removal from domestic wastewater using limestone and granular activated carbon. *Desalination*, **271**; 265 – 272.

Ikehata, K. and Gamal El-Din, M. (2006) Aqueous pesticide degradation by hydrogen peroxide/ultraviolet irradiation and Fenton-type advanced oxidation processes: a review. *Journal of Environmental Engineering and Science*, **5**(2); 81 – 135.

Ismail, Z. Z. (2012) Kinetic study for phosphate removal from water by recycled date-palm wastes as agricultural by-products. *International Journal of Environmental Studies*, **69** (1); 135 – 149.

IUPAC: International Union of Pure and Applied Chemistry (1982) Reporting Physisorption Data for Gas/Solid Systems with Special Reference to the Determination of Surface Area and Porosity. *Pure & Appl. Chem.*, **54** (11); 2201 – 2218.

Jha, V. K. and Hayashi, S. (2009) Modification on natural clinoptilolite zeolite for its NH4+ retention capacity. *Journal of Hazardous Materials*, **169**; 29 – 35.

Ji, X. D., Zhange, M. L., Ke, Y. Y. and Song, Y. C. (2013) Simultaneous immobilization of ammonium and phosphate from aqueous solution using zeolites synthesized from fly ashes. *Water Science & Technology*, **67** (6); 1324 – 1331.

Jiang, C., Jia, L., Zhang, B., He, Y. and Kirumba, G. (2014) Comparison of quartz sand, anthracite, shale and biological ceramsite for adsorptive removal of phosphorus from aqueous solution. *Journal of Environmental Sciences*, **26**; 466 – 477.

Jung, Y., Koh, H., Shin, W. and Sung, N. (2005) Wastewater treatment using combination of MBR equipped with non-woven fabric filter and oyster-zeolite column. Environ. Eng. Res. 10, 247-256.

Johansson Westholm, L. (2006) Substrates for phosphorus removal – Potential benefits for on-site wastewater treatment? *Water Research*, **40**; 23 – 26.

Jorgensen, T. C. and Weatherley, L. R. (2003) Ammonia removal from wastewater by in exchange in the presence of organic contaminants. *Water Research*, **37**;1723 – 1728.

Kamel, A. A. (2015) Phosphorus Compounds in Pharmaceutical Drugs and Their Rising Role as Antioxidants and Antidiabetics: A Review. *Int. J. Chem. Biomed. Sci.* **1**; 56–69.

Kang, S.-K., Choo, K.-H. and Lim, K.-H. (2003) Use of Iron Oxide Particles as Adsorbents to Enhance Phosphorus Removal from Secondary Wastewater Effluent. *Separation Science and Technology*, **38** (15); 3853 – 3874.

Kang, S. A., Li, W. Lee, H. E., Phillips, B. L. and Lee, Y. J. (2011) Phosphate uptake by TiO_2: Batch studies and NMR spectroscopic evidence for multisite adsorption. *J. of Colloid and Interface Science*, **364**; 455 – 461.

Karadag, D., Koc, Y., Turan, M. and Armagan, B. (2006) Removal of ammonium ion from aqueous solution using Turkish clinoptilolite. *Journal of Hazardous Materials*, **B136**; 604 – 609.

Karageorgiou, K., Paschalis, M. and Anastassakis, G. N. (2007) Removal of phosphate species from solution by adsorption onto calcite used as natural adsorbent. *Journal of Hazardous Materials*, **A139**; 447 – 452.

Karapinar, N. (2009) Application of natural zeolite for phosphorus and ammonium removal from aqueous solutions. *Journal of Hazardous Materials*, **170**; 1186 – 1191.

Karelid, V., Larsson, G. and Bjorlenius, B. (2017) Pilot-scale removal of pharmaceuticals in municipal wastewater: Comparison of granular powdered activated carbon treatment at three wastewater treatment plants. *J. of Environmental Management*, **193**; 491 – 502.

Krasner, S. W., Mitch, W. A., McCurry, D. L., Hanigan, D., and Westeroff, P. (2013) Formation, precursors, control and occurrence of nitrosamines in drinking water: a review. *Water Research*, **47**; 4435 – 4450.

Krishnan, K. A. and Haridas, A. (2008) Removal of phosphate from aqueous solutions and sewage using natural and surface modified coir pith. *Journal of Hazardous Materials*, **152**; 527 – 535.

Kumar, E., Bhatnagar, A., Hogland, W., Marques, M. and Sillanpää, M. (2014a) Interaction of inorganic anions with iron-mineral adsorbents in aqueous media – A review. *Advances in Colloid and Interface Science*, **203**; 11 – 21.

Kumar, E., Bhatnagar, A., Hogland, W., Marques, M. and Sillanpää, M. (2014b) Interaction of anionic pollutants with Al-based adsorbents in aqueous media – A review. *Chemical Engineering Journal*, **241**; 443 – 456.

Kunaschk, M., Schmalz, V., Dietrich, N., Dittmar, T. and Worch, E. (2015) Novel regeneration method for phosphate loaded granular ferric (hydr)oxide – A contribution to phosphorus recycling. *Wat. Res.* **71**; 219 – 226.

Latimer, R., Rohrbacher, J., Nguyen, V., Khunjar, W. O., Jeyanayagam, S. (2015) Towards a Renewable Future: Assessing Resource Recovery as a Viable Treatment Alternative (NTRY1R12b). Water Environment Research Foundation.

LeCorre, K. S., Valsami-Jones, E., Hobbs, P. And Parsons, S. A. (2005) Impact of calcium on struvite crystal size, shape and purity. *Journal of Crystal Growth*, **283**; 514 – 522.

LeCorre, K. S., Valsami-Jones, E., Hobbs, P. and Parsons, S. A. (2009) Phosphorus Recovery from Wastewater by Struvite Crystallization: A Review. *Critical Reviews in Environmental Science and Technology*, **39** (6): 433-477.

Lee, K. M., Lai, C. W., Ngai, K., S. and Juan, J. C. (2016) Recent developments of zinc oxide based photocatalyst in water treatment technology: a review. *Wat. Res.*, **88**; 428 – 448.

Legrini, O., Oliveros, E. and Braun, A. M. (1993) Photochemical Processes for Water Treatment. *Chem. Rev.*, **93**; 671 – 698.

Lew, B., Tarre, S., Beliavski, M., Dosoretz, C. and Green, M. (2009) Anaerobic membrane bioreactor (AnMBR) for domestic wastewater treatment. *Desalination*, **243**; 251 – 257.

Li, G., Gao, S., Zhang, G and Zhang, X (2014) Enhanced adsorption of phosphate from aqueous solution by nanostructured iron(III)-copper(II) binary oxides. *Chemical Engineering Journal*, **235**: 124 – 131.

Li, R., Kelly, C., Keegan, R., Xiao, L., Morrison, L. and Zhan, X. (2013) Phosphorus removal from wastewater using natural pyrrhotite. *Colloids and Surfaces A: Physicochem. Eng. Aspects*, **427**: 13 – 18.

Li, M., Liu, J., Xu, Y. and Qian, G. (2016) Phosphate adsorption on metal oxides and metal hydroxides: A comparative review. *Environ. Rev.*, **24**; 319 – 332.

Li, M., Zhu, X., Zhu, F., Ren, G., Cao, G. and Song, L. (2011) Application of modified zeolite for ammonium removal from drinking water. *Desalination*, **271**; 295 – 300.

Li, L., and Stanforth, R. (2000). Distinguishing adsorption and surface precipitation on phosphate and goethite (α-FeOOH). *Journal of Colloid and Interface Science*, 230, 12-21.

Liu, H., Dong, Y., Wang, H. and Liu, Y. (2010a) Ammonium adsorption from aqueous solutions by strawberry leaf powder: Equilibrium, kinetics and effects of coexisting ions. *Desalination*, **263**; 70 – 75.

Liu, H., Dong, Y., Wang, H. and Liu, Y. (2010b) Adsorption behavior of ammonium by a bioadsorbent – Boston ivy leaf powder. *Journal of Environmental Sciences*, **22** (10); 1513 – 1518.

Liu, H., Dong, Y., Liu, Y. and Wang, H. (2010c) Screening of novel low-cost adsorbents from agricultural residues to remove ammonia nitrogen from aqueous solution. *Journal of Hazardous Materials*, **178**; 1132 – 1136.

Liu, J., Zhou, Q., Chen, J., Zhang, L. and Chang, N. (2013) Phosphate adsorption on hydroxyl-iron-lanthanum doped activated carbon fiber. *Chemical Engineering Journal*, **@15-216**; 859 – 867.

Long, F., Gong, J.-L., Zeng, G.-M., Chen, L., Wang, X.-Y., Deng, J.-H., Niu, Q.-Y., Zhang, H.-Y. and Zhang, X.-R. (2011) Removal of phosphate from aqueous solution by magnetic Fe-Zr binary oxide. *Chemical Engineering Journal*, **171**; 448 – 455.

Long, X.-L., Cheng, H., Xin, Z.-L., Xiao, W.-D., Li, W. and Yuan, W.-K. (2008) Adsorption of ammonia on activated carbon from aqueous solutions. *American Institute of Chemical Engineers Environ Prog*, **27**; 225 – 233.

Lopez-Periago, A. M., Fraile, J., Lopez-Aranguren, P., Vega, L. F. and Domingo, C. (2013) CO2 capture efficiency and carbonation/calcination kinetics of mirco and nanosized particles of supercritically precipitated calcium carbonate. *Chemical Engineering Journal*, **226**; 357 – 366.

Love, N., Bronk, D. A. and Mulholland, M. R. (2010). Nutrients and Their Effects on the Environment. In *Nutrient Removal: WEF Manual of Practice No. 34.*; Water Environment Federation® (2010). WEF Press. Alexandria, VA.

Lu, J., Liu, H., Liu, R., Zhao, X., Sun, L. and Qu, J. (2013) Adsorptive removal of phosphate by a nanostructured Fe-Al-Mn trimetal oxide adsorbent. *Powder Technology*, **233**; 146 – 154.

Luster, E. Avisar, D., Horovitz, I., Lozzi, L., Baker, M. A., Grilli, R. and Mamane, H. (2017) N-doped TiO_2-coated ceramic membrane for carbamazepine degradation in different water qualities. *Nanomaterials*, **7**, 206; doi:10.3390/nano7080206.

Maher, W., and Woo, L. (1998). Procedures for the storage and digestion of natural waters for the determination of filterable reactive phosphorus, total filterable phosphorus and total phosphorus. *Analytica Chimica Acta* , **375**, 5-47.

Mahmudov, R. and Huang, C. P. (2011) Selective adsorption of oxyanions on activated carbon exemplified by Filtrasorb 400 (F400). *Separation and Purification Technology*, **77**; 294 – 300.

Maizel, A. C. and Remucal, C. K. (2017). The effect of advanced secondary municipal wastewater treatment on the molecular composition of dissolved organic matter. *Water Research*, **122**; 42 – 52.

Malato, S., Blanco, J., Maldonado, M.I., Fernández-Ibánez, P. and Campos, A. (2000) Optimizing solar photocatalytic mineralization of pesticides by adding inorganic oxidizing species; application to the recycling of pesticide containers. *Appl. Catal. B Environ*. **28**; 163 -174.

Manassero, A., Passalia, C., Negro, A. C., Cassano, A. E. and Zalazar, C. S. (2010) Glyphosate degradation in water employing the H2O2/UVC process. *Wat. Res.*, **44**; 3875 – 3882.

Mangat Echavia, G. R., Matzusawa, F. and Negishi, N. (2009) Photocatalytic degradation of organophosphate and phosphonoglycine pesticides using TiO_2 immobilized on silica gel. *Chemosphere*, **76**; 595 – 600.

Malovanyy, A., Sakalova, H., Yatchyshyn, Y., Plaza, E. and Malovanyy, M. (2013) Concentration of ammonium from municipal wastewater using ion exchange process. *Desalination*, **329**; 93 – 102.

Martin, B. D., Parsons, S. A. and Jefferson, B. (2009) Removal and recovery of phosphate from municipal wastewaters using a polymeric anion exchanger bound with hydrated ferric oxide nanoparticles. *Water Science & Technology*, **60** (10); 2637 – 2645.

Mayer, B. K., Gerrity, D., Rittmann, B. E., Reisinger, D. and Brandt-Williams, S. (2013) Innovative strategies to achieve low total phosphorus concentrations in high water flows. *Critical Reviews in Environmental Science and Technology*, **43**(4); 409 – 441.

Mehta, C., Khunjar, M., Wendell, W., Nguyen, V., Tait, S. and Batstone, D. (2015) Technologies to recover nutrients from waste streams: a critical review. Crit. Rev. Env. Sci. Tec. 45 (4), 385 - 427.

Mineralienatlas.de (2012) HEU zeolite structure group. <http://www.mineralienatlas.de/lexikon/index.php/MineralData?mineral=HEU%20zeolite%20structure%20group> (Retrieved April 29, 2014).

Mohan, D. and Pittman Jr., C. U. (2007) Arsenic removal from water/wastewater using adsorbents – A critical review. *Journal of Hazardous Materials*, **142**; 1 – 53.

Moharami, S. and Jalali, M. (2013) Removal of phosphorus from aqueous solutions by Iranian natural adsorbents. *Chemical Engineering Journal*, **223**; 328 – 339.

Moharami, S. and Jalali, M. (2014) Effect of TiO_2, Al_2O_3, and Fe_3O_4 nanoparticles on phosphorus removal from aqueous solution. *Environmental Progress & Sustainable Energy*, **33** (4); 1209 – 1219.

Molinos-Seneante, M., Hernandez-Sancho, F., Sala-Carrido, R. and Garrido-Baserba, M. (2010) Economic Feasibility Study for Phosphorous Recovery Process. *AMBIO*, **40**; 408 – 416.

Molle, P., Lienard, A., Grasmick, A., Iwema, A. and Kabbabi, A. (2005) Apatite as an interesting seed to remove phosphorus from wastewater in constructed wetlands. *Water Sci. Technol.* **51**(9); 193–203.

Molle, P., Martin, S., Esser, D., Besnaulth, S., Morlay, C. and Harouiya, N. (2011) Phosphorus removal by the use of apatite in constructed wetlands: Design recommendations. *Water Practice & Technology*, **6** (3); doi:10.2166/wpt.2011.046.

Moran, M. A. and Zepp, R. G. (1997) Role of photoreactions in the formation of biologically labile compounds from dissolved organic matter. *Limnology and Oceanography*, **42**(6); 1307 – 1316.

Mulder, A. (2003) The quest for sustainable nitrogen removal technologies. *Water Science & Technology*, **48** (1); 67 – 75.

Murayama, N., Tanabe, M., Tamamoto, H. and Shibata, J. (2003) Reaction, Mechanism and Application of Various Zeolite Syntheses from Coal Fly Ash. *Materials Transactions*, **44** (12); 2475 – 2480.

Murphy, M., Walczak, M. S., Hussain, H., Acres, M. J., Muryn, C. A., Thomas, A. G., Silikas, N., Lindsay, R. (2016) An *ex situ* study of the adsorption of calcium phosphate from solution onto TiO_2(110) and Al_2O_3(0001). *Surface Science*, **646**; 146 – 153.

Namasivayam, C. and Sangeetha, D. (2004) Equilibrium kinetic studies of adsorption on phosphate onto $ZnCl_2$ activated coir pith carbon. *Journal of Colloid and Interface Science*, **280**; 359 – 365.

Nawrocki, J. and Andrzejewski, P. (2011) Nitrosamines and water. *Journal of Hazardous Materials*, **189**; 1 - 18.

Nguyen, T. A. H., Ngo, H. H., Guo, W. S., Zhang, J., Liang, S. and Tung, K. L. (2013) Feasibility of iron loaded 'okara' for biosorption of phosphorous in aqueous solutions. *Bioresource Technology*, **150**; 42 – 49.

Ning, P., Bart, H.-J., Li, B., Lu, X. and Zhang, Y. (2008) Phosphate removal from wastewater by model-La(II) zeolite adsorbents. *Journal of Environmental Sciences*, **20**; 670 – 674.

NIST (National Institute of Standards and Technology). Standard Reference Database 46; National Institute of Standards and Technology. Gaithersburg, MD, 2001.

Nowack, B. (2003) Environmental chemistry of phosphonates. *Wat. Res.*, **37**; 2533 – 2546.

Nur, T., Johir, M. A. H., Loganathan, P., Nguyen, T., Vigneswaran, S., and Kandasamy, J. (2013) Phosphate removal from water using an iron oxide impregnated strong base anion exchange resin. *Journal of Industrial and Engineering Chemistry*, http://dx.doi.org/ 10.1016/j.jiec.2013.07.009.

Oh, Y.-M., Hesterberg, D.L. and Nelson, P.V. (1999) Comparison of phosphate adsorption on clay minerals for soilless root media. *Commun. Soil Sci. Plant Anal.*, **30**; 747–756.

Ohno, T., Sarukawa, K., Tokieda, K. and Matsumura, M. (2001) Morphology of a TiO2 Photocatalyst (Degussa, P-25) Consisting of Anatase and Rutile Crystalline Phases. *J. of Catalysis*, **203**; 82 – 86.

O'Neal, J. A. and Boyer, T. H. (2013) Phosphate recovery using hybrid anion exchange: Applications to source-separated urine and combined wastewater streams. *Water Research*, **47**; 5003 – 5017.

Ozacar, M. (2003) Short Communication: Adsorption of phosphate from aqueous solution onto alunite. *Chemosphere*, **51**; 321 – 327.

Parsons, S. A. & J. A. Smith (2008) Phosphorus Removal and Recovery from Municipal Wastewaters. *Elements*, **4**(2), 109-112.

Peng, L., Dai, H., Wu, Y., Peng, Y. and Lu, X. (2018) A comprehensive review of phosphorus recovery from wastewater by crystallization process. Chemosphere, **197**; 768 – 781.

Qin, C., Liu, H., Liu, L., Smith, S., Sedlak, D. L. and Gu, A. Z. (2015) Bioavailability and characterization of dissolved organic nitrogen and dissolved organic phosphorus in wastewater effluents. *Science of the Total Environment*, **511**; 47 – 53.

Qu, X., Alvarez, P. J. J. and Li, Q. (2013) Applications of nanotechnology in water and wastewater treatment. *Water Research*, **47**; 3931 – 3946.

Rahman, M. M., Salleh, M. A. M., Rashid, U., Ahsan, A., Hossain, M. M. and Ra, C. S. (2014) Production of slow release crystal fertilizer from wastewaters through struvite crystallization – A review. *Arabian Journal of Chemistry*, **7**; 139 – 155.

Ren, Z., Shao, L. and Zhang, G. (2012) Adsorption of Phosphate from Aqueous Solution Using an Iron – Zirconium Binary Oxide Sorbent. *Water Air Soil Pollut*, **223**; 4221 – 4231.

Riahi, K., Thayer, B. B., Mammou, A. B., Ammar, A. B. and Jaafoura, M. H. (2009) Biosorption characteristics of phosphates from aqueous solution onto *Phoenix dactylifera* L. date palm fibers. *Journal of Hazardous Materials*, **170**; 511 – 519.

Rittman, B.E., Mayer, B., Westerhoff, P. and Edwards, M. (2011) Capturing the lost phosphorus – Review. *Chemosphere*, **84**; 846 – 853.

Robards, K., McKelvie, I. D., Benson, R. L., Worsfold, P. J., Blundell, N. J. and Casey, H. (1994) Determination of carbon, phosphorus, nitrogen and silicon species in waters. *Analytica Chimica Acta*, **287**, 3; 147 – 190.

Rodrigues, L. A., Caetano, M. L. and da Silva, P. (2010) Adsorption kinetic, thermodynamic and desorption studies of phosphate onto hydrous niobium oxide prepared by reverse microemulsion method. *Adsorption* **16**; 173 – 181.

Ruiz-Martinez, A., Garcia, N. M., Romero, I., Seco, A. and Ferrer, J. (2012) Mircoalgae cultivation in wastewater: Nutrient removal from anaerobic membrane bioreactor effluent. Bioresource Technology, 126: 247 – 253.

Saad, R., Belkacemi, K and Hamoudi, S. (2007) Adsorption of phosphate and nitrate anions on ammonium-functionalized MCM-48: Effects of experimental conditions. *Journal of Colloid and Interface Science* **311**; 375 – 381.

Sarma, J. and Mahiuddin, S. (2014) Specific ion effect on the point of zero charge of α-alumina and on the adsorption of 3,4-dihydroxybenzoic acid onto the α-alumina surface. *Colloids and Surfaces A: Physicochemical and Engineering Aspects*, **457**; 419 – 424.

Schreier, M. and Regalbuto, J.R. (2004) A fundamental study of Pt tetraammine impregnation of silica 1. The electrostatic nature of platinum adsorption. *Journal of Catalysis*, **225**; 190 – 202.

Sedlak, R. I., (1991) Phosphorus and Nitrogen Removal from Municipal Wastewater: Principles and Practice, 2nd Edition, Lewis Publishers, New York. 229 pages.

Seckler, M. M., Bruinsma, O. S. L. and van Rosmalen, G. M. (1996) Calcium phosphate precipitation in a fluidized bed in relation to process conditions: a black box approach. *Wat. Res.*, **30**; 1677 – 1685.

Sendrowski, A. and Boyer, T.H. (2013) Phosphate removal from urine using hybrid anion exchange resin. *Desalination*, **322**; 104 – 112.

Shah, D. N., Feldkamp, J. R., White, J. L. and Hem, S. L. (1982) Effect of the pH-zero point charge relationship on the interaction of ionic compounds and polyols with aluminum hydroxide gel. *Journal of Pharmaceutical Sciences*, **71** (2); 266 – 268.

Shifu, C. and Yunzhang, L. (2006) Study on the photocatalytic degradation of glyphosate by TiO_2 photocatalyst. *Chemosphere*, **67**; 1010 – 1017.

Shon, H. K., Vigneswaran, S. & Snyder, S. A. (2006) Effluent Organic Matter (EfOM) in Wastewater: Constituents, Effects, and Treatment. *Critical Reviews in Environmental Science and Technology*, **36**(4); 327-374.

Sindelar, H. R., Brown, M. T. And Boyer, T. H. (2015) Effects of natural organic matter on calcium and phosphorus co-precipitation. *Chemosphere*, **138**; 218 – 224.Smith, A.L., Stadler, L.B., Love, N.G., Skerlos, S.J. and Raskin, L. (2012) Perspectives on anaerobic membrane bioreactor treatment of domestic wastewater: a critical review. Bioresource Technology, 122: 149 – 159.

Smith, D. S., I. Takács, S. Murthy, G. Diagger, and A. Szabó (2008). Phosphate complexation model and its implications for chemical phosphorus removal. *Water Environment Research* **80**, 428–438.

Smith, D. S. (2007). Solution of simultaneous chemical equilibria in heterogeneous systems: implementation in Matlab. (https://www.researchgate.net/publication/228415676_ Solution_of_simultaneous_chemical_equilibria_in_heterogeneous_systems_implementation_in_Matlab) (accessed: 22 April 2018).

Sohrabnezhad, S., Moghaddam, M. J. M. and Salavatiyan, T. (2014) Synthesis and characterization of CuO-montmorillonite nanocomposite by thermal decomposition method and antibacterial activity of nanocomposite. *Spectrochimica Acta Part A: Molecular and Biomolecular Spectroscopy*, **125**; 73 – 78.

Sperlich, A. (2010) Phosphate adsorption onto granular ferric hydroxide (GFH) for wastewater reuse. Dissertation, University of Berlin.

Standard Methods (Standard Methods for the Examination of Water and Wastewater), 2005. 21st ed., American Public Health Association/American Water Works Association/Water Environment Federation, Washington, DC, USA.

Su, Y., Cui, H., Li, Q., Gao, S. and Shang, J. K. (2013) Strong adsorption of phosphate by amorphous zirconium oxide nanoparticles. *Water Research*, **47**; 5018 – 5026.

Tanada, S., Kabayama, M., Kawasaki, N., Sakiyama, T., Nakamura, T., Araki, M. and Tamura, T. (2003) Removal of phosphate by aluminum oxide hydroxide. *Journal of Colloid and Interface Science*, **257**; 135 – 140.

Tchobanoglous, G. Burton, F. L. and Stensel, H. D. (2003) Wastewater engineering: treatment and reuse. Metcalf & Eddy, Inc. 4th ed. McGraw-Hill, New York.

Thompson, J. G. and Cuff, C. (1985) Crystal structure of kaolinite: dimethylsuloxide intercalate. *Clay and Clay Minerals*, **33** (6); 490 – 500.

Thorton, A., Pearce, P. and Parsons, S. A. (2007) Ammonium removal from solution using ion exchange on to MesoLite, an equilibrium study. *Journal of Hazardous Materials*, **147**; 883 – 889.

USEPA, 2007. Advanced wastewater treatment to achieve low concentration of phosphorus. EPA 910-R-07e002.

Valsami-Jones, E. 2001 Mineralogical controls on phosphorus recovery from wastewaters. *Mineralogical Magazine*, **65** (5); 611 – 620.

van Loon, G. W. and Duffy, S. J. (2000). *Environmental chemistry a global perspective*. New York, NY: Oxford University Press.

Vela, N., Calin, M., Yanez-Gascon, M. J., Garrido, I., Perez-Lucas, G., Fenoll, J. and Navarro, S. (2018) Photocatalytic oxidation of six pesticides listed as endocrine disruptor chemicals from wastewater using two different TiO_2 samples at pilot plant scale under sunlight irradiation. *Journal of Photochemistry and Photobiology A: Chemistry*, **353**; 271 – 278.

Vlad, S. (2015) "Treatment of the Cyanotoxin Anatoxin-a via Activated Carbon Adsorption". *UWSpace. http://hdl.handle.net/10012/9392*.

Wahab, M. A., Jellali, S. and Jedidi, N. (2010) Ammonium biosorption onto sawdust: FTIR analysis, kinetics and adsorption isotherms modeling. *Bioresource Technology*, **101**; 5070 – 5075.

Wang, J., Burken, J. G. and Zhang, X. (J.) (2006) Effect of seeding materials and mixing strength on struvite precipitation. *Water Environ. Res.* **78** (2); 125 – 132.

Wang, S. and Peng, Y. (2010) Natural zeolites as effective adsorbents in water and wastewater treatment – Review. *Chemical Engineering Journal*, **156**; 11 – 24.

Wang, Y. Q., Liu, S. J., Xu, Z., Han, T.W., Chuan, S. and Zhu, T. (2006) Ammonia removal from leachate solution using natural Chinese clinoptilolite. *Journal of Hazardous Materials*, **136**; 735–740.

Wang, Y., Lin, F. and Pang, W. (2008) Ion exchange of ammonium in natural and synthesized zeolites. *Journal of Hazardous Materials*, **160**; 371 – 375.

Wang, Z., Shi, M., Li, J., Wang, Z and Zheng, Z. (2013) Sorption of dissolved inorganic and organic phosphorus compounds onto iron-doped ceramic sand. *Ecological Engineering*, **58**; 286 – 295.

Wendling, L. A., Douglas, G. B., Coleman, S. and Yuan, Z. (2013) Nutrient and dissolved organic carbon removal from natural waters using industrial by-products. *Science of the Total Environment*, **442**; 63 – 72.

Westerhoff, P., Moon, H., Minakata, D. and Crittenden, J. (2009) Oxidation of organics in retentates from reverse osmosis wastewater reuse facilities. *Water Research*, **43**, 3992 – 3998.

Wilfert, P., Kumar, P. S., Korving, L., Witkamp, G.-J. and van Loosdrecht, M. C. M. (2015) The relevance of phosphorus and iron chemistry to the recovery of phosphorus from wastewater: A review. *Environ. Sci. Technol.*, **49**; 9400-9414.

Wu, R. S. S., Lam, K. H., Lee, J. M. N. and Lau, T. C. (2007) Removal of phosphate from water by a highly selective La(III)-chelex resin. *Chemosphere*, **69**; 289 – 294.

Wu, K., Liu, T., Ma, C., Chang, B., Chen, R. and Wang, X. (2014) The role of Mn oxide doping in phosphate removal by Al-based bimetal oxides: adsorption behaviors and mechanisms. *Envrion Sci Pollut Res*, **21**; 620 – 630.

Xie, J., Wang, Z., Wu, D. and Kong, H. (2014) Synthesis and properties of zeolite/hydrated iron oxide composite from coal fly ash as efficient adsorbent to simultaneously retain cationic and anionic pollutants from water. *Fuel*, **116**; 71 – 76.

Xie, M., Shon, H. K., Gray, S. R. and Elimelech, M. (2016) Membrane-based processes for wastewater nutrient recovery: technology, challenges and future direction. *Water Research*, **89**; 210 -221.

Xing, B., Chen, H., and Zhang, X. (2017a) Efficient degradation of organic phosphorus in glyphosate wastewater by catalytic wet oxidation using modified activated carbon as a catalyst. *Environmental Technology*, doi.org/10.1080/09593330.2017.1310935.

Xing, B., Chen, H. and Zhang, X. (2017b) Removal of organic phosphorus and formaldehyde in glyphosate wastewater by CWO and the lime-catalyzed formose reaction. *Water Science & Technology*, **75** (6); 1390 – 1398.

Xiong, W. and Peng, J. (2008) Development and characterization of ferrihydrite-modified diatomite as a phosphorus adsorbent. *Water Res*, **42**; 4869 – 4877.

Xu, Z., Cai, J. and Pan, B. (2013) Mathematically modeling fixed-bed adsorption in aqueous systems. *J. of Zhejiang University – SCIENCE A (Applied Physics & Engineering)*, **14**(3); 155 – 176.

Yan, L., Xu, Y., Yu, H., Xin, X., Wei, Q. and Du, B. (2010) Adsorption of phosphate from aqueous solutions by hydroxyl-aluminum, hydroxyl-iron and hydroxyl-iron-aluminum pillared bentonites. *Journal of Hazardous Materials*, **179**; 244 – 250.

Yao, Y., Gao, B., Inyang, M., Zimmerman, A. R., Cao, X., Pullammanappallil, P. and Yang, L. (2011) Biochar derived from anaerobically digested sugar beet tailings: Characterization and phosphate removal potential. *Bioresource Technology*, **102**; 6273 – 6278.

Yao, Y., Gao, B., Zhange, M., Inyang, M. and Zimmerman, A. R. (2012) Effect of biochar amendment on sorption and leaching of nitrate, ammonium, and phosphate in a sandy soil – Short Communication. *Chemosphere*; **89**; 1467 – 1471.

Ye, Y., Ngo, H. H., Guo, W., Liu, Y., Li, J., Liu, J. Liu, Y., Zhang, X. and Jia, H. (2017) Insight into chemical phosphate recovery from municipal wastewater. *Science of the Total Environment*, **576**; 159 – 171.

Yeoman, S., Stephenson, T., Lester, J. N. and Perry, R. (1988) The removal of phosphorus during wastewater treatment: A review. *Environmental Pollution*, **49**; 183 – 233.

Yin, H., Yun, Y., Zhange, Y. and Fan, C. (2011) Phosphate removal from wastewaters by a naturally occurring, calcium-rich sepiolite. *Journal of Hazardous Materials*, **198**; 362 – 369.

Yin, H., Kong, M. and Fan, C. (2013) Batch investigations on P immobilization from wastewaters and sediment using natural calcium rich sepiolite as a reactive material. *Water Research*, **47**; 4247 – 4258.

Zaranyika, M. F. and Nyandoro, M. G. (1993) Degradation of glyphosate in the aquatic environment: an enzymatic kinetic model that takes into account microbial degradation of both free and coloidal (or sediment) particle adsorbed glyphosate. J Agric FoodChem **41**; 838–842.

Zhang, B., Wu, D., Wang, C., He, S., Zhang, Z. and Kong, H. (2007) Simultaneous removal of ammonium and phosphate by zeolite synthesized from coal fly ash as influenced by acid treatment. *Journal of Environmental Sciences*, **19**; 540 – 545.

Zhang, C. and Chen, Y. (2009) Simultaneous Nitrogen and Phosphorus Recovery from Sludge-Fermentation Liquid Mixture and Application of the Fermentation Liquid to Enhance Municipal Wastewater Biological Nutrient Removal. *Environ. Sci. Technol*. **43**; 6164 - 6170.

Zhang, Y., Desmidt, E., Van Looveren, A., Pinoy, L., Meesschaert, B., and Van der Bruggen, B. (2013) Phosphate separation and recovery from wastewater by novel electrodialysis. *Environ. Sci. Technol.*, **47**, 5888 – 5895.

Zhang, Y., Zhang, W. and Pan, B. (2015) Struvite-based phosphorus recovery from the concentrated bioeffluent by using HFO nanocomposite adsorption: effect of solution chemistry. *Chemosphere*, **141**; 227 – 234.

Zhou, Y., Gao, B., Zimmerman, A. R., Chen, H., Zhang, M. and Cao, X. (2014) Biochar-supported zerovalent iron for removal of various contaminants from aqueous solutions. *Bioresource Technology*, **152**; 538 – 542.